The human GPCR Nicotinic Acid Receptor 1: Heterologous Overproduction in *Pichia pastoris* and the Reconstitution of its Complex with β-Arrestin 1 *in vivo* and *in vitro*

Dissertation
zur Erlangung des Doktorgrades
der Naturwissenschaften

vorgelegt beim Fachbereich
Chemische und Pharmazeutische Wissenschaften
der Johann Wolfgang Goethe Universität
Frankfurt am Main

von
Jan Griesbach
aus Augsburg, Deutschland

Frankfurt am Main, 2007
D30

vom Fachbereich Chemische und Pharmazeutische Wissenschaften der Johann Wolfgang Goethe – Universität als Dissertation angenommen

Dekan: Prof. Dr. Harald Schwalbe

1. Gutachter: Prof. Dr. Clemens Glaubitz
2. Gutachter: Prof. Dr. Hartmut Michel

Datum der Disputation:

As I stand here, the ground beneath is nothing more than one point of view

(Dave Matthews – Raven)

Table of Content

Abstract

Nicotinic acid has been used in the clinical treatment of elevated blood lipid levels for over 50 years. Although it has a beneficial effect on myocardial infarction and blood lipid profiles, its widespread use has been hampered by side effects such as skin rashes and a burning sensation on the upper body. Since elevated blood lipid levels, especially ones of VLDL and LDL cholesterol are a frequent indication and high risk factor for coronary and cardiac diseases, finding a compound with an enhanced pharmacological profile, still holding the desired effects, but without inconvenient side effects, is a very appealing aim to many pharmaceutical companies. These efforts have already produced two marketed drugs, Acipimox and Acifran, but they have not been able to overcome the restrictions already imposed on the treatment by nicotinic acid. Although proposed long before, in the year 2000 the gene for the nicotinic acid receptor in mouse PUMA-G was cloned, and in 2003 the discovery of the genes HM74 and HM74A followed, which comprise the homologous low and high affinity receptors for nicotinic acid in humans. The discovery of this G Protein-coupled receptor target allowed a more directed approach for the search of alternative compounds.

This work is the first report of the heterologous overexpression of the high affinity GPCR gene HM74A in the methylotrophic yeast *Pichia pastoris*. The protein product, NAR1, was pharmacologically characterized, and displayed a binding affinity of 224.8 nM to its ligand nicotinic acid, showing a similar activity profile compared to those displayed in human tissue, which were determined to be 60 nM to 90 nM. Additionally, inhibitory constants (K_i) for Acifran and Acipimox were determined to be 4.5 µM and 50.5 µM, respectively. Furthermore, the total yield of NAR1 reached 42 pmol/mg membrane protein, which corresponds to 0.4 mg of receptor produced per liter yeast culture, opening up the perspective of large scale protein production to facilitate high throughput screening drug discovery efforts and structural studies. In addition, NAR1 could be solubilized in n-decyl-β-D-maltopyranoside and purified to homogeneity after immobilized metal affinity chromatography and a second affinity chromatography step on immobilized monomeric avidin, yielding a single peak on gel filtration, while the purified receptor was able to bind ligand, as shown in NMR Saturation Transfer Difference (STD) measurements.

It could be shown that NAR1 is desensitized by β-arrestin 1 *in vivo* in confocal microscopy studies on HEK and BHK cells. This finding provides a native binding partner for the stabilization of the receptor upon solubilization and purification.

Finally human β-arrestin 1 could be produced as a constitutively active variant, comprising residues 1-382 in *Pichia pastoris* and *Escherichia coli*. The purified protein was used for *in vitro* binding experiments and shown to be capable of interacting with NAR1. Although the interaction and formation of the complex was only possible to a limited extent, it leaves open the perspective of crystallizing NAR1 in its active conformation, bound to nicotinic acid and β-arrestin 1.

Zusammenfassung

Nikotinsäure wird seit über fünfzig Jahren in der klinischen Therapie eingesetzt. Damals entdeckten Robert Altschul und Kollegen [11], dass Nikotinsäure Blutfettwerte verbessern und den Cholesterinspiegel senken kann. Diesen Effekt erzielt Nikotinsäure durch die Inhibition der Lipolyse in Fettgewebe [12]. Dies führt zu einer Konzentrationsminderung von freien Fettsäuren und Triglyceriden im Blutplasma, wodurch die Synthese von Triacylglyceriden und Very Low Density Lipoproteins (VLDLs) in der Leber, mangels Substrat, reduziert wird. Damit einhergehend verschiebt sich das Gleichgewicht von Very Low Density Lipoproteins (VLDLs) und Low Density Lipoproteins (LDLs) und darin enthaltenem Cholesterin („schlechtes Cholesterin“) zu Gunsten der High Density Lipoproteins (HDLs) und darin gebundenem Cholesterin („gutes Cholesterin“) (Abbildung 6). Im Jahr 2000 gelang es der Gruppe von U. Schwabe den G-Protein gekoppelten Rezeptor für Nikotinsäure in Mäusen (PUMA-G, Protein Upregulated in Macrophages by Interferon-γ) zu identifizieren [13], und 2003 publizierten 3 Gruppen unabhängig voneinander die Identifizierung zweier Gene für die humane Nikotinsäurerezeptoren HM74 (GPR109B) und HM74-A (GPR109A) [14-16]. Die Sequenzhomologie dieser beiden Gene beträgt 96 %, und ihre physikalische Nähe auf Chromosom 12q24.31 lassen auf kürzlich zurückliegende Genverdopplung schließen. Das Gen mit der Bezeichnung HM74A codiert für den hoch affinen Rezeptor, und seine Nukleinsäuresequenzhomologie zu dem murinen PUMA-G beträgt 82 %.

Dadurch ergibt sich für die therapeutische Wirkung von Nikotinsäure folgender Effekt. Nikotinsäure aktiviert den G-Protein gekoppelten Rezeptor HM74A, der über die Kopplung mit heterotrimeren G-Proteinen der G_i Familie die Adenylylcyclase inhibiert, und zu einer Aktivitätsminderung der hormonsensitiven Triglyceridlipase führt (Abbildung 6). Dadurch entstehen die oben bereits beschriebenen Effekte. Allerdings sind für die Therapie mit Nikotinsäure oral einzunehmende Dosen von 1,5 g – 3.0 g täglich nötig, und werden seit jeher von ungewollten Nebenwirkungen begleitet. Diese sind vor allem Vasodilation, die zu einer deutlichen Rötung im Gesicht und am Oberkörper, sowie ein sonnenbrandähnliches Gefühl an ebendiesen Stellen führen. Wenn auch die Nebenwirkungen nicht dramatisch sind, schränken sie die Akzeptanz der Patienten bei länger anhaltenden Therapie drastisch ein. Der Nikotinsäurerezeptor wird neben Fettgewebe auch in dermalen dendritischen Zellen und Makrophagen exprimiert, in denen durch G_i Kopplung und Phospholipase A2 Aktivierung

Arachidonsäure freigesetzt wird. Arachidonsäure wird von der Cyclooxygenase-1 zu Prostaglandin D2 und E2 umgewandelt, und verursacht so die beschriebenen Nebenwirkung. Die derzeit verfügbaren, alternativen Medikamente Acifran und Acipimox mildern die Nebenwirkungen, vermeiden sie aber auch nicht.

Diese Arbeit beschreibt erstmals die heterologe Überexpression des Nikotinsäurerezeptors in der methylotrophen Hefe *Pichia pastoris*. Dies beinhaltet die Generierung verschiedener Vektorkonstrukte, die Transformierung von *Pichia pastoris* Zellen und die Isolierung von Klonen, die mehrere Kopien des Expressionskonstruktes in ihr Genom integriert haben, und eine hohe Expression des Nikotinsäurerezeptorproteins (NAR1) ermöglichen. Der auf diese Weise produzierte Rezeptor wurde eingehend charakterisiert, und es konnte gezeigt werden, dass seine pharmakologischen Eigenschaften denen des Rezeptors aus homologem Gewebeproben entsprechen. Die Affinität für Nikotinsäure liegt mit 224.8 nM unter den in nativem Gewebe gemessenen Werten, die zwischen 60 nM und 90 nM liegen. Die Inhibitionskonstanten (K_i) für Acifran (K_i = 4,57 µM) und Acipimox (K_i = 50,5 µM) sind auch dementsprechend verschoben. Diese Beobachtung wurde aber bereits für andere Rezeptoren gemacht, und liegt in der Tatsache begründet, dass sowohl die Zusammensetzung der Membranlipide in *Pichia pastoris* anders ist als auch Proteinkomponenten, welche die Aktivität von GPCRs modulieren, gar nicht vorhanden sind. Die maximale Produktionsmenge des Nikotinsäurerezeptors lag bei einem B_{max}-Wert von 42 pmol/mg Membranprotein. Dies entspricht 0.4 mg Rezeptorprotein pro Liter Hefekultur. Die hier produzierte Menge erlaubt erstmals Hochdurchsatz Screening Methoden *in vitro* durchzuführen, und neue therapeutische wirksame Substanzen zu identifizieren. Zusätzlich konnte die Auswirkung verschiedener Pufferkomponenten in funktionellen Tests gemessen werden. So konnte gezeigt werden, dass der heterolog exprimierte Rezeptor sensitiv gegenüber hohen Konzentration an Natriumionen ist. Dies stimmt mit den Messungen von Lorenzen et al. 2001 [13] überein, die in nativem Gewebe ebenfalls eine Aktivitätsabnahme in Gegenwart hoher Natriumkonzentrationen beschreiben. GPCRs der Familie A wie der Nikotinsäurerezeptor haben alle eine konservierte Disulfidbrücke zwischen den extrazellulären Verbindungen der Transmembranhelices zwei und drei, sowie vier und fünf. Diese ist für strukturelle und funktionelle Integrität des Rezeptors unerlässlich, und es konnte gezeigt werden, dass die Reduktion dieser durch Zugabe von DTT zu einem Aktivitätsverlust führt.
Des Weiteren ermöglicht die hier produzierte Menge erstmals umfassende Studien zu Solubilisierung und Proteinreinigung, die neben der funktionellen Expression die ersten

wichtigen Schritte auf dem Weg zu Experimenten zur Strukturaufklärung sind. Es konnte gezeigt werden, dass aus einem Testsatz von 18 Detergenzien alle mit Ausnahme von n-Decyl-β-D-Glucopyranosid in der Lage waren den Nikotinsäurerezeptor NAR1 aus der Membran zu extrahieren. Die Messung der Bindungsaktivität wurde jedoch durch die Verwendung von Detergenzien erschwert. Durch die Extraktion des Rezeptors aus der Membran ist zum einen eine Abnahme der Affinität zu erwarten, zum anderen muss der ungebundene Ligand von dem freien separiert werden, was durch das Auflösen der Membran nicht mehr mit dem bisherigen Filtrationsversuch möglich ist. Dies konnte dadurch gezeigt werden, dass bei Erreichen der kritischen mizellaren Konzentration (cmc) von Detergenz im Bindungstest keinerlei Aktivität mehr zu messen war. Titrationskurven mit den Detergenzien n-Decyl-β-D-Maltopyranosid, n-Dodecyl-β-D-Maltopyranosid und Cymal-6 belegen dies eindeutig. Es konnte weiterhin gezeigt werden, dass die anschließende Extraktion des Detergenz zu einer partiellen Rückgewinnung der Aktivität führte. Die besten Werte lieferte dabei n-Decyl-β-D-Maltopyranosid mit über 30 % der Ausgangsaktivität. Ein Proteinstabilitätsscreening konnte zusammen mit verschiedensten Reinigungsstrategien n-Decyl-β-D-Maltopyranosid als am besten geeignetes Detergenz bestätigen, weil es das größte Ausmaß an Rezeptorstabilität und Funktionalität gewährleistet. Letztlich konnte der Rezeptor über Immobilisierte Metall-Affinitätschromatographie und einen zweiten affinitätschromatographischen Schritt mit Hilfe immobilisierten monomeren Avidins gereinigt werden. Der so vorliegende Rezeptor ergab ein einzelnes Signal in der analytischen Gelfiltration, das von einer homogenen Proteinpräparation zeugt. Die Aktivität des gereinigten Rezeptors konnte mittels NMR basierenden STD (Saturierungs Transfer Differenz) Messungen gezeigt werden.

Die Kristallisation von Membranproteinen gestaltet sich häufig schwierig, da in vielen Fällen die hydrophilen Anteile des Proteins nicht über die Detergenzmizelle hinausreichen, und somit kaum eine Möglichkeit zur Ausbildung von Kristallkontakten besteht. Um dieses Problem zu lösen werden Anitkörperfragmente an das zu kristallisierende Membranprotein gebunden, um die polare Oberfläche zu vergrößern, was die Bildung von Kristallkontakten ermöglicht. Da die Suche nach einem geeigneten Antikörperfragment schwierig und langwierig ist, wurde nach Alternativen gesucht, und β-Arrestine als potentielle Kandidaten entdeckt. Der Aktivitätszyklus eines G-Protein gekoppelten Rezeptors stellt sich wie folgt dar: Der Rezeptor bindet den extrazellulären Liganden, und wird so durch eine Konformationsänderung in den aktiven Zustand überführt. Dieser ermöglicht die Aktivierung

des gekoppelten heterotrimeren G-Proteins, dessen α-Untereinheit sich von dem βγ-Komplex löst und beide Effektorenzyme aktivieren. Der dissozierte βγ-Komplex rekrutiert G-Protein gekoppelte Rezeptorkinasen, die Tyrosin-, Serin- und Threoninseitenketten phosphorylieren. Die Phosphoaminosäuren stellen zusammen mit der aktiven Rezeptorkonformation die Bindungsstelle für Arrestinproteine dar, die zum einen die Aktivierung weiterer heterotrimerer G-Proteine unterbinden und die Verbindung zu Clathrin ummantelten Vesikeln herstellen. Der Komplex aus Rezeptor Ligand und Arrestin ist langlebig, da Arrestin den Rezeptor zu den Endosomen begleitet, wo über seine Wiederverwendung oder Abbau bestimmt wird. Mit 40 kDa ist β-Arrestin ähnlich groß wie der Rezeptor, aber ein lösliches Protein, und vergrößert so die hydrophile Oberfläche des Komplexes im Vergleich zu der des Rezeptors alleine.

In vivo Experimente mit HEK- (Human Embryonic Kidney) und BHK- (Baby Hamster Kidney) Zellen zeigten erstmals die Interaktion beider Proteine nach Stimulation mit Nikotinsäure. Hierzu wurden Plasmide mit GFP markiertem Nikotinsäurerezeptor und CFP markiertem β-Arrestin hergestellt und in die Zellen transfiziert. Daraufhin konnte beobachtet werden, dass sich die blaue Fluoreszenz β-Arrestins als Volllängenkonstrukt, als auch in der konstitutiv aktiven Variante der Aminosäuren 1 bis 382 im Zytoplasma befindet, während sich die grüne Fluoreszenz des Rezeptors auf die Zellmembran und definierte intrazelluläre Membrankompartimente beschränkte. Zugabe von Nikotinsäure zum Medium bewirkte eine Verlagerung des β-Arrestin Fluoreszenzsignals an die Membran, zu dem Rezeptor.

β-Arrestin 1 konnte als konstitutiv aktive Variante, die die Aminosäuren 1 bis 382 (β-Arrestin 1-382) umfasst, sowohl in *Pichia pastoris*, als auch in *Escherichia coli* produziert werden, wobei die Ausbeute in *Pichia pastoris* das vierfache der Menge in *Escherichia coli* betrug. Jedoch ist die Handhabung von *Escherichia coli* deutlich angenehmer, und die Verwendung von *Pichia pastoris* nicht zwingend. In beiden Expressionssystemen gestaltete sich die Expression von β-Arrestin 2 als schwierig, und brachte nicht die erforderlichen Proteinmengen ein. Ein [^{15}N] markierte Präparation der konstitutiv aktiven Version β-Arrestin 1-382 stellte sich in NMR-spektroskopischen Messungen als dynamisch gefaltetes Protein dar, jedoch waren die spektralen Eigenschaften β-Arrestins 1-382 nicht ausreichend um eine Auflösung eines Signals für jede Aminosäure zu ergeben. Dadurch war die Zuordnung und Strukturbestimmung mittels NMR nicht möglich. Auch konnte keine Interaktion mit einem

Rezeptorpeptid beobachtet werden, die eine Eingrenzung der interagierenden Aminosäuren erlaubt hätte.

Dennoch konnte *in vivo* gezeigt werden, dass der gereinigte Rezeptor an β-Arrestin 1 bindet, und sich somit die Möglichkeit zur Herstellung einer konformationssensitiven Affinitätsmatrix bietet. Ebenso eröffnet die Interaktion die Möglichkeit der Kristallisation des Komplexes aus Nikotinsäurerezeptor, dem Agonisten Nikotinsäure und β-Arrestin 1. Jedoch war die Rekonstitution des Komplexes nicht quantitativ, und erfordert zusätzliche Erkenntnisse, über die Faktoren, die die Ausbildung des Komplexes bestimmen, um die angeführten Ziele letztendlich in die Tat umzusetzen. Ein hierbei augenscheinliches Problem stellt der oligomere Zustand des Rezeptors dar. Für eine Vielzahl von Rezeptoren [17-20], unter anderem Rhodopsin [6, 21], konnte gezeigt werden, dass sie in der Membran als Dimere vorliegen. Auch wurde im Falle von Rhodopsin gezeigt, dass diese Organisation durch Zugabe von Detergenz bis zur Solubilisierung aufgelöst wird. Da sich zusätzlich die Daten mehren, dass β-Arrestin das Rezeptordimer bindet [22, 23], muss die Suche nach Bedingungen, die zum einen den dimeren Zustand des Rezeptors konservieren, als auch die quantitative Bindung mit β-Arrestin verstärken, eines der dringendsten Ziele sein. Diese könnten dann zur Herstellung der oben genannten konformationssensitiven Affinitätsmatrix genutzt werden und die Kristallisation des Komplexes aus dem Nikotinsäurerezeptor NAR1, Nikotinsäure und β-Arrestin ermöglichen.

1 Introduction

1.1 Signal Transduction

"Life just wants to be there!" is a quote from Bill Bryson's Aventis-Prize for Science Books 2004 award winning book "A Short History of Nearly Everything" [24]. But living imposes certain requirements on every cell, the smallest living entity, and the building block of multi-cellular organisms. One of these requirements is certainly the capability to perceive environmental stimuli and react accordingly. The field of research dedicated to these processes is called signal transduction. The term was originally used by physical scientists and electronic engineers to describe the conversion of energy and information from one form into another. It first occurred in biological literature in 1974 and as a title word in 1979. Its widespread use was triggered by an important review by Martin Rodbell, published in 1980 [25]. He was the first to draw attention to the role of GTP and GTP-binding proteins in metabolic regulation and he deliberately borrowed the term to describe their role. By the year 2000, 12% of all papers using the term cell also employed the term signal transduction [25, 26].

The environmental stimuli a cell has to perceive are manifold, such as light, ions, gases like nitric oxide, small organic molecules such as biogenic amines, lipids or nucleotides, steroids and sugars to peptides and even entire proteins. Some of these signaling molecules can readily cross the cell's membrane and act within the cytoplasm on their cognate receptors, like the steroid hormones testosterone and cortisol that bind to steroid receptors and modulate transcription, or nitric oxide that binds to nitric oxide sensitive guanylate cyclase and changes its enzymatic activity. Other signaling molecules are either too hydrophilic or just too large to cross the cell membrane, and therefore need specific target receptors on the cell's surface, that translate the signal into the cell's own language. These molecules act predominantly on three classes of transmembrane receptors.

The first of these are the ligand-gated ion channels. They serve in the nervous system for the rapid conversion of a chemical signal into an electrical one. Neurotransmitters like acetylcholine, glutamate, γ-aminobutyricacid (GABA) or glycine bind to their cognate ion channel and lead to its opening or closing. The passage of ions into or out of the cell leads then to a change in the membrane potential.

The second class of transmembrane receptors is the family of receptor tyrosine kinases (RTKs). The roughly 60 members of this family identified to date can be further divided into 20 subfamilies, according to either a prototypic ligand or receptor [27]. They all share a common architecture, which is made up by an extracellular ligand binding domain, a single membrane spanning helix followed by a juxtamembrane region and a conserved intracellular protein tyrosine kinase domain as well as regulatory sequences. Most of their ligands are protein hormones. Hormone binding to the receptor leads to a clustering of monomeric forms, or the rearrangement of pre-existing dimers, juxtaposing the kinase domains for mutual phosphorylation, activation and initiation of downstream signaling.
Tyrosine phosphorylation within regulatory segments creates binding sites for proteins containing SH2 or PTB domains, and leads to passing the signal on to Phosphatidylinositol-3-Kinase, Phospholipase Cγ, the Ras- and MAPK-pathways or STAT proteins for example.

The third class of transmembrane receptors are G-protein coupled receptors (GPCRs) and are now discussed in more detail.

1.1.1 GPCRs

1.1.1.1 GPCR Evolution

The evolution of the 5 major classes of GPCRs in the human genome (Glutamate, Rhodopsin, Adhesion, Frizzled and Secretin) took place before the split of the nematode from the chordate linage, as has been shown by recent phylogenetic analyses [5, 8]. The large expansion in GPCR numbers is thought to have arisen from genome duplication events that occurred 650-350 million years ago in early chordate [28], or in two waves, the latter 430-80 million years ago, at the time of the mouse-human split and a first at the vertebrate-amphioxus split about 750-430 million years ago [8, 29]. Since that time GPCRs constitute the major class of transmembrane receptors. The nematode *Caenorhabditis elegans* has as many as 1149 predicted GPCRs [5], comprising 5% of its entire genome. Mammalian genomes are less dominated by GPCRs, although they still comprise the largest gene family. Mice have approximately 1318 predicted GPCRs [5], and there are 720-800 functional GPCRs found in the human genome, which accounts for about 2% of all its genes [4].
GPCRs are found throughout the eukaryotic kingdom (Figure 1), but not in prokaryotes [8].

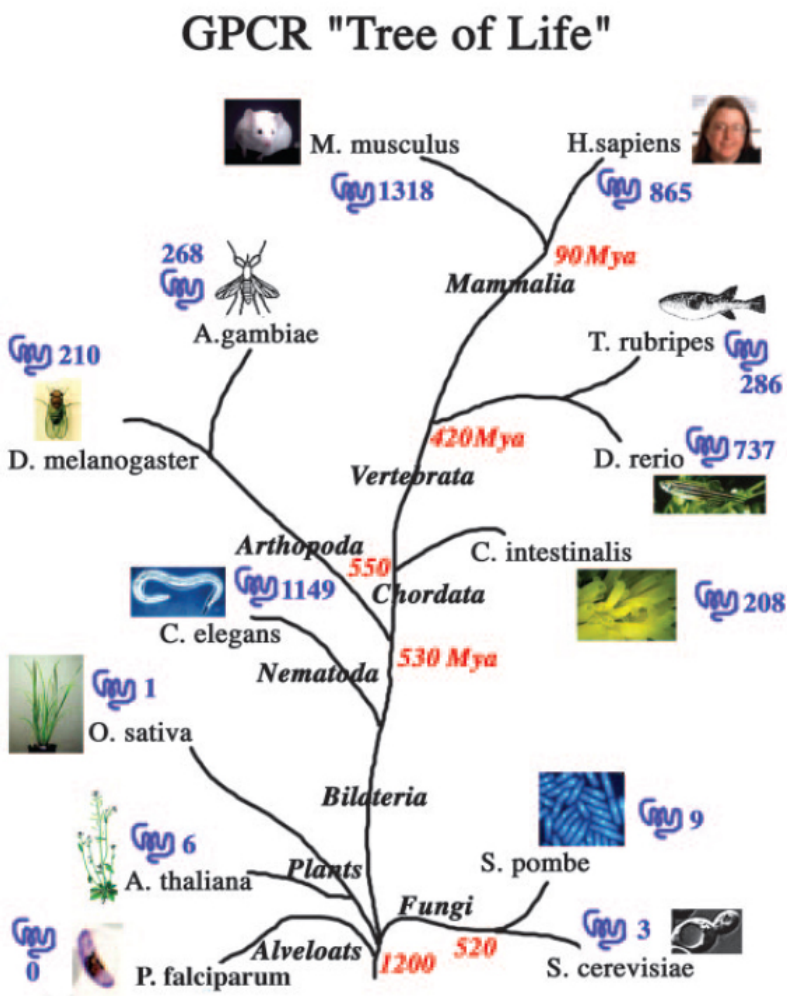

Figure 1: Phylogenetic GPCR tree of the different species. Numbers in red indicate the time in million years since the split at that node occurred. Blue GPCRs and numbers give the number predicted in this species, based upon [5], taken from [8].

1.1.1.2 GPCR Distribution among Species

Among the classes of transmembrane receptors, the GPCR superfamily is the largest [8]. They can be found in almost every eukaryotic organism, including plants [30], fungi and throughout the bilateria [5]. In yeast, only a few GPCRs are found. In the yeast *Saccharomyces cerevisiae* only three GPCRs have been described, including the yeast pheromone receptors (Ste2 and Ste3) and one of the *Adhesion*-family (Gpr1) being a sugar sensing receptor. Nine are found in the genome of *Schizosaccharomyces pombe*, and further ones have been found in the fungal pathogen *Cryptococcus neoformans*, among which is the amino acid methionine sensing Gpr4, which is coupled via the G-protein α subunit Gpa1 to the cAMP-PKA pathway. Other yeasts are able to grow in diverse environments and are therefore confronted with a wider

variety of environmental stimuli. They need to have extensive sensing and signaling capacities. In the genome of *Neurospora crassa* ten putative GPCRs have been identified, belonging to families of microbial opsins, pheromone receptors, glucose sensors, nitrogen sensors and one sharing similarity with sequences from *Dictyostelium discoideum*, in which four related cARs (cAMP receptors) sense cyclic AMP (cAMP) levels during multicellular development and sporulation. Similarity exists as well to predicted proteins in *Caenorhabditis elegans* and *Arabidopsis thaliana* [31].

Although a few proteins sharing the 7TM signature motif have been identified in plants, only one, the *Arabidopsis thaliana* Gcr1, shares similarity to a *Dictyostelium discoideum* cAMP receptor and has been shown to interact with the single Gα subunit Gpa1 of *A. thaliana* [32]. Nevertheless, it is not yet clear to what extent signaling occurs through heterotrimeric G-proteins and Gcr1's effect on seed germination is at least in part heterotrimeric G-protein independent [33].

1.1.1.3 GPCR Identification

GPCRs are characterized by a signature motif of seven transmembrane helices, and their functional coupling to a heterotrimeric G-proteins. With the availability of fully sequenced genomes of higher eukaryotes, the prediction of formerly unknown genes and putative GPCRs has become possible.

In the absence of high degrees of sequence similarity [34, 35] and functional data of G-protein coupling, GPCRs were predicted by the mere existence of seven stretches of 25 to 35 predominantly hydrophobic amino acids expected to form seven membrane-crossing α helices. The first helix is preceded by an extracellular N-terminus of varying size, and the seven transmembrane helices (TM1-7) spanning the lipid bilayer in alternating orientation are connected by hydrophilic loops, termed either extracellular loop (EL) 1-3 or intracellular loop (IL) 1-3 according to their appearance, alternating between the inside and the outside of the cell. The seventh helix is followed by a C-terminal tail, which frequently contains a palmitoylated cysteine residue. This initial ordering led to several synonyms for this protein superfamily, like 7-transmembrane receptors, heptahelical receptors and serpentine-like receptors [36].

1.1.1.4 Retinal Binding Proteins vs. GPCRs

Interestingly, the fold of seven helices criss-crossing the membrane not only occurs in GPCRs but as well in bacterial retinal-binding proteins and subunit III of the cytochrome *c* oxidase. With bacteriorhodopsin being the model protein for the class of bacterial retinal-binding proteins, and rhodopsin being the best studied GPCR and a retinal-binding protein as well, some confusion arose about the origin of GPCRs. However they are two functionally distinct groups of membrane proteins. Bacteriorhodopsin is a light-driven proton pump, having all-*trans*-retinal as a covalently bound chromophore which photo isomerizes upon light absorption to 13-*cis*-retinal. It is not involved in signal transduction. The GPCR in contrast binds an extracellular ligand and drives intracellular changes mediated by a heterotrimeric G-protein. There is though one GPCR, rhodopsin, that somehow belongs to both classes. It binds retinal and therefore belongs to the class of retinal-binding proteins. But on the other hand it couples light absorption of its chromophore 11-*cis*-retinal and photo isomerization to all-*trans*-retinal to the activation of the heterotrimeric G-protein transducin. Rhodopsin is the protein responsible for vision, and although it binds the same chromophore as the bacterial retinal-binding proteins, there is no homologue found in bacteria. Furthermore there is no obvious evolutionary relationship between these two proteins, regarding sequence similarities or gene organization. This was further demonstrated in 2000, when the structure of bovine rhodopsin [37] became available and was compared to the one of bacteriorhodopsin from 1997 [38]. It was found that the helices are arranged in a different way [39].

1.1.1.5 GPCR Classification

Human GPCRs have been classified in three main families based on their amino acid sequence. Family A consists of the rhodopsin-like receptors, and constitutes the largest and best studied family. It contains the opsins, olfactory GPCRs, small molecule and peptide hormone receptors as well as the glycoprotein hormone receptors (Figure 2A-C). Despite their low overall sequence homology, they are characterized by several highly conserved amino acids within the core of the seven transmembrane helix bundle. The only residue that is conserved among all family A GPCRs is the arginine residue within the highly conserved DRY motif at the cytoplasmic end of transmembrane helix 3 [40]. Apart from very few exceptions (melanocyte stimulating/adrenocorticotropic hormone (MSH/ACTH) and cannabinoid receptors), a disulfide bridge between conserved cysteine residues bridging extracellular loops one and two is also highly conserved. The high degree of conservation of

these residues implies that they are crucial for maintaining the structure and function of the receptor. In addition, most of them contain a palmitoylated cysteine in their intracellular cytoplasmic tail [41]. The binding of small molecules occurs within the core of the seven transmembrane helix bundle (Figure 2A) and that of peptides (Figure 2B) and glycoprotein hormones (Figure 2c) at the N-terminus, the extracellular loops and the loop proximal parts of the transmembrane helices [4].

The secretin-like family B receptors share none of the above mentioned characteristic features of family A receptors, with the exception of the disulfide bond bridging the first and second extracellular loop (Figure 2D). They are characterized by a relatively long N-terminal tail, in general about 100 amino acids, that contains three additional conserved disulfide bonds, forming a network and contributing to the globular domain structure which is, alongside with the seven juxtamembrane regions of the transmembrane helices, implicated in ligand binding. Like family A receptors, family B receptors share a number of conserved proline residues within the transmembrane segments, which are believed to be responsible for conformational dynamics of the receptor[4, 40]. Members of this family are the calcitonin, CGRP and CRF receptors, the PTH and PTHrP receptors, the glucagon, glucagon-like peptide, GIP, GHRH, PACAP, VIP, secretin receptors and the laxotroxin receptor [40].

Family C GPCRs are characterized by an extraordinarily long N-terminal tail (500-600 amino acids) and a long C-terminal tail (Figure 2E). The disulfide bridge between extracellular loops one and two is found in family C receptors too. Another characteristic element is a short third extracellular loop. A few of the conserved residues found in family A receptors are also conserved among family C receptors, indicating a common origin of these two families. The large N-terminal domain contains a cysteine rich domain (CRD) which links the transmembrane core to another domain that resembles bacterial periplasmic binding proteins. This so-called “venus flytrap” module contains the ligand binding site. For the metabotropic glutamate receptor, the crystal structures of the venus flytrap module have been solved in the liganded and unliganded state, showing a disulfide linked homodimer that undergoes considerable conformational rearrangement upon ligand binding [4, 40]. Family C contains the metabotropic glutamate receptors, the metabotropic GABA receptors, calcium receptors, vomeronasal receptors and the taste receptors.

A fourth family of receptors comprises the members of the frizzled-smoothened family, for which direct coupling to heterotrimeric G-proteins is still a matter of debate.

Despite the low overall homology between GPCRs, within each family and their 7 transmembrane core region, the families' members share in general more than 25% of sequence similarity.

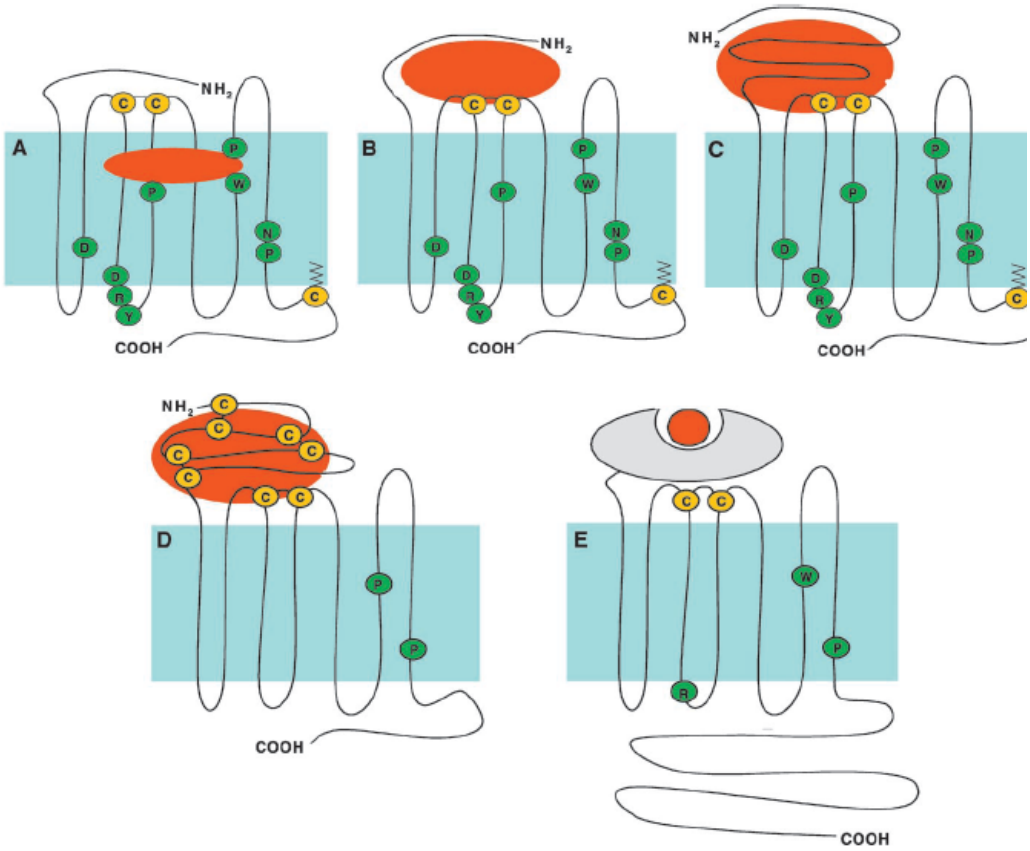

Figure 2: Classification of GPCRs in 3 main families. A-C depict variations of rhodopsin-like family A GPCRs, A. binding of small biogenic amine ligand; B. peptide binding GPCR and C. glycoprotein ligand (Ligand binding regions depicted in red). Highly conserved residues are displayed in green, and the conserved disulfide bond between ECL1 and ECL2 is given in yellow). D. Family B GPCRs and E. family C GPCRs. Taken from Jacoby et al., 2006 [4]

A further distinction has to be made among GPCRs according to the origin of their ligands [4]. On the one hand are the pheromone, odorant, tastant and light receptors as sensory receptors, responding to environmental stimuli and on the other are those that respond to endogenous ligands.

Of the 720-800 predicted human GPCRs about 380 have been identified as unique, functional and nonsensory. For these, endogenous ligands are either known or expected to be found.

These are referred to as *endo*-GPCRs that modulate various physiological functions. From a comparative analysis between mouse and human GPCR sequences, 367 were found in humans and 392 in mouse, with 343 present as homologues in both species [42]. Of these 367 human receptors 284 belong to the family A rhodopsin-like GPCRs, including 98 receptors without any known ligand, therefore termed orphan receptors. 50 belong to the family B secretin receptor-like GPCRs, 34 of which are orphan receptors, 17 to family C with 6 orphan receptors, and 11 to the frizzled/smoothened receptor-like family (F/S). In total, the human genome comprises 224 receptors with an identified ligand and 143 orphan receptors, for which the search of a ligand is still ongoing [42].

Due to recent phylogenetic analyses, a reclassification of the GPCRs in the human genome into five major groups has taken place. These groups are, as noted already above the Glutamate-, Rhodopsin-, Adhesion-, Frizzled/taste2- and Secretin-like groups, and the new system is called GRAFS. This new GRAFS system displays some differences to the A, B, C system outlined above. First, the adhesion receptors are formed by Family B receptors that have a long N-terminus forming adhesion molecule repeats like EGF domains. These are expressed in leukocytes and the nervous system and thought to be involved in cell-cell interactions. Second, the taste receptors have been subdivided into the glutamate group and the frizzled/taste2 group [43] [4].

1.1.1.6 GPCR Research History

The first GPCR that was purified was the β_2-adrenergic receptor in 1979 in Robert Lefkowitz's laboratory [44]. With the protein in hand and the identification of small peptide stretches, researchers at Merck were able to design oligonucleotide probes and identify and clone the β_2-adrenergic receptor gene from a hamster cDNA library [45]. The purification and the cloning the β_2-adrenergic receptor heralded the dawn of the molecular age of GPCR research. With the sequencing of the entire human genome, the identification of putative GPCRs has become fairly simple. Depending on the stringency of data mining methods, there are 720-800 GPCRs identified in the human genome, which comprises about 2 % of all open reading frames, making them the largest gene family therein [4]. And as large as their number is the diversity of the signals they respond to, reaching from photons in the case of rhodopsin, to extracellular endogenous chemical messengers like biogenic amines, purines and nucleic acid derivatives, lipids, peptides and proteins, ions like calcium, and protons to environmental stimuli like tastants, pheromones and odorants.

1.1.2 GPCR Signaling

1.1.2.1 Heterotrimeric G proteins

The name G Protein-Coupled Receptors stems from their ability to recruit and activate intracellular heterotrimeric G proteins composed of a guanosine nucleotide binding α-subunit (G_α) and a stable complex of a β and a γ subunit ($G_{\beta\gamma}$). Ligand binding to the receptor triggers conformational changes and rearrangement of the helix bundle that enable the receptor to act as a nucleotide exchange factor on the heterotrimeric G protein. The activated receptor induces a conformational change within the α-subunit of its associated heterotrimeric G protein, releasing GDP and thus allowing GTP to enter the now empty nucleotide binding site, GTP binding induces further conformational changes that distort the binding interface between G_α and $G_{\beta\gamma}$ which results in the dissociation of G_α and $G_{\beta\gamma}$. In its GTP-bound state the G_α-subunit is capable of activating downstream effector enzymes. The same is true for the $G_{\beta\gamma}$-complex [40]. G_α and $G_{\beta\gamma}$ are permanently localized to the cell membrane due to lipid anchors on G_α and G_γ, which locate them in the vicinity of receptors and effector enzymes.
The human genome contains at least 20 genes for α-subunits, 5 for β-subunits and 15 for γ-subunits. The α-subunits are further divided into 4 classes termed $G_{\alpha s}$, $G_{\alpha i}$, $G_{\alpha q}$ and $G_{\alpha 12}$. All theoretical combinations of G_α and $G_{\beta\gamma}$-complexes produces more than thousand possible heterotrimeric G Proteins. Although not all of them are known to exist *in vivo*, this potential demonstrates the incredible opportunities of diverse and flexible signaling inherent to GPCRs. This is further highlighted by reports, where receptors signal in a context specific manner through different G proteins. The β_2-adrenoreceptors signals upon initial ligand binding through G_s, activating adenylyl cyclase and in turn PKA. PKA phosphorylates residues within the third intracellular loop, and redirects signaling to G_i, which inhibits adenylyl cyclase. The fact that GPCRs may signal in a context specific manner through G_α-subunits with opposing effects on effector enzymes, and that $G_{\beta\gamma}$-complexes may oppose the effect of their G_α-subunit in a context specific manner, as $G_{\alpha s}$ stimulates but $G_{\beta\gamma}$ inhibits adenylyl cyclase, demonstrates the complexity of these signaling networks.

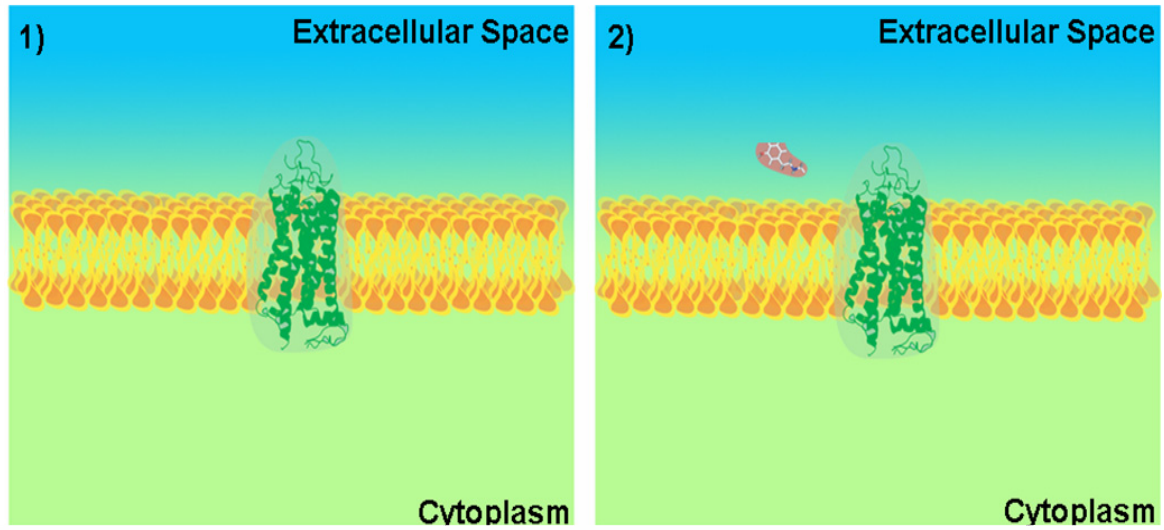

Figure 3: Classical Scheme of GPCR signaling: 1) GPCR (ribbon diagram of rhodopsin) resides in the membrane; 2) Ligand (here epinephrin) is present in the extracellular fluid;

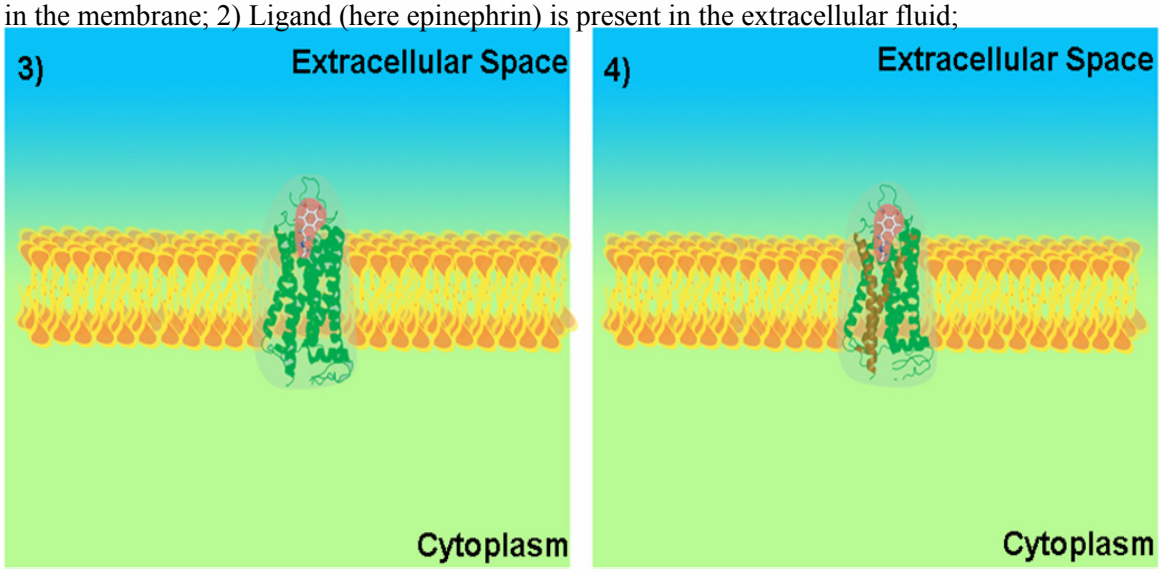

3) the ligand binds, and 4) activates the GPCR.

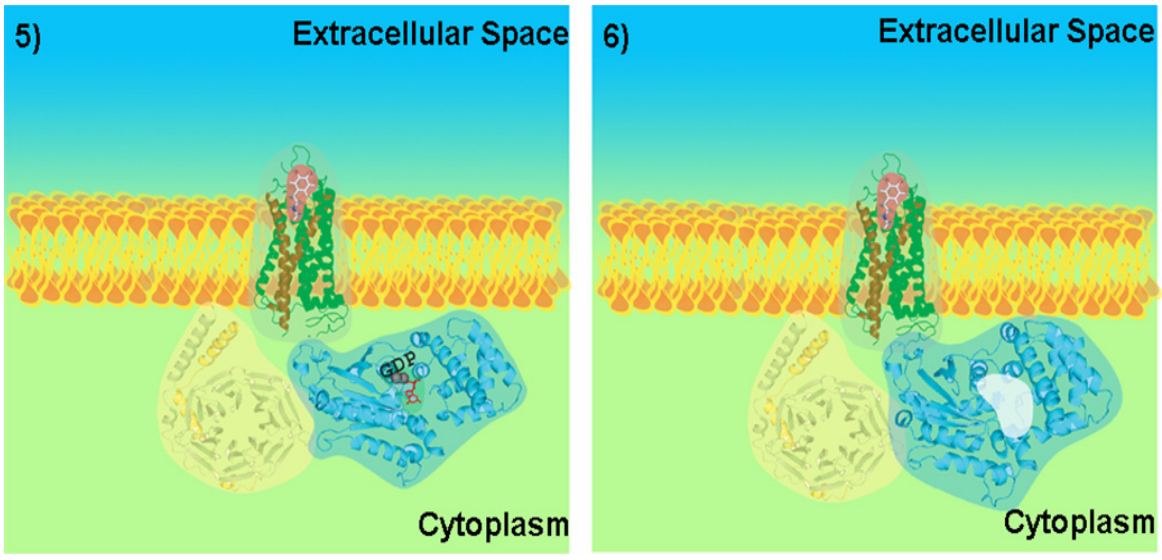

5) The heterotrimeric G protein, bound to GDP, is stimulated by the activated GPCR to release 6) GDP

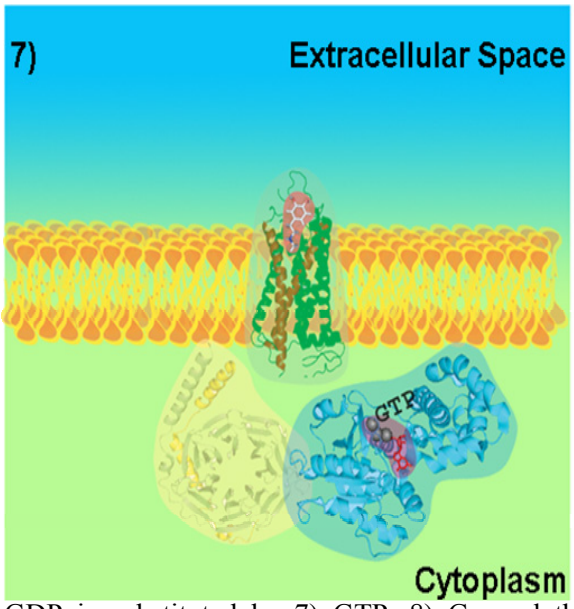

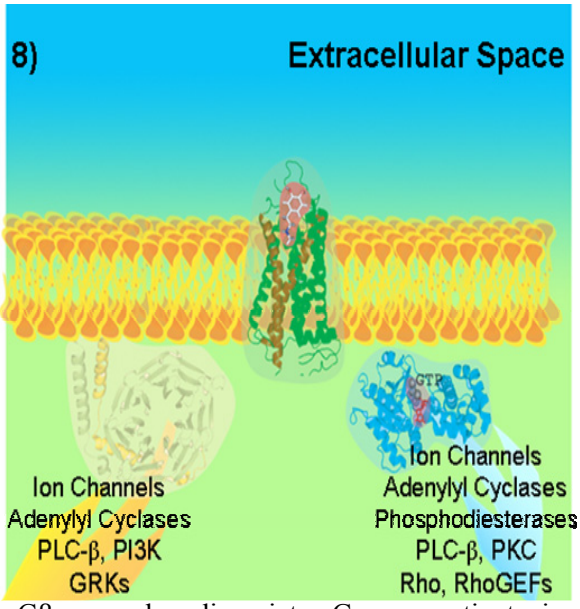

GDP is substituted by 7) GTP. 8) Gα and the Gβγ complex dissociate. Gα can activate ion channels, adenylyl cyclases, phosphodiesterases, PLC-β, PKC, DAG, Rho and RhoGEFs; the Gβγ complex acts on ion channels, adenylyl cyclases, PLC-β, PI3-K and GRKs.

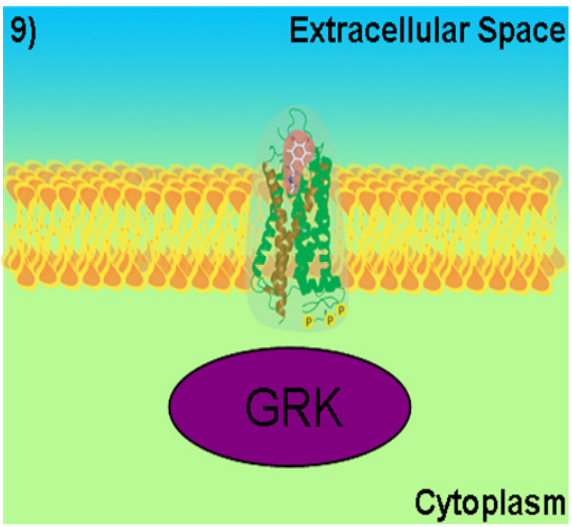

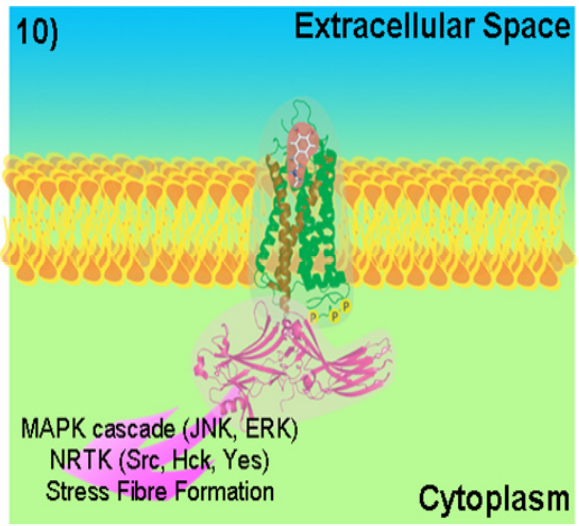

9) The GRK phosphorylates serine and threonine residues, leading to 10) arrestin recruitment. Arrestin can initiate signaling via the MAPK cascade, NRTKs and stress fiber formation.

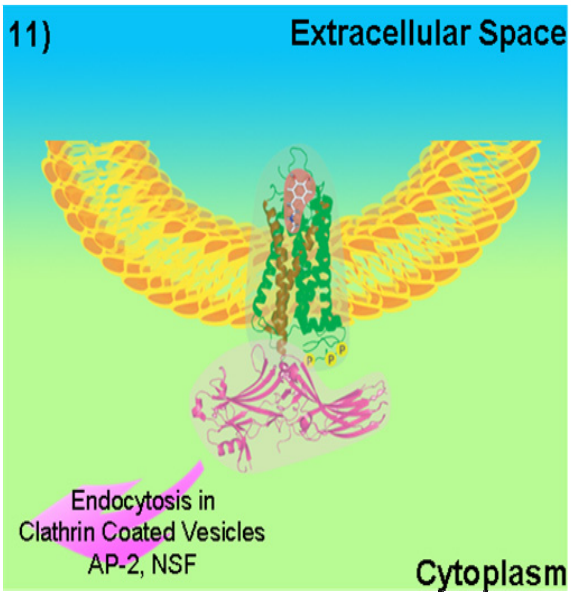

11) Finally the receptor is removed from the cell surface by endocytosis, mediated by interaction between arrestins, AP-2 and NSF.

PLC-β: Phospholipase Cβ; PKC: Protein kinase C; DAG: Diacylglycerol; Rho: a small G-protein; RhoGEFs: Rho Guanidine Exchange Factors; GRK: G-Protein Coupled Receptor Kinase; MAPK: Mitogen Activated Protein Kinase; NRTKs: Non-Receptor Tyrosine Kinases; AP-2: Adaptor Protein 2; NSF: N-maleimide sensitive factor.

1.1.2.1.1 Gα Subunits

- $G_{\alpha s}$-subunits are characterized by their upregulation of adenylyl cyclase, hence the name stimulatory, and drive the opening of Ca^{2+} channels. Furthermore, they are constitutively activated by Cholera toxin, which ADP ribosylates an arginine residue, permanently inactivating its intrinsic GTPase activity. This leads to a permanent activation of downstream effector enzymes without being stimulated by a hormone [46].
- $G_{\alpha i}$-subunits in contrast decrease Ca^{2+} influx through channels, but open potassium channels. In addition they inhibit the activity of adenylyl cyclase, which lead to the subscript $_i$ for inhibitory, and stimulate the activity of cGMP specific phosphodiesterase. Pertussis toxin ADP ribosylates a cysteine residue near the C-terminus, which prevents activation of the G-protein by the receptor, permanently blocking signal transmission. In the case of $G_{\alpha t}$ (transducin) cholera toxin deactivates as well the GTPase activity by arginine ADP ribosylation [46].
- $G_{\alpha q}$-subunits couple to phospholipase cβ in an activating manner, and they are not sensitive to pertussis toxin [46].
- $G_{\alpha 12}$-subunits use Rho specific nucleotide exchange factor proteins as downstream effector molecules and the GTPase activating protein RasGAP [46].

One thing that all G_α-subunits share is their low intrinsic GTPase activity, leaving G_α a long time in the activated GTP bound state. For example, k_{cat} values of GTP hydrolysis for $G_{\alpha t}$ are in the range of $0.05s^{-1}$. The relatively long time they remain in the activated state ensures the productive coupling to downstream effector molecule, which frequently act as GTPase-activating proteins (GAP), increasing the k_{cat} value of GTP hydrolysis up to two orders of magnitude, turning the signal off, once it is received by a downstream effector enzyme [46].

1.1.2.1.1.1 Effector Enzymes

Activated G proteins pass the ligand initiated signal on to enzymes or channels, which catalyze concentration changes of small diffusible signaling molecules called second messengers. Among these second messengers are cAMP, cGMP, diacylglycerol (DAG), inositol trisphosphate (IP_3) and Ca^{2+} ions.

- The first GPCR effector enzyme was adenylyl cyclase. It catalyzes the formation of 3'-5'-cyclic AMP (cAMP) from ATP. Its activity can be stimulated by $G_{\alpha s}$ *GTP,

Ca^{2+}/calmodulin, protein kinase C (PKC) and $G_{\beta\gamma}$-subunits, resulting in an increase of intracellular cAMP concentration, or inhibited by $G_{\alpha i}$ *GTP, Ca^{2+} and $G_{\beta\gamma}$-subunits causing the opposite effect. cAMP was the first second messenger to be discovered, and acts mostly through the activation of protein kinases. Kinases that are activated by cAMP are classified as protein kinase A (PKA). They exist in the cytosol as tetramers, composed of two regulatory subunits and two kinase subunits. Upon binding of cAMP to the regulatory subunits, the kinase subunits are released from the regulatory subunits and their inhibitory effect. Apart from the kinases, cAMP effects cAMP gated ion channels. cAMP binding on their cytoplasmic side results in their opening or closing. The effect of the adenylyl cyclases is opposed by an enzyme called phosphodiesterase, which degrades existing cAMP molecules, thus restoring the resting state level of cAMP.

- The second most prominent effector enzymes belong to the class of phospholipases Cβ. Phospholipases are enzymes that cleave off the headgroups of membrane lipids, and are differentiated according to their attack point on the lipid. Cleavage of phosphatidylinositol-4,5-bisphosphate (PIP_2) by phospholipase Cβ produces two second messengers. The first being inositol-1,4,5-trisphosphate (IP_3) and the second being diacylglycerol (DAG) [46].
- Inositol trisphosphate (IP3) mobilizes Ca^{2+} release from specific storage compartments in the ER and mitochondria. The free cytosolic Ca^{2+} concentration in resting cells is very low, about 10^{-7}M, compared to the high Ca^{2+} concentrations in specific compartments within the cytosol and in the extracellular space, which reach millimolar concentrations. IP_3 binds to the IP_3 Receptor that opens Ca^{2+}-channels, leading to efflux of Ca^{2+} ions from intracellular storage compartments, and giving rise to a steep increase in cytosolic Ca^{2+} concentrations. Ca^{2+} signals are three dimensional, according to time, space and concentration, and are deciphered by a wide variety of Ca^{2+} binding proteins within the cell's cytosol. Among the Ca^{2+} binding proteins within the cell, Calmodulin is outstanding. Upon Ca^{2+} binding it undergoes a structural rearrangement that allows it to bind further proteins. Members of the G-protein coupled receptor kinases, IP_3Receptors, protein kinases and phosphatases are targets of Ca^{2+}/calmodulin, which regulates their activity, thus affecting regulation of proliferation, mitosis, neuronal signal transduction, muscle contraction and glucose metabolism.

Diacylglycerol has at least two functions. First, it is an important source for the release of arachidonic acid, being a precursor in the prostaglandin biosynthesis, and second it stimulates the activity of protein kinase C (PKC) [46].

1.1.2.1.2 Gβγ-Complex

Although neglected as a competent partner in GPCR signaling for a long time, we now turn to the $G_{\beta\gamma}$-complex. Upon release from the G_{α}-subunit, previously masked interaction surfaces become available on the $G_{\beta\gamma}$-complex. A number of proteins that interact with and are regulated by the $G_{\beta\gamma}$-complex have been identified. Adenylyl cyclase, phospholipase C, potassium channels, Ca^{2+} channels, G-protein coupled receptor kinases (GRKs), phosducin, regulators of G protein signaling (RGS) and PI3-kinase (Phosphatidylinositol 3 kinase) type γ are some of them, and from that large array of interaction partners, the $G_{\beta\gamma}$-complex has evolved in our understanding from a previously passive partner to versatile contributor of GPCR signaling. Only one of its functions needs to be described here in more detail. The $G_{\beta\gamma}$-complex recruits the G-protein coupled receptor kinase (GRK) to the membrane, by exposure of an interaction surface, previously masked by the G_{α}-subunit. The GRK becomes activated by membrane recruitment and IP_3 and in turn phosphorylates serine and threonine residues within cytoplasmic loops and the C-terminal tail of activated receptors, rendering them incapable of activating further heterotrimeric G-proteins on the one hand, and creating a binding site for β-arrestin on the other hand.

1.1.2.2 Arrestins

Arrestins are proteins involved in the desensitization of GPCRs. Four arrestin genes have been identified in the human genome: two of them are expressed exclusively in the retina, the remaining two, called β-arrestin 1 and β-arrestin 2, are expressed ubiquitously. These two β-arrestins are thought to be involved in the downregulation of signaling of most non-visual GPCRs.

1.1.2.2.1 Desensitization and Endocytosis

Weakening of a long lasting GPCR signal is a process that is called desensitization. This effect is mediated by arrestins and was their classically attributed role. They function as

molecular coincidence detectors, scanning for activated receptor conformations and binding only to GRK phosphorylated receptors. In addition to decoupling the receptor from G proteins, they serve as a scaffold for the assembly of signaling complexes. Upon GPCR binding arrestins undergo a large conformational rearrangement and expose further binding sites for other proteins (Figure 4).

They redirect signaling to the MAPK pathway, by recruiting JNK, ERK or recruitment of non-receptor tyrosine kinases via a poly-proline SH3 interaction like c-Src and Hck. Arrestin serves also as scaffold for proteins of the endocytotic machinery like Clathrin, AP-2 and NSF [47]. By means of endocytosis, brought about by arrestins bridging receptors to endocytotic proteins, the receptor-ligand complex is sequestered from the plasma membrane. The receptor containing vesicles traffic to endosomes. Here the sorting machinery decides upon the receptor's fate of either being degraded by the lysosomal pathway, or being recycled back to the membrane. After disassembly of the clathrin coat and arrestin, dephosphorylation and removal of the ligand the receptor is ready for a new round of signal reception and transduction.

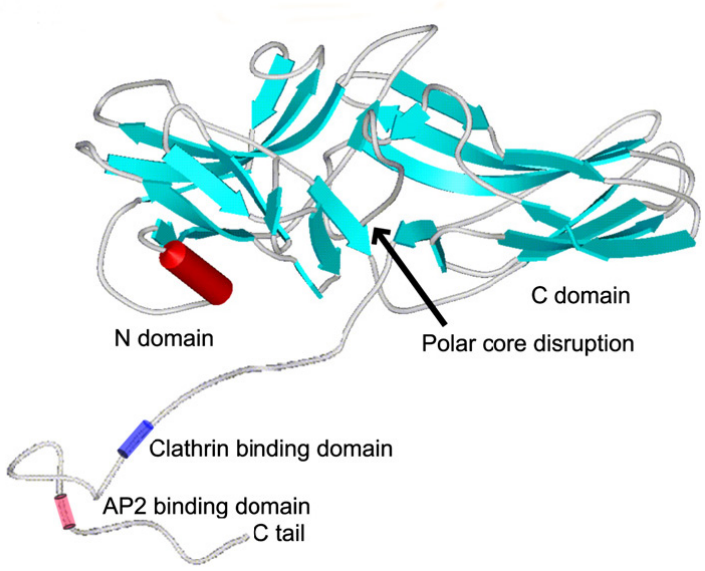

Figure 4: β-arrrestin structure: Active conformation of β-arrestin1, adapted from Xiao et. al. 2004 [3], showing the concave shaped N- and C-domain, and the released tail that contains peptide motifs for interaction with AP-2 and Clathrin. Figure taken from [7].

1.1.3 Dimerization

Another aspect of GPCR signaling that has recently come to close investigation is the phenomenon of dimerization. A number of GPCRs have been shown to form homo- or

heterodimers and complex receptosomes that incorporate in a context-dependent manner intra- and extracellular soluble proteins and other membrane proteins. For some receptors, dimerization is required for correct membrane transport [18], while for others modulation of ligand specificity has been reported, as well as negative and positive cooperativity [4, 17, 48]. Even the stoichiometry of the most important GPCR interactions is still a matter of debate. It was assumed that one GPCR interacts with one heterotrimeric G protein. However, evidence now accumulates that a large number of receptors exists as dimers, raising the question of whether a receptor dimer interacts with a single heterotrimeric G protein or with two of them. The same speculation exists for the interaction with arrestins. While most textbooks still show a complex of one rhodopsin molecule with either one heterotrimeric G protein or one arrestin molecule, a recent study suggested a model of a rhodopsin dimer interacting with one heterotrimeric G protein or one molecule of arrestin [6, 49].

1.1.4 GPCRs as Drug Targets

Long before the first GPCR was purified and sequenced, drugs were used in clinics that had GPCRs as targets, including β blockers, antihistamines, anticholinergics, analgesic opiates and neuroleptics. Abnormalities in GPCR signaling affects most tissues and organs in our body, and are the causative agents in disorders such as hyperfunctioning thyroid adenoma, precocious puberty, nephrogenic diabetes and color blindness [50]. Around 30% of today's marketed prescription drugs are directed against GPCRs, furthermore they comprise 30% of all drug targets investigated so far, rendering them the most successful therapeutic target family [4]. A wide variety of medical indications is covered by drugs targeting GPCRs. They are used in the treatment of allergies, hypertension, gastric ulcers, migraine, cancer, neurological pain, stroke, schizophrenia and asthma. In addition, they have been implicated in additional diseases and further medical indications. The human immunodeficiency virus (HIV) for example uses the chemokine receptors CCR5 and CXCR4 as co-receptors along with CD-4 to enter leukocytes [17]. Virally encoded GPCRs have been implicated in Kaposi's sarcomagenesis and atherosclerosis. The potential of drug development against GPCR targets seems to be inexhaustible [4].

1.1.4.1 Structure Based Drug Design for GPCRs

The high resolution structure of rhodopsin opened up the perspective of structure based drug design for GPCRs. Homology modeling techniques, in combination with ligand receptor

interaction data obtained by mutagenesis and the substituted-cysteine accessibility method allowed the discovery of new antagonists for the NK_1, the dopamine D3, the muscarinic M1 and the vasopressin V1a receptors for example[3, 51, 52]. Because the structure of rhodopsin is in the off-state, it can only be used as a model for the antagonist bound state, and virtual screening for agonists has been more complicated and less successful to date. Our understanding of how the transition to the active state is brought about and what it looks like is very limited. It is assumed that agonist induced activation of GPCRs disrupts an ionic lock between transmembrane helices three and six, resulting in a separation of these two helices accompanied by a twist of the latter. This results in an opening of the seven helix bundle. The rearrangement of the helices exposes the cytoplasmic end of helices two, three, six and seven, with the cytoplasmic ends of helices four and five retracted into the membrane. The intrinsic thermodynamic constraints and the limited conformational entropy imposed on the receptor by folding are overcome by these agonist-induced perturbations [50]. As mentioned above, dimerization is becoming more and more an issue in GPCR research, and it is not yet clear how that fits into this picture. A recent study supported by molecular modeling described how the G Protein Transducin binds Rhodopsin dimers and tetramers [6, 21]. Another study on the leukotriene B4 BLT1 receptor suggests the formation of a pentameric complex consisting of two receptor molecules and one heterotrimeric G Protein [53]. But still we know very little about how an activated GPCR looks, and how it interacts with the heterotrimeric G Proteins and Arrestins. Given the fact, that it is already becoming feasible not only to drug active sites of proteins, but also protein-protein interfaces by small molecules, as demonstrated for the interface between a $G_{\beta\gamma}$-complex and Phospholipase Cβ2 or PI-3Kinase γ, we need to know more about the interaction of GPCRs and their effectors [54, 55].

1.2 Crystallization of Membrane Proteins

A full understanding of how GPCRs work will require more high resolution structures of GPCRs, not just one the one of rhodopsin in the inactive state. It will require structures of multiple receptors bound to different ligands, agonists, partial agonists, inverse agonists and antagonists, and further it will require complex structures of receptors interacting with their modulators and downstream effectors like G proteins or arrestin. A systematic approach, improving expression, purification and crystallization and joining X-ray crystallography and NMR spectroscopy will eventually lead to a structural understanding of GPCRs and their modes of signaling [4]. Unfortunately the elucidation of membrane protein structures has been

tricky. Despite the fact that membrane proteins make up 30% of all open reading frames in the genome of every cell, the number of their structures in the protein data base are underrepresented. This is due to the amphipathic surface of membrane proteins. They are designed to integrate into the hydrophobic interior of the lipid bilayer and simultaneously protrude out into a hydrophilic environment, resulting in an amphipathic surface. This dual nature of their surface makes them difficult to handle in a standard biochemical aqueous buffer system, and to accommodate them in solution, the use of surfactants or detergents has been established. Typical detergents are small amphipathic molecules with a hydrophilic headgroup and a hydrophobic hydrocarbon tail that form spherical or elliptic aggregates capable of shielding the hydrophobic surface of a membrane proteins' transmembrane domain, thus preventing their aggregation by unspecific hydrophobic interactions. Despite the fact that in some cases the suitability of detergents for the purpose of membrane protein handling was questioned because of their destabilizing effect, alternatives like lipid cubic phases and amphipols are being developed, but are still in their infancy. Therefore the method of choice in membrane protein biochemistry remains the use of detergents and dealing with the requirements they impose. A detergent solubilized membrane protein carries a detergent micelle around its transmembrane domain like a life belt. The bigger the hydrophilic domains, the further they extend away from the micellar life belt and the more likely is the occurrence of protein-protein contacts and their potential arrangement in a crystal lattice. Membrane proteins with limited polar surfaces, like class A GPCRs, have less mass to extend out of the detergent micelle and are therefore harder to crystallize. One method to overcome this obstacle is the use of antibody fragments (Figure 5).

Proteolytically produced F_{ab}- or recombinant F_v–fragments can bind to the hydrophilic portion of a membrane protein with high affinity and reach out of the detergent micelle, extending the polar surface and allowing the formation of stable crystal contacts. A number of membrane proteins have been crystallized due to this method, like the cytochrome *c* oxidase [56], the *bc*1 complex [57] and KcsA [58]. The crystal lattice is clearly brought about by the antibody fragments outreaching the detergent micelle. Further advantages of the use of antibody fragments are their potentially stabilizing effect on the conformation of the protein and providing a simple immuno-affinity purification method [1, 59]. However, raising conformationally sensitive antibodies that bind with high affinity without adversely affecting protein functionality is a difficult and time consuming task.

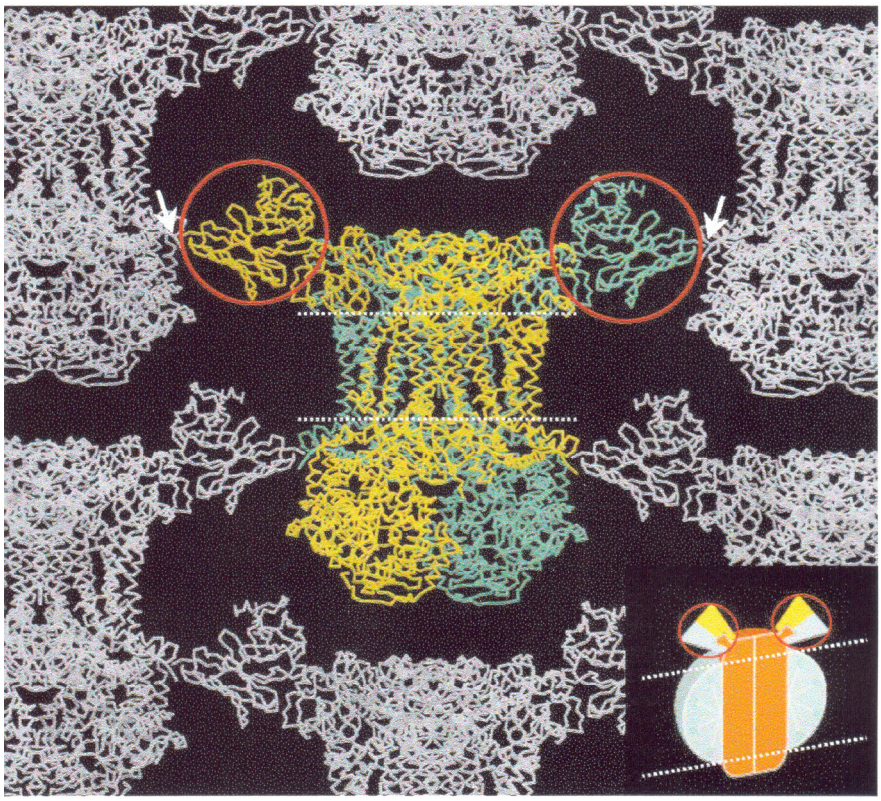

Figure 5: Crystal Packing is mediated by an antibody fragment in the crystallization of the bc1 complex [1].

1.3 Nicotinic Acid Receptor

1.3.1 Nicotinic Acid in Clinical Use

Nicotinic acid (Niacin) belongs to the water-soluble vitamin B complex. Alongside its effect of being a vitamin, it was discovered more than 50 years ago by Robert Altschul *et al.* [11] that nicotinic acid could modify lipoprotein profiles in humans. Roughly ten years later, in 1963, Carlson and coworkers found that nicotinic acid inhibits lipolysis in adipose tissue, resulting in a rapid decrease of free fatty acid levels in blood plasma. After a delay of approximately one day, it is followed by a decrease of triacylglycerol (TAG), very-low-density lipoprotein (VLDL) and low-density lipoprotein (LDL) cholesterol levels and accompanied by an increase in high-density lipoprotein (HDL) and HDL cholesterol concentration. Soon after these observations, nicotinic acid was introduced into clinics as the first antidyslipidemic drug. In the Coronary Drug Project and its follow-up study, it was shown that nicotinic acid, administered in oral doses (1.5-3.0 g/day) reduced myocardial infarction and had a beneficial effect on mortality respectively [60, 61]. Unfortunately, the

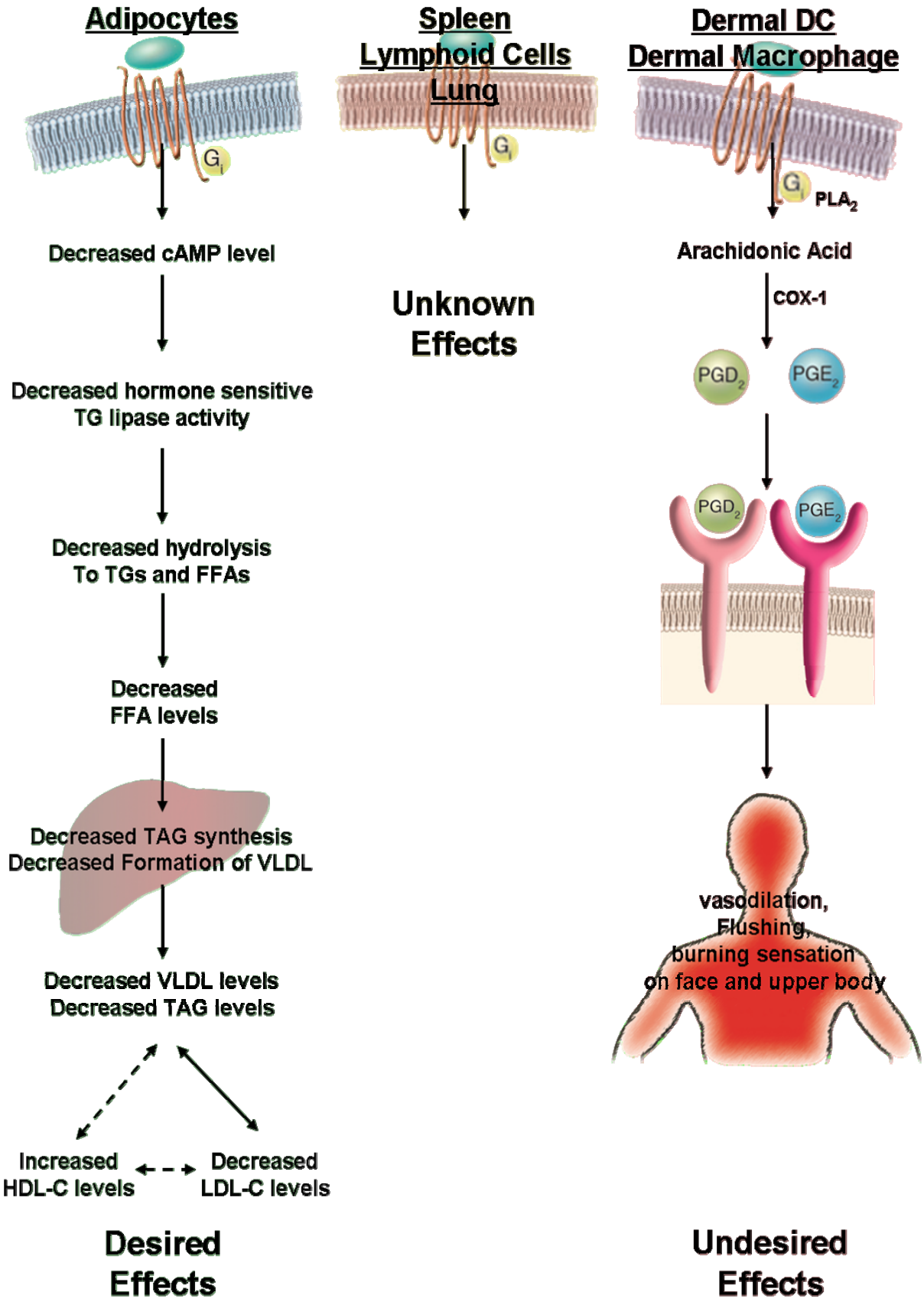

Figure 6: Physiological effects of nicotinic acid on different types of tissues, create desired effects in adipocytes and undesired effects in dermal dendritic cells and dermal macrophages. Adapted from [2] and [9]

administration of nicotinic acid is accompanied by side effects including rashes of the skin and a burning sensation in the upper body. These side effects, although harmless, reduce the compliance of patients dramatically.

1.3.2 Discovery of the Nicotinic Acid Receptor

Although the existence of a GPCR for nicotinic acid had been proposed long before, it was only in 2003 that three research groups independently cloned the human gene for the nicotinic acid receptor, called HM74A (GPR109A) [14-16]. HM74A turns out to be the high affinity receptor for nicotinic acid, while two closely related genes, both located in close proximity on chromosome 12q24.31, and called HM74 (GPR109B) and GPR81 only bind nicotinic acid with low affinity or not at all, respectively. The sequence similarity between HM74A and HM74 is 96%, and the similarity to GPR81 is 64%. The high degree of similarity in these GPCR genes suggests a fairly recent gene duplication, especially for HM74 and HM74A. The ortholog mouse receptor termed PUMA-G (Protein Upregulated in Macrophages by Interferon-γ), shares 82% sequence similarity with HM74A.

1.3.3 Nicotinic Acid Receptor Drugs

Currently, two compounds that mimic the effect of nicotinic acid are marketed: one is called Acipimox, which is selective for HM74A (GPR109A, NAR1) and PUMA-G, and does not activate HM74 (GPR109B), while the other one, Acifran is an agonist for both receptors. No ligand that activates GPR81 has been described, and so it still waits for its deorphanization.

1.3.4 Nicotinic Acid Receptor Expression and Signaling

The nicotinic acid receptor is expressed preferentially in adipocytes, spleen, lymphoid cells, lung, dermal dendritic cells and dermal macrophages (Figure 6). It couples to G proteins of the $G_{\alpha i}$ family. In adipocytes, the result is a decrease in cytosolic cAMP levels, which in turn inhibits PKA and results ultimately in the dephosphorylation of hormone sensitive triglyceride lipase, reducing its activity. The hydrolysis of triglycerides and free fatty acids from storage fat is thereby abolished. The antilipolytic effects brought about by the treatment with nicotinic acid results in increased HDL (“good cholesterol”) levels in plasma, while the plasma levels of “bad cholesterol”, VLDL and LDL, are decreased.

Unfortunately, on bone marrow derived cells like dermal dendritic cells and dermal macrophages, the result of stimulation of the nicotinic acid receptor is different. Activation of $G_{\alpha i}$ in cells of this origin raises intracellular Ca^{2+} levels, which in turn activates phospholipase A_2 that liberates arachidonic acid from membrane lipids. Arachidonic acid is subsequently converted by cyclooxigenase 1 (Cox1) into prostanoids like prostaglandin D2 (PGD2) and prostaglandin E2 (PGE2). PGD2 and PGE2 mediate in an auto- and paracrine fashion the stimulation of Prostaglandin D2- (DP), prostaglandin E2- (EP2) and prostaglandin E4- (EP4) receptors leading to cutaneous vasodilation, which evokes flushing and the sensation of burning on the face and in the upper body. How nicotinic acid affects other tissues like spleen, lymphoid cells and lung is not yet known (Figure 6).

1.3.5 Physiological Ligand

Nicotinic acid levels in plasma never reach concentrations that are required for the activation of HM74A (GPR109A). Despite the fact that this receptor was deorphanized by finding its activation by agonists such as nicotinic acid, Acifran and Acipimox, the physiological ligand remains to be discovered. Recent data have suggested D-β-hydroxybutyrate as a potential physiological ligand [62].

D-β-hydroxybutyrate, acetoacetate and acetate are small water-soluble carboxylic acids and belong to the group of ketone bodies. During starvation, storage fat in adipose tissue is released and transported to the liver via the blood stream. Hepatic breakdown of free fatty acids and synthesis of ketone bodies from acetyl-CoA derived from β-oxidation is an important energy source for the brain and other tissues during prolonged fasting. Serum levels are usually around 50 μM after a meal and reach overnight to levels of up to 400 μM. Upon prolonged fasting, D-β-hydroxybutyrate levels plateau at ~6-8 mM. Hepatic formation of ketone bodies is at least in part limited by lipolysis in adipose tissue. Activation of GPR109A by D-β-hydroxybutyrate at millimolar concentrations could represent a negative feedback-loop to prevent ketoacidosis, by exerting an antilipolytic effect and controlling the rate of free fatty acid release during starvation.

1.4 Aim of the Project

The aim of this PhD project was to find a means for the supply of large quantities of the human GPCR HM74A/GPR109A which has a low abundance in native tissues and is an important drug target. This ought to be accomplished by the heterologous overexpression in the methylotrophic yeast *Pichia pastoris*. The produced protein material had to be functionally characterized whether it resembles activity profiles of the receptor in native tissues. Upon characterization a way for the large scale production of the receptor should be found, to supply enough material suitable for structural studies and eventually future crystallization trials, with the ultimate goal of structure determination. Therefore the receptor should be solubilized by detergent and purified while its activity is to be carefully monitored to preserve it in an active and native-like state.

A second aspect of this project was to find a native binder, which interacts with the GPCR HM74A/GPR109A tightly and could potentially substitute for Fv fragments in the crystallization process. Therefore its interaction with β-arrestins had to be shown *in vivo*. Upon that they needed to be overexpressed and purified, thereby comparing the two heterologous host organisms *P. pastoris* and *E. coli*. Finally the complex of β-arrestin and HM74A/GPR109A in its active conformation with nicotinic acid bound should be reconstituted *in vitro* and evaluated regarding the possibility of crystallizing this complex.

2 Material & Methods

2.1 Chemicals

2.1.1 General Chemicals

All chemicals that were used in this work that are not listed below were either purchased from Sigma-Aldrich Chemie GmbH, Steinheim, Germany, Carl Roth GmbH &Co, Karlsruhe, Germany (depicted Roth below) or AppliChem, Darmstadt, Germany in ultra pure quality, p.a. grade.

a-Cyano-3-hydroxy cinnamic acid	Bruker Daltonic GmbH, Bremen, Germany
Acifran	Sanofi-Aventis Deutschland GmbH
Acipimox	Sanofi-Aventis Deutschland GmbH
Acrylamide ready.made solutions for polyacrylamide gels 40 and 30% (37.5:1)	Roth, Karlsruhe, Germany
Agarose, Seakem LE, for electrophoresis	Cambrex BioScience Inc., Rockland, ME USA
Asolectin	Sigma, Steinheim, Germany
Ammonium-persulfate	Sigma, Steinheim, Germany
Ampicillin, sodium salt	Sigma, Steinheim, Germany
Bacto agar, Difco	Becton, Dickinson and Co., Sparks, MD, USA
Bacto tryptone, Difco	Becton, Dickinson and Co., Sparks, MD, USA
Bacto yeast extract, Difco	Becton, Dickinson and Co., Sparks, MD, USA
Biotin	Roth, Karlsruhe, Germany
Bovine Serum Albumin (BSA)	Sigma, Steinheim, Germany
BCIP (5-Bromo-4-chloro-3-indolylphosphate, 4-toluidine salt	MBI Fermentas GmbH, St. Leon-Rot, Germany
β-Cyclodextrin	Sigma, Steinheim, Germany
Cholesteryl hemisuccinate (CHS)	Sigma, Steinheim, Germany
Coomassie Brilliant Blue R-250	Serva Electrophoresis GmbH, Heidelberg, Germany
Deoxynucleoside-5'-phosphates (dNTPs) (supplied with AccuPrime)	Invitrogen GmbH, Karlsruhe, Germany
DMF	Roth, Karlsruhe, Germany

DMSO (Dimethyl sulfoxide)	Roth, Karlsruhe, Germany
DTT	Biomol Feinchemikalien GmbH, Hamburg
Ethidium-bromide	Bio-Rad Laboratories GmbH, Munich
EDTA(ethylenediaminetetratacetic acid, disodium salt)	Roth, Karlsruhe, Germany
G418, Geniticin sulfate	Calbiochem, Merck Bioscience, Darmstadt, Germany
Glass beads (0.5mm)	Euler, Frankfurt am Main, Germany
Glycine	GERBU Biotechnik GmbH, Gaiberg, Germany
Glutathione (reduced)	Sigma, Steinheim, Germany
HEPES	Roth, Karlsruhe, Germany
Imidazole	Roth, Karlsruhe, Germany
Isopropanol	Roth, Karlsruhe, Germany
IPTG (Isopropyl-β-D-thiogalactoside)	Sigma, Steinheim, Germany
Kanamycin	Roth, Karlsruhe, Germany
Leupeptin	Biomol Feinchemikalien GmbH, Hamburg
Methanol, p.a.	Roth, Karlsruhe, Germany
Milk powder, non-fat	Roth, Karlsruhe, Germany
Nicotinic acid	Sigma, Steinheim, Germany
NBT (Nitrobluetetrazolium, toluidine salt)	Biomol Feinchemikalien GmbH, Hamburg
Pepstatin A	Biomol Feinchemikalien GmbH, Hamburg
Peptone	Sigma, Steinheim, Germany
PMSF (Phenylmethylsulfonylfluoride)	Roth, Karlsruhe, Germany
Polyethyleneimine (PEI)	Sigma, Steinheim, Germany
Scintillation mix Rotiszint eco plus	Roth, Karlsruhe, Germany
Streptavidin PVT SPA Scintillation Beads	GE Healthcare Europe GmbH, Munich, Germany
Streptavidin YSi SPA Scintillation Beads	GE Healthcare Europe GmbH, Munich, Germany
TEMED (N,N,N'N'-tetramethylethylendiamine)	Sigma, Steinheim, Germany
Tris-(hydrooxymethyl)-aminomethane	Roth, Karlsruhe, Germany
Tween 20	New Brunswick Scientific Deutschland GmbH, Nürtingen, Germany

Yeast Nitrogen Base (YNB), w/o amino acids, with ammonium sulphate, Difco	Becton, Dickinson and Co., Sparks, MD, USA

2.1.2 Labeled Chemicals

[^{3}H]-nicotinic acid	BioTrend, Cologne, Germany
[^{14}C]-nicotinic acid	BioTrend, Cologne, Germany
[^{15}N] NH_4Cl	EURISO-TOP GmbH, Saarbrücken, Germany
[^{15}N] NH_4SO_4	EURISO-TOP GmbH, Saarbrücken, Germany
[^{2}H]-Glycerol	EURISO-TOP GmbH, Saarbrücken, Germany
1,2-Dimyristoyl-*sn*-Glycero-3-Phosphoethanolamine-N-(Lissamine Rhodamine B Sulfonyl) (Ammonium Salt) (14:0 Lissamine Rhodamine PE)	Avanti Polar Lipids, Inc., Alabaster, AL, USA
Oregon Green ® 488 1,2-dihexadecanoyl-sn-glycero-3-phosphoethanolamine (Oregon Green ® 488 DHPE)	Molecular Probes Europe BV, Leiden, The Netherlands

2.1.3 Detergents

n-octyl-β-D-glucopyranoside (OG)	Glycon Biochemicals, Luckenwalde, Germany
n-nonyl-β-D-glucopyranoside (NG)	Glycon Biochemicals, Luckenwalde, Germany
n-decyl-β-D-glucopyranoside (DG)	Glycon Biochemicals, Luckenwalde, Germany
n-decyl-β-D-maltopyranoside (DM)	Glycon Biochemicals, Luckenwalde, Germany
n-undecyl-β-D-maltopyranoside (UM)	Glycon Biochemicals, Luckenwalde, Germany

n-dodecyl-α-D-maltopyranoside (α-LM)	Anatrace, Maumee, OH, USA
n-dodecyl-β-D-maltopyranoside (LM)	Glycon Biochemicals, Luckenwalde, Germany
C12E9 (nonaethylene glycol monodecyl ether)	Sigma, Steinheim, Germany
Cymal-6 (Cyclohexyl-hexyl-β-D-maltopyranoside)	Anatrace, Maumee, OH, USA
Digitonin	Sigma, Steinheim, Germany
Laurylsucrose (LS) (n-Dodecanoylsucrose)	Calbiochem, Merck Bioscience, Darmstadt Germany
CHAPS (3-[(3-cholamidopropyl)-dimethylammonio]-1-propane sulfonate)	Sigma, Steinheim, Germany
FOS-Choline 12 (FOS-12) (N-dodecylphosphocholine)	Synphabase AG, Muttenz, Switzerland
FOS-Choline 14 (FOS-14) (N-tetradecylphosphocholine)	Synphabase AG, Muttenz, Switzerland
FOS-Choline 16 (FOS-16) (N-hexadecylphosphocholine)	Synphabase AG, Muttenz, Switzerland
LDAO (n-dodecyl-N,N-dimethylamine-N-oxide)	Fluka Chemie GmbH, Buchs, Switzerland
Zwittergent 3-12 (N-Dodecyl-N,N-dimethyl-3ammonio-1-propanesulfonate)	Sigma, Steinheim, Germany
Cholate (sodium salt)	Sigma, Steinheim, Germany
SDS (sodium-dodecyl-sulfate)	Sigma, Steinheim, Germany

2.1.4 Columns, Chromatographic Matrices & Prepacked Columns

Polypropylene Columns, 2 ml with glass frits	Pierce Laboratories GmbH, Munich, Germany
Polypropylene Columns, 5 ml with glass frits	Pierce Laboratories GmbH, Munich, Germany
Liquid Chromatography Columns, Luer Lock, non-jacketed, 2.5 cm x 10 cm	Sigma, Steinheim, Germany
Liquid Chromatography Columns, Luer Lock, non-jacketed, 1.0 cm x 20 cm	Sigma, Steinheim, Germany
Immobilized Monomeric Avidin	Pierce Laboratories GmbH,

	Munich, Germany
Ni-NTA agarose	Qiagen GmbH, Hilden, Germany
Glutathione Sepharose 4B	GE Healthcare Europe GmbH, Munich, Germany
HisTrap HP, 1 ml	GE Healthcare Europe GmbH, Munich, Germany
DEAE Sepharose™ FastFlow, 1 ml	GE Healthcare Europe GmbH, Munich, Germany
Q Sepharose™ FastFlow, 1 ml	GE Healthcare Europe GmbH, Munich, Germany
ANX Sepharose™ 4FastFlow, 1 ml	GE Healthcare Europe GmbH, Munich, Germany
SP Sepharose™ FastFlow, 1 ml	GE Healthcare Europe GmbH, Munich, Germany
CM Sepharose™ FastFlow, 1 ml	GE Healthcare Europe GmbH, Munich, Germany
HiTrap Blue HP, 1 ml	GE Healthcare Europe GmbH, Munich, Germany
Superdex 75 10/30GL	GE Healthcare Europe GmbH, Munich, Germany
Superose 6 PC 3.2/30	GE Healthcare Europe GmbH, Munich, Germany
HiTrap Heparin HP, 5 ml	GE Healthcare Europe GmbH, Munich, Germany
Bio-Gel P60-Gel	Bio-Rad Laboratories GmbH, Munich, Germany
Bio-Gel P100-Gel	Bio-Rad Laboratories GmbH, Munich, Germany

2.1.5 Antibodies

M2 anti-FLAG antibody (Mouse)	Sigma, Steinheim, Germany
Anti-polyhistidine antibody (Mouse)	Sigma, Steinheim, Germany
Streptavidin, alkaline phosphatase conjugated	Promega GmbH, Mannheim, Germany

Anti-Mouse alkaline phosphatase conjugated	Sigma, Steinheim, Germany
Goat Anti-Mouse IgG G 12nm	Dianova, Hamburg, Germany

2.1.6 Enzymes

*Bam*HI	MBI Fermentas GmbH, St. Leon-Rot, Germany
*Bgl*II	New England Biolabs GmbH, Schwalbach, Germany
*Eco*RI	MBI Fermentas GmbH, St. Leon-Rot, Germany
*Not*I	New England Biolabs GmbH, Schwalbach, Germany
*Pme*I	New England Biolabs GmbH, Schwalbach, Germany
AccuPrime *Taq* Polymerase	Invitrogen GmbH, Karlsruhe, Germany
CIAP (Calf Intestine Alkaline Phosphatase)	MBI Fermentas GmbH, St. Leon-Rot, Germany
Quick Ligase	New England Biolabs GmbH, Schwalbach, Germany
Endo-H (Endoglycosidase H)	New England Biolabs GmbH, Schwalbach, Germany
PNGase F	New England Biolabs GmbH, Schwalbach, Germany
Lysozyme	Sigma, Steinheim, Germany
Benzonase	Merck KgaA, Darmstadt, Germany

2.1.7 Kits & Markers

Qiagen PCR purification kit	Qiagen GmbH, Hilden, Germany
Qiagen gel excision kit	Qiagen GmbH, Hilden, Germany
Qiagen plasmid miniprep kit	Qiagen GmbH, Hilden, Germany
BCA protein assay kit	Interchim, Montluçon, France
Prestained protein marker, broad range	New England Biolabs GmbH,

	Schwalbach, Germany
Prestained Seeblue+2	Invitrogen GmbH, Karlsruhe, Germany
Gene Ruler DNA Ladder Mix	MBI Fermentas GmbH, St. Leon-Rot, Germany
λ *Eco*RI/*Hind*III 3	MBI Fermentas GmbH, St. Leon-Rot, Germany

2.1.8 Filters, Membranes & Concentrators

Cellulose acetate 0.2 µm filters	Satorius, Göttingen, Germany
Amicon Ultra-4/15 (30/50 kDa) Concentrators	Millipore GmbH, Schwalbach, Germany
Gel blotting paper	Schleicher & Schuell BioScience GmbH, Dassel, Germany
GF/C filters for binding assay	Whatman International LtD, Maidstone, UK
1.2 µm membranes RA	Millipore GmbH, Schwalbach, Germany
0.45 µm membranes HA	Millipore GmbH, Schwalbach, Germany
Prefilters AP25	Millipore GmbH, Schwalbach, Germany
PVDF membrane	Millipore GmbH, Schwalbach, Germany
RED Devices	Pierce Laboratories GmbH, Munich, Germany
Sterivex GP 0.22 µm 2L	Millipore GmbH, Schwalbach, Germany
Sterile Filters Filtropur 0.22 µm	Sarstedt, Nümbrecht, Germany
Nitrocellulose membrane	Schleicher & Schuell BioScience GmbH, Dassel, Germany
ZelluTrans/ Roth Dialysis Membranes T1 MWCO 4000-6000	Roth, Karlsruhe, Germany

2.1.9 Buffers & Solutions

Agarose gel (1 %)	1 g Agarose 100 ml 1x TAE buffer 2.5 µl Ethidium bromide (10 mg/ml)
TAE buffer (50x)	2 M Tris/HCl 1 M Acetic Acid 50 mM EDTA

Loading buffer 6x (DNA)	30 mM EDTA
	0.036 % (w/v) Xylene cyanol
	0.03 % (w/v) Bromophenol blue
	30 % Glycerol
Ampicillin Stock Solution	100 mg/ml inH_2O (filter sterilized, stored at -20 °C)
AP buffer	100 mM Tris/HCl, pH 9.5
	100 mM NaCl
	5 mM $MgCl_2$
APS	10 % (w/v) in H_2O
BCIP-Solution	50 mg/ml in DMF (stored at -20°C)
Pre-Soak buffer	50 mM Tris/HCl pH 7.4
	0.3 % PEI (v/v)
Binding buffer (1x)	50 mM Tris/HCl, pH 7.4
	1 mM $MgCl_2$
	0.02 % CHAPS (w/v)
Binding buffer (5x)	250 mM Tris/HCl, pH 7.4
	5 mM $MgCl_2$
	0.1 % CHAPS (w/v)
Blotting buffer (1x)	38 mM Glycine
	10 mM Tris
	20 % (v/v) Methanol
Blotting buffer (5x)	190 mM Glycine
	50 mM Tris
TBST buffer	10 mM Tris/HCl, pH 8.0
	150 mM NaCl
	0.05 % Tween 20
Breaking buffer	50 mM Sodium-Phosphate buffer, pH 7.4
	100 mM NaCl
	1 mM EDTA
	5 % Glycerol
	1 mM PMSF
	Pepstatin A (1 µg/ml)
	Leupeptin (0.1 µg/ml)
Lysis buffer	25 mM Tris pH 8.5

	150 mM NaCl
	5 mM DTT/ 10 mM β-Mercaptoethanol
	10 % Glycerol (v/v)
CB50	25 mM Tris pH 8.5
	50 mM NaCl
	5 mM DTT/ 10 mM β-Mercaptoethanol
	10 % Glycerol (v/v)
CB100	25 mM Tris pH 8.5
	100 mM NaCl
	5 mM DTT
	10 % Glycerol (v/v)
CB1000	25 mM Tris pH 8.5
	1000 mM NaCl
	5 mM DTT
	10 % Glycerol (v/v)
NPB0	25 mM Hepes pH 7.5 / 25 mM Tris pH 9.0
	0 mM NaCl
	5 mM $MgCl_2$
	10 % Glycerol (v/v)
	0.12 % DM / 0.015 % LM / 0.04 % Cymal-6
	0.024 % / 0.003 % / 0.008 % CHS
	Asolectin (optional)
	0.5 mM nicotinic acid (optional)
NPB100A	25 mM Hepes pH 7.5 / 25 mM Tris pH 9.0
	100 mM NaCl
	5 mM $MgCl_2$
	0 mM Imidazole
	10 % Glycerol (v/v)
	0.12 % DM / 0.015 % LM / 0.04 % Cymal-6
	0.024 % / 0.003 % / 0.008 % CHS
	Asolectin (optional)
	0.5 mM nicotinic acid (optional)
NPB100B	25 mM Hepes pH 7.5 / 25 mM Tris pH 9.0
	100 mM NaCl

	5 mM $MgCl_2$
	300 mM Imidazole
	10 % Glycerol (v/v)
	0.12 % DM / 0.015 % LM / 0.04 % Cymal-6
	0.024 % / 0.003 % / 0.008 % CHS
	Asolectin (optional)
	0.5 mM nicotinic acid (optional)
NPB1000	25 mM Hepes pH 7.5 / 25 mM Tris pH 9.0
	1000 mM NaCl
	5 mM $MgCl_2$
	10 % Glycerol (v/v)
	0.12 % DM / 0.015 % LM / 0.04 % Cymal-6
	0.024 % / 0.003 % / 0.008 % CHS
	Asolectin (optional)
	0.5 mM nicotinic acid (optional)
NPB-low salt	10 mM Hepes pH 7.5 / 10 mM Tris pH 9.0
	0 mM NaCl
	1 mM $MgCl_2$
	10 % Glycerol (v/v)
	0.12 % DM / 0.015 % LM / 0.04 % Cymal-6
	0.024 % / 0.003 % / 0.008 % CHS
	Asolectin (optional)
	0.5 mM nicotinic acid (optional)
IMA blocking buffer	100 mM Na-Phosphate pH 7.0
	150 mM NaCl
	2 mM D-Biotin
IMA regeneration buffer	100 mM Glycine, pH 2.8
Coomassie Stain	2 g Coomassie Brilliant Blue R250
	600 ml H_2O
	100 ml glacial acetic acid
	300 ml Methanol
Destain	600 ml H_2O
	100 ml glacial acetic acid
	300 ml Methanol

Kanamycin Stock Solution (1000x)	50 mg/ml in H_2O, stored at 4 °C
Loading buffer 4x (SDS-PAGE)	250 mM Tris/HCl, pH 6.8
	8 % SDS
	40 % Glycerol
	400 mM DTT
	0.004 % Bromophenol blue
Running buffer (10x)	500 mM Tris/HCl
	1.92 M Glycine
	1 % SDS
Running buffer (1x)	50 mM Tris/HCl
	192 mM Glycine
	0.1 % SDS
Lower Tris (4x)	0.4 % SDS
	3 M Tris/HCl pH 8.84
Upper Tris (4x)	0.4 % SDS
	0.5 M Tris/HCl pH 5.8
PMSF Stock Solution	200 mM PMSF in Isopropanol
	(stored room temperature)
Pepstatin A Stock Solution (1000x)	1 mg/ml in Methanol (stored at -20 °C)
Leupeptin Stock Solution (100x)	1 mg/ml in H_2O (stored at -20 °C)
TB salts (10x) 100 ml	2.31 g KH_2PO_4
	12.54 g K_2HPO_4
M9 Salts (10x) 1 l	60 g Na_2HPO_4
	30 g KH_2PO_4
	5 g NaCl
	10 g NH_4Cl
TFB-I	30 mM Potassium acetate pH 5,8
	10 mM $CaCl_2$
	50 mM $MnCl_2$
	100 mM RbCl
	15 % Glycerol
TFB-II	10 mM MOPS/KOH pH 6,8
	10 mM RbCl
	75 mM $CaCl_2$

15 % Glycerol

2.1.10 Vectors

pPIC9K	Invitrogen GmbH, Karlsruhe, Germany
pPIC3.5K	Invitrogen GmbH, Karlsruhe, Germany
pcDNA3.1	Invitrogen GmbH, Karlsruhe, Germany
pTrcHIS2A	Invitrogen GmbH, Karlsruhe, Germany
pET	Merck Biosciences, Darmstadt, Germany
pGEX	GE Healthcare Europe GmbH, Munich, Germany

2.1.11 cDNA-Templates

All templates for human β-arrestin1, human β-arrestin 2 and HM74-A/GPR109A were provided by our industrial collaborator Sanofi-Aventis Deutschland GmbH, and verified by DNA sequencing.

2.1.12 Primers

2.1.12.1 Cloning

barr1for	5'-ATCCGGAATTCGATGAGAACCTGTACTTCCAGGGCATGGG CGACAAAGGGACCCGAGTGTTCAAGAAGGCC-3
barr1-BamHIrev	5'-**P**-GAGATACTCAGGATCGACCAGGACCACACC-3'
barr1-BamHIfor	5'-**P**-GGTGTGGTC CTGGTCGATCCTGAGTATCTC-3'
barr1-EcoRIrev	5'-**P**-CCAGACGCACAGAATTTCGCTTGTGGATCTTCTCCTCC-3'
barr1-EcoRIfor	5'-**P**-GGAGGAGAAGATCCACAAGCGAAATTCTGTGCGTCTGG-3'
barr1-flrev	5'-**P**-ATAAGAATGCGGCCGCTCATCTGTTGTTGAGCTGTGGA GAGCCGG-3'
barr1R169Erev	5'-**P**-CCTCTCTGGGGCATACTGAACCTTCTCGATGACCAGAC GC-3'
barr1R169Efor	5'-**P**-GCGTCTGGTCATCGAGAAGGTTCAGTATGCCCCAGAGA GG-3'

barr1-382rev	5’-ATAAGAATGCGGCCGCTCATGTGTCAAGTTCTATGAGATTGG-3’
barr1-393	5'-ATAAGAATGCGGCCGCTCAAGCAAAGTCCTCAAATACAATGTCG-3'
barr1-origfor	5'-CATGCCATGGGCGACAAAGGGACC-3'
barr1-origrev	5'-CCCAAGCTTTCATGTGTCAAGTTCTAT-3'
barr1-NcoI1for	5'-**P**-GGAGATCTATTACCACGGAGAACCCATCAGC-3'
barr1-NcoI1rev	5'-**P**-GCTGATGGGTTCTCCGTGGTAATAGATCACC-3'
barr1-NcoI2for	5'-**P**-GTGCCCTGTTGCAATGGAAGAGGC-3'
barr1-NcoI2rev	5'-**P**-GCCTCTTCCATTGCAACAGGGCAC-3'
barr2for	5'-ATCCGGAATTCGATGAGAACCTGTACTTCCAGGGCATGGGGGAGAAACCCGGGACCAGG-3'
barr2-382rev	5'-ATAAGAATGCGGCCGCTCAGGTATCAAATTCAATGAGGTTGG-3'
barr2-393rev	5'-ATAAGAATGCGGCCGCTCAGGCAAAGTCCTCAAACACAATGTCATCATCTGTGGC-3'
barr2-flrev	5'-ATAAGAATGCGGCCGCTGAGCTAGCGCCTGAACCTCCGGAGC-3'
NAR1for	5’-TCACGGGGATC CCAATCGGCACC-3’
NAR1-BamHIrev	5’-P-GGGAGCCAGAAGATGCGGAGCCGCACAACCAC GCTGG-3’
NAR1-BamHIfor	5’-P-CCAGCGTGGTTGTGCGGCTCCGCATCTTCTGG CTCC-3’
NAR1rev	5’-CCGGTGCCGCCGCCGAATTC-3’
pPIC9Kfor	5’-GGTGGGAGATCTAAACGATGAGATTTCCTTCAATTTTTACTG-3’
pPIC9KOLrev	5’-**P**-CCCTGAAAATAAAGATTCTCTCTAGCACCCAACCAAGCTTCAACATCTCTTTTCTCGAGAGATACCCC-3’

pPIC9KOLfor	5’-**P**-GTGCTAGAGAGAATCTTTATTTTCAGGGCGGATCCGAGG CTGAAGCTTACGT AGAATTCC-3’
pIC9Krev	5’-CACGGTGCCTGACTGCGTTAGC-3’
stab-for	5’-GGGTGGGAATTCGAGAATCTTTATTTTCAGGGCGGCGGCG GCACCGGCGGC-3’
AOX1rev	5’-GGCAAAT GGCATTCTGACATCC-3’
GSTfor	5’-ATCGCGGATCCGCCATGTCCCCTATACTAGGTTATTGGAAA ATTAAGGGCC-3’
GSTrev	5’-ATGCGGAATTCCGGATTTTGGAGGATG GTCGCCACCACC-3’
MCSfor	5'-**P**-CTAGCCGCGGGATCCCGCGGAATTCCGAAATATGCGGCC GCTATAAACCCA-3'
MCSrev	5'-**P**-AGCTTGGGTTTATAGCGGCCGCATATTTCGGAATTCCGCG GGATCCCGCGG-3'
GFPfor	5'-ATCCGGAATTCATGGTGAGCAAGGGCGAGGAGC-3'
GFPrev	5'-ATCCGGAATTCGATGAGAAACTGTACTTCCAGGGCATGGG GGAGAAACCCGGGACCAGG-3'
CFPfor	5'-GTGTGTGGATCCTCTGGAATGGTGAGCAAGGGCGAGGAGC-3'
CFPrev	5'-GTGTGAATTCCTTGTACAGCTCGATCCATGCCG-3'

2.1.12.2 Sequencing

pTrcHISfor	5'-GAGGTATATATTAATGTATCGATTAAATAAGGAGG-3'
pTrcHISrev	5'-GGCTGAAAATCTTCTCTCATCCGC-3'

AOX1for	5'-GACTGGTTCCAATTGACAAGC-3'
AOX1rev	5'-GGCAAAT GGCATTCTGACATCC-3'
alpha for	5'-CTACTATTGCCAGCATTGCTGCT-3'
T7 prom	5'-TAATACGACTCACTATAGG-3'
T7 term	5'-TAGTTATTGCTCAGCGGTGG-3'
pGEX 5'	5'-GGCCTTTGCAGGGCTGGCAAGCCACGTTTGGTG-3'
pGEX 3'	5'-CCTCTGACACATGCAGCTCCCGG-3'
BGH seq	5'-TAGAAGGCACAGTCGAGG-3'

2.1.13 Strains

2.1.13.1 E. coli

- Mach1™-T1^R

  F$^-$ φ80(*lacZ*)ΔM15 Δ*lac*X74 *hsd*R($r_K^- m_K^+$) Δ*rec*A1398 *end*A1 *ton*A

  Invitrogen, Karlsruhe, Germany
- BL21(DE3)pLysS

  F–, *omp*T, *hsd*S_B (r_B–, m_B–), *dcm*, *gal*, λ(DE3), pLysS, Cm^r

  Promega GmbH, Mannheim, Germany
- BL21 Codon Plus®(DE3)-RIPL

  E. coli B F– *ompT hsdS*(rB– mB –) *dcm*+ Tetr *gal* λ(DE3) *endA* Hte [*argU proL* Camr] [*argU ileY leuW* Strep/Specr]

  Stratagene Europe, Amsterdam, The Netherlands
- Rosetta(DE3)

  F – ompT hsdSB(rB– mB–) gal dcm (DE3) pRARE6 (CamR)

  Merck Biosciences, Darmstadt, Germany

2.1.13.2 P. pastoris

- SMD1163
  Mut+, His-, protease deficient (*his4*, *pep4*, *prb*)
  From Invitrogen GmbH, Karlsruhe, Germany

2.1.13.3 Mammalian Cells

- BHK cells
  European Collection of Cell Cultures, UK

- HEK-293 cells
  Sanofi-Aventis Deutschland GmbH, Frankfurt a. M., Germany

2.1.14 Media

2.1.14.1 Stock Solutions

Biotin (500x) 0.02 % biotin
Filter sterilize
store at room temperature, shelf life approx. one year

G418 50 mg/ml
filter sterilize
store at -20 °C

Glucose (10x) 20 %
Glucose 200 g/l
filter sterilize
store at room temperature, shelf life approx. one year

Glycerol (10x) 10 % (v/v)
autoclave
store at room temperature, shelf life approx. one year

M9 salts (10x)

Na_2HPO_4	60 g/l
KH_2PO_4	30 g/l
NaCl	5 g/l
NH_4Cl	10 g/l

autoclave

store at room temperature, shelf life is greater than one year

[^{15}N]-M9 salts (10x)

Na_2HPO_4	60 g/l
KH_2PO_4	30 g
NaCl	5 g/l
[^{15}N]-NH_4Cl	10 g/l

autoclave

store at room temperature, shelf life is greater than one year

Potassium phosphate buffer (10x)

K_2HPO_4	23.0 g/l
KH_2PO_4	118.1 g/l

adjust pH to 6.0 with phosphoric acid or KOH

autoclave

store at room temperature, shelf life is greater than one year

TB salts (10x)

KH_2PO_4	2.31 g/100 ml
K_2HPO_4	12.54 g/100 ml

autoclave

store at room temperature, shelf life is greater than one year

Yeast Nitrogen Base (YNB) (10x)

YNB w/o amino acids, with ammonium-sulfate	34 g/l
NH_4SO_4	100 g/l

filter sterilize

store at room temperature, shelf life is approx. one year

[^{15}N]-Yeast Nitrogen Base (YNB) (10x)

YNB w/o amino acids, w/o ammonium-sulfate	134 g/l
[^{15}N]-NH_4SO_4	100 g/l

filter sterilize

store at room temperature, shelf life is approx. one year

2.1.14.2 E. coli

LB Media

Bacto tryptone	10 g/l
Bacto yeast extract	5 g/l
NaCl	10 g/l
Bacto agar (for plates)	15 g/l

TB Media

Bacto tryptone	12 g/l
Bacto yeast extract	24 g/l
Glycerol	4 ml/l
10x TB salts	100 ml/l

M9 Minimal Media

ddH_2O	879 ml/l

autoclave, cool down and add:

10x M9 salts (autoclaved)	100 ml/l
$MgSO_4$ (1M) (autoclaved)	1 ml/l
$CaCl_2$ (100mM) (autoclaved)	10 ml/l
Glucose Solution (20%) (filter sterilized)	10 ml/l

2.1.14.3 P. pastoris

BMGY

Peptone	20 g/l
Bacto yeast extract	10 g/l
ddH_2O	700 ml/l

autoclave, cool down and add:	
Potassium phosphate buffer (10x)	100 ml/l
YNB (10x)	100 ml/l
Glycerol (10x)	100 ml/l
Biotin (500x)	2 ml/l
store at room temperature, the shelf life is approx. two month	

BMMY

Peptone	20 g/l
Bacto yeast extract	10 g/l
ddH_2O	800 ml/l
autoclave, cool down and add:	
Potassium phosphate buffer (10x)	100 ml/l
YNB (10x)	100 ml/l
Methanol	5 ml/l
Biotin (500x)	2 ml/l
store at room temperature, the shelf life is approx. two month	

BMG

ddH_2O	700 ml/l
autoclave, cool down and add:	
Potassium phosphate buffer (10x)	100 ml/l
YNB (10x)	100 ml/l
Glycerol (10x)	100 ml/l
Biotin (500x)	2 ml/l
store at room temperature, the shelf life is approx. two month	

BMM

ddH_2O	800 ml/l
autoclave, cool down and add:	
Potassium phosphate buffer (10x)	100 ml/l
YNB (10x)	100 ml/l
Methanol	5 ml/l
Biotin (500x)	2 ml/l

store at room temperature, the shelf life is approx. two month

MD plates

Bacto agar	15 g/l
ddH_2O	800 ml/l
autoclave, cool down and add:	
Glucose (10x)	100 ml/l
YNB (10x)	100 ml/l
Biotin (500x)	2 ml/l

store at 4 °C, the shelf life is several month

YPD

Peptone	20 g/l
Bacto yeast extract	10 g/l
Bacto agar (optional, for plates)	20 g/l
ddH_2O	900 ml/l
autoclave, cool down and add:	
Glucose (10x)	100 ml
G418 (optional, for G418 plates)	appropriate conc.

store at 4 °C, the shelf life is at least six month

2.1.14.4 Mammalian Cell Culture

Dulbecco's Modified Eagle's Medium (DMEM) w/o L-Glutamine	Cell Concepts, Umkirchen Germany
Iscove's Media	Cell Concepts, Umkirchen Germany
Fetal Calf Serum (FCS)	GibcoBRL, Life Technologies GmbH, Karlsruhe
PBS	Cell Concepts, Umkirchen Germany

L-Glutamine	GibcoBRL, Life Technologies GmbH, Karlsruhe
Ham's F-12 Media	PAA Laboratories, Pasching, Austria

2.1.15 General Apparatus General

Desintegrator-C	Bernd Euler, Frankfurt a. M., Germany
Electrophoresis System Xcell SureLock with 1 mm cassettes	Invitrogen, Carlsbad, CA, USA
Electroporation Device Gene Pulser	Bio-Rad, Munich, Germany
Scintillation Counter TRI-CARB 1500	Camberra-Packard, Frankfurt a. M., Germany
Wallac Micro Beta TriLux	PerkinElmer LAS (Germany) GmbH, Rodgau-Jügesheim, Germany
Brandel Harvester	Adi Hassel, Munich, Germany
MicroBeta Filtermate-96 Harvester	PerkinElmer LAS (Germany) GmbH, Rodgau-Jügesheim, Germany
Shakers	Infors AG, Bottmingen, Switzerland
Spectrophotometer	Thermo Spectronic, Cambridge, UK
Microplate Reader Power Wave	Bio-Tek Instruments GmbH, Bad Friedrichshall, Germany
OMNIFLEX MALDI TOF MS	Bruker Daltonik GmbH, Bremen, Germany
DRX 600 Spectrometer	Bruker BioSpin GmbH, Rheinstetten, Germany
EM 208 Electron Microscope	FEI Company, Hillsboro, OR, USA
Molecular Imager Gel Doc XR	Invitrogen, Carlsbad, CA, USA

2.1.15.1 Centrifuges

Sorvall RC-5B	Du Pont de Nemours GmbH, Bad Homburg, Germany
Avanti J-20 XPI	Beckman-Coulter, Fullerton, CA, USA
Optima LE-80K ultracentrifuge	Beckman-Coulter, Fullerton, CA, USA
Optima MAX ultracentrifuge (tabletop)	Beckman-Coulter, Fullerton, CA, USA

Sigma 3K 12 (tabletop)	Sigma-Aldrich Chemie GmbH, Steinheim, Germany
Centrifuge 5415D	Eppendorf GmbH, Hamburg, Germany

2.2 Methods

2.2.1 Genetic Engineering

2.2.1.1 *E. coli* Cell Growth

E. coli cells of the strain Mach1 were grown at 37 °C at 250 rpm shaking in LB media over night for the amplification of desired plasmids or preparation of glycerol stocks. Ampicillin was added at a concentration of 100 mg/ml for plasmid maintenance. Glycerol stocks were prepared by adding 15 % of sterile Glycerol, flash frozen in liquid nitrogen and stored at -80 °C for later use. For plasmid preparation cells were harvested by centrifugation at 5000 g, 10 min, at 4 °C and handled as described in plasmid preparation (2.2.1.4).

2.2.1.2 Competent Cell Preparation

Competent cells were essentially prepared according to Hanahan [63]. 50 ml LB media were inocculated with 100 µl of an over night culture, and grown at 37 °C, 240 rpm shaking until they reached an optical density OD_{600} = 0.5. The culture was chilled on ice for 10 min, and then harvested by centrifugation for 10 min, 2000 g at 0 °C. The pellet was carefully resuspended in 1ml ice cold TFB-I, and another 6.5 ml TFB-I were added, and mixed by gentle invertation. Cells were then incubated on ice for one hour, and pelleted by centrifugation for 10 min at 3000 g and 0 °C. The cell pellet was resuspended in 2 ml ice cold TFB-II. 100 µl aliquots were then prepared on ice, snap frozen in liquid nitrogen and stored at -80 °C for further use.

2.2.1.3 *E. coli* Transformation

Transformation of all *E. coli* strains was done essentially according to a protocol by Hannahan [63]. An aliquot of competent cells was thawed on ice, and 0.2 µg plasmid DNA, or 10 µl of the ligation reaction were added, swirled and incubated on ice for 30 min. The reaction was then heat-shocked for 45 seconds at 42 °C and chilled on ice for 2 min. After addition of 600

µl plain LB media cells were allowed to recover and grow for 60 min at 37 °C with vigorous shaking. The transformation reaction was then pelleted at 2000 rpm on a tabletop microfuge and excess media discarded. The cell pellet was resuspended in 100 µl LB media and plated onto LB-agar plates containing the appropriate antibiotic (ampicillin 100 µg/ml, kanamycin 25 mg/ml). Transformed colonies were selected the following day after incubation over night at 37 °C.

2.2.1.4 Plasmid Preparation

E. coli Mach1 cells were grown and harvested as described above (*E. coli* cell growth). The cell pellets were processed essentially as described in the Qiagen plasmid miniprep kit manual. DNA concentration was measured at UV absorption of 260 nm. Plasmid DNA was stored at -20 °C for further use.

2.2.1.5 PCR

PCR reactions typically had a volume of 50 µl. For amplification of sequences from plasmid DNA typically 0.05 µg were used as template, for reamplification of previously obtained PCR products 1 µl of the purified amplificated was used as template. 0.3 µM of forward and reverse primers were added, 5µl of the supplied 10x reaction buffer, containing dNTPs (2 µM) and $MgCl_2$ (1.5 mM) and 50 units of AccuPrime DNA polymerase. The reaction was started by a heat denaturing step to activate the enzyme for 2 min at 94 °C. The melting reaction was carried out according to the manufacturer's recommendations at 94 °C for 30 s. The annealing step lasted 30 s and the temperature was calculated on the basis of the pairing primer sequence according to equation

$$T_m = 81.5 + 0.41(\%\ GC) - 675/N - \%\ mismatch$$

N = length of the pairing sequence of the primer
% GC = the content of G and C nucleotides in the pairing sequence
% mismatch = the content of mismatching nucleotides.

Temperature for the extension step was 68 °C according to the manufacturer suggestions and the time was calculated according to the length of the amplificate and the enzymes processivity (1 kb/min). In general between 16 and 25 cycles were used.

All PCR products were purified using the Qiagen PCR purification kit according to the protocol supplied.

2.2.1.6 Restriction Digest

All restriction endonucleases used in this work are of type 2, leaving cohesive overlapping ends at one strand. Restriction digestions were always carried out according to the manufacturer's guidelines and performed in the supplied buffers at recommended temperatures. Plasmids that were opened by restriction digest for insert uptake were additionally treated with 5 Units/100 pmol termini calf intestine alkaline phosphatase (CIAP) to remove 5' phosphates and minimize relegation. The reaction was performed in the restriction buffer for 30 min at 37 °C. All restriction digest reactions were purified using the Qiagen PCR purification kit.

2.2.1.7 Ligation

Stoichiometric amounts of insert and vector DNA, according to agarose gel electrophoresis were mixed in a volume of 10 µl. 10 µl of 2x Ligation buffer were added and 0.5 µl Quick Ligase. The reaction was mixed thoroughly and incubated at room temperature for 20 min, chilled on ice for 5 min and mixed with competent cells as described in *E. coli* transformation.

2.2.1.8 Preparation of β-arrestin 1 Sequence for Cloning

To remove intrinsic *Bam*HI and *Eco*RI sites from the coding sequence of β-arrestin 1, a set of PCR overlap extensions was carried out. Three reactions with primers pairs barr1for and barr1-BamHIrev, barr1-BamHIfor and barr1-EcoRIrev, barr1-EcoRIfor and barr1-flrev, respectively were performed, and all three fragments were gel excised and purified with the Qiagen Gel Excision Kit, and subsequently used as templates in a new PCR reaction using primers barr1-for and barr1-flrev. The resulting fragment of 1291 bp was used as template for further cloning and amplification procedures of β-Arrestin 1.

2.2.1.9 Introduction of the Activating Mutation R169E

The amino acid arginine169 in β-arrestin 1 was substituted by a glutamate in a PCR overlap extension reaction. A 5'-fragment and a 3' fragment were amplified by PCR, using primer

pairs barr1for and barr1R169Erev, and barr1R169Efor and barr1flrev, respectively. Both fragments were gel excised, and purified by the Qiagen gel extraction kit. Both purified fragments were then used as templates for another PCR reaction, using primers barr1for and barr1flrev, resulting in a fragment of ~1300 bp termed β-arrestin 1R169E.

2.2.1.10 Removal of the Intrinsic *Bam*HI Site from HM74A

To facilitate cloning of the coding sequence of HM74A/GPR109B it was required to remove the intrinsic *Bam*HI site from the sequence. Two fragments were amplified by PCR using AccuPrime, a 5'-fragment of 738 bp with the primer combination NAR1for and NAR1-BamHIrev. A 3'-fragment with the primers NAR1-BamHIfor and NAR1rev that produced a fragment of 445 bp length. The two PCR fragments were gel excised and purified by the Qiagen gel extraction kit. These two fragments and the primers NAR1for and NAR1rev amplified the entire coding sequence in another PCR reaction. These primers introduced additionally desired restriction enzyme sites for directed cloning and affinity tags or the coding sequence for protease cleavage sites.

2.2.1.11 Cloning of HM74A

2.2.1.11.1 Construction of pPIC9K Derivatives

For NAR1 expression in *P. pastoris* a different affinity tag, the nano9-tag, was employed that is used as affinity handle in conjunction with a Streptavidin matrix. In a first step the *Bam*H1 site that exists in the unmodified pPIC9K vector at position 938 was disrupted. The sequence between the *Bgl*II site up to the MCS was amplified by PCR, using a forward primer pPIC9Kfor and a reverse primer pPIC9KOLrev. This primer introduced the coding sequence for the nano9-tag and a TEV recognition site. In a second reaction the sequence from the MCS of the pPIC9K fhT-Tbio was amplified with a forward primer pPIC9KOLfor and a reverse primer pPIC9Krev. Both fragments were gel excised and purified with the Qiagen gel extraction kit. In a new PCR reaction both fragments were used as templates with primers pPIC9Kfor and pPIC9Krev, producing a fragment of 739 bp. This fragment was purified with the Qiagen PCR purification kit, digested with *Bgl*II and *Not*I and ligated into the pPIC9K vector previously treated with *Bam*HI, *Not*I and CIAP. Ligation of compatible *Bam*HI sticky ends to *Bgl*II sticky ends disrupts the *Bam*HI site. Ligation was done with the Quick Ligase and transformed into *E. coli* Mach-1 cells. Transformed clones were grown according to

instructions given in the manual of Qiagen miniprep kit, DNA isolated and analyzed by restriction digest. Positive clones were verified by DNA sequencing. The resulting vector was called pPIC9KnT.

In a second step the different C-terminal fusion sequences, Stab-tag, β-arrestin 1-382 and β-arrestin 1-fl were amplified by PCR using the primers stab-for and AOX1rev for the stab-tag, barr1-for and barr1-382rev for the truncated β-arrestin 1, and primers barr1-for and barr1-flrev for the full length construct of β-arrestin 1. The resulting fragments were then digested by *Eco*RI and *Not*I restriction endonucleases and cloned into the likewise treated vector pPIC9KnT, additionally treated with CIAP. The prepared vector and amplificate were mixed, ligated using Quick Ligase, and transformed into competent *E. coli* Mach-1 cells (Stratagene). DNA of colonies growing on LB-ampicillin plates was purified using the Qiagen miniprep kit and analyzed by restriction digest and the desired DNA sequence of positive clones was verified by DNA sequencing, producing vectors pPIC9KnT-Tstab, pPIC9KnT-Tβarr1-382 and pPIC9KnT-Tbarr1-fl.

2.2.1.11.2 Cloning into *P. pastoris* Vectors

The modified coding sequence of HM74A was then digested by restriction endonucleases *Bam*HI and *Eco*RI and cloned into the likewise prepared vectors that additionally were treated with CIAP. The prepared vectors and amplificate were mixed, ligated using Quick Ligase (NEB) and transformed into competent *E. coli* Mach-1 cells (Stratagene). DNA of colonies growing on LB-ampicillin plates was purified using the Qiagen miniprep kit and analyzed by restriction digest and the desired DNA sequence was verified by DNA sequencing.

2.2.1.12 Cloning of β-Arrestins

2.2.1.12.1 pPIC3.5K GST-β-Arrestin

The DNA coding for the Glutathione-S-Transferase was amplified from a pGEX vector by a PCR reaction using primers GSTfor and GSTrev. The amplificate was purified by the Qiagen PCR purification kit and digested with *Bam*HI and *Eco*RI. The pPIC3.5K vector was likewise digested and treated with CIAP. Both, vector and amplificate, were purified with the Qiagen PCR purification kit, ligated and transformed into *E. coli* Mach-1 cells. The resulting vector, pPIC3.5KGST, was analyzed by restriction digest and positive clones were verified by DNA sequencing.

The β-arrestin sequences were amplified by PCR using primer and template combinations as depicted in table 1, and cloned into *Eco*RI and *Not*I sites of the vector pPIC3.5KGST. Positive clones were analyzed by restriction digest, and the correct sequence was verified by DNA sequencing.

	forward primer	**reverse primer**	**template**
β-arrestin 1-382	barr1for	barr1-382rev	β-arrestin 1
β-arrestin 1-393 R169E		barr1-39rev3	β-arrestin 1R169E
β-arrestin 1-fl		barr1-flrev	β-arrestin 1
β-arrestin 2-382	barr2for	barr2-382rev	β-arrestin 2
β-arrestin 2-393		barr2-393rev	
β-arrestin 2-fl		barr2-flrev	

Table 1: Templates and primer used for the amplification of various β-arrestin constructs

2.2.1.12.2 pET HIS-β-Arrestin

The pET His vector was a kind gift from Dr. K. Saxena, University Frankfurt, and contained a hexahistidine-tag. The vector was opened with *Eco*RI and *Not*I, and dephosphorylated by CIAP. The β-arrestin cDNAs were amplified according to table 1, and the resulting fragments were cloned via *Eco*RI and *Not*I sites into the pET His vector, and transformed into Mach-1 *E. coli* competent cells. Clones were analyzed by restriction digest and positive ones were further analyzed by DNA sequencing.

2.2.1.12.3 pGEX β-Arrestin

Cloning of β-arrestin constructs into the pGEX vector was done essentially as described above for the pET vector.

2.2.1.12.4 pTrc β-Arrestin 1-382

Cloning of β-arrestin 1-382 was done essentially as described [64]. To facilitate cloning as described, two *Nco*I sites in the original sequence of β-arrestin 1 had to be removed. Therefore three PCR reactions were carried out, the first using primers barr1-origfor and barr1-NcoI1rev, the second using the primer pair barr1-NcoI1for and barr1-NcoI2rev, and the

third the primer pair barr1-NcoI2for and barr1-origrev. All three fragments were gel excised and used altogether as template for a new PCR, using primers barr1-origfor and barr1-origrev, resulting in a β-arrestin 1 sequence without *Nco*I restriction sites. This β-arrestin 1-382 sequence was cloned into the pTrcHisB between *Nco*I and *Hind*III sites, thus eliminating the his-tag. Positive clones were analyzed by restriction digest, and clones containing the appropriate DNA fragment were verified by DNA sequencing.

2.2.1.12.5 pcDNA3.1

The pcDNA3.1 vector was a kind gift from Dr. S. Marino. The old multiple cloning site was excised by *Nhe*I and *Hind*III restriction, and thoroughly dephosphorylated. A new multiple cloning site was produced by annealing primers MCSfor and MCSrev, that contained restriction sites *Bam*HI, *Eco*RI and *Not*I in the desired orientation, and ligated into the vector, now termed pcDNA3.1J. The resulting clones were analyzed by restriction digest and positive clones were verified by DNA sequencing.

In the following eGFP was amplified by PCR using primers GFPfor and GFPrev, and cloned between *Eco*RI and *Not*I restriction sites of pcDNA3.1J. Positive clones were analyzed by restriction digest and DNA sequencing. In the following the sequence of NAR1 was amplified using primers NAR1for and NAR1rev, and ligated into *Bam*HI and *Eco*RI restriction sites, creating a fusion of NAR1 and eGFP.

Likewise eCFP was amplified by PCR using primers CFPfor and CFPrev, and ligated between *Bam*HI and *Eco*RI sites of pcDNA3.1J. Clones were analyzed by restriction digest and positive ones verified by DNA sequencing. In a second step the various sequences of β-arrestin 1 were cloned between *Eco*RI and *Not*I sites. Therefore β-arrestin 1 was amplified using primers pairs as listed in table 1, digested with *Eco*RI and *Not*I and ligated into the pcDNA3.1J vector previously equipped with eCFP. Positive clones were analyzed by restriction digest and verified by DNA sequencing.

2.2.2 Transformation of *P. pastoris*

2.2.2.1 Preparation of Competent Cells

P. pastoris cells of the strain SMD1163 were grown in YPD media till they reached an optical density of ~1.5. Cells were pelleted by centrifugation, 5 min, 2000 g at 4 °C. The pellet was resuspended in 1 culture volume of ice cold sterile H_2O, and pelleted again as described

above. The supernatant was discarded, and cells were then resuspended in 2/50 volume of the original culture volume ice cold sterile 1 M sorbitol, and pelleted again. In a final step cells were resuspended 1/500 ice cold sterile 1 M sorbitol.

2.2.2.2 Electroporation

80 µl of the competent cells were mixed with 10 µg linearized vector DNA in an elctroporation cuvette, 0.2 mm gap, and incubated on ice for 5 min. The vector DNA was electroporated into the cells with the Gene Pulser, which was set to 1500 V, 25 µF and 600 Ω. The cells were removed from the cuvette with 1 ml ice cold, sterile 1 M sorbitol, spread onto 3 MD plates and incubated for 3 days at 30 °C.

2.2.2.3 Selection of Positive Transformands

The selection of transformands was performed on MD agar plates. This is possible due to the fact that the strain is deficient in histidine biosynthesis, and therefore only the ones that incorporated the plasmid DNA that provides the gene encoding for histidinol dehydrogenase can grow on this media.

2.2.2.4 Multi-copy Clone Selection

2.2.2.4.1 G418 Screen

The standard procedure suggested by the manufacturer for selection of multi-copy clones is screening of increased antibiotic resistance of the transformands. A high integration number results in a high gene dosage of the Kanamycin resistance gene from Tn903, that confers tolerance to higher G418 (Geneticin) concentrations. Out of all transformands 96 were selected and transferred each into 200 µl YPD media in a sterile 96 well plate and grown for two days at 30 °C. Cultures were resuspended and 20 µl aliquots were transferred into a new 96 well plate containing 180 µl YPD media to ensure similar cell densities. Cultures were then stamped onto YPD plates containing 0.05, 0.075, 0.1, 0.2, 0.3, 0.5 and 1.0 mg/ml Geneticin®. First Geneticin® resistant colonies appeared after 3-5 days at 30 °C.

2.2.2.4.2 Direct-Expression Colony-Blot

This method was essentially done as described by Böttner et al. [65] with slight modifications. For the purpose of the direct-expression colony-blot cells from each of the 96 cultures were spotted onto a nitrocellulose membrane covered BMGY agar plates and grown at 30 °C until they all reached approximately the same size. These nitrocellulose membranes were then transferred onto inducing BMMY agar plates, grown at 30 °C and harvested after 48 and 72 hours. The membranes were placed on three layers of Whatman paper soaked in 100 mM Tris/HCl pH 8.5, 20 mM EDTA, 9 M urea, 2 % SDS and 150 mM β-mercaptoethanol and incubated for 3 h at 65 °C. The remaining cells were washed off the membranes, which were then treated like Western Blots.

2.2.3 Protein Expression

2.2.3.1 *E. coli* Expression Culture Growth

2.2.3.1.1 Small Scale Expression Test

5 ml pre-cultures were grown over night in the desired media at 37 °C, 250 rpm. Cell density was measured at OD_{600} and 25 ml of the same media were inoculated to an optical density of 0.05. Cells were then grown at 30 °C until they reached an OD_{600} of 0.5 and protein expression was induced by the addition of IPTG to a final concentration of 1 mM. Cultures were grown for the indicated time at the indicated temperature, and then harvested by centrifugation for 10 min at 16000 g and 4 °C. Cell pellets were resuspended in 4x SDS-PAGE loading buffer, boiled at 95 °C for 5 min and analyzed by SDS-PAGE.

2.2.3.1.2 Large Scale Culture Growth

500-1000 ml culture was grown in LB media containing the appropriate antibiotic over night at 37 °C, 250 rpm shaking. The Pre-Culture was used to inoculate 6-12 l LB media containing the appropriate antibiotic to a cell density of OD_{600} of 0.05. Cells were then grown at 30 °C and 170 rpm shaking in baffled flasks until cell density reached an OD_{600} of 0.5. Cells were induced by the addition of IPTG to a final concentration of 1 mM, and grown four additional hours, harvested by centrifugation 10 min, 10000 g at 4 °C. Cell pellets from 1 l culture were resuspended in 10 ml Lysis Buffer.

2.2.3.1.3 Metabolic Labeling with [^{15}N]

100-200 ml of *E. coli* pre-culture from a freshly streaked plate were grown in LB, containing 100 µg/ml Ampicillin at 37 °C at 250 rpm shaking over night. The pre-culture was used to inoculate a second preculture of 2 l [^{15}N]-M9 minimal media, containing 100 µg/ml ampicillin, and was grown overnight at 30 °C and 170 rpm shaking in a 5 l baffled flask. The second pre-culture was used to inoculate 12 l [^{15}N]-M9 minimal media, containing 100 µg/ml ampicillin, in six 5 l baffled flasks to an OD_{600} of 0.1. Cells were then grown at 30 °C and 170 rpm shaking until they reached an OD_{600} of 0.5 and were induced with IPTG at a final concentration of 1 mM. The culture was then transferred to 20 °C, 170 rpm and grown overnight. Cells were harvested by centrifugation 10 min, 10000 g at 4 °C. Cell pellets from 1 l culture were resuspended in 10 ml Lysis Buffer.

2.2.3.2 *P. pastoris* Expression Culture Growth

2.2.3.2.1 Small Scale Culture Growth

Clones were freshly streaked from a glycerol stock onto YPD plates, and grown at 30 °C for 3 days. A chunk of these cells was used to inoculate a 5 ml pre-culture in BMGY liquid media grown at 30 °C and 225 rpm over night. Optical cell density was measured at 600 nm, and just enough cells were pelleted at 2500 g at 4 °C for 5 min to be resuspended in 25 ml BMMY media containing 0.5 % methanol to reach a starting OD_{600} of 1. The 25 ml small scale expression culture was grown for 24 h at 30 °C with 225 rpm. After 18 h growth additional methanol was added to reach again a concentration of 0.5 %. Cells were harvested by centrifugation 5000 g, 10 min, 4 °C, washed once with ice cold breaking buffer, and either snap frozen in liquid nitrogen or directly entered membrane preparation.

2.2.3.2.2 Optimization of Expression Conditions

2.2.3.2.2.1 Expression Time

Small scale cultures were inoculated as described above. Then cultures were grown either at 22 °C or at 30 °C, and starting after 12 h every 6 h one 25 ml culture was harvested as described above, membranes prepared, protein content determined and subjected to radioligand binding analysis and Western-blotting.

2.2.3.2.2.2 DMSO & Nicotinic Acid

For the optimization of culture conditions regarding DMSO and nicotinic acid cultures were grown as described above, with the difference that the culture media contained 0 %, 0.5 %, 1 %, 2 %, 3 %, 5 % or 7.5 % DMSO or 0 nM, 100 nM, 1 µM, 10 µM, 100 µM or 1 mM nicotinic acid. Cultures were harvested after 24 h, membranes prepared, protein content determined and subjected to radioligand binding analysis and Western-blotting.

2.2.3.2.2.3 Large Scale Expression Culture Growth (Optimized Conditions)

Clones were freshly streaked from a glycerol stock onto YPD plates, and grown for 3 days at 30 °C. A chunk of these cells was used to inoculate a 5 ml pre-culture in BMGY liquid media grown over night at 30 °C and 225 rpm. The culture was used to inoculate 1 l BMGY media in a 5 l baffled flask, and grown for 24 h to 48 h at 30 °C and 225 rpm till the optical density OD_{600} reached ~6. The culture was pelleted by centrifugation at 2500 g, 5 min at 20 °C, resuspended in inducing BMMY media containing 2% DMSO (v/v), and used to inoculate six 5 l baffled flasks containing 1 l BMMY with 2 % DMSO (v/v) each. Cultures were then grown for 24 h at 22 °C and 225 rpm. After 18 h another 5 ml methanol were added. Cells were harvested after 24 h by centrifugation, 5000 g, 10 min at 4 °C, resuspended in breaking buffer, and again centrifuged at 5000 g for 10 min at 4 °C. Cell pellets were weighed, and resuspended in breaking buffer to give a 50 % (w/v) cell suspension, and either membranes were directly prepared or the cell suspension snap frozen in liquid nitrogen and stored at -80 °C (NAR1).

For preparation of cytosolic fractions containing β-arrestins, no DMSO was added to the culture media, and cell suspension were flash frozen in liquid nitrogen and stored at -80 °C for later use.

2.2.3.2.3 Metabolic Labeling with [^{15}N]

A 1st pre-culture of 20 ml BMGY media in a 100 ml baffled flask, containing 50 µg/ml kanamycin was inoculated with a chunk of *P. pastoris* cells from a freshly streaked MD plate and grown overnight at 30 °C and 225 rpm shaking. 500 µl were used to inoculate a 2nd pre-culture of 25 ml BMG media in a 100 ml baffled flask, containing 50 µg/ml Kanamycin and grown at 30 °C, 225 rpm overnight. This culture was used to inoculate a 3rd pre- culture 200 ml [^{15}N]-BMG media, containing 50 µg/ml kanamycin in a 1 l baffled flask, and was grown for 48 h until it reached an OD_{600} of 10. The cells were harvested by centrifugation, 2500 g,

10 min at room temperature and resuspended in 2 l [^{15}N]-BMM expression media containing 50 µg/ml kanamycin and distributed into two 5 l baffled flasks. The expression culture was grown for 80 h, further addition of 5 ml methanol per liter culture every 24 h. Cells were harvested by centrifugation, 5000 g, 10 min at 4 °C, resuspended in breaking buffer, and again centrifuged at 5000 g for 10 min at 4 °C. Cell pellets were then resuspended in 20ml lysis buffer, flash frozen in liquid nitrogen and stored at -80 °C.

2.2.4 Cytosol & Membrane Preparation

2.2.4.1 *E. coli* Lysis

1ml lysozyme (10 mg/ml) and 2 µl benzonase and PMSF to a final concentration of 1 mM were added to the cell suspension (per liter of culture), mixed thoroughly and incubated on ice for 30 min. Cells were broken by sonication on ice, six cycles 60 s on, 60 s off. Lysates were cleared by centrifugation at 40000 g, 20 min, at 4 °C. The supernatant was passed through a 0.2 µM filter and used directly for purification.

2.2.4.2 *P. pastoris* Breakage

2.2.4.2.1 Small Scale Breakage

For small scale membrane preparation 50 % cell suspension (w/v) of above described cultures was prepared by resuspending in ice cold breaking buffer with freshly added PMSF (1 mM) and 1 ml thereof added into a 2 ml microfuge tube that was filled with glass beads (0.5 mm diameter) until a distance of 1-1.5 mm from beads to the surface of the liquid is reached. These were vortexed for 30 s and incubated on ice for 30 s, 8 cycles. The glass bead cell mixture was transferred into propylene columns with a glass fiber frit, and centrifuged at 3000 g for 1 min at 4 °C. Glass beads were washed with 1 additional ml of ice cold breaking buffer, and again centrifuged at 3000 g, 4 min, at 4 °C to pellet cellular debris.

2.2.4.2.2 Large Scale Breakage

Cells of the suspension prepared as described above were broken at 4 °C in the desintegrator-C filled with 80 ml glass beads. Therefore they were passed through the machine 3-4 times,

till ~90 % of the cells were broken. The cell homogenate was centrifuged at 5000 g for 10 min at 4 °C to remove cellular debris, organelles and unbroken cells.

2.2.4.3 Separation of Membrane & Cytosolic Fractions

2.2.4.3.1 Small Scale

The cellular debris was pelleted as described above and the glass beads were retained in the polypropylene column. The homogenate (Small Scale *P. pastoris* Break Up) was transferred to a 1.5 ml ultracentrifuge tube, and centrifuged at 100000 g for 1 h at 4 °C. The supernatant was used if cytosolic fractions were intended to be recovered (β-arrestins), otherwise it was discarded and the pelleted membranes were resuspended by pottering in 500 µl membrane buffer (NAR1). Cytosolic Fractions entered purification or analysis immediately, while membranes were either used directly or were flash frozen in liquid nitrogen and stored for further use at -80 °C.

2.2.4.3.2 Large Scale

The homogenate (Large Scale *P. pastoris* Breakage) was centrifuged at 100000 g, for 1 h at 4 °C. If β-arrestins were to be purified, the supernatant was passed through a 0.4 µM filter and entered purification procedures immediately. If membranes were intended (NAR1), the supernatant was discarded and pellets were resuspended in ~10 ml membrane buffer per 1 g of membranes with a homogenizer. A sample of the membrane suspension was used for the determination of the protein concentration as described below (2.2.14.4), and the remainder was aliquoted, snap frozen in liquid nitrogen and stored at -80 °C for later use.

2.2.5 Radioligand Binding Assay

2.2.5.1 Screening Conditions

Functionality of GPCR containing membranes is routinely tested by their capability to bind their cognate radio labeled ligand. Therefore 50 µg of membrane protein were incubated with 250 µM [^{3}H]-nicotinic acid, in a buffer of 50 mM Tris/HCl pH 7.4, 1 mM $MgCl_2$, and 0.02 % (w/v) CHAPS in a total volume of 250 µl. For non-specific binding 1 mM unlabelled nicotinic acid was added, and incubated at room temperature for 3.5 h. The receptor with bound ligand

was separated from the unbound ligand by filtration using a Brandel Harvester over GF/C glass fiber filters, previously equilibrated in Pre-Soak buffer and washed twice with 2 ml ice cold H_2O [13]. After sample Filtration, GF/C filters were washed 4 times with 2 ml ice cold H_2O. The remaining radioactivity on the filters was then measured by liquid scintillation counting after 48 h. All samples were prepared in triplicates.

Screen II was essentially prepared as above, except that a nicotinic acid mixture composed of [^{1}H]-nicotinic acid and [^{3}H]-nicotinic acid in a ratio of 50:1 was used, to reduce the amount of costly [^{3}H]-nicotinic acid. This mixture was added to a final concentration of nicotinic acid of 2 µM. The concentration of diluted radio ligand allowed binding assays at saturating conditions 10 times above the K_d. Further activity calculations were corrected for this dilutional effect by reducing the specific activity by a factor of 50. Additionally the incubation time was reduced to 2 h.

2.2.5.2 Evaluation of Buffer Components

250 µl binding assay samples containing 50 µg membrane protein in binding buffer were prepared according to screening conditions (2.2.5.1) and the desired chemical (NaCl, KCl, LiCl, NH_4Cl) was added to a final concentration of 0 mM, 1 mM, 2 mM, 5 mM, 10 mM, 50 mM, 100 mM and 250 mM. For DTT concentrations were 0 mM, 0.0625 mM, 0.125 mM, 0.5 mM, 1 mM, for imidazole 0 mM, 0.25 mM, 2.5 mM, 25 mM, 100 mM and 250 mM and for DMSO 0 %, 0.5 %, 1 %, 2 %, 5 % and 10 %. For pH dependence of NAR1 binding different binding buffers were used to adjust the pH accordingly (pH 4.5: Na-acetate, pH 5.0 and pH 5.5: Na-citrate, pH 6.0: MES, pH 6.5: ADA, pH 7.0: MOPS, pH 7.5: HEPES, pH 8.0, pH 8.5 and pH 9.0: Tris, pH 9.5: CAPSO) but contained corresponding to the standard buffer a final concentration of 1 mM $MgCl_2$ and 0.02 % CHAPS in the sample. After 3.5 h incubation samples were harvested as described above. For the determination of unspecific binding 1 mM of [^{1}H]-nicotinic acid was added. All experiments were performed in triplicates.

2.2.5.3 Evaluation of Detergent Effects

To evaluate the effect of detergent on the radio ligand binding assay, detergent stock solutions were prepared according to table 2, and added to the binding assay in concentrations of 0.1 times cmc, at 1 time cmc and 10 times cmc. Samples were prepared in triplicates, and non specific binding was determined as described above (screening conditions, 2.2.5.1).

For the detergent mixtures DM+CHS, LM+CHS and Cymal-6+CHS detergent inhibition curves were recorded. Therefore detergent was added from 0.00005 % to 1%, covering at least ranges from 1/500 cmc (LM+CHS) to 10 times cmc (DM+CHS). Samples were then processed as described above.

2.2.5.4 Binding Kinetics: NAR1 On- & Off-Rate

To determine the on-rate of nicotinic acid, samples were prepared as described under screening conditions (2.2.5.1), and harvested after 30 min, 60 min, 120 min and 210 min. For the determination of background binding samples were prepared that contained 1 mM [^{1}H]-nicotinic acid and were harvested at the same indicated time points. Harvesting and counting was done as described above. All measurements were performed in triplicates.

For the determination of the off-rate of nicotinic acid binding to NAR1 samples were prepared as described above (2.2.5.1), after 3.5 h a pulse of 1 mM [^{1}H]-nicotinic acid was added, and samples were harvested 1 min, 2 min, 5 min, 10 min, 20 min, 30 min, 45 min and 60 min thereupon. Control samples did not contain the pulse and were harvested at the same indicated intervals.

2.2.5.5 Saturation Binding Curves

Determination of the total amount of receptor present in a given membrane preparation can only be determined inaccurately by a single point measurement. The method of choice for calculating the total amount of receptor is the recording of binding curves, and fitting of the data to the model receptor ligand association according to Cheng & Prussof [66]. In an experiment the unoccupied receptor and the free ligand are in equilibrium with the receptor ligand complex. It is described by the equation

$$R + L \Leftrightarrow RL \qquad \text{(equation 1)}$$

The equilibrium constants are given by the following equations

$$R + L \xrightarrow{k_{+1}} RL; \qquad RL \xrightarrow{k_{-1}} R + L$$

$$K_a = [RL]/[R][L] = k_{+1}/k_{-1} = 1/K_d \qquad \text{(equation 2)}$$

The specific binding between the ligand and receptor is saturable, and the more ligand is added to a fixed amount of receptor, an increasing amount of binding sites is occupied. The total number of binding sites B_{max} in a given sample at equilibrium is represented by the number of unoccupied receptors plus the number of receptors bound to ligand. Unfortunately the amount of unbound receptor cannot be measured. But substituting [R] in the equation by B_{max}-[RL] and rearrangement, we derive following equation

$$[RL] = B_{max}*[L] / K_d+[L] \qquad \text{(equation 3).}$$

The plotted data, [RL] vs. [L] can then be fitted by non-linear regression using equation 3.
The program used for non-linear regression fitting was KaleidaGraph.

For this procedure 50 µg of membrane protein were mixed in binding buffer with a nicotinic acid mixture composed of [^{1}H]-nicotinic acid and [^{3}H]-nicotinic acid in a ratio of 50:1, to reduce the amount of costly [^{3}H]-nicotinic acid. The total nicotinic acid concentrations were 2 µM, 1 µM, 0.5 µM, 0.25 µM, 0.125 µM, 0.0625 µM, 0.03125 µM and 0.01625 µM, and unspecific binding was measured by addition of 1 mM [^{1}H]-nicotinic acid. Samples were processed as described above, and plotting of free ligand vs. bound ligand and correction for the 50 fold dilution of the radiolabeled ligand resulted in binding curves that were fitted to equation 3, and B_{max} and K_D values were calculated accordingly. All samples were prepared in triplicates.

2.2.5.6 Inhibition Curves

Inhibition curves were recorded by preparing samples that contained 25 µg of membrane protein in binding buffer and a concentration of [^{3}H]-nicotinic acid of 27 nM. Increasing amounts of [^{1}H]-nicotinic acid, Acifran or Acipimox were added at concentrations of 0 nM, 3 pM, 10 pM, 30 pM, 0.1 nM, 0.3 nM, 1 nM, 3 nM, 10 nM, 30 nM, 0.1 µM, 0.3 µM, 1 µM, 3 µM, 10 µM, 30 µM, 0.1 mM, 0.3 mM, 1 mM, 3 mM and 10 mM. Total sample volume was 250 µl. All samples were produced in triplicate, incubated, harvested and measured as described above.

The data obtained from the inhibition curve is described by the equation

$$Y = \text{Nonspecific} + (\text{Total-Nonspecific})/1+10^{\log[D]-\log(IC50)} \quad \text{(equation 4).}$$

This equation can be simplified to

$$Y = \text{Nonspecific} + ((\text{Total-Nonspecific})/1+[\text{Drug}]/IC_{50}) \quad \text{(equation 5)}$$

and according to Cheng and Prussoff [66] K_i and IC_{50} values can be calculated.

$$K_i = IC_{50}/(1+[\text{radioligand}]/K_d) \quad \text{(equation 6)}$$

Assuming that in a homologous inhibition experiment, the hot and the cold ligand have the same affinities the K_d can be obtained from the equation

$$K_d = K_i = IC_{50} - [\text{Radioligand}] \quad \text{(equation 7).}$$

2.2.6 Solubilization

2.2.6.1 Detergent Efficiency Test

For solubilization membrane preparations were adjusted to a concentration of 5 mg/ml with buffer NPB100A and detergent:CHS (5:1) stock solutions were added to a concentration 1 % (w/v). Exceptions were Fos-16, that was used at a concentration of 0.1 % (w/v) and OG and CHAPS that were used at a concentration of 2.5 % (w/v). Solubilization samples were incubated for 1 h at 4°C with gentle shaking and centrifuged at 100000 g for 1 h at 4 °C to remove insoluble material. Supernatants were analyzed by Western-blotting, as well as pellets, resuspended in 4x loading buffer.

Detergent	MW [Da]	cmc [mM]	cmc [%]	stock [%]
β-LM	510,6	0,17	0,0086	10
α-LM	510,6	0,17	0,0076	10
NG	306,7	6,5	0,199	10

OG	292,4	20	0,58	10
UM	496,4	0,59	0,029	10
DM	482,6	1,8	0,086	10
DG	322,4	2,2	0,07	10
LS	524,6	0,3	0,015	10
FOS 12	351,5	1,5	0,052	10
FOS 14	380,5	0,12	0,0046	10
FOS 16	409,5	0,013	0,00053	1
LDAO	229,41	1,4	0,032	10
Cymal-6	508,5	0,56	0,028	10
C12E9	582,5	0,1	0,0058	10
Zwittergent 3-12	335,5	4	0,13	10
CHAPS	614,9	10	0,61	10
SDS	288,4	10	0,288	10

Table 2: List of Detergents used in this study and their properties, molecular weight (MW) and critical micellar concentration (cmc), concentration of the stock solution.

2.2.6.2 Large Scale Solubilization for Purification

Membrane preparations of large scale *P. pastoris* cultures in general contained membrane protein concentrations 20-25 mg/ml. These were diluted in the buffer NPB100A to obtain a membrane protein concentration of 5 mg/ml. Detergent was added to a final concentration of 1 % and 0.2 % CHS. Solubilization mixture was incubated for 1 h at 4 °C with gentle stirring, and centrifuged 100000 g at 4 °C to remove insoluble material. The supernatant was passed through a 0.4 μM filter and used for purification.

2.2.7 Protein Purification

All protein purifications procedures were carried out in the cold room at 4 °C.

2.2.7.1 β-Arrestin 1

2.2.7.1.1 Glutathione Sepharose 4B – Batch Mode

Cleared cell lysates of GST-β-arrestin 1-382/393R169E/fl were incubated with 1 ml glutathione beads per liter culture at 4 °C for 1 h with gentle agitation. Beads were then washed with 10 bed volumes of buffer CB50, and were eluted three times with 5 ml of buffer CB50 containing 10 mM glutathione. Throughout the purification on Glutathione Sepharose 4B 5 mM DTT was used as reducing agent.

2.2.7.1.2 HisTrap™HP (IMAC)

Cleared cell lysates of His-β-arrestin 1-382 were loaded onto a 5 ml HisTrap HP column in lysis buffer containing 10mM imidazole with a flow rate of 5 ml/min, using an Äkta Purifier. The column was then washed with lysis buffer containing 10 mM imidazole until baseline of UV280 nm monitor was reached. His-β-arrestin 1-382 was then eluted with a linear gradient of imidazole from 0 mM to 300 mM in buffer CB50 over 50 column volumes. Fractions were analyzed by SDS-PAGE and His-β-arrestin 1-382 containing fractions were pooled. Instead of DTT, the reducing agent β-mercaptoethanol was used at 5 mM throughout purifications on HisTrap HP material.

2.2.7.1.3 TEV Cleavage (optional)

If removal of the affinity tag (GST/His) was desired, pooled GST-β-arrestin 1-382/393R169E/fl or His-β-arrestin1-382 were incubated with 200 µg TEV per 2 mg pooled elute overnight at 4 °C.

2.2.7.1.4 HiTrap Heparin HP

Purification of β-arrestins on HiTrap Heparin HP column was essentially carried out as described by Han et al 2001 [64].

Pooled elutes from Glutathione Sepharose 4B or HisTrap HP were loaded onto a 5 ml HiTrap Heparin HP column with a flow rate of 2 ml/min on an Äkta Purifier. The column was washed with buffer CB100 for 10 column volumes and eluted with a linear gradient from 400 mM to 1000 mM NaCl over 10 column volumes at a flow rate of 1 ml/min. Fractions were analyzed by SDS-PAGE and β-arrestin containing fractions were pooled.

2.2.7.1.5 Superdex75 Gel Filtration (Preparative)

Gel filtration was done as described by Han et al 2001 [64]. Only β-arrestin 1-382 was used, and tags were removed as described under TEV cleavage (2.2.7.1.3). Up to 2 ml of concentrated β-arrestin 1-382 were loaded onto the Superdex 75 gel filtration column that was previously equilibrated with 2 column volumes of buffer CB100. Fractions were analyzed by SDS-PAGE and β-arrestin 1-382 containing fractions were pooled and either snap frozen in liquid nitrogen and stored at -80 °C or immediately used for further experiments.

2.2.7.2 NAR1

2.2.7.2.1 HisTrap™HP (IMAC)

Solubilized NAR1 was loaded onto a 1 ml HisTrap HP column, previously equilibrated in buffer NPB100A, containing 10mM imidazole with an Äkta Purifier at 1 ml/min. The column was then washed with buffer NPB100A until baseline of UV280 nm monitor was reached, washed to baseline with 15 % NPB100B buffer until baseline was reached. Additionally the column was washed with buffer NPB-low salt for 10 column volumes. NAR1 was eluted with a linear gradient 15 % to 100 % NPB100B buffer over 15 column volumes. Fractions were analyzed by SDS-PAGE and occasionally Western-blotting, NAR1 containing fractions were pooled and used for further purification.

2.2.7.2.2 TEV Cleavage (optional)

If NAR1 was to be cleaved off the tags, 200 µg TEV protease were added to 500 µg of NAR1, and digested overnight at 4 °C.

2.2.7.2.3 Inverse HisTrap™HP

For inverted HisTrap HP purification, NAR1 samples were pooled after HisTrap HP chromatography, TEV added as described above and dialyzed into buffer NPB100A overnight at 4 °C. The dialyzed sample was then treated as described under HisTrap HP, except the Flow Through was kept and a shallow linear gradient from 0 % to 15 % NPB100B buffer was applied and fractions were analyzed by SDS-PAGE.

2.2.7.2.4 Ion Exchange Chromatography: DEAE Sepharose™FastFlow, Q Sepharose™FastFlow, ANX Sepharose™4FastFlow, CM Sepharose™FastFlow, SP Sepharose™FastFlow

Ion exchange chromatography separates proteins on the basis of the charge density on their surfaces, which differs largely according to the folding state of the protein. Unfolded proteins are usually in a random coil state that varies a lot and does not display a defined surface charge density. A good estimation of which resin a protein will bind to can be made by calculating the pI of the protein and deriving which charge it will have at a given pH. For membrane proteins on the other hand it should be considered that the transmembrane portion that in solution is shielded by the detergent might not contribute the relevant surface charges.
All Ion Exchange Columns were equilibrated with buffer NPB0 for 5 column volumes. NAR1 as obtained from IMAC (2.2.7.2.1) was diluted in ten volumes of buffer NPB0, to reduce ionic strength, facilitate binding to the ion exchange resin, and loaded onto the various ion exchange columns, 1 ml/min. The column was washed with 5 column volumes of buffer NPB0 and eluted with linear gradient from 0 % NPB1000 buffer to 20 % NPB1000 buffer over 20 column volumes, and further by a second linear gradient from 20 % NPB1000 buffer to 100 % NPB1000 buffer over another 20 column volumes. Fractions were analyzed by SDS-PAGE and Western Blotting.

2.2.7.2.5 HiTrap Blue HP

The HiTrap Blue Column material was tested, which is composed of the dye Cibacron™ Blue F3G-A, which structurally resembles naturally occurring co-factors NAD^+ and $NADP^+$, and allowed for the affinity purification of different enzymes that required either one. Additionally it has been used for the purification of a number of different proteins, and given the fact that it contained a nicotine amide moiety, which is closely related to nicotinic acid and might be used as a ligand column.
NAR1 as obtained from IMAC (2.2.7.2.1) was diluted in ten volumes of NPB0 buffer, to reduce ionic strength, and loaded onto a 1ml HiTrapHP Blue column, previously equilibrated with 5 column volumes NPB0 buffer. The column was washed with 5 column volumes of NPB0 buffer and NAR1 was eluted with linear gradient from 0% NPB1000 buffer to 20 % NPB1000 buffer over 20 column volumes, and further by a second linear gradient from 20 % NPB1000 buffer to 100 % NPB1000 buffer over another 20 column volumes. Fractions were analyzed by SDS-PAGE and Western Blotting.

2.2.7.2.6 Immobilized Monomeric Avidin

2 ml resin were packed into a 5 ml column (manufactured in the MPIBP workshop), and blocked with 50 column volumes IMA blocking buffer, and regenerated with 20 column volumes IMA regeneration buffer. Then the column was equilibrated with 5 column volumes NPB100A buffer. After IMAC (2.2.7.2.1) purification NAR1 containing fractions were loaded onto the immobilized monomeric avidin column, 0.2 ml/min, and washed until baseline of UV280 nm monitor was reached. NAR1 was eluted with NPB100A buffer containing 2 mM D-biotin. Upon formation of a stable baseline at UV absorbance at 280 nm, the column was washed with IMA regeneration buffer. All fractions were pooled and analyzed by SDS-PAGE.

2.2.7.2.7 Superose 6 Gel Filtration (Analytical)

Superose 6 gel filtration was performed on a SMART system. The column was equilibrated with 4 ml NPB100A buffer. The NAR1 samples were concentrated, and 60µl thereof were run through a 0.2 µM spin filter, 4 min, 2000 g at 4 °C. 50 µl were injected onto the column at a flow rate of 50 µl/min.

2.2.8 Stability Screen

For the stability screen, 3x buffers were prepared using detergents DM+CHS, LM+CHS, Cymal-6+CHS, C12E9+CHS, Fos-12+CHS and Fos-14+CHS, that adjusted the pH (4.0-9.5), NaCl (0 mM, 100 mM, 500 mM) and detergent (1x cmc, 3x cmc) conditions according to table 3. The reservoir of a CrystalQuickSW plate (Greiner) was filled with a 200 µl of a mixture of 3x buffer, H_2O and NPB0 in a ratio 1:1:1. Two out of three wells were filled by a Cartesian Robot with 100 nl of the corresponding 3x buffer, 100 nl of either TEV (1:10 diluted into H_2O) or H_2O and 100 nl NAR1 as obtained from HisTrap HP (IMAC, 2.2.7.2.1) purification. Stability Screen plates were stored at 4 °C and analyzed after 18 h, 42 h, 72 h, 96 h and 168 h for visible precipitates, and ranked accordingly.

	3x Buffer	TEV/H_2O	NAR1 1 mg/ml
pH 4.0	100 nl 100 mM Na-formiate 0/0.3/1.5 M NaCl 3x/9x cmc detergent	100 nl TEV (1:10) or 100 nl H_2O	100 nl NAR1
pH 4.5	100 nl 100 mM Na-acetate 0/0.3/1.5 M NaCl 3x/9x cmc detergent	100 nl TEV (1:10) or 100 nl H_2O	100 nl NAR1
pH 5.0	100 nl 100 mM Na-citrate 0/0.3/1.5 M NaCl 3x/9x cmc detergent	100 nl TEV (1:10) or 100 nl H_2O	100 nl NAR1
pH 5.5	100 nl 100 mM Na-citrate 0/0.3/1.5 M NaCl 3x/9x cmc detergent	100 nl TEV (1:10) or 100 nl H_2O	100 nl NAR1
pH 6.0	100 nl 100 mM MES 0/0.3/1.5 M NaCl 3x/9x cmc detergent	100 nl TEV (1:10) or 100 nl H_2O	100 nl NAR1
pH 6.5	100 nl 100 mM ADA 0/0.3/1.5 M NaCl 3x/9x cmc detergent	100 nl TEV (1:10) or 100 nl H_2O	100 nl NAR1
pH 7.0	100 nl 100 mM MOPS 0/0.3/1.5 M NaCl 3x/9x cmc detergent	100 nl TEV (1:10) or 100 nl H_2O	100 nl NAR1
pH 7.5	100 nl 100 mM HEPES 0/0.3/1.5 M NaCl 3x/9x cmc detergent	100 nl TEV (1:10) or 100 nl H_2O	100 nl NAR1

pH 8.0	100 nl 100 mM Tris 0/0.3/1.5 M NaCl 3x/9x cmc detergent	100 nl TEV (1:10) or 100 nl H_2O	100 nl NAR1
pH 8.5	100 nl 100 mM Tris 0/0.3/1.5 M NaCl 3x/9x cmc detergent	100 nl TEV (1:10) or 100 nl H_2O	100 nl NAR1
pH 9.0	100 nl 100 mM Na-Borate 0/0.3/1.5 M NaCl 3x/9x cmc detergent	100 nl TEV (1:10) or 100 nl H_2O	100 nl NAR1
pH 9.5	100 nl 100 mM CAPSO 0/0.3/1.5 M NaCl 3x/9x cmc detergent	100 nl TEV (1:10) or 100 nl H_2O	100 nl NAR1

Table 3: List of buffers used for the stability screen, and the composition of the drops.

2.2.9 Activity Measurements

2.2.9.1 Immobilization on IMAC-Beads

NAR1 as obtained from HiTrap HP (IMAC) purification (2.2.7.2.1), was dialyzed against NPB0, to remove excess imidazole overnight at 4 °C, and rebound for 30 min to Ni-NTA beads, with gentle agitation. NAR1 was then incubated with [^{3}H]-nicotinic acid:[^{1}H]-nicotinic acid mixture 1:50 (2 µM) for 2 h in NPB0 buffer at room temperature. Beads were then pelleted by centrifugation at 4 °C for 2 min at 500 g, the supernatant removed, beads were washed three times with 500 µl ice cold NPB0 buffer and pelleted again. Remaining radioactivity was measured by scintillation counting, negative control experiments were performed in the presence of 1 mM [^{1}H]-nicotinic acid.

2.2.9.2 Immobilization on Streptavidin Coated Plates

NAR1 as obtained from HiTrap HP (IMAC) purification (2.2.7.2.1) was bound to the wells of Streptavidin coated plates for 30 min and washed once with NPB0 buffer. NAR1 was then incubated with [^{3}H]-nicotinic acid:[^{1}H]-nicotinic acid mixture 1:50 (2 µM) for 2 h in NPB0 buffer at room temperature. The wells were washed 3 times with 200 µl ice cold NPB0 buffer and remaining radioactivity, bound to NAR1 was eluted with 200 µl IMA regeneration buffer, and measured by scintillation counting. Control experiments were carried out in the presence of 1 mM [^{1}H]-nicotinic acid, to determine non specific binding [67].

2.2.9.3 Gel Filtration

BioGel P60-Gel medium was packed into 5 ml polypropylene columns. NAR1 as obtained from HiTrap HP (IMAC) purification (2.2.7.2.1) was diluted to reduce the imidazole content of the sample five fold in NPB0 buffer, and reconcentrated. NAR1 was then mixed with [^{3}H]-nicotinic acid:[^{1}H]-nicotinic acid mixture 1:50 (2 µM) for 2 h in NPB0 buffer at room temperature and then chilled on ice for 5 min. 200 µl of sample were applied to the top of the column, and allowed to enter the chilled (4 °C) resin by gravity flow. After the sample had entered the column completely, additional 2 ml of ice cold buffer NPB0 were added to the reservoir of the column and allowed to enter the matrix by gravity flow. Elution fractions were collected in 100 µl steps, and analyzed by scintillation counting [68].

2.2.9.4 Scintillation Proximity Assays (SPA)

For SPA 50 µl NAR1 was mixed with 50 µl streptavidin PVT or YSi SPA scintillation beads suspension in NPB0 buffer and 50 µl [^{3}H]-nicotinic acid (200 nM, final concentration) or [^{14}C]-nicotinic acid (20 nM, final concentration). Light emission was measured in a MicroBeta Scintillation Counter after 60 min, 120 min and 180 min at 25 °C. Unspecific binding was determined in the presence of 2 µM [^{1}H]-nicotinic acid.

2.2.9.5 Equilibrium Dialysis

NAR1 as obtained from HiTrap HP (IMAC) purification (2.2.7.2.1) was diluted to reduce the imidazole content of the sample five fold in NPB0 buffer, and reconcentrated. NAR1 was then mixed with [^{3}H]-nicotinic acid:[^{1}H]-nicotinic acid mixture 1:50 (2 µM) and filled into

the sample chamber of the RED device. The buffer reservoir was filled with NPB0. 50 µl samples from the sample chamber and the buffer reservoir were analyzed by liquid scintillation counting after 1 h, 2 h and 3.5 h. Control experiments contained 2 mM [^{1}H]-nicotinic acid.

2.2.9.6 Saturation Transfer Difference Spectroscopy (STD)

Reference solutions of each compound (nicotinic acid, Acifran, Acipimox) were prepared at 1 mM in NPB0 with [^{2}H]-glycerol. 1D [^{1}H] NMR spectra were recorded on a DRX600 spectrometer using following parameters:

Parameters	**DRX 600**
Pulse Sequence	**Normal 1D [^{1}H]** (standard BRUKER pulse program) with 3-9-19 WATERGATE sequence for water suppression, gaussian shaped pulses
T (K)	298
Number of Scans	128
Spectral window [ppm]	13.979
O1P [ppm]	4.701
TD	32768

NAR1 was concentrated after HisTrap HP (IMAC) purification (2.2.7.2.1) and diluted into NPB0 buffer prepared with [^{2}H]-glycerol and re-concentrated. This procedure was repeated twice, to reduce the amount of [^{1}H]-glycerol. The final concentration was determined at 10 µM in a volume of 450 µl. 50 µl of D_2O and 10µM TSPA (as concentration reference) were added.

1D [^{1}H] Saturation Transfer Difference (STD) spectra were recorded on a DRX600 spectrometer using the following parameters:

Parameters	**DRX 600**
Pulse Sequence	**STD** (standard BRUKER pulse program) with 3-9-19 WATERGATE sequence for water suppression,

	gaussian shaped pulses
T (K)	298
Number of Scans	128
Spectral window [ppm]	13.979
O1P [ppm]	4.701
TD	32768
Delay (D7) between two scans [µs]	2000
Fq1 on-resonance [Hz]	480-500
Fq1 off-resonance [Hz]	-10000

2.2.10 Reconstitution

2.2.10.1 Activation of BioBeads™

BioBeads were activated by washing 10 g of BioBeads with 100 ml methanol for 15 min at room temperature and thorough stirring. The methanol is then removed, and the BioBeads are washed again in 250 ml methanol. The BioBeads are then hydrated in 500 ml dH_2O. The water is drained and then the BioBeads are resuspended in 1000 ml dH_20 and ready for use.
The detergent binding capacity of BioBeads is now ~100 mg/g.

2.2.10.2 Reconstitution of Solubilized NAR1

2.2.10.2.1 BioBeads™

NAR1 containing membranes were solubilized in DM+CHS, LM+CHS, Fos-12+CHS, C12E9+CHS and Cymal-6+CHS at membrane protein concentration of 5 mg/ml with 1 % of detergent, and cleared by ultracentrifugation as described in solubilization. 1ml of the cleared solubilizate was mixed with 50 mg of BioBeads for 12 h, vigorous shaking at 4 °C. The BioBeads were removed, and the mixture was again incubated with 50 mg of BioBeads. This procedure was repeated twice more. At each time point a sample was taken, analyzed for the membrane protein content and measured as described in Binding Assay Screening Conditions II (2.2.5.1).

Alternatively instead of cleared lysate, purified NAR1 in the corresponding detergent:CHS:asolectin mixture (5:1:5) was used. For each of the 4 consecutive BioBead treatment cycles, the amount of BioBeads was chosen to remove half of the detergent present in the purified sample (5 mg BioBeads/mg detergent) according to the manufacturer's suggestions.

2.2.10.2.2 Gel Filtration

This method was adapted with slight modifications from Cerione et al [69]. 50 µg of lipid thin film (Asolectin/Asolectin:PS 1:2, containing 1 mol% of rhodamine labeled PE) were resolubilized with100 µl of NAR1 (0.1 mg/ml). 100 µl sample were then loaded onto a 1x20 cm column packed with BioGel-P100 and pre-equilibrated with 100 µl of equilibration vesicles (same lipid as above, but solubilized by sonication) in 3 column volumes NPB0 buffer w/o detergent. Upon entering the bed, the reconstitution sample of NAR1 was followed by a pulse of 200 µl detergent stock (10x cmc). The column was then flown at 9 ml/hr and 0.5 ml fractions collected on an Abimed Gilson FC 204 fraction collector. Fluorescence signal of rhodamine labeled PE was traced in 96 well plate and read at 590 nm emission wave length (excitation 550 nm). The first fluorescent peak contained NAR1 reconstituted into liposomes. These were analyzed by Radioligand Binding Assays (Screening Conditions; 2.2.5.1) and Electron Microscopy (2.2.11).

2.2.10.2.3 Cyclodextrin Method

This method was essentially performed as described by DeGrip et al. [70]. Purified NAR1 samples, containing 0.15 % DM, 0.03 % CHS and 0.15 % Asolectin and 1 mol% of the tracer lipid Oregon Green labeled phosphatidylethanolamine (PE), were mixed with β-cyclodextrin at concentrations equimolar to the detergent concentration and incubated on ice for 30 min. Separation of the proteoliposomes from the β-cyclodextrin detergent complexes was achieved by centrifugation through a sucrose step gradient (45 % sucrose, 20 % sucrose, 10 % sucrose and 10 % sucrose containing 10 mM β-cyclodextrin in a ratio of 2:3:2:2), on which the sample was layered carefully. Centrifugation was carried out at 4 °C for 12 h at 200000 g. The proteoliposome fraction containing the Oregon green labeled tracer lipid PE indicated the position of the proteoliposome fraction, which was recovered and used for binding assay as described in Screening Conditions (2.2.5.1) and electron microscopic analysis as described in 2.2.11. A control experiment where no β-cyclodextrin was added did not show such a band.

2.2.10.2.4 Dilution Method

This method was essentially done as described by Cerione et al. [69] and Ambudkhar et al. [71]. 1 ml of purified NAR1, containing 0.15 % DM, 0.03 % CHS and 0.15 % asolectin and 1 mol% of the tracer lipid Oregon Green labeled phosphatidylethanolamine (PE) was diluted in 9 ml NPB0 buffer at once or in a stepwise fashion into 1 ml, this mixture then into 2 ml and again into 6 ml of buffer NPB0, thus lowering the detergent concentration below cmc. After each dilution step the samples were incubated on ice for 10 min. Proteoliposomes were recovered by ultracentrifugation 1 h at 4 °C and 100000 g. The fluorescent proteoliposome pellet was recovered in 200 µl 1x binding buffer and resuspended. Proteoliposomes were then analyzed by the binding assay as described in Screening Conditions (2.2.5.1) and electron microscopy (2.2.11).

2.2.11 Electron Microscopic Imaging

2.2.11.1 Freeze Fracture

Small amounts of the NAR1 vesicle suspensions were enclosed between two 0.1 mm copper profiles as used for the sandwich double-replica technique. The sandwiches were snap frozen by freeze plunging in liquid ethane, cooled to -180 °C by liquid nitrogen. Freeze-fracturing was performed in a BAF400T (BAL-TEC, Liechtenstein) freeze-fracture unit at -140 °C at a pressure of 2 x 10^{-7} mbar using a double-replica stage. The fractured samples were shadowed without etching with 2–2.5 nm Pt/C at an angle of 45°. Additional carbon shadowing was performed at an angle of 90°. The heavy metal replicas were plunged in water and cleaned with 40-50 % CrO_3 H_2SO_4 from adhesive organic materials over night. Finally, they were rinsed in distilled water and mounted onto Formvar® coated copper grids for examination in an EM 208 electron microscope (FEI). All freeze-fracture micrographs were mounted with direction of shadowing from bottom to top.

2.2.11.2 On-Grid – Immuno-Gold Labeling

1-4 µl liposome solution were absorbed to poly-L-lysine (0.01 %) laced Formvar® coated copper grids. Grids were washed twice with PBS (pH 7.5), blocked for 10 min with PBS containing 2 % glycine, and washed again with PBS (pH 7.5). Samples were then blocked again with PBS (pH 7.5) containing 0.1 % BSA, and incubated with M2-Flag Antibody (8 mg/µl). Grids were then washed four times with PBS (pH 7.5)/0.1 % BSA. The secondary

goat anti mouse IgG G12 nm antibody was used in a dilution 1:50 for labeling. Grids were washed three times with PBS (pH 7.5), fixed with 0.5 % glutharaldehyd/PBS (pH 7.5) and rinsed with ddH_2O. Staining was performed with 0.5 % uranylacetate, and mounted for examination in an EM 208 electron microscope (FEI).

2.2.12 NMR Spectroscopic Measurements

2.2.12.1 TROSY Spectra

The [^{1}H, ^{15}N] spectra signifying high quality conditions for NMR experiments were recorded on a DRX600 using the following parameters.

Parameters	**DRX 600**
Pulse Sequence	**TROSYF3GPGHSI19** (standard BRUKER pulse program) using phase sensitivity improvement by Echo/Antiecho method on f3-channel; water suppression by Watergate sequence
T (K)	283/298/310
Number of Scans	96
Spectral window (F2) [ppm]	17.959
Spectral window (F1) [ppm]	36.0015
O1P [ppm]	4.701
O3P [ppm]	119.21
TD (F2)	2048
TD (F1)	128

2.2.12.2 Heteronuclear Overhauser Effects (HetNOEs)

Pairs of 1D [^{1}H]-[^{15}N] HetNOE spectra were recorded at a DRX800 spectrometer. In each pair of spectra, the first spectrum is recorded with 3 s presaturation of amide protons (NOE buildup time) and the second spectrum is without proton presaturation. Gradient selection was utilized to minimize solvent saturation transfer effects in HetNOE data.

Parameters	DRX 800
Pulse Sequence	**hetnoe1dpr** recording NOE/noNOE with WATERGATE gradients with/without presaturation of amide protons
T (K)	283/298/308
Number of Scans	2048
Spectral window [ppm]	14.076
Spectral window (F1) [ppm]	36.0015
O1P [ppm]	4.701
O3P [ppm]	117.00
TD (F2)	4096
Presaturation [µs]	3000

As seen in Figure 14, one dimensional HetNOE data can characterize protein folding as fully folded ([^{1}H]-[^{15}N] HetNOE effect is positive), as unfolded states (effect is negative). Or the protein sample may exist in a dynamic equilibrium between both states (effect is approximately zero) or in an intermediate state, e.g. as a molten globule protein, respectively.

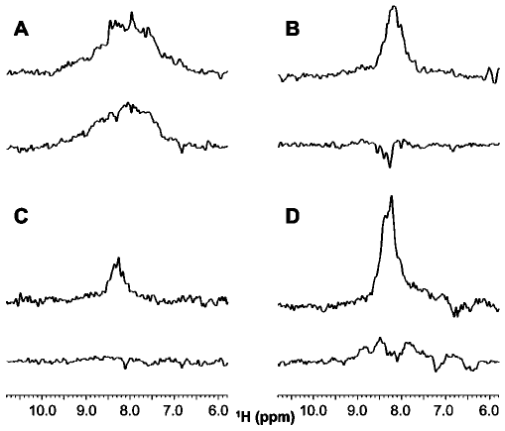

Figure 14: (A) HetNOE spectra of a typical folded protein displaying amide proton chemical shift dispersion and relative similarity in intensities between spectra with and without saturation. (B) HetNOE spectra of a typical unfolded protein with the expected narrow range of amide proton chemical shifts and negative signal intensity when the spectrum is recorded following proton presaturation. (C-D) HetNOE spectra of proteins which are characterized as poor/unfolded by 2D TROSY spectra. Weak positive signals in HetNOE spectra are obtained with amide proton presaturation. These data are interpreted as indicating an equilibrium between unfolded and folded proteins or some partial folded character in the solution state (Figure taken from Snyder et al., 2005 [10]).

2.2.13 Mammalian Cell Culture

2.2.13.1 Cell Growth

BHK (Baby Hamster Kidney) and HEK (Human Embryonic Kidney) cells were used for transient transfection, and confocal microscopy studies. Therefore both cell types were grown in Dulbecco's Modified Eagle's Medium (DMEM) and Iscove's 1:1, supplemented with 5 mM glutamate and 10 % fetal calf serum (FCS), at 37 °C and 5 % CO2. Cells were passaged at a confluency of 70 %, after washing with PBS and detachment with trypsin.

2.2.13.2 Transient Transfection of Mammalian Cells

Mammalian cells, BHK and HEK cells, were transfected by the calcium phosphate method [72, 73]. ~25000 cells were seeded into each of the 4 chambers of a Lab-Tek slide, and grown overnight. Cells were washed with PBS at a confluency of 30 % to 40 % and 300 µl of Ham's F-12 media, supplemented with 5 mM Glutamate and 10 % FCS were added. 1 µg of plasmid DNA was mixed with 16.2 µl 1xHBS buffer, and 1 µl of $CaCl_2$ (2.5 M), and all components were mixed thoroughly, and incubated for 30min at room temperature. The transfection mixture was then added to each well in a drop wise fashion with gentle swirling. The cells were then incubated for 6 h at 37 °C, 5 % CO_2 and another 500 µl Ham's F-12 medium were added. Cells were then grown for another 24 h and analyzed by confocal laser scanning microscopy.

2.2.13.3 Confocal Microscopy

Cells were analyzed on a Zeiss LSM 510 confocal microscope in a climate box (37 °C, 5 % CO_2, 50 % humidity). CFP was excited with a 405 nm diode laser, and detected with a 420-480 nm band pass filter. GFP was excited with 488 nm argon laser and detected with a 505 nm long pass filter. Doubly fluorescent cells were identified in the laser scanning mode. Time track mode was initiated taking pictures sequentially of CFP and GFP every 2 min (line average: 2). After the first image, 500 µM nicotinic acid were added to stimulate NAR1 and trigger β-arrestin 1 translocation. Images were analyzed using programs Imaris and QuantX.

2.2.14 Interaction of β-Arrestin 1-382 with NAR1

100 µg purified GST-β-arrestin 1-382 were mixed with a 300-500 µg purified NAR1 in 1 ml NPB0 containing appropriate amounts of detergents DM+CHS, LM+CHS or Cymal-6+CHS, supplemented with 500 µM nicotinic acid and asolectin. 100 µl of Glutathione 4B resin were added and the mixture was incubated for 60 min at 4 °C with gentle agitation. The resin was pelleted by centrifugation, 500 g, 4 min, at 4 °C and the supernatant removed. The resin was washed twice with 1 ml NPB0 supplemented with detergents DM+CHS, LM+CHS or Cymal-6+CHS, 500 µM nicotinic acid and asolectin. The beads were then resuspended in 100 µl Loading Buffer 4x (SDS-PAGE) and analyzed by SDS-PAGE and Western Blotting.

2.2.15 General Techniques

2.2.15.1 Agarose Gel Electrophoresis

DNA fragments were separated according to size on agarose gels from 1 % to 2 % (w/v). Gels were prepared by boiling appropriate amounts of agarose in 1xTAE buffer until the agarose was dissolved completely. 2.5 µl ethidium bromide solution were added and poured onto a flat bed gel electrophoresis apparatus, equipped with combs. Combs were removed from solidified gels to free the wells for loading, and the gel was covered with 1xTAE buffer. Appropriate amounts of DNA sample mixed with loading buffer 6x (DNA) were filled into the wells and gels run at 75 V until the dye front reached the bottom of the gel. DNA a bands were detected due to intercalating ethidium bromide on a Molecular Imager Gel Doc XR system (Invitrogen) under UV light.

2.2.15.2 Phenol-Chloroform Extraction (DNA Purification)

200 µl sample were mixed with 200 µl chloroform/phenol/isoamylalcohol (25:24:1) and vortexed thoroughly. The sample was then centrifuged for two minutes at room temperature at 13000 g, and the supernatant was transferred to a fresh tube. 200 µl of chloroform/isoamylalcohol (24:1) were added, and vortexed thoroughly. The sample was centrifuged again at room temperature for two min at 13000 g. The supernatant was removed and submitted to ethanol precipitation.

2.2.15.3 Ethanol Precipitation (DNA Concentration)

200 µl of sample were mixed with 20 µl 3 M Na-acetate, pH 5.2, 2.5 volumes of ice cold ethanol and the sample was vortexed thoroughly. The DNA was precipitated for 30 min at -80 °C, and centrifuged at 4 °C and 13000 g for 20 min. The pellet was washed with ice cold 70 % (v/v) ethanol and centrifuged again for at 4 °C and 13000 g 5 min. The pellet was dried in a speed vac for 5 min at 30 °C, and then dissolved in sterile ddH_2O at 65 °C for 5 min.

2.2.15.4 BCA Assay (Protein Concentration Determination)

For quantification of protein content the BCA (bichinonic acid) method was used according to Smith et al, 1985 [74] and the manufacturer's instructions for measurement in 96-well plates. The membrane samples were diluted 1 in 10 into ddH_2O and 1 µg, 2 µg, 4 µg, 6 µg, 8 µg, 10 µg and 12 µg of bovine serum albumin were used to record a calibration curve. Samples were incubated at 37 °C for 30 min and read in a 96-well plate spectrophotometer at 562 nm.

2.2.15.5 TCA Precipitation of Proteins

Trichloroacetic acid (TCA) precipitation was carried out essentially as described by Tornquist and Belfrage (1976) [75]. 500 µl of sample were mixed with 12.5 µl 1 % (w/v) Na-deoxycholate and incubated at room temperature for 15 min. Upon addition of 500 µl ice cold 12 % (w/v) TCA the sample was centrifuged at 4 °C at 10000 g for 20 min. The supernatant was removed, the sample was then additionally centrifuged for 2 min, 4 °C at 10000 g. Residual liquid was removed, and the sample dried at room temperature for 10min. The sample was resuspended in 20 µl to 100 µl 2.5 % (w/v) SDS, incubated for 15 min at 37 °C and analyzed by SDS-PAGE.

2.2.15.6 SDS-PAGE

SDS-PAGE analysis was carried out according to a modification of the Laemmli protocol [76] by Fling and Gregerson [77]. Gels were poured according to table 4 (given below). Samples were mixed with an appropriate amount of 4x SDS-PAGE loading buffer and loaded into sample pockets without heating. Gels were run at 140 V through the stacking gel and at 180 V in the separation gel, until the dye front reached the bottom of the gel. Gels were stained by Coomassie Blue, or used for Western blotting.

	Stacking Gel	Separation Gel 10%	Separation Gel 12%
H2O	11.7 ml	18.1 ml	15.1 ml
Lower Tris (4x)	-	11.25 ml	11.25 ml
Upper Tris (4x)	5 ml	-	-
Acrylamide Solution	3.3 ml	15 ml	18 ml
APS (10%)	60 µl	600 µl	600 µl
TEMED	15 µl	40 µl	40 µl

Table 4: Preparation of SDS-Acrylamide Gels: Pipeting scheme for 8 cassettes.

2.2.15.7 Western-Blotting

For Western blotting the gel was stacked onto three layers of Whatman paper, previously equilibrated in blotting buffer (1 h), covered with a PVDF membrane, previously activated in methanol (5 min) and equilibrated in blotting buffer (1 h), and again covered by three layers of as above described equilibrated Whatman papers. Electrotransfer was carried out at 0.75 mA/cm^2 for 75 min. The membrane was then blocked in 50 ml TBST containing 5 % (w/v) milk powder for 1 h at room temperature, washed twice with TBST and incubated either with the primary antibody (Anti-His, Anti-Flag) or alkaline phosphatase conjugated streptavidin for 30 min at room temperature. The membrane was washed three times for 5 min with 50 ml TBST, and incubated with the secondary antibody (Anti-Mouse alkaline phosphatase conjugated). Secondary antibody incubation was done for 30 min at room temperature, and then washed again three times with 50 ml TBST for 10 min at room temperature. Development was carried out by equilibration of the membrane in 10 ml AP buffer for 1 min and then incubated with 330 µg/ml NBT and 165 µg/ml BCIP in 10 ml AP buffer.

2.2.15.8 Detergent Assay

Detergent concentration was measured with the phenol-sulfuric acid method according to Mikkelsen 2004 [78]. 12.5 µl sample were combined in a 96 well plate with 12.5 µl 5 % (w/v) phenol. A calibration curve was done by serial dilutions of a 1 % LM stock solution. The plate is placed on ice and 125 µl of concentrated sulphuric acid were added. The plate was covered

and incubated at 80 °C for 30 min. Sulfuric acid hydrolyzes polysaccharides to their constituent monosaccharides, which are dehydrated to reactive intermediates. In the presence of phenol, these form yellow products. The absorbance is measured at 492 nm in 96 well plate spectrophotometer.

2.2.15.9 Mass Spectroscopy

For mass spectroscopy all tubes and scalpels were rinsed with detergent and 50% acetonitrile/trifluoracetic acid 0.1 %. The Coomassie stained band was excised and incubated for 45 min at 37 °C in 200 µl 100 mM NH_4HCO_3/50 % acetonitrile. Gel pieces were shrunk in 100 % acetonitrile for 10 min and dried in a speed vac for 15 min at room temperature. Gel pieces were then soaked with 20 µl trypsin solution (20 µg/ml), until their white color disappeared. Remaining trypsin solution was removed, and the gel pieces were covered with 40 µl 40 mM NH_4HCO_3 and incubated for digest over night at 37 °C. The sample was sonicated for 5 min, the supernatant removed, combined with 2 µl 10 % trifluoracetic acid and kept. Remaining gel pieces were covered with 50 µl 50 % acetonitrile/5 % trifluoracetic acid, sonicated for 5 min, and incubated at room temperature with vigorous shaking for 1 h. The supernatant was removed, pooled with the previous supernatant and the procedure repeated. Combined supernatants were dried in a speed vac, washed with 10 µl 1 % trifluoracetic acid and dried again. The pellets were resuspended in 5 µl 70 % acetonitrile/0.1 % trifluoracetic acid by sonication and vortexing.

A saturated solution of a-cyano-3-hydroxy cinnamic acid was prepared in a solution of 10 mg NH_4HCO_3 in 1 ml 50 % acetonitrile, and 0.5 µl were spotted onto the target with 0.5 µl peptide sample solution. The dried matrix was washed four times with 0.1 % trifluoracetic acid and analyzed in a Bruker Daltonic OMNIFLEX MALDI TOF MS mass spectrometer.

3 Results

3.1 Production of the human GPCR HM74A in *P. pastoris*

3.1.1 Cloning

Pichia pastoris was chosen as the heterologous host system for the expression of NAR1, since its success in the production of GPCRs had been shown previously [79-82].

All pPIC9K vectors employed for this study contain the α-factor mating type prepropeptide cDNA of *Saccharomyces cerevisiae* that serves as signal for membrane insertion. The pPIC9K fhT-Tbio vector has an N-terminal Flag-tag for immunodetection and a stretch of ten consecutive histidine residues as an affinity handle. A second vector series (pPIC9KnT-T) encodes for the nano9-tag as the affinity handle in conjunction with a streptavidin matrix. To stabilize the receptor two proteins were used as fusions to the C-terminus:

- The first fusion protein, in the case of the pPIC9KfhT-Tbio is the biotinylation domain of the transcarboxylase of *Propionibacterium shermanii*. The fusion protein has a twofold effect: on the one hand it allows for affinity purification using immobilized monomeric avidin that specifically binds to the biotin moiety, on the other hand it has a positive effect on the stability and functionality of heterologously expressed GPCRs in *Pichia pastoris* [79, 80, 83].
- For the pPIC9KnT-Tstab vector the Stab-tag, which is a modified version of the biotinylation domain, was used. The biotin accepting lysine 56 is replaced by an arginine (Dr. H. Reiländer) to prevent biotin attachment, but preserve the stabilizing effect of the fusion protein.
- Two different length constructs of β-arrestin 1 were introduced as a fusion partner of the GPCR: i) a truncated version, residues 1-382, that is constitutively active (pPIC9KnanoT-Tβarr1-382) and ii) the full length sequence (pPIC9KnanoT-Tβarr1-fl). Reports indicate a stabilizing and protecting effect of such a fusion and an enhanced pharmacological profile [84].

The Stab-tag was amplified by PCR with primers stab-for and AOX1rev from the template pSK+Stab (kindly provided by G. Maul & Dr. H. Reiländer), β-arrestin 1-382 using primers βarr1for and βarr1-382rev, β-arrestin 1-fl with primers βarr1for and βarr1-flrev from the template provided by Sanofi-Aventis Deutschland GmbH. These DNA fragments were ligated after restriction digestion into the *Eco*RI and *Not*I sites of pPIC9KnT (Genetic Engineering 2.2.1).

All vectors contain two Tobacco etch virus (TEV) cleavage sites flanking the *Bam*H1 and *Eco*R1 restriction sites for integration of the GPCR sequence, to allow the removal of all flexible tags.

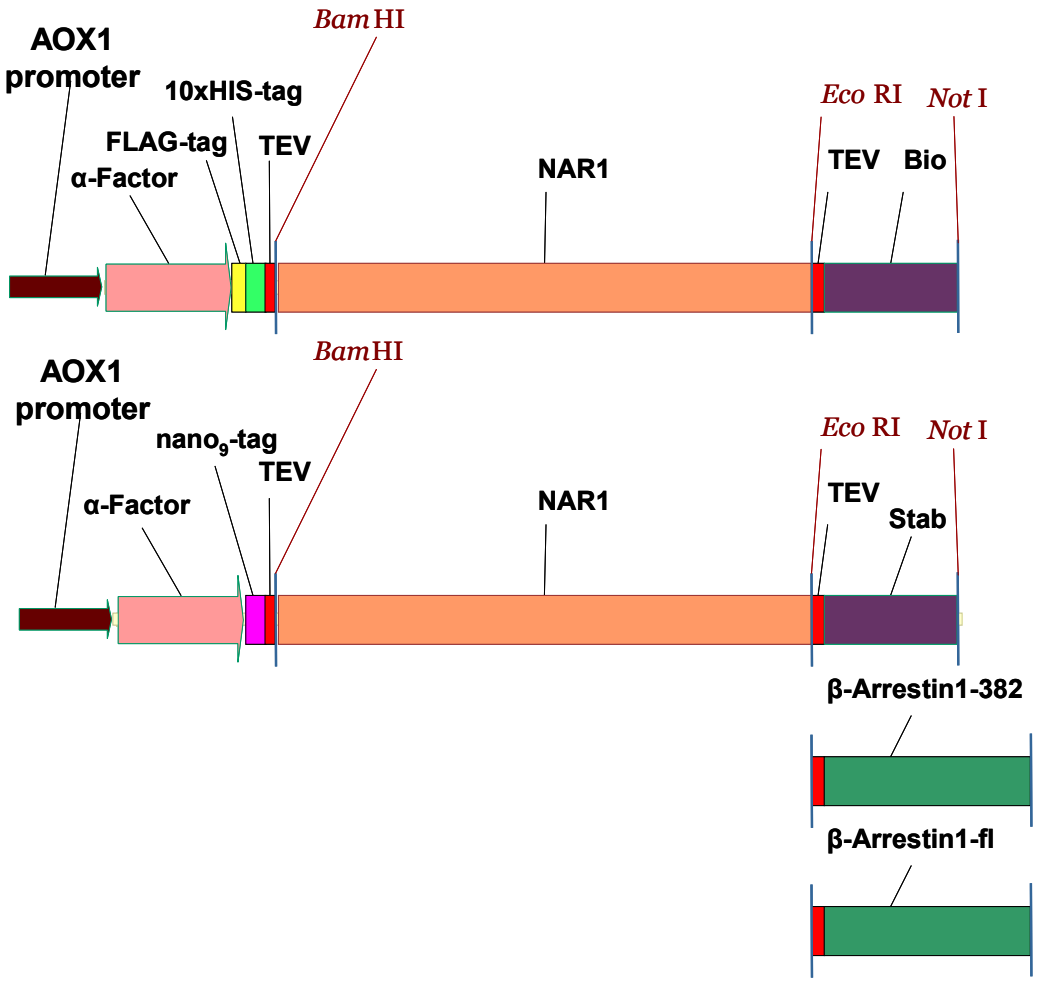

Figure 7: Schematic drawing of constructs for the expression of NAR1 in *P. pastoris*. *Bam*HI, *Eco*RI, *Not*I: Restriction enzyme sites; TEV: Tobacco Etch Virus Protease cleavage site; Bio: Biotinylation Domain; Stab: Stab-Tag; NAR1: coding sequence of the gene HM74A;

The HM74A/GPR109A DNA was mutated to remove an intrinsic *Bam*HI site (Genetic Engineering 2.2.1). The modified DNA of HM-74A/GPR109A was amplified by PCR (primers: NAR1for, NAR1rev) resulting in a band of apparent size of ~1100bp and successfully cloned between *Bam*HI and *Eco*RI sites into the pPIC9K fhT-Tbio and the newly engineered derivatives pPIC9KnanoT-Tstab, pPIC9KnanoT-Tβarr1-382 and pPIC9KnanoT-

Tβarr1-fl. These four vectors were called pPIC9KfhT-NAR1-Tbio, pPIC9KnanoT-NAR1-Tstab, pPIC9KnanoT-NAR1-Tβarr1-382 and pPIC9KnanoT-NAR1-Tβarr1-fl (Figure 7).

3.1.2 Transformation & Multi-Copy Clone Selection

The vector DNAs were linearized with *Pme*I and subsequently transformed into the protease deficient *Pichia pastoris* strain SMD1163, and selection of transformed clones on histidine deficient media was performed.

The task was to identify the highest expressing clone of each NAR1 construct. Although not observed in the production of soluble proteins, it was observed in our laboratory that highest G418 resistance did not always correlate with the highest receptor expression level [79]. Therefore a screen of two different methods for the selection of the highest expressing clone was used. These two methods included the standard antibiotic concentration dependent resistance screen, selecting colonies on the basis of the vector integration number, and a direct-expression colony-blot, selecting on the basis of the target protein expression. Clones selected by both methods were compared on the basis of functional expression in radioligand binding assays and Western-Blot analysis.

96 clones were randomly selected out of the transformands for each expression construct and selection of clones that grew between 0.05 and 1.0 mg/ml final concentration of G418 followed. Based on tolerance to G418, a total of five colonies of pPIC9KfhT-NAR1-Tbio were identified. Clone 1A10 behaved inconsistently in growing on 0.05 mg/ml G418 and on 0.3 mg/ml, but not on intermediate concentrations, and clones 1B2 and 1C4 grew on 0.075 mg/ml, but not on 0.05 mg/ml. Similarly for pPIC9KnanoT-NAR1-Tstab, pPIC9KnanoT-NAR1-Tβarr1-382 and pPIC9KnanoT-NAR1-Tβarr1-fl four, eleven and seven colonies were selected, respectively.

The same 96 clones were analyzed in a direct-expression colony-blot. Instead of the mere copy number of the vector that is the selection basis in the G418 resistance screen, this procedure allows a direct assessment of the production of the desired target protein. For construct pPIC9KfhT-NAR1-Tbio, six clones were selected on the basis of the direct-expression colony-blots.

The direct-expression colony-blot did not allow the identification of nano9-tagged proteins (pPIC9KnanoT-NAR1-Tstab, pPIC9KnanoT-NAR1-Tβarr1-382, pPIC9KnanoT-NAR1-Tβarr1-fl), since streptavidin cross reacts with intracellular biotinylated proteins. Therefore it was neither possible to verify the G418 positive clones, nor to identify additional ones.

Only two clones growing on G418 containing media produced a signal in the direct-expression colony-blots. On the basis of these two methods, a total number of nine clones for pPIC9KfhT-NAR1-Tbio was selected for further analysis, three exclusively on the basis of the G418 screen, four exclusively by the direct-expression colony-blot, and two in agreement to both methods.

3.1.3 Expression Analysis

These nine clones were used for small scale culture growth (2.2.3.2.1) and membrane preparation and entered the second stage of analysis along with the 22 clones obtained for pPIC9KnanoT-NAR1-Tstab, pPIC9KnanoT-NAR1-Tβarr1-382 and pPIC9KnanoT-NAR1-Tβarr1-fl constructs.

3.1.3.1 Western Blotting

For the comparison of NAR1 expression levels, Western-Blots with equal amounts of membrane protein were performed. Western Blot analysis was done using either M2-Flag antibody or Anti-His antibody both directed against N-terminal tag sequences, or with a

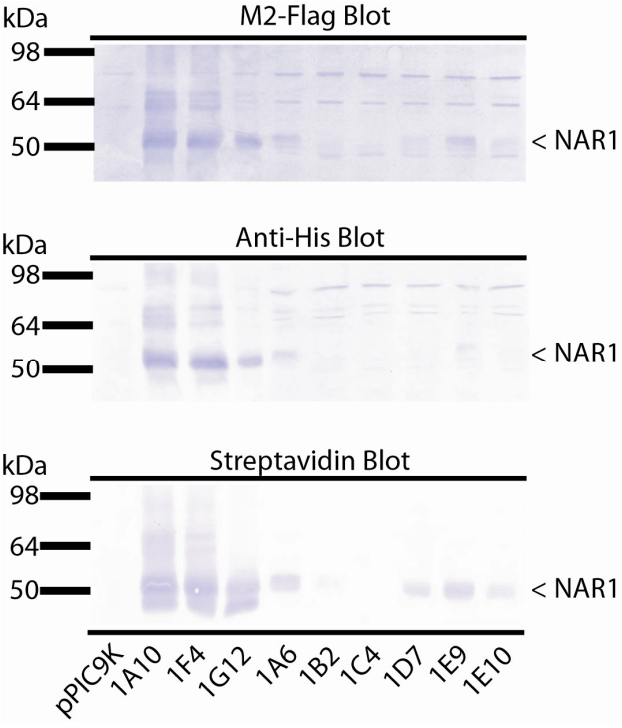

Figure 8: Western Blot analysis of membranes from pPIC9KfhT-NAR1-Tbio clones, 10 µg membrane protein loaded in each lane. Upper pannel: developed with Anti M2-Flag Antibody. Middle pannel: developed with Anti-His antibody. Lower pannel: developed with alkaline phosphatase conjugated Streptavidin.

streptavidin conjugate directed against the C-terminal biotinylation domain. Clones 1A10, 1F4 showed a strong band with either antibody, migrating at an apparent size of 55kDa, in good agreement with the calculated molecular weight of the NAR1 construct. A smaller signal with all three antibodies was observed for clones 1A6, 1E9, and 1G12. Clones 1D7 and 1E10 only showed a signal in M2-Flag and streptavidin blots, but not in the Anti-His blot. Empty pPIC9K transformed cells showed no such band (Figure 8).

All the six clones that were selected on the basis of the direct-expression colony-blot also showed expression in the Western-Blot analysis. Out of the five clones selected due to their resistance to G418, only three produced NAR1 protein according to Western-Blot analysis. The two clones 1A10 and 1F4 that exhibited highest expression levels in the Western-Blot analysis are the two that were selected in both screens, the G418 screen and the direct-expression colony-blot.
Membranes prepared from cultures of clones for the pPIC9KnanoT-NAR1-Tstab, pPIC9KnanoT-NAR1-Tβarr1-382 and pPIC9KnanoT-NAR1-Tβarr1-fl constructs failed to produce a clear signal in a Streptavidin-Blot.

3.1.3.2 Radioligand Binding Assay

The membrane preparations of nine selected clones of pPIC9KfhT-NAR1-Tbio, four of pPIC9KnT-NAR1-Tstab, eleven of pPIC9KnT-NAR1-Tβarr1-382 and the seven clones of pPIC9KnT-NAR1-Tβarr1-fl were also subjected to a functional analysis. Radioligand binding analysis of pPIC9KfhT-NAR1-Tbio clones showed that the two clones 1A10 and 1F4 were binding nicotinic acid above 6000 specific cpm, and another one, 1G12 producing approximately 2500 specific cpm above background. The remaining clones bound radioligand only at low levels, barely above the background value, as determined with membranes from cells transfected with empty pPIC9K vector. Calculation of NAR1 content in membranes revealed at this stage an expression level of 1 pmol/mg for two clones 1A10 and 1F4, although the radioligand binding assay was carried out at non saturating levels of nicotinic acid. These two clones yielding the highest binding level were also the ones that exhibited high level expression in the Western-Blot analysis (Figure 9) (Table 5).

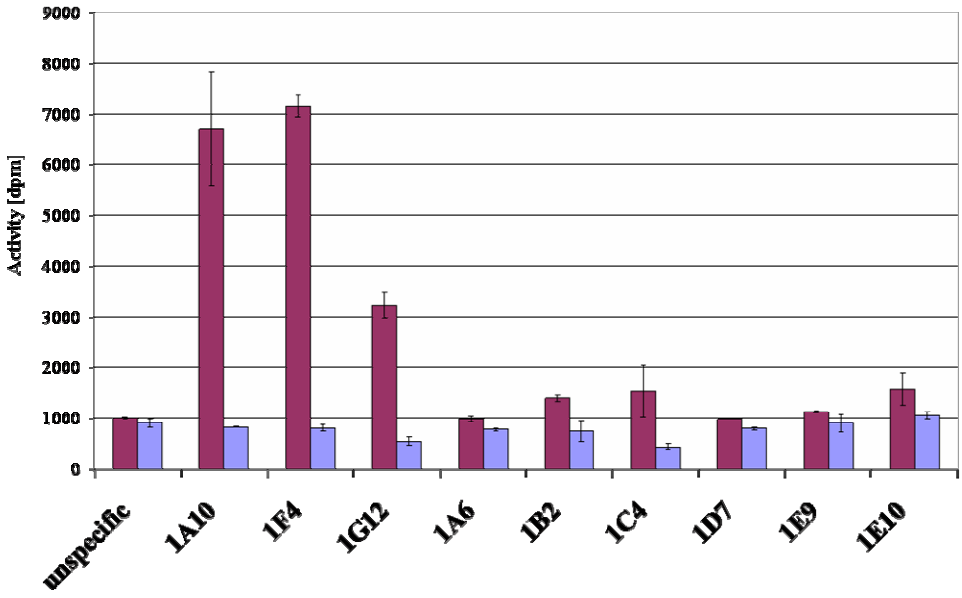

Figure 9: Binding analysis of [^{3}H]-nicotinic acid (97.7 nM) to membranes (50 µg protein) from clones of pPIC9KfhT-NAR1-Tbio. Red: Total binding, blue: Background binding. Unspecific binding was determined with membranes of *P. pastoris* clones transformed with empty pPIC9K vector. The values are the mean of three independent experiments.

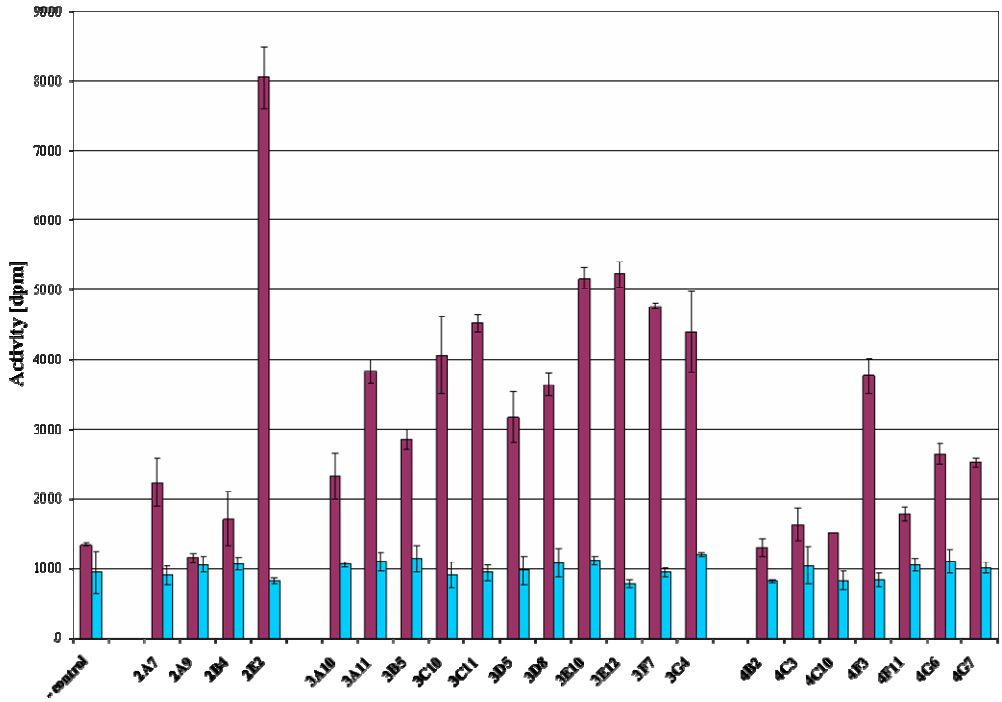

Figure 10: Binding analysis of [^{3}H]-nicotinic acid (111.5 nM) to constructs pPIC9KnT-NAR1-Tstab, pPIC9KnT-NAR1-Tβarr1-382 and pPIC9KnT-NAR1-Tβarr1-fl. Red: Total Binding, blue: Background binding. Background levels were determined with membranes prepared from *P. pastoris* clones transformed with empty pPIC9K vector. Values are the mean of three different experiments.

Out of four clones of pPIC9KnT-NAR1-Tstab, one, 2E2, exhibited binding at a level of 8000 dpm above a background of 1000 dpm. Six of the clones selected for pPIC9KnT-NAR1-Tbarr 1-382 exhibited binding between ~3000 and ~4000 specific dpm, while the remaining clones displayed binding between ~1000 and ~2800 specific dpm. All seven clones of pPIC9KnT-NAR1-βarr1-fl showed low level binding, with the best, 4F3, having ~2800 specific dpm (Figure 10).

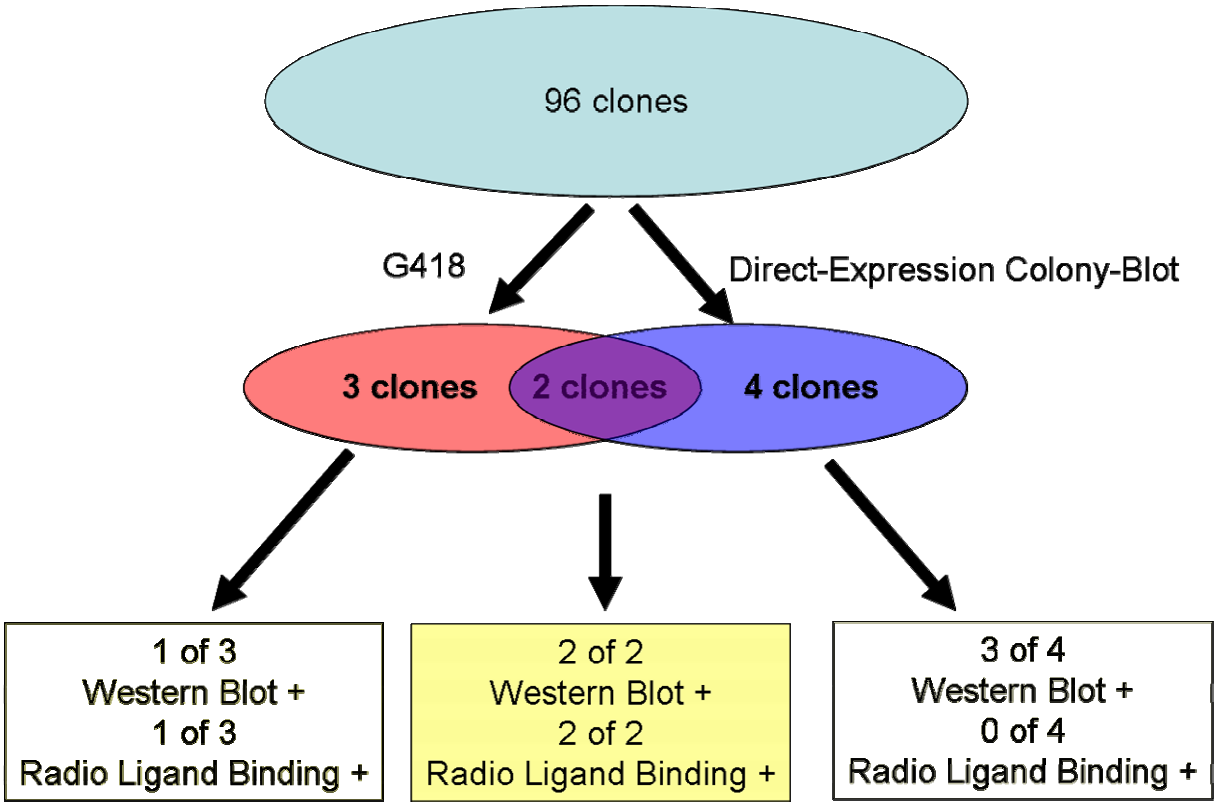

Figure 11: Flow chart of clone selection for pPIC9KfhT-NAR1-Tbio expression construct.

Out of the 96 clones that were selected for high level expression screening of pPIC9KfhT-NAR1-Tbio, only two were found to express NAR1 at levels suitable for future experiments. The initial screening methods, the G418 resistance screen and the direct expression blot, have a limited success rate. Out of all positive clones produced by the G418 screening method, only 40 % could be verified by thorough analysis, while from the direct colony blot 34 % could be verified. By combining both methods and selecting their intersection, both high level expressing clones were obtained (Figure 11).

	-cont	1A10	1F4	1G12	1A6	1B2	1C4	1D7	1E9	1E10
G418 (mg/ml)		0.05 0.3	0.05 0.075	0.05		0.075	0.075			
Direct Blot		+	+		+			+	+	+
M2 Membrane	-	++	++	+	+	-	-	+	+	+
His Membrane	-	++	++	+	+	-	-	-	+	-
Strep Membrane	-	++	++	+	+	-	-	+	+	+
Binding Assay (cpm)	**94.7**	**5886.9**	**6366.6**	**2699.1**	**212.4**	**660.2**	**1098.4**	**189.6**	**231.1**	**525.6**
Binding Assay (pmol/mg)	**0.017**	**1.063**	**1.147**	**0.486**	**0.038**	**0.119**	**0.198**	**0.035**	**0.042**	**0.095**

Table 5: Summary of data collected on clones for pPIC9Kfht-NAR1-Tbio. The G418 row gives the antibiotic concentration the selected clones tolerated. A + in the Direct Blot row indicates identification of the clone due to the direct expression colony blot. M2 shows whether the clones produced a signal in the M2 anti Flag blot, ++: strong signal; +: lower signal; -: no signal. The His row shows whether the clones produced a signal in the anti-His blot, ++: strong signal; +: lower signal; -: no signal. The Strep row shows whether the clones produced a signal in the Streptavidin blot, ++: strong signal; +: lower signal; -: no signal. Binding assay (cpm) gives the values of specific radio active signal observed in single point measurements, and Binding assay (pmol/mg) gives the calculated amount of NAR1 observed due to single point measurements.

3.1.3.3 Determination of the Total Amount of NAR1 produced

For each construct, the clone with the highest expression level was selected for analysis of total amount of receptor produced. To determine the total amount of receptor accurately, saturation binding curves were recorded. Binding curves were recorded for the best clone of all four constructs and allowed for the calculation of B_{max} and K_d values. Clone 1F4, (pPIC9KfhT-NAR1-Tbio) produced NAR1 initially at a level of 14.3 pmol/mg and a K_d of 224 nM (Figure 12).

The other clones containing NAR1 in constructs pPIC9KnT-NAR1-Tstab, pPIC9KnT-NAR1-Tβarr1-382 and pPIC9KnT-NAR1-Tβarr1-fl revealed slightly lower K_ds, 140 nM, 149 nM and 186 nM respectively, but the expression level was also lower than in clone 1F4. The level for clone 2E2 (pPIC9KnT-NAR1-Tstab) was 10.7 pmol/mg and those for pPIC9KnT-NAR1-Tβarr1-382 and pPIC9KnT-NAR1-Tβarr1-fl were 3.7 pmol/mg and 5.5 pmol/mg,

respectively. Therefore, clone 1F4 of pPIC9KfhT-NAR1-Tbio was selected for further expression optimization.

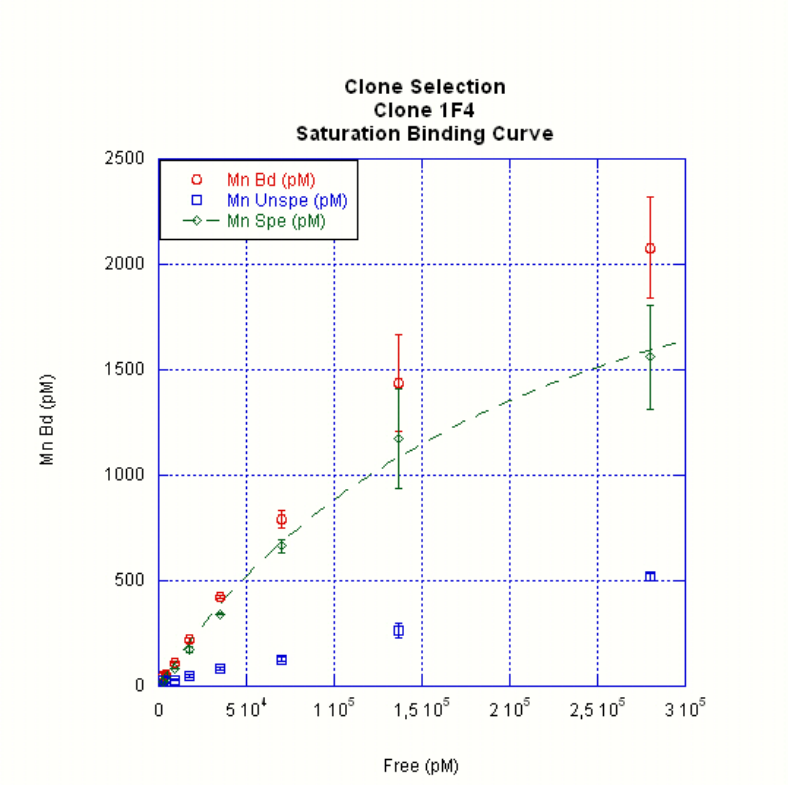

Figure 12: Initial binding curve recorded for construct pPIC9KfhT-NAR1-Tbio clone 1F4 yielded a B_{max} value of 14.3 pmol/mg and a K_d of 224.8 nM. ○: Total Binding of [^{3}H]-nicotinic acid; □:Unspecific binding, determined in the presence of 1mM unlabelled nicotinic acid; -◊-: Specific Binding.

3.1.4 Expression Optimization

According to the pattern developed by André et al, 2006 [79], to improve the amount of functional expression of GPCRs, four parameters were adjusted.

- the temperature during expression
- the addition of DMSO to the expression media
- the addition of a ligand for the receptor to the expression media
- the addition of histidine to the expression media

Cells were either grown at 22 °C or 30 °C and every six hours samples were analyzed for the amount of functional receptor and cell mass. Expression level of NAR1 peaked at 30 °C after 18 h, dropped sharply after and rose again at 36 h. At 22 °C the expression level rose steadily up to 24 h and plateaued between 24 h and 30 h. The cell mass between the expression at 30

°C for 18 h and 22 °C for 24 h to 30 h was nearly identical. Therefore, the expression time and temperature were adjusted for the final expression condition to be 22 °C and 24 hours. DMSO had been shown previously to have a positive effect on the level of functional receptor produced if added to the culture media [79, 85]. The DMSO concentration was screened ranging from 0 % as control to 7.5 %, and it was found that 2 %DMSO increased the B_{max} by 50 % (Figure 13), although it did not seem to have an effect on the total amount of receptor produced, according to Western Blot analysis (data not shown).

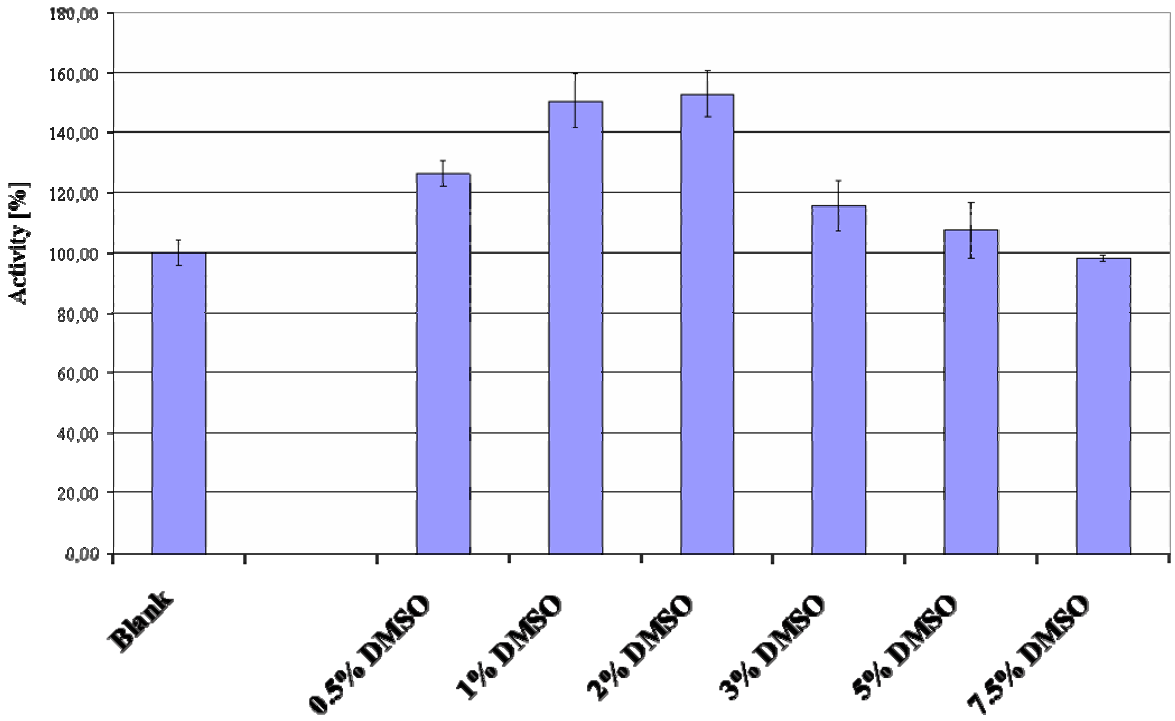

Figure 13: Increased binding observed on membranes from cultures grown in media with DMSO added.

In the MePNet screen [79], the positive effect of ligands, agonists as well as antagonists, on the amount of functional receptor production has been observed, but for the addition of nicotinic acid no positive effect on the production level of NAR1 was observed. The addition of histidine also had no observable effect.

No difference could be seen whether membranes from freshly harvested cells were used, or whether membranes were frozen before analysis (data not shown). No effect was found for

the cell disruption method, whether small scale vortexing with glass beads, larger scale stirring with a baffled steel stick or the cell disruptor was used (data not shown).
The incubation time of the radio ligand binding assay could be reduced from three and a half hours [13, 15] to two hours (Figure 14) as, after that time, the measurable activity did not

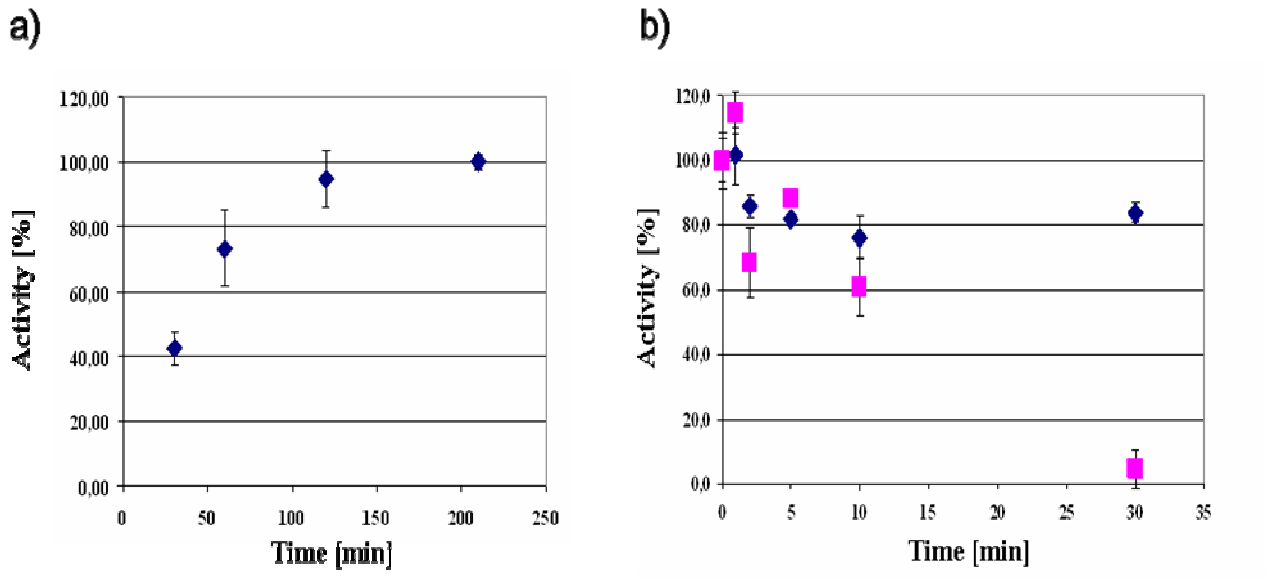

Figure 14: a) Time dependent saturation of NAR1 with [^{3}H]-nicotinic acid in *P. pastoris* membranes, b) Blue: control experiment without cold ligand, total binding barely decreases over time; Pink: [^{3}H]-nicotinic acid displacement by excess unlabelled nicotinic acid.

increase significantly. Furthermore, it was observed that incubation at 22 °C yielded about 60 % more total activity than at 30 °C. Additionally, in a pulse-chase experiment, it was determined that a pulse of excess unlabeled nicotinic acid could displace all previously bound radiolabeled nicotinic acid molecules from the receptor within 30 min (Figure 14).

After optimizing handling parameters and assay conditions as described above, the B_{max} value increased three-fold up to 42 pmol/mg in saturation binding experiments, while the K_d remained in a similar range at 252 nM (Figure 15 a, b). Homologous competition experiments, where unlabeled nicotinic acid was used to compete out radiolabeled nicotinic acid resulted in an affinity of 328 nM and comparable B_{max} (Figure 16 b). Heterologous inhibition curves were performed with the agonists Acifran and Acipimox (Figure 16 a), and resulted in inhibitory constants of 4.57 µM for Acifran and 50.5 µM for Acipimox (Figure 16 b).

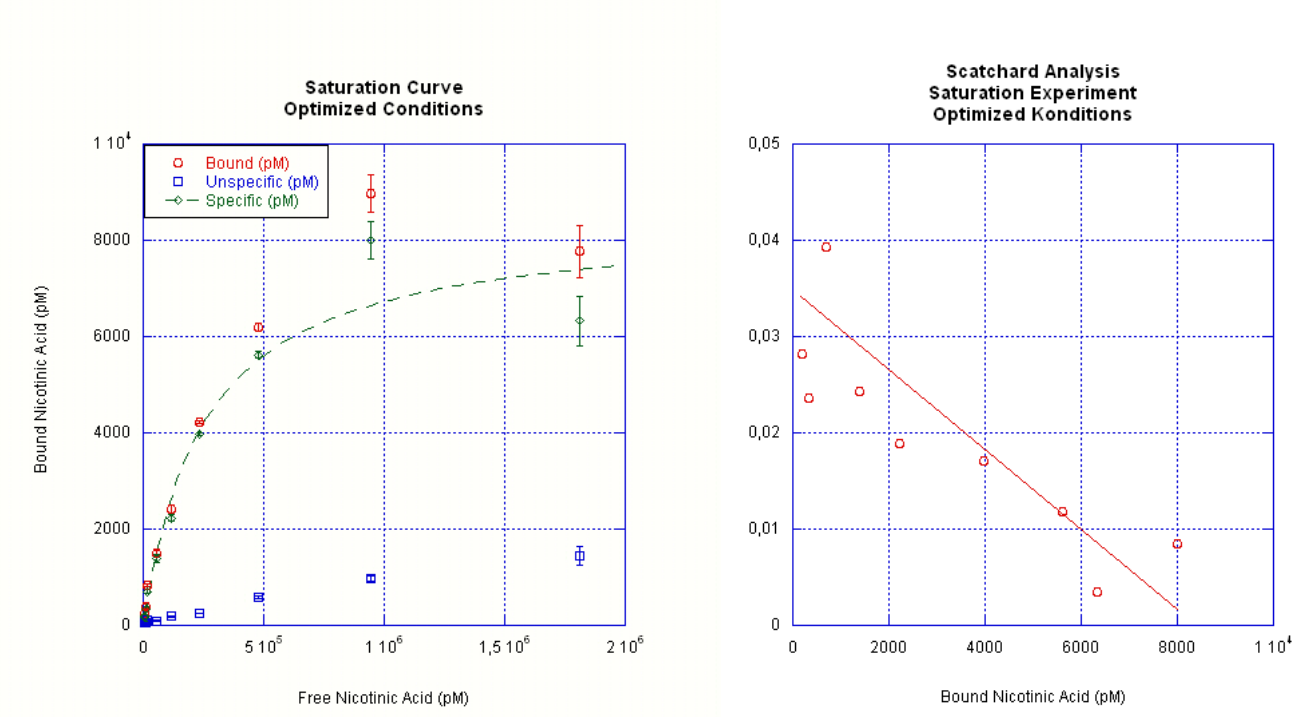

Figure 15: a) Saturation Binding Curve of NAR1 Clone 1F4, B_{max}: 42 pmol/mg, K_d: 252 nM; ○: Total binding of [^{3}H]-nicotinic acid (max.: 2 µM); □:Unspecific binding, determined with 2 mM unlabelled nicotinic acid; -◊-: Specific Binding; 50 µg total membranes; b) Scatchard analysis of binding experiment a), B_{max}: 42 pmol/mg, K_d: 252 nM.

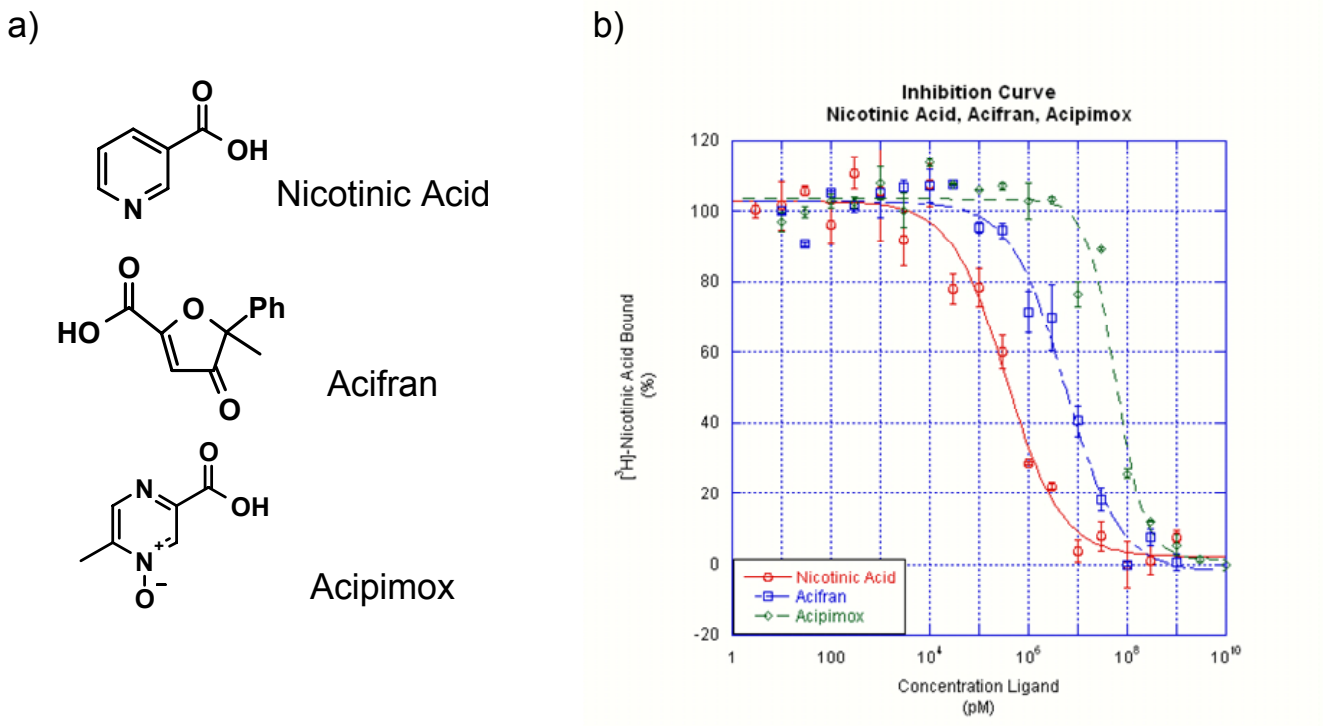

Figure 16: a) Structure of Nicotinic Acid and the Agonists Acifran and Acipimox. b) Inhibition curves, 25 µg membrane protein with 27 nM [^{3}H]-nicotinic acid displaced with ○ [^{1}H]-nicotinic acid concentrations ranging from 3 pM to 1 mM, calculated K_d: 328 nM; □ Acifran, calculated K_i: 4.57 µM; and -◊-Acipimox over a concentration range from 3 pM to 10 mM, calculated K_i: 50.5 µM.

3.1.5 Effect of Various Buffer Components: cations, pH, imidazole, DMSO and DTT

Buffer conditions during future solubilization and purification experiments must be varied to meet the experiments' requirements. Therefore, the influence of various components common to solubilization and purification buffers was assessed, and measured by monitoring the ligand binding activity of NAR1 in membranes and the presence of increasing amounts of additives such as NaCl, DTT, imidazole and DMSO.

It has been shown before for NAR1 that agonist binding is diminished by high concentrations of sodium ions [13], while for other receptors an enhancing effect on antagonist binding was demonstrated [86, 87]. Therefore, different cations were screened in various concentrations to monitor ligand binding properties of NAR1 in membranes in this respect. NaCl had the most detrimental effect on nicotinic acid binding by NAR1. Potassium and lithium chloride had a somewhat less severe effect and it appeared that ammonium chloride, or the ammonium cation, affected the binding reaction least. Ammonium chloride reduced the amount of functionally observed receptor at 250 mM only to 70 % of the initial value without salt, whereas sodium chloride reduced the detectable binding to less than 20 % at concentrations of 100 mM (Figure 17a).

Furthermore, the pH optimum of the receptor ligand interaction was determined. It is evident from the data that the binding optimum for the receptor is at a physiological pH of around 7.0 (Figure 17b).

The effect of imidazole in the binding reaction was assessed because it is used routinely to elute proteins from metal chelate affinity resins. Imidazole shares a similar scaffold with nicotinic acid as it comprises a nitrogen substituted aromatic ring structure. Therefore, it was crucial to know if imidazole competes with nicotinic acid and would impair the binding experiments. Imidazole did reduce the observed binding in radioligand binding assays to 80 % at concentrations of 100 mM and further to a level of 25 % of the initial value recorded without imidazole at 250 mM imidazole (Figure 17c).

DMSO is a solubilizing agent that is frequently used for the preparation of pharmacological compound stock solutions that are poorly soluble in water. The question of whether DMSO would impair the binding of nicotinic acid to NAR1, and therefore render NMR STD Saturation Transfer Difference) studies or binding experiments with compounds in DMSO useless, was addressed. DMSO dramatically affects the observable binding of NAR1 to nicotinic acid in the standard radioligand binding filtration assay.

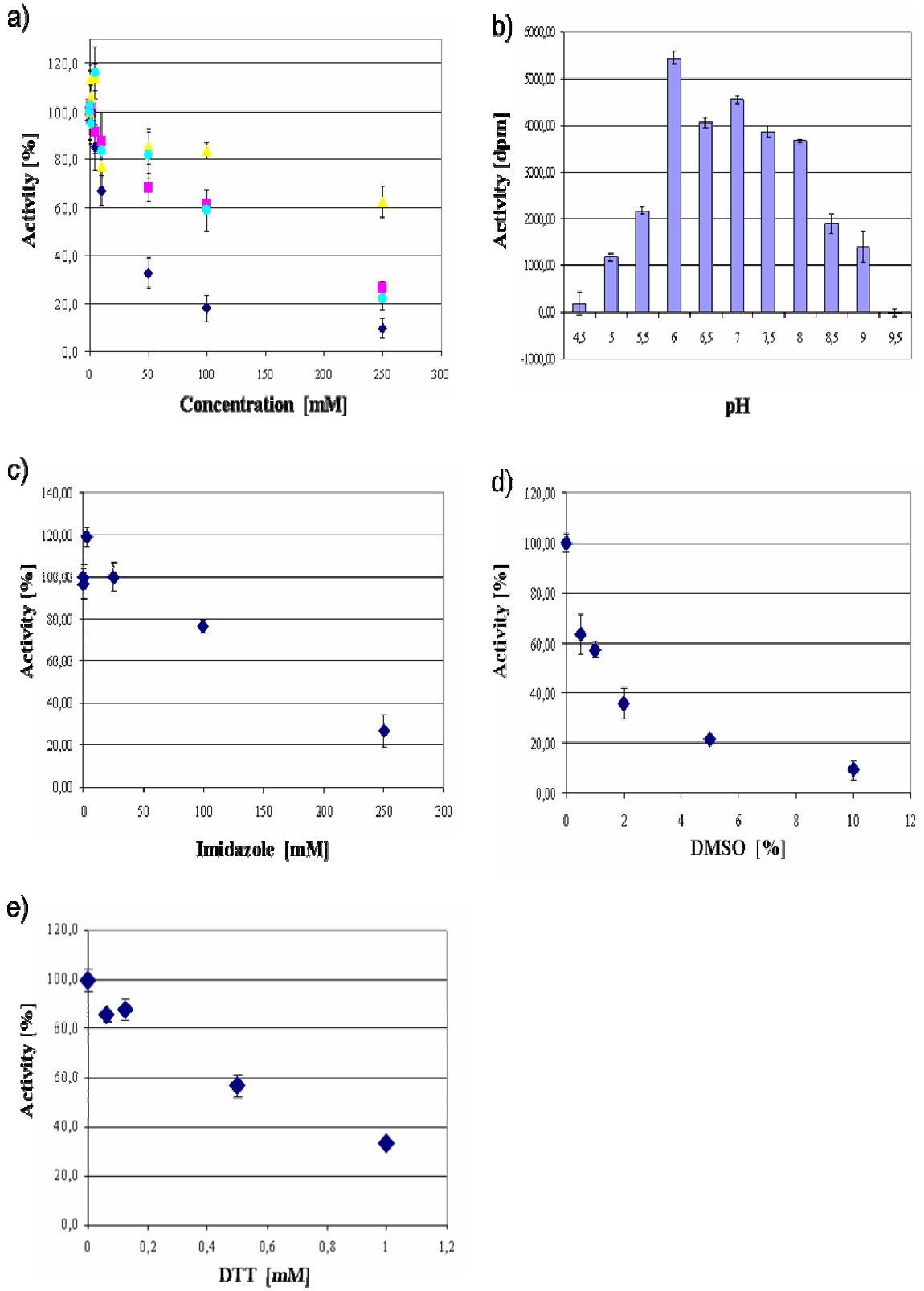

Figure 17: a) Cation concentration dependence of NAR1 binding to [^{3}H]-nicotinic acid. ♦ NaCl, ■ KCl, ● LiCl, ▲ NH_4Cl; b) NAR1 binding to [^{3}H]-nicotinic acid at different pH values; c) Effect of the imidazole concentration on NAR1 binding to [^{3}H]-nicotinic acid; d) Effect of DMSO concentration on NAR1 binding to [^{3}H]-nicotinic acid; e) Effect of the concentration of reducing agent DTT on [^{3}H]-nicotinic acid binding to NAR1

Concentrations of 1 % DMSO reduce the detectable binding to less than 60 % and at 5 % DMSO only little more than 20 % is observed compared to initial binding without DMSO (Figure 17d).

As already mentioned previously, a disulfide bond between the extracellular loops 2 and 3 is a common feature in family A GPCRs. Its pivotal function in receptor activity can be shown by the addition of reducing agents like DTT that reduce binding activity.

In contrast to protein portions on the extracellular side of the membrane, intracellular portions need to be protected from oxidation by addition of reducing agents like DTT to the buffer. Otherwise non-specific formation of disulfide bonds between free cysteine residues can occur and lead to protein aggregation. In any standard preparation of the cytosolic β-arrestin, reducing agents would be present, therefore it was assessed how much DTT could be added along with β-arrestin for complexation with the receptor without affecting its structural and functional integrity. The radioligand binding activity of NAR1 in the presence of increasing amounts of DTT was measured and 1 mM DTT reduced receptor binding to 20 % of its original value. The detrimental effect of DTT on receptor activity furthermore confirms the crucial role for the conserved disulfide bond between extracellular loops 2 and 3 (Figure 17e).

3.1.6 Solubilization

As mentioned already in this work (1.2), the standard procedure for purification of membrane proteins is their extraction from the membrane and solubilization in detergents. In an initial experiment it was tested which out of a standard set of 18 detergents (LM, α-LM, NG, OG, UM, DM, DG, D/C, L-sucrose, Fos-12, Fos-14, Fos-16, LDAO, Cymal-6, C12E9, Zwittergent3-12, CHAPS and SDS) is capable of extracting NAR1 from *Pichia pastoris* membranes. The Western Blot analysis showed that all of the 18 chosen detergents can extract NAR1 from the membranes with the exception of DG (Figure 18).

An additional preliminary screen addressed the question of whether the addition of detergent would have an effect on the observable binding of NAR1 in membranes. Therefore each detergent was added to the binding assay at a concentration of either ten times below and at the critical micellar concentration (cmc). Radioligand binding analyses showed that below the cmc, with the exception of SDS, all detergents were tolerated by the assay format and NAR1.

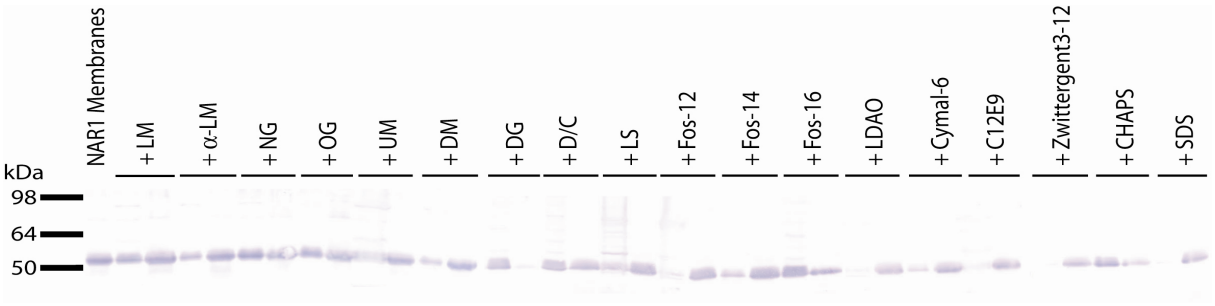

Figure 18: Solubilization of NAR1 from *P. pastoris* membranes with 18 detergents. For each detergent: 1st lane: Solubilization Mixture, 2nd lane: Supernatant; 10 µg membrane protein per lane.

Still, variations in the binding level were also observed in all cases. α-LM, UM, DM, DG, LS, Fos-14, Fos-16 Cymal-6 and C12E9 led to even higher binding levels, while OM, LDAO and Zwittergent3-12 reduced binding levels compared to control membranes. At detergent concentrations of one time cmc, only with α-LM, DM, Fos-16, Cymal-6 and C12E9 significant binding activity could be detected (Figure 19). The same detergents shown above

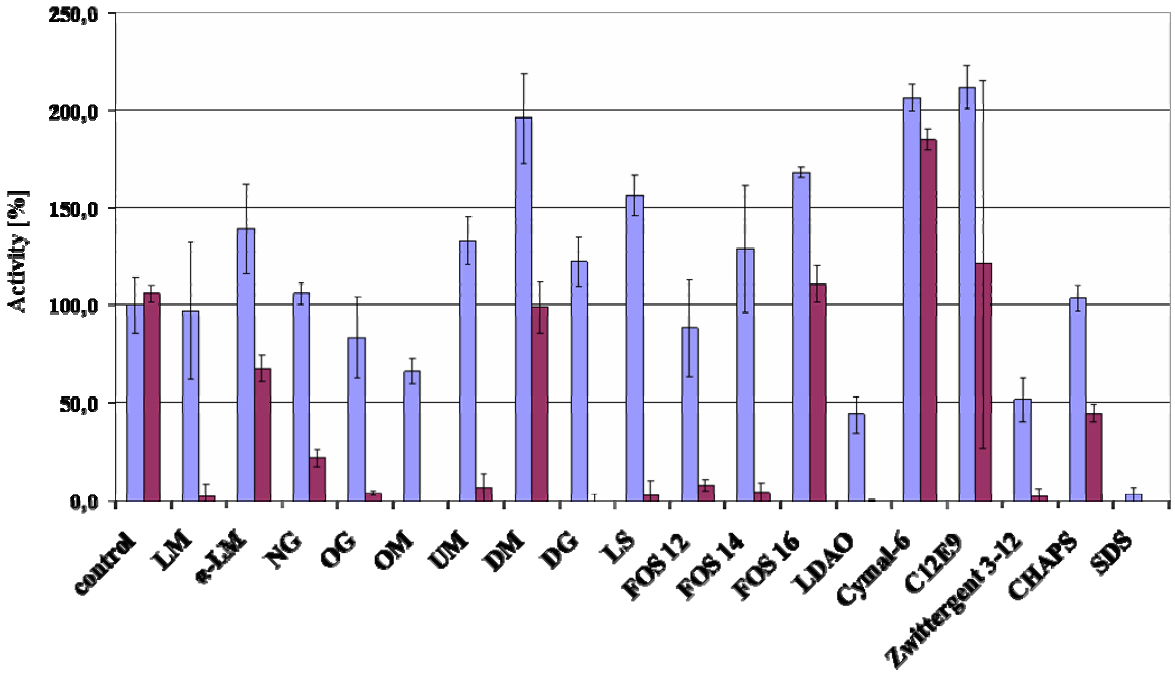

Figure 19: Detergent effect on NAR1 binding to [^{3}H]-nicotinic acid. Blue Bars: Binding activity at 0.1 times the cmc of the detergent in the binding assay, Red Bars: Binding activity at the cmc of the detergent added to binding assay. Control was performed on membranes without detergent.

were tested at concentrations routinely used for solubilization. At detergent concentrations ten times above the cmc no binding was observed in the filtration radioligand binding assay for any of the detergents (data not shown).

Detergent	Solubilization Western Blot	Ligand Binding [%] 0,1x cmc		Ligand Binding [%] 1x cmc	
LM	++	69,3	+/- 15,2	4,2	+/- 4,2
α-LM	++	95,1	+/- 1,8	41,2	+/- 7,3
NG	++	56,9	+/- 2,9	10,3	+/- 3,9
OG	++	46,0	+/- 3,3	1,1	+/- 0,3
OM	++	39,2	+/- 1,2	2,2	+/- 4,1
UM	++	71,1	+/- 12,3	3,8	+/- 1,5
DM	++	97,9	+/- 10,4	62,7	+/- 1,3
DG	-	61,3	+/- 3,9	-0,6	+/- 6,8
LS	++	84,1	+/- 6,9	1,8	+/- 5,2
Fos-12	++	42,7	+/- 9,3	3,6	+/- 1,3
Fos-14	++	66,5	+/- 16,0	1,1	+/- 3,7
Fos-16	+	86,7	+/- 2,4	61,6	+/- 5,1
LDAO	++	22,6	+/- 2,9	-0,3	+/- 0,6
Cymal-6	++	104,2	+/- 1,1	108,8	+/- 1,4
C12E9	++	95,0	+/- 3,6	65,5	+/- 48,5
Zwittergent 3-12	++	27,1	+/- 4,9	1,5	+/- 0,3
CHAPS	+	52,1	+/- 4,1	25,1	+/- 1,0
SDS	++	0,5	+/- 0,9	-25,6	+/- 10,2

Table 6: Summary of data collected on radioligand binding assays in the presence of detergents with CHS without centrifugation prior to the assay. Column Solubilization Western Blot shows the capability of the detergent to extract NAR1 from the membrane: ++: all receptor was Solubilized; +: most of the receptor was Solubilized; -: the receptor was not Solubilized. Columns Ligand Binding [%] give the amount of ligand binding at detergent concentrations in the assay of 0.1 cmc and the cmc. Values are given relative to those measured in membrane samples assayed without detergent.

In a further set of experiments the question asked was whether the loss of binding due to detergent addition was reversible. NAR1 containing membranes were solubilized with 1% detergent (w/v) containing 0.2 %(w/v) cholesteryl hemisuccinate, insoluble material was pelleted by centrifugation and then the detergent was subsequently removed with BioBeads. BioBead treatment did not show any effect on the binding activity of unsolubilized membranes, while DM/CHS solubilized membranes showed a recovery rate of up to 35 % of binding activity. The recovery rate with LM/CHS was much lower and yielded finally 15 % recovery of binding activity. Cymal-6/CHS behaved in a similar way, but yielded 20 % of the reference value after complete detergent removal. Furthermore the amount of detergent left in the DM/CHS, LM/CHS and Cymal-6/CHS samples was determined and recovery of the activity could only be seen once the detergent had been removed completely (Figure 20a, b).

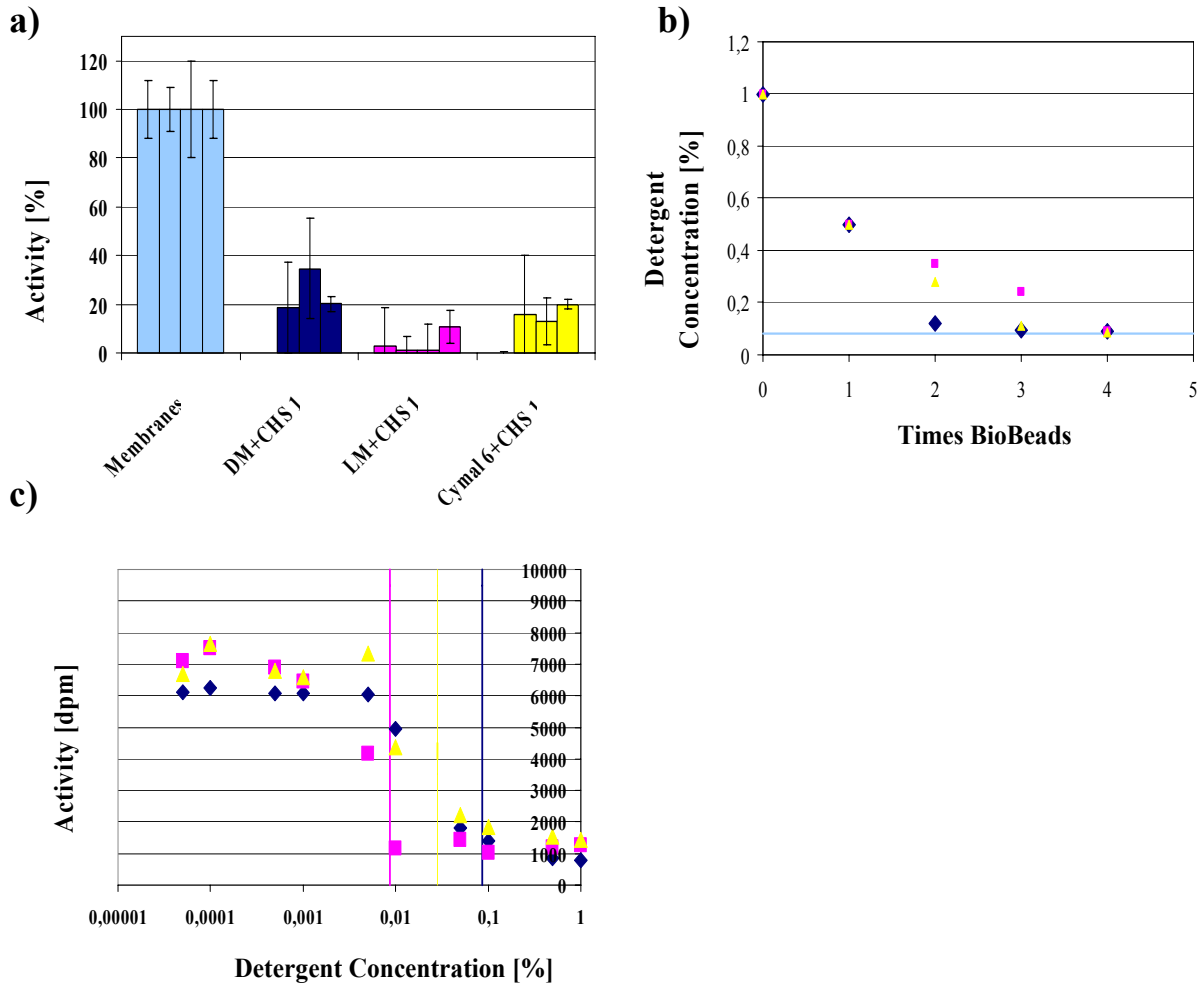

Figure 20: a) Recovery of ligand binding activity after solubilization and stepwise detergent removal with BioBeads (4 rounds); light blue bars: membranes; dark blue: DM+CHS solubilized NAR1 membranes; pink bars: LM+CHS solubilized NAR1 membranes; yellow bars: Cymal-6/CHS solubilized NAR1 membranes; b) remaining detergent in samples from a) ♦: DM concentration; ■: LM concentration; ▲: Cymal-6 concentration; ▬: membranes without detergent. c) Loss of [^{3}H]-nicotinic acid binding of NAR1 with increasing detergent concentrations; ♦: DM+CHS; ■: LM+CHS; ▲: Cymal-6+CHS; ▌DM cmc (~0.086 %(w/v)); ▌LM cmc (~0.0086 %(w/v)); ▌Cymal-6 cmc (~0.028 %(w/v)).

It was more thoroughly investigated at which concentration detergents inhibit the interaction between NAR1 and nicotinic acid or that with the receptor and the glass fiber filter. Therefore increasing amounts of DM+CHS, LM+CHS and Cymal-6+CHS mixtures were added to the binding reaction and the remaining ligand binding activity was analyzed. It is clearly evident, that as soon as the detergent concentrations come close to the critical micellar concentration, the measurable binding activity is lost (Figure 20c).

3.1.7 Purification & Enzymatic Processing

3.1.7.1 HisTrap™HP (IMAC)

The first purification step was chosen to be an immobilized metal affinity chromatography (IMAC) step that uses the decahistidine tag for specific interaction with the nickel loaded resin. The cleared solubilizate of membrane proteins was loaded onto a HisTrap HP column and eluted initially with a shallow linear gradient up to 300 mM imidazole. It was found that NAR1 remained tightly bound to the column up to concentrations of 60 mM imidazole (Figure 21a). Additionally it was found that an endogenous *Pichia pastoris* protein running at an apparent molecular weight of 40 kDa, that appeared as recurrent impurity in the purification of several other proteins expressed in *Pichia pastoris*, could be significantly reduced by the introduction of an additional no-salt washing step (Figure 21b) (C. Reinhart, personal communication).

3.1.7.2 Post-Translational Modifications & TEV Cleavage

Crude preparations of NAR1 were used for characterization of the post translational state of the protein and cleavability by TEV protease. SDS-PAGE and Western-Blot analysis confirmed the identified band, migrating at an apparent molecular weight of 55 kDa as NAR1. Additionally, TEV cleavage produced a truncated fragment of an apparent molecular weight of ~40 kDa that corresponds to the expected size of the untagged NAR1 expression construct (Figure 22). Furthermore, the signal for that band disappeared in the anti-His Western-Blot. The Coomassie gel excised band was identified as NAR1 by mass spectrometric analysis at the laboratories of Sanofi-Aventis Deutschland GmbH.

One problem that arises with the heterologous overexpression of membrane proteins is the differential glycosylation pattern compared to its pattern in a homologous organism. The NAR1 amino acid sequence evaluated with a bioinformatics tool, NetOGlyc 3.1 [88], identifies two potential consensus sequences for O-linked glycosylation, Threonine 360 and Serine 361. A similar tool, NetNGlyc 1.0 [89], predicts N-linked glycosylation sites, and found two within the NAR1 sequence, Lysine 140 (**N**RTA) and Lysine 335 (**N**KTR) (Figure 23a). All these signature sequences are found within the cytosolic parts of NAR1, and therefore not subjected to glycosylation, which occurs only at the extracellular portions of proteins. This *in silico* prediction could be confirmed by enzymatic assays using PNGase F

and Endo-H. After treatment with these two enzymes no altered mobility on SDS-PAGE could be observed (Figure 23b).

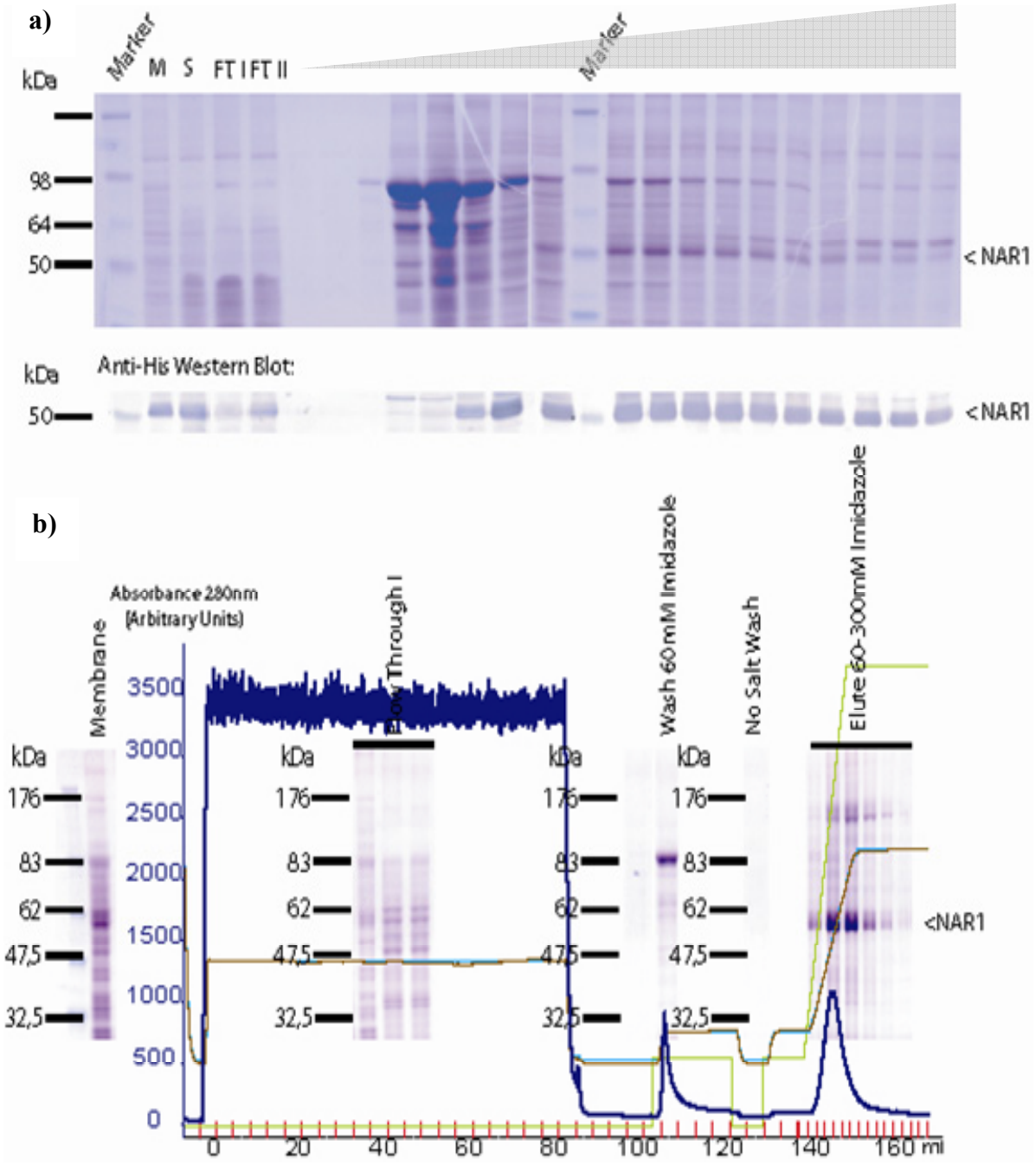

Figure 21: a) 10 % SDS-PAGE, Coomassie stained and corresponding Anti-His Western-Blot of initial NAR1 IMAC purifiaction, with DM+CHS as detergent. M: Membranes (10 µg); S: Solubilizate; FT I: First Flow Through Fraction; FT II: Second Flow Through Fraction; The grey bar indicates 15 µl samples of 2 ml fractions from the imidazole gradient (0 mM – 300mM). b) Chromatogram of final purification and corresponding Coomassie stained 12 % SDS-PAGE.

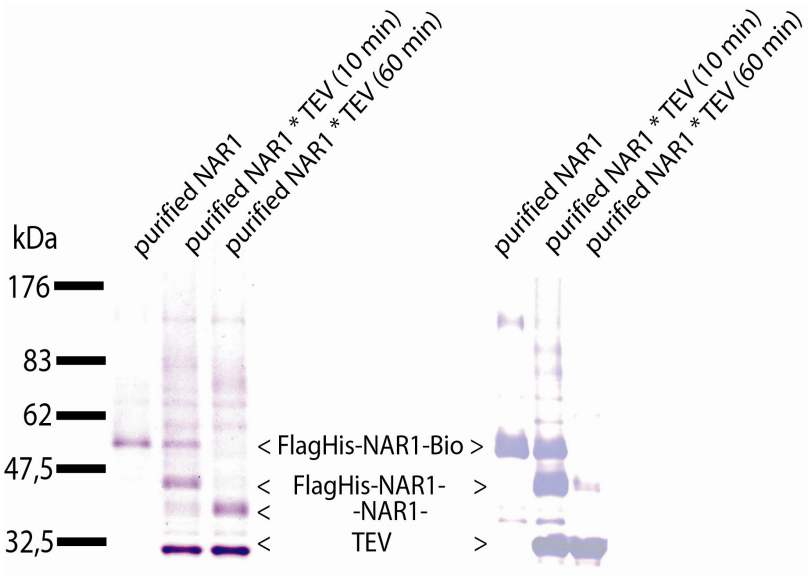

Figure 22: left panel: 12% SDS-PAGE, Coomassie stained (10µg total protein loaded each lane); NAR1 cleaved by TEV protease; right pannel: Corresponding Anti-His Western-Blot (10µg total protein loaded each lane).

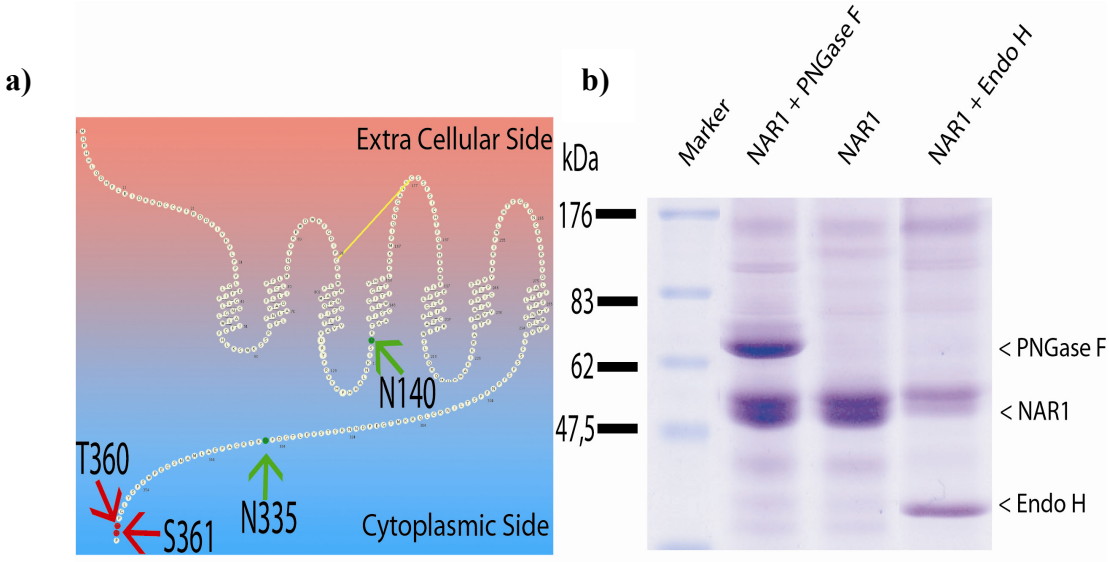

Figure 23: a) NAR1 piktogram, predicted N-linked glycosylation sites (N140, N335) marked with a green arrow, predicted O-linked glycosylation sites (T360, S361) are indicated by a red arrow. b) 10 % SDS-PAGE showing PNGase F treated NAR1, NAR1 and EndoH treated NAR1 (10 µg total protein loaded each lane).

After TEV cleavage most of the NAR1 protein precipitated, and the intended inverse affinity chromatography was not possible. Therefore a number of different chromatographic steps were evaluated as a second one, to separate unfolded precipitating species after TEV cleavage from folded ones.

3.1.7.3 Ion Exchange Chromatography of TEV cleaved NAR1

Five different ion exchange columns, the anion exchange resins DEAE, Q and ANX Sepharose as well as the cation exchange materials CM and SP Sepharose were tested according to their ability to separate folded from unfolded, precipitating NAR1.

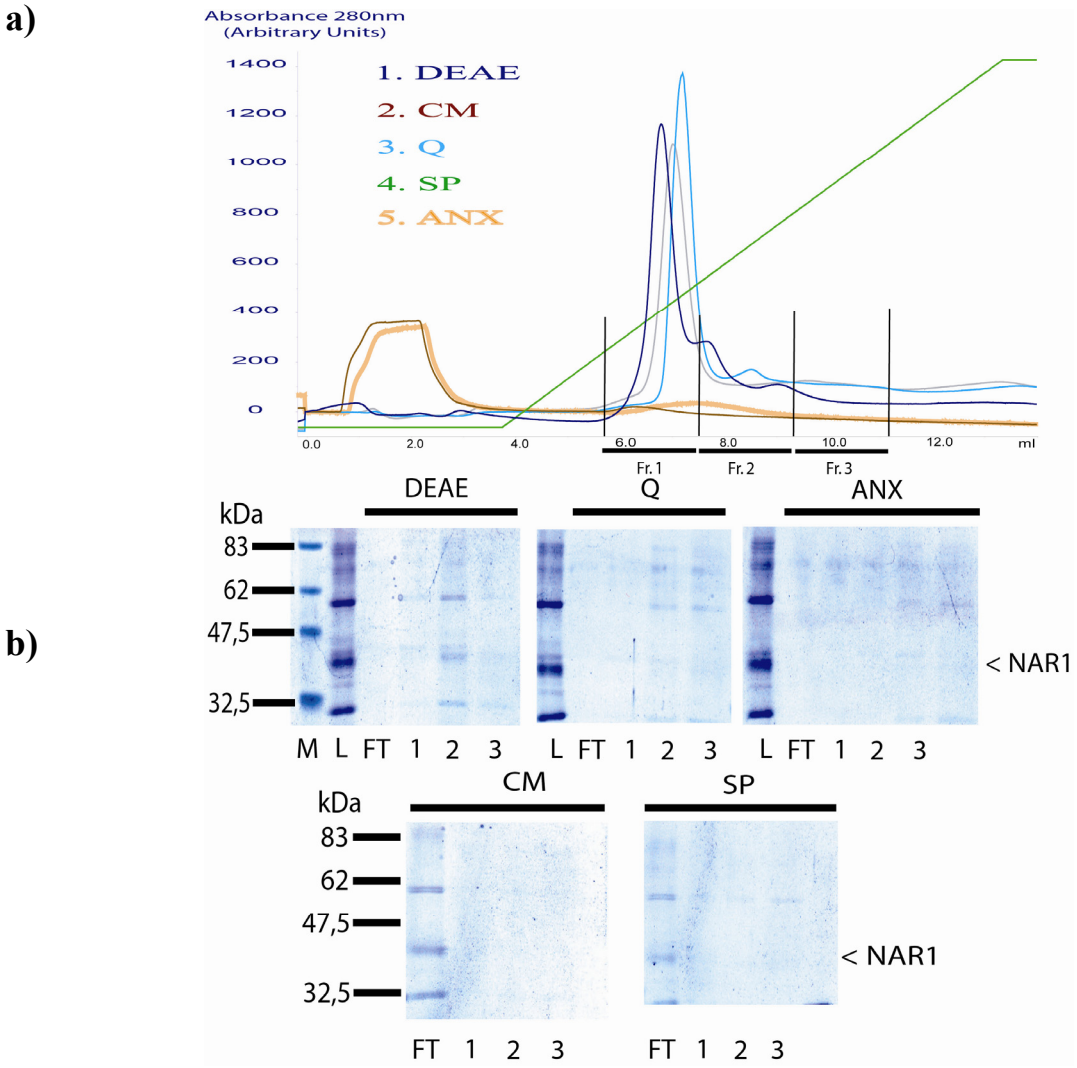

Figure 24: a) Chromatogram comparison of NAR1 purification on various ion exchange resins. Blue: DEAE; Light Blue: Q; Grey: ANX; Red: CM; Yellow: SP; Green: Gradient; Orange: Conductivity. b) 12 % SDS-PAGE, Coomassie stained. Lanes show 15 µl samples of the indicated fractions from the different column materials. M: Marker; L: Load; FT: Flow Through; 1: Fr. 1from a); 2: Fr. 2 from a); 3: Fr.3. from a).

NAR1 was initially purified on an IMAC column as described above (3.1.7.1), genetically engineered tags were removed by TEV cleavage, loaded onto the various resins, and eluted with a linear salt gradient.

The cation exchangers CM and SP did not bind NAR1 and did not result in an increased purity of the sample. Anion exchange columns did bind the receptor and NAR1 was eluted in

a salt concentration dependent manner. SDS-PAGE analysis showed however that the major peak did not correspond to the receptor. NAR1 was found in DEAE and Q elution profiles in the fraction following the major peak. In the DEAE column elution profile, this corresponds to a distinct shoulder of the major peak. The fraction that contained NAR1 in the SDS-PAGE did not show a peak in the Q elution profile. No fraction could be identified that contained NAR1 in the ANX elution profile. In fact, the NAR1 protein did not appear in any of the ANX fractions (Figure 24). Although the DEAE column improved protein purity slightly, the major problem remained protein stability and could not be overcome by the addition of ligand and asolectin. The major part of the protein precipitated either during TEV cleavage, during the second chromatography step or shortly after.

3.1.8 Stability Screen

Finding buffer conditions that preserved the activity of NAR1 was an important goal. The tested conditions varied with respect to pH, detergent type, detergent concentration, ionic strength and, for the tag-containing and the TEV processed state the NAR1 construct. An artificial stability score was set up, where samples were attributed a value of 2 for clear samples without precipitation, and 0 for massive precipitation. Intermediate scores of 0.5 and 1 were attributed to samples that displayed only slight precipitation. Tested detergents included DM/CHS, LM/CHS, Cymal-6/CHS, C12E9/CHS and the harsher detergents Fos-12/CHS and Fos14/CHS that produced good results for other receptors in our group. The detergent concentrations were varied between 1.5 times the cmc and 3 times the cmc. Furthermore, the pH was varied between 4.0 and 9.5, and the NaCl concentration was tested at values of 0 mM, 100 mM and 500 mM.

The results of this stability screen showed that differences between detergents are tremendous. While in DM/CHS the addition of TEV protease led to the precipitation of nearly all conditions within 24 hours, harsher detergents like Fos-12/CHS were capable of keeping NAR1 in solution for more than 144 hours, despite TEV cleavage (Figure 25a). Another observation showed increased stability at higher detergent concentrations for cleaved NAR1. For example at 3 times cmc TEV cleaved NAR1 was stable in DM/CHS for up to 48 hours, compared to only 24 hours at 1.5 times cmc (Figure 25b). The phenomenon of prolonged solubility was also observed at higher salt concentrations (Figure 25c). Yet, most importantly, even in milder detergents at low concentrations, the tagged NAR1 was more stable than the

a)

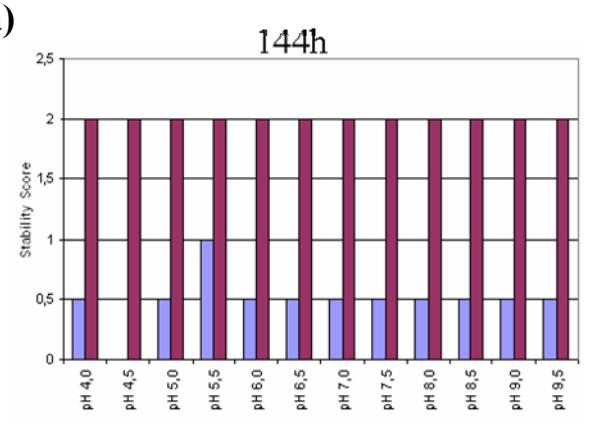

Figure 25: a) Comparison of NAR1 stability in respect to detergents DM and Fos-12 after 144h. Blue Bars: 1x cmc DM + TEV showed precipitation at all conditions and were attributed scores between 0 and 1; Red Bars: 1x cmc Fos12 + TEV remained clear throughout the experiment and were attributed the score 2.

b)

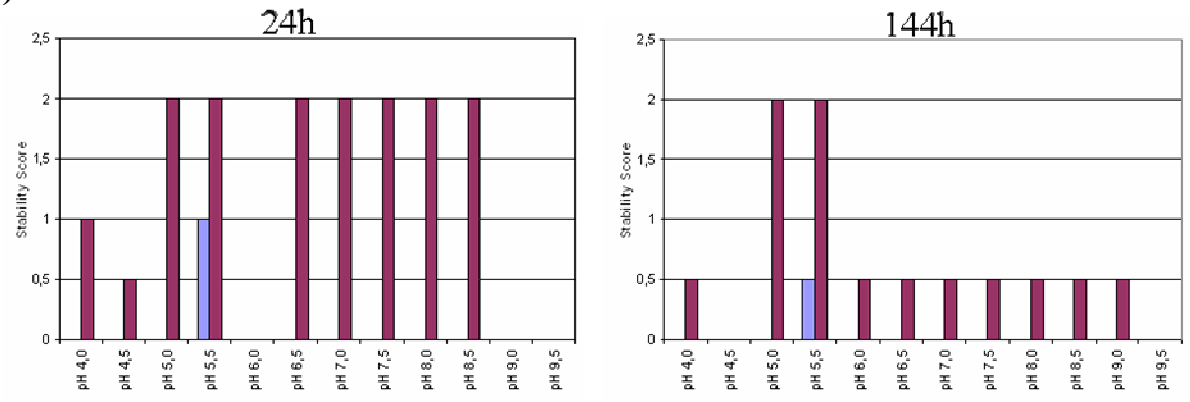

Figure 25: b) Comparison of NAR1 stability with respect to detergent concentration without TEV at 24 h and 144 h, Blue Bars: 1x cmc DM/CHS; after 24 h only at pH 5.5 slight precipitation occurred and increased after 48 h. All other samples showed massive precipitation. Red Bars: 3x cmc DM; Most samples remained clear and were attributed score 2. After 48 h precipitation increased but was less severe than at lower DM concentrations

c)

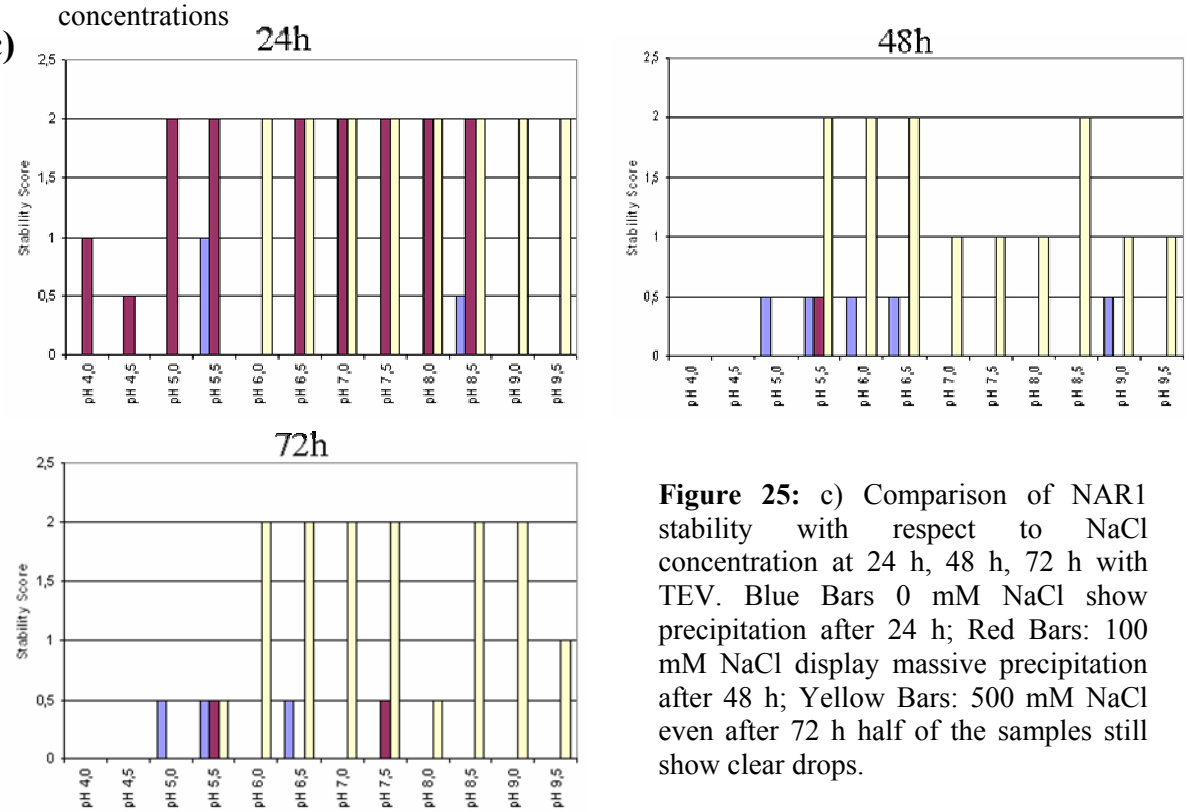

Figure 25: c) Comparison of NAR1 stability with respect to NaCl concentration at 24 h, 48 h, 72 h with TEV. Blue Bars 0 mM NaCl show precipitation after 24 h; Red Bars: 100 mM NaCl display massive precipitation after 48 h; Yellow Bars: 500 mM NaCl even after 72 h half of the samples still show clear drops.

d)

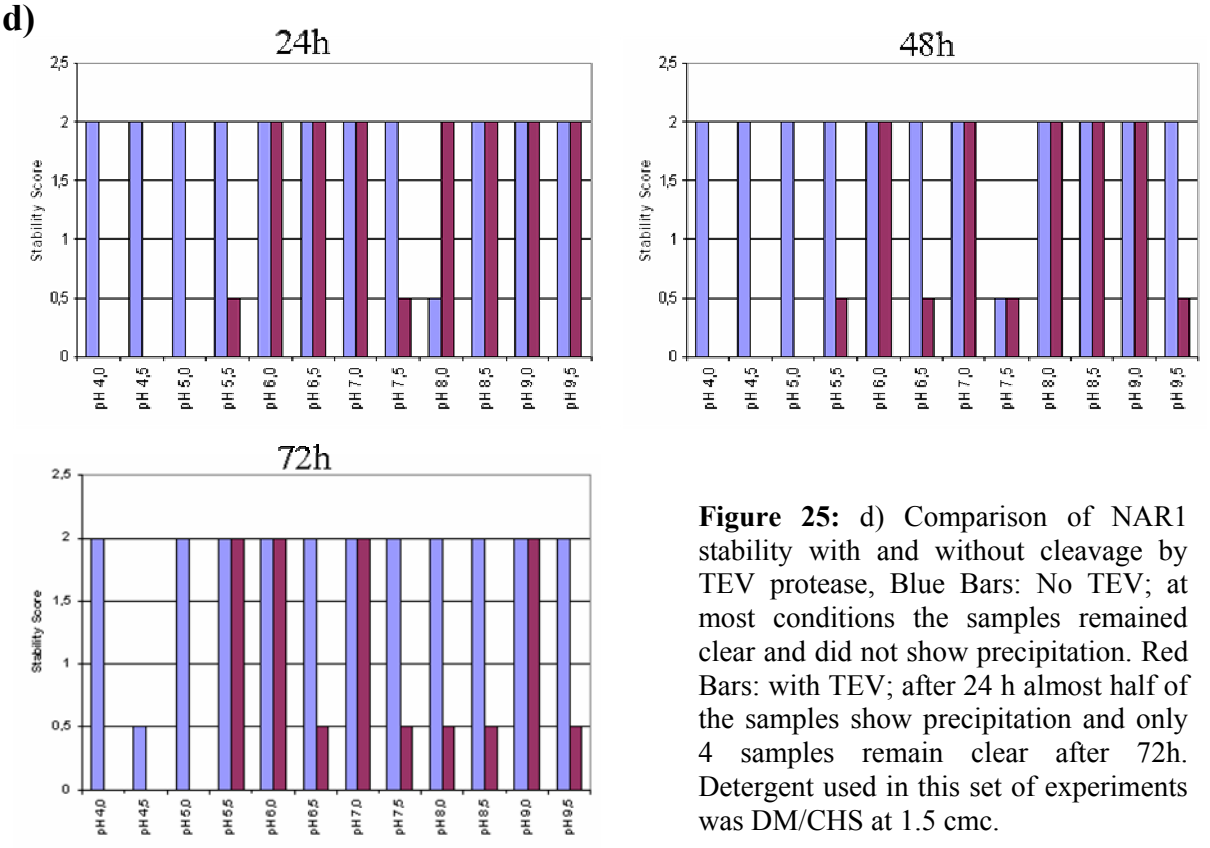

Figure 25: d) Comparison of NAR1 stability with and without cleavage by TEV protease, Blue Bars: No TEV; at most conditions the samples remained clear and did not show precipitation. Red Bars: with TEV; after 24 h almost half of the samples show precipitation and only 4 samples remain clear after 72h. Detergent used in this set of experiments was DM/CHS at 1.5 cmc.

cleaved one which precipitated rapidly after tag removal. Furthermore, it was observed that three pH values, pH 6.0, pH 7.0 and pH 9.0, irrespective of detergent, salt concentration and TEV cleavage, did not result in precipitation, or at least less severe precipitation than at other pH values (Figure 25d).

3.1.9 Chromatographic Purification of NAR1 (with tags)

Further purifications were run at pH 5.5, 6.0, 7.0 (both solubilized and loaded on HisTrapHP material at pH7.4) and pH 9.0 using six detergents (Fos-12/CHS, Fos-14/CHS, C12E9/CHS, DM/CHS, LM/CHS, Cymal-6/CHS) and subsequently compared. Results from the stability screen could not easily be adapted to large scale preparations, since TEV cleavage of NAR1 in detergents Fos-12/CHS, Fos-14/CHS and C12E9/CHS that showed no precipitation in the stability screen resulted in massive precipitation in large scale preparations. Elution from the HisTrapHP material at pH 5.5 and 6.0 resulted also in massive precipitation. The focus then turned again onto LM/CHS, DM/CHS and Cymal-6/CHS which already indicated positive results in previous functional assays. In comparable purification runs 50% more protein was

eluted at pH 9.0 than at pH 7.0 according to peak height at UV monitor at 280nm. Further analysis of initial purified NAR1 was done by analytical gel filtration.

3.1.9.1 Analytical Gel Filtration

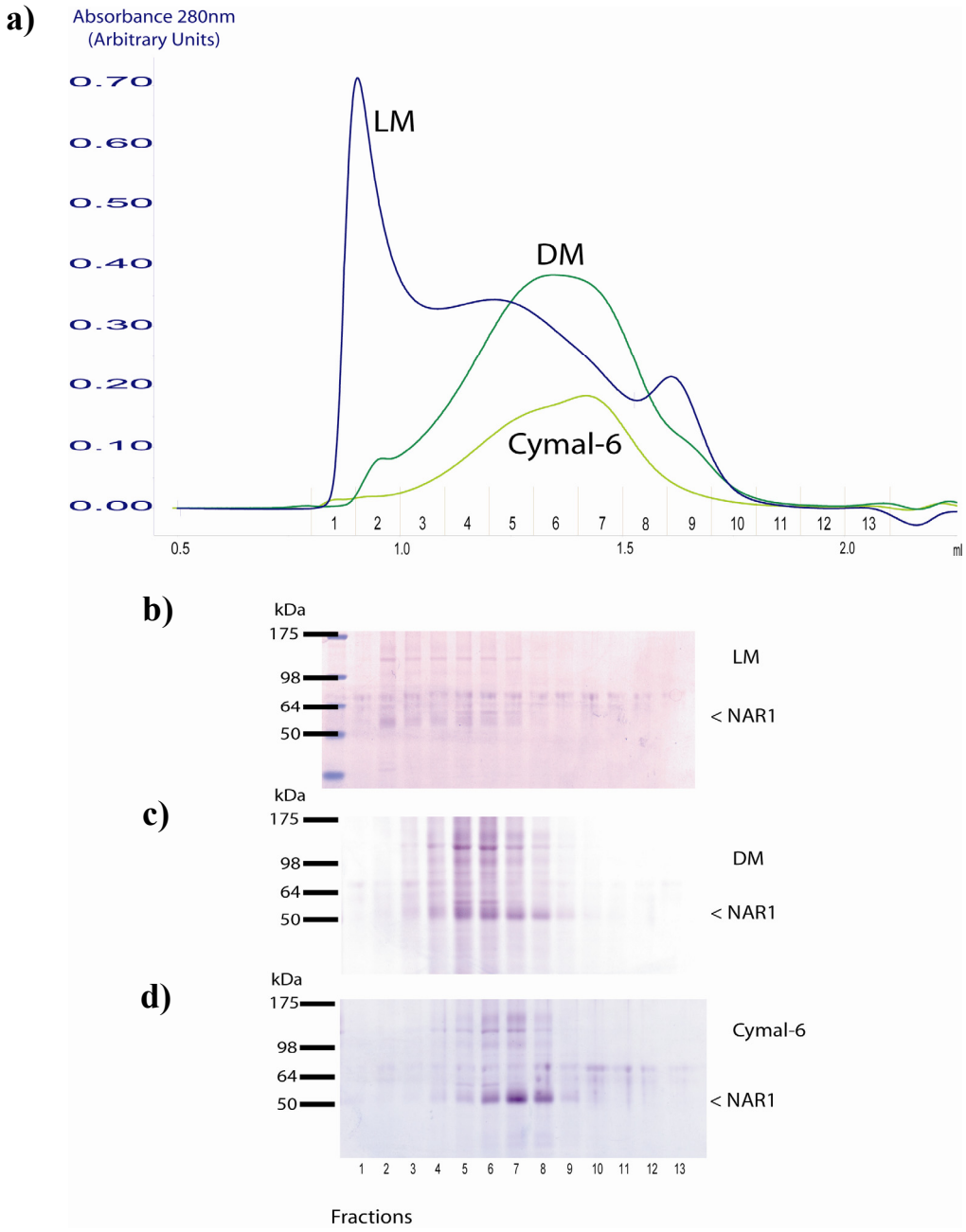

Figure 26: Superose 6 Gel Filtration of NAR1 after Ni-NTA purification. a) Chromatogram Blue: with LM, CHS and Asolectin; Green: with DM, CHS and Asolectin; Yellow: with Cymal-6, CHS and Asolectin. b) 12 % SDS-PAGE 15 µl samples of 2 ml fractions from LM run as indicated above, Coomassie stained, c) 12 % SDS-PAGE 15 µl samples of 2 ml fractions from DM run as indicated above, Coomassie stained, d) 12 % SDS-PAGE 15 µl samples of 2 ml fractions from Cymal-6 run as indicated above, Coomassie stained.

NAR1 protein in DM/CHS, LM/CHS, or Cymal-6/CHS purified by immobilized metal affinity chromatography at pH 7.0 or pH 9.0 was subjected to analytical gel filtration. Protein purified at pH 7.0 did not elute from the gel filtration column, indicating aggregation on the prefilter or the column. Protein preparation at pH 9.0 in contrast prevented this aggregation. LM/CHS showed a pronounced peak in the void volume, indicating higher order oligomerization or aggregation of the protein. DM/CHS and Cymal-6/CHS showed profiles without such a pronounced aggregation peak but the elution profile was still a broad one, consisting of multiple species. SDS-PAGE analysis of the gel filtration run showed that NAR1 was present in the highest concentration in the void volume peak if LM/CHS was used as detergent, while when purified in DM/CHS or Cymal-6/CHS it was found in the broad peak of the elution profile, with none detectable in the void volume (Figure 26).
As already seen in the reversibility of solubilization (Solubilization 3.1.7) the detergents DM/CHS and Cymal-6/CHS seem to be tolerated best by NAR1 with respect to ligand binding.

3.1.9.2 Purification on Immobilized Monomeric Avidin

Immobilized monomeric avidin column was tested as a second affinity purification step following IMAC purification. The performance of the resin further increased the purity of NAR1 (Figure 27a, b). Most dramatically was its effect on the gel filtration behavior of NAR1 (Figure 27c).
The concentrated NAR1 protein gave a single peak on the gel filtration column after IMAC and immobilized monomeric avidin purification (Figure 27c). This peak corresponds to a monomeric form of the receptor, if the retention volume on the Superpose-6 is compared to other GPCRs purified in our group. Furthermore, the fractions of this peak correspond to the fractions of the broad gel filtration profile just after immobilized metal affinity chromatography that contained the receptor. However, significant amounts of protein were lost on the immobilized monomeric Avidin column and only eluted under harsh column regeneration conditions. Typically, only 10% to 20 % of NAR1 that was bound on the column was eluted with biotin, while the remainder could only be eluted under regeneration conditions at pH 2.8.

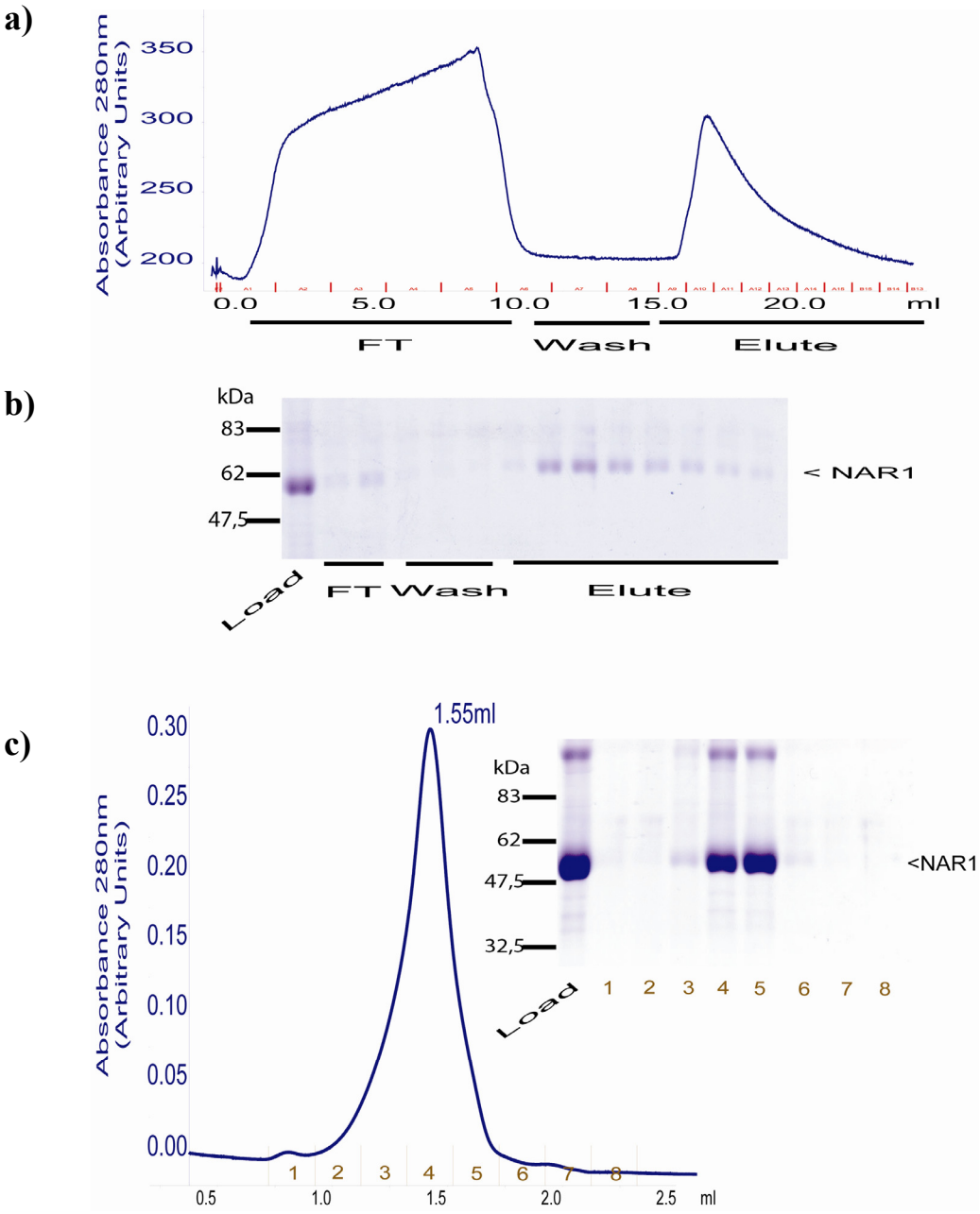

Figure 27: Purification of NAR1 on immobilized monomeric avidin and by gel filtration on superpose 6. a) monomeric avidin affinity chromatography of NAR1: Chromatogram and b) 12 % SDS-PAGE analysis. Black bars indicate fractions from the chromatogram. c) Superose 6 gel filtration of NAR1 after monomeric avidin: Chromatogram and 12 % SDS-PAGE of fraction indicated.

3.1.9.3 Alternative Chromatographic Steps to increase the purification yield

The HP Blue material was tested as additional resin. It is made of a dye that contains a nicotinic acid moiety and was evaluated as ligand column. NAR1 did not bind to this material, either at pH 7.0 or pH 9.0.

The DEAE column material which already proved to bind cleaved NAR1 at pH 7.5 was used again. Scouting purification runs were performed for pH values 6.0, 7.0, 8.0 and 9.0. NAR1 bound to the column at all pH values, indicated by no UV280 nm absorbance during loading.

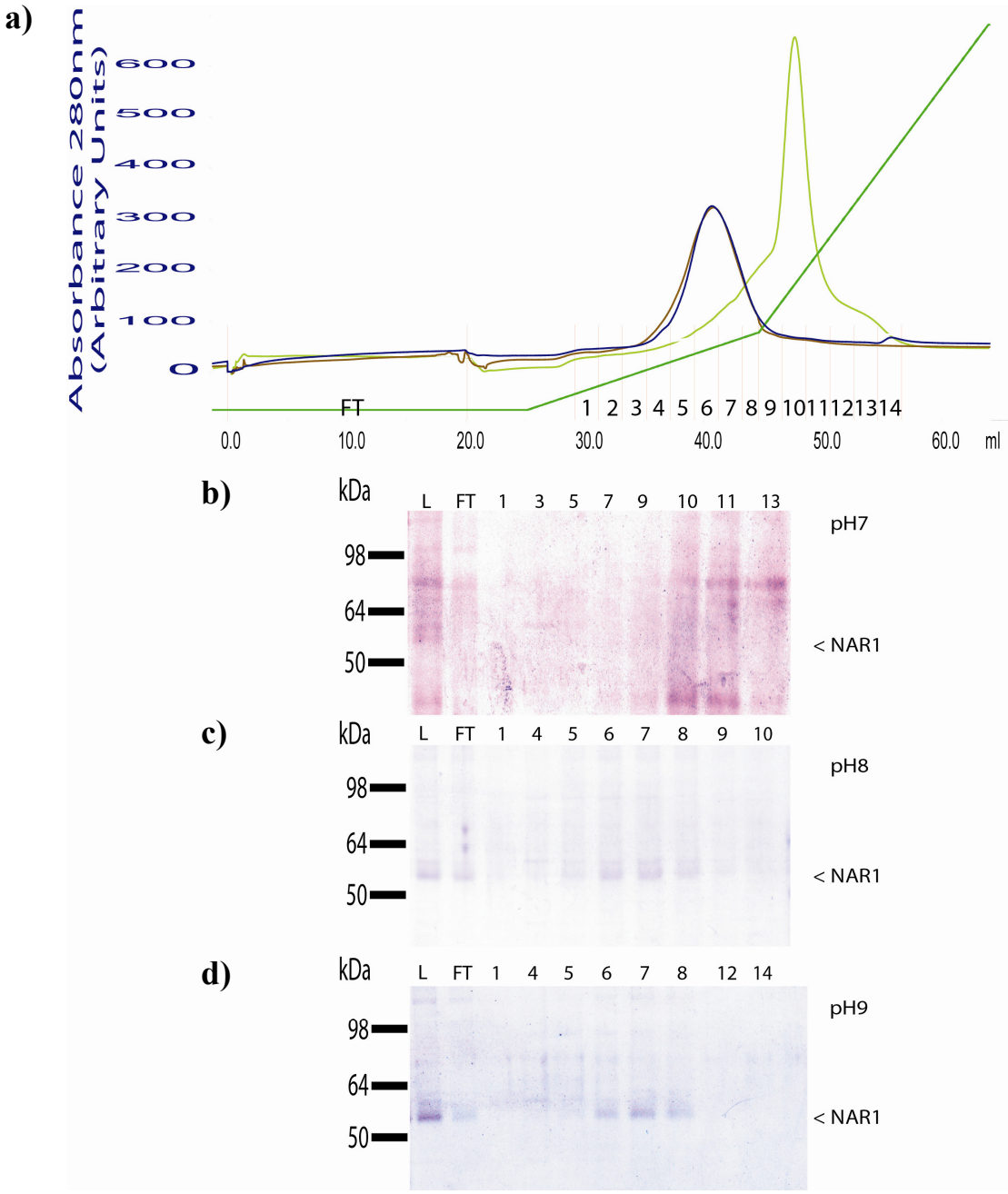

Figure 28: DEAE ion exchange chromatography at different pH values: a) Chromatograms, Blue: pH 9; Red: pH 8; Yellow: pH 7; Green: Gradient. b) 12 % SDS-PAGE, Coomassie stained, 15 µl samples of fractions indicated above, run at pH 7. c) 12 % SDS-PAGE, Coomassie stained, 15 µl samples of fractions indicated above, run at pH 8. d) 12 % SDS-PAGE, Coomassie stained, 15 µl samples of fractions indicated above, run at pH 9. Lane 1: load; following lanes are samples from the fractions corresponding to the ones in the chromatogram.

Elution with increasing salt concentration resulted in peaks only for pH values of 7.0, 8.0 and 9.0. The sharpest and highest peak was observed at pH 7.0, but according to SDS-PAGE this peak did not contain any NAR1. In contrast, pH 8.0 and pH 9.0 which resulted in a comparable elution chromatogram contained NAR1 (Figure 28). Although the purity could be increased, the loss of protein was severe, and the purification on immobilized monomeric avidin could not be rivaled.

3.2 Interaction of NAR1 with β-Arrestin 1 *in vivo*

To prove the hypothesis that β-arrestin 1 interacts with NAR1 *in vivo*, NAR1 was cloned into a pcDNA3.1 derivative and equipped with a C-terminal GFP fusion partner resulting in vector construct pcDNA3.1 NAR1-GFP. A truncated version of human β-arrestin 1 (residues 1-382) and the wild type full length sequence were cloned into the same pcDNA3.1 derivative and equipped with an N-terminal CFP fusion, resulting in vectors pcDNA3.1 CFP-βarr1-382 and pcDNA3.1 CFP-βarr1-fl. In both constructs the fluorescent protein variant was separated from the target protein by a spacer of ten amino acids. The resulting vectors were analyzed by restriction digestion and verified by DNA sequencing.

Transfection of the different constructs into Human Embryonic Kidney (HEK) or Baby Hamster Kidney (BHK) cells yielded the expected fluorescence, and confocal laser scanning microscopy showed the correct cellular localization of both constructs. NAR1-GFP was correctly localized at the plasma membrane and internal membranes, indicated by a clearly fluorescent cell periphery and further fluorescence around the nucleus, while the CFP fluorescence of both arrestin constructs was distributed evenly throughout the cytoplasm (Figure 29).

Cotransfection of the pcDNA3.1 NAR1-GFP construct with either pcDNA3.1 CFP-βarr1 construct yielded double fluorescent cells with easily distinguishable signals for both proteins, β-arrestin 1 being in both cases distributed throughout the cytoplasm, while NAR1 was located in the plasma membrane or in internal membrane compartments of the secretory pathway (Figure 29).

Addition of nicotinic acid resulted in the recruitment of cytosolic β-arrestin to the membrane, as evidenced from the CFP-fluorescence signal, where the GFP signal indicated the presence of NAR1 (Figure 30). Control cells that were not co-transfected with NAR1, and therefore devoid of GFP fluorescence, did not react to the addition of nicotinic acid. CFP-fluorescence remained in the cytoplasm of the cell and did not translocate to its membrane.

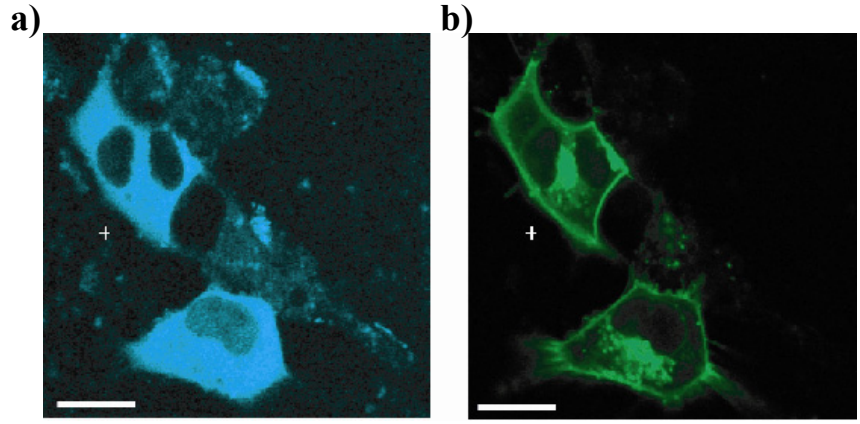

Figure 29: Doubly transfected HEK cells, a) CFP-βarr1-fl fluorescence imaging, excitation 405 nm, detection 420–480 nm. b) NAR1-GFP fluorescence image; excitation 488 nm, detection > 505 nm. White bar corresponds to 20 µm.

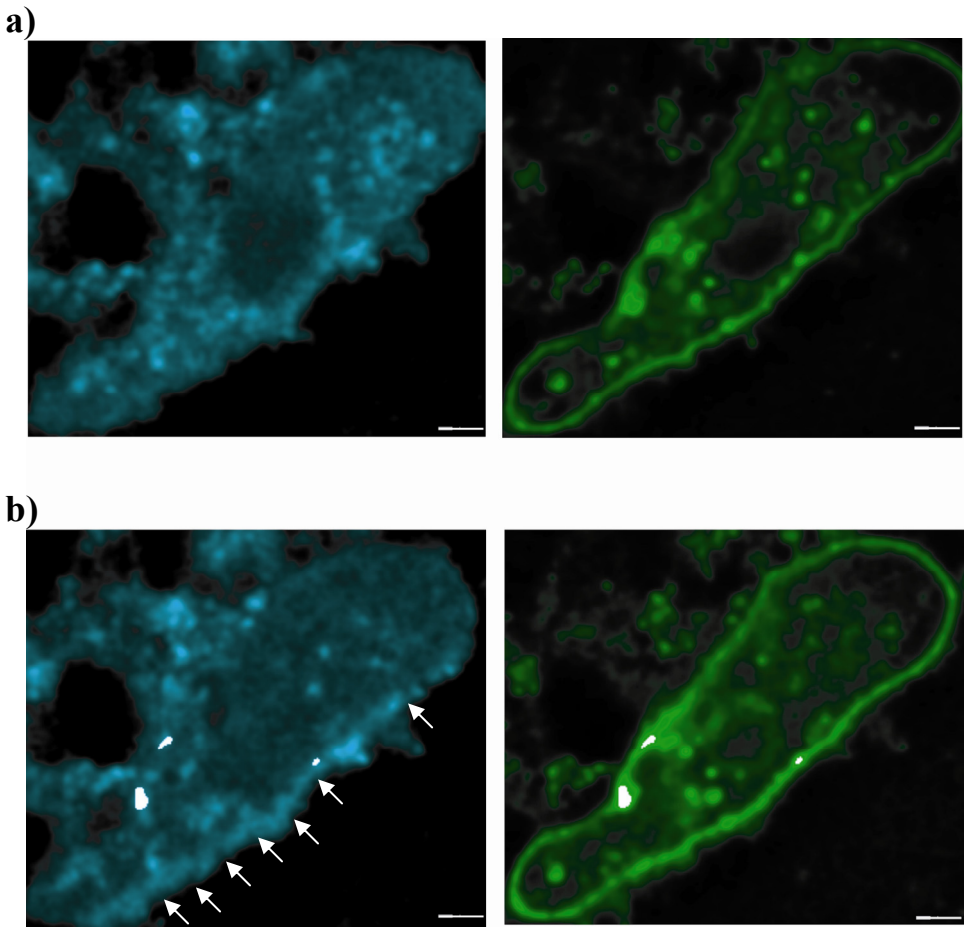

Figure 30: BHK cells cotransfected with CFP-βarr1-382 (excitation 405 nm; emission detection 420-480 nm) and NAR1-GFP (excitation 488 nm; emission detection >505 nm). a) before nicotinic acid addition, left: CFP-βarr1-382, right: NAR1-GFP. b) 10 min after nicotinic acid stimulation, left CFP-βarr1-382 translocation marked by white arrows, right: NAR1-GFP. The white bar corresponds to 4 µm.

3.3 Comparative Multi-Host Expression of β-Arrestins in *E. coli* and *P. pastoris*

3.3.1 Cloning & Expression

The amino acid sequence of the crystallized bovine β-arrestin 1 [64] was aligned with the sequences of human β-arrestin 1 and human β-arrestin 2. The sequence identity between the bovine and the human isoforms of β-Arrestin 1 is 99 %, within the length of the crystallized fragments only two amino acids differ. The identity between human β-arrestin 1 and β-arrestin 2 is 74 %. The major differences are found in loop regions while the secondary structure elements are well conserved. The regions flanking the activating mutation R169E [90] and the truncation of the crystallized constructs, comprising residues 1 to 382 and 1 to 393, are well conserved, and easily identified in the human sequences (Figure 31). Additionally, the shortest crystallized version of β-arrestin 1 (residues 1-382) has been shown to be another constitutively active variant [89].

To increase the hydrophilic portions of NAR1 and potentially stabilize it, the reconstitution of the complex with β-arrestin 1 should be attempted. For the production of β-arrestin 1 a comparative expression in two heterologous systems, *E. coli* and *P. pastoris* was set up. For reasons of completeness constructs of β-arrestin 2 were included. Therefore, both β-arrestin sequences were amplified by PCR introducing restriction sites *Eco*RI and *Not*I and an N-terminal TEV cleavage site in three different versions, comprising residues 1-382, 1-393 and full length. The amplified DNA 1-393 was derivatized by a PCR overlap extension exchanging arginine169 for a glutamate in β-arrestin 1 (R169E), arginine170 for a glutamate in β-arrestin 2 (R170E), and all versions were ligated into a pPIC3.5K vector derivative with an N-terminal GST-tag for *P. pastoris* expression resulting in vectors pPIC3.5K GST-βarr1-382, pPIC3.5K GST-βarr1-393R169E and pPIC3.5K GST-βarr1-fl for β-arrestin 1 and pPIC3.5K GST-βarr2-382, pPIC3.5K GST-βarr2-393R170E and pPIC3.5K GST-βarrr2-fl for β-arrestin 2.
The same β-arrestin cDNAs were ligated into a pGEX vector, containing an N-terminal GST moiety, a pET vector derivative, containing an N-terminal hexahistidine tag, resulting in vectors pGEX βarr1-382, pGEX βarr1-393R169E, pGEX βarr1-fl, pGEX βarr2-382, pGEX βarr2-393R170E, pGEX arr2-fl and pET βarr1-382, pET βarr1-393R169E, pET βarr1-fl, pET βarr2-382, pET βarr2-393R170E and pET βarr2-fl, respectively. Additionally, the DNAs were amplified without the TEV recognition site and ligated into a pTrc vector, resulting in

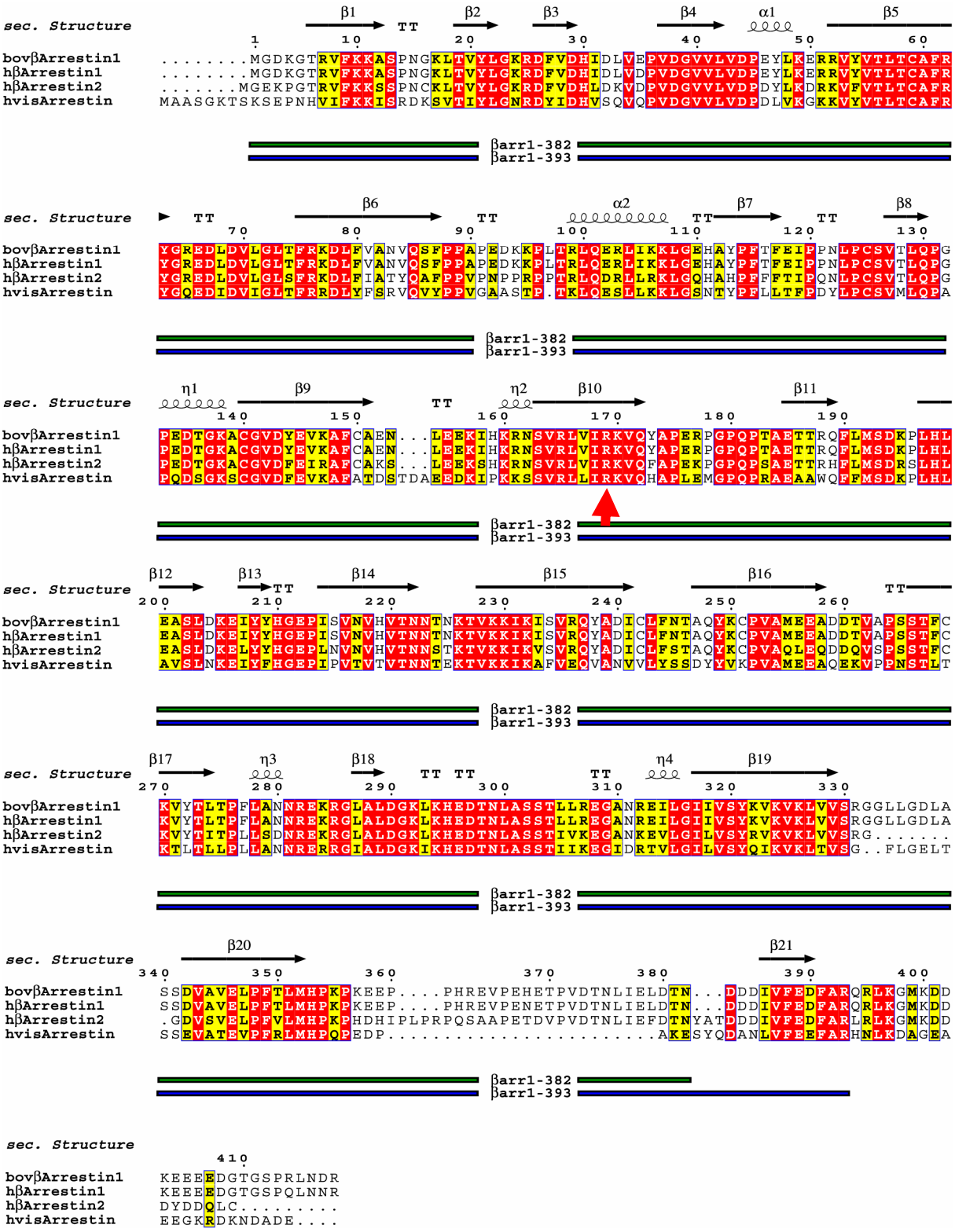

Figure 31: Sequence Alignment of arrestins (bovine β-arrestin 1; human β-arrestin 1; human β-arrestin 2; human visual arrestin). Secondary structure elements depicted above are derived from the structure of bovine β-arrestin 1. Strictly conserved residues are given in red, conservatively exchangeded residues in yellow. The length of truncated constructs is depicted below, and the activating mutation R169E in β-arrestin 1 is marked with a red arrow.

vectors pTrc βarr1-382, pTrc βarr1-393R169E, pTrc βarr1-fl, pTrc βarr2-382, pTrc βarr2-393R170E and pTrc βarr2-fl.

All pPIC3.5K vectors were transformed into protease deficient *P. pastoris* strain SMD1163, and multi-copy clones selected on G418-containing YPD plates. *E. coli* vectors were transformed into strains BL21 DE3, BL21 Codon plus and Rosetta gami DE3 pRARE and tested for expression (Figure 32).

The β-arrestin 1 variants were expressed significantly better than the β-arrestin 2 constructs, and the best expression was achieved with the shortest version of β-arrestin 1, pET βarr1-382. The full length wild type construct pET βarr1-fl showed lower expression levels. The worst expression among β-arrestin 1 constructs was pET βarr1-393R169E. Furthermore, the pET derivative containing the HisTEV-tag displayed a higher expression than the pTrc constructs without the modifications. Expression in both LB and M9 minimal media was possible. Compared to LB medium, M9 minimal medium had a lower expression. For LB medium, the induction time of four hours, and a growth temperature of 25°C were sufficient. Higher temperature led to more insoluble material, and longer expression time did not obviously increase the amount of produced protein.

Although significant overexpression of GST-β-Arrestin constructs was not evident from *E. coli* whole cell lysates, conditions were adapted so that the GST-fusion proteins could be detected on Glutathione Sepharose 4B beads after incubation with *E. coli* whole cell lysates.

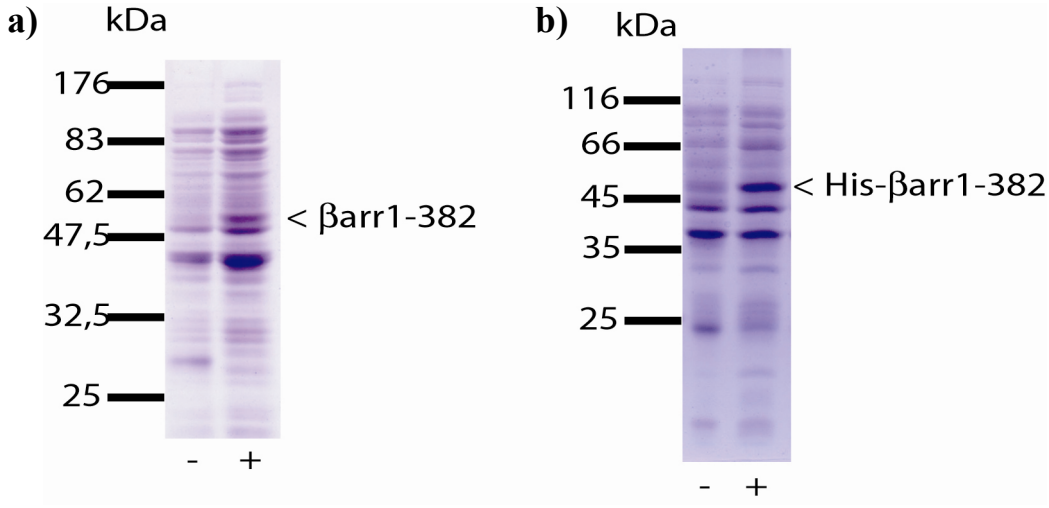

Figure 32: Whole Cell Lysates of β-arrestin in *E.coli*. a) BL21 DE3 cells with pTrc βarr1-382, producing βarr1-382, grown in M9 medium, 25 °C; -: uninduced, +:4 h after induction. 12 % SDS-PAGE, Coomasssie stained, b) BL21 Codon Plus cells with pET βarr1-382, producing His-βarr1-382, grown in LB media, 25 °C; -: uninduced, +: 4 h after induction; 14 % SDS-PAGE, Coomassie stained.

SDS-PAGE analysis of GST- β-arrestin 1 immobilized on glutathione beads allowed the selection of the *P. pastoris* clone with the highest apparent expression. The shortest construct, pPIC3.5K GST-βarr1-382 and the pPIC3.5K GST-βarr1-fl construct yielded the best expression; the construct version pPIC3.5K GST- βarr1-393R169E displayed lower expression, while no clones derived from vectors pPIC3.5K GST-βarr2-382, pPIC3.5K GST-βarr2-393R170E and pPIC3.5K GST-βarrr2-fl could be detected that expressed β-arrestin 2 in any version.

3.3.2 Purification

An affinity purification step initiated β-arrestin 1 purification. HisTrap HP resin was used in the case of the His-tagged version, and a Glutathione Sepharose 4B matrix for GST constructs.

MALDI-TOF analysis of the fragments derived from tryptic digestion was used to confirm the identity of the protein. 17.7% of the proteins' sequence was covered by the retrieved

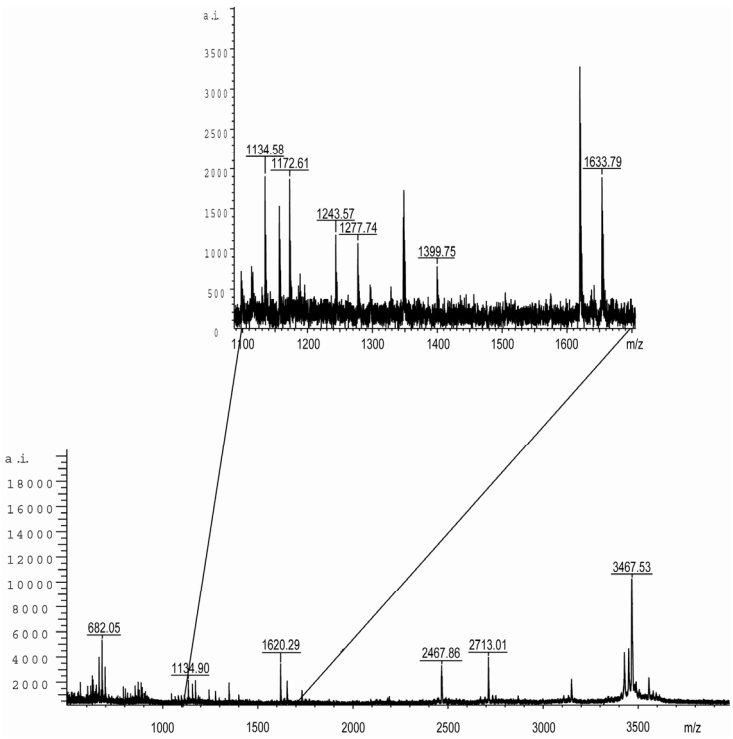

Figure 33: Mass Spectrometric Identification of β-arrestin 1-382 produced in *P. pastoris* after Tryptic Digest.

fragments of characteristic masses (Figure 33), which along with the fact that the protein was susceptible to TEV cleavage and displayed an altered mobility in SDS-PAGE analysis afterwards unambiguously identified the protein.

Fragment Position	Peptide Sequence	Calculated Mass	Observed Mass
26-49	DFVDHDILVPDVDGVVLVDPEYLK	2711.3813	2711.35
52-62	RVYVTLTCAFR	1399.7514	1277.74
53-62	VYVTLTCAFR	1172.6132	1172.64
53-62 Cys 59PAM	VYVTLTCAFR	1243.6503	1243.66
63-76	YGREDLDVLGLTFR	1653.8594	1653.85
66-76	EDLDVLGLTFR	1277.6735	1277.74
313-322	EILGIIVSYK	1134.6768	1134.68

Table 7: Masses of observed peptide fragments of β-arrestin 1-382 by mass spectrometric analysis.

The second chromatographic step employed a HiTrap HeparinHP column. Elution with increasing ionic strength yielded a single peak for GST- β-arrestin 1-382 and two peaks for the TEV-cleaved and the His-tagged protein product. SDS-PAGE analysis of each peak demonstrated that each of them contained pure GST- β-arrestin 1-382 or pure β-arrestin 1-382 respectively. In case of the TEV cleaved product, the TEV protease and GST moieties could be separated from β-arrestin 1-382.

Since the HiTrap Heparin HP column yielded two peaks for the cleaved β-arrestin 1-382 that were only partially resolved by elution with a linear salt gradient, anion exchange chromatography was assessed for its purification. Chromatographic analysis on a Q-Sepharose column yielded a single homogeneous peak that contained only β-arrestin 1-382 according to SDS-PAGE analysis. Both samples of the HiTrap Heparin HP column and the Q-Sepharose column were compared by Gel Filtration on a Superdex 75 10/30GL column and by 1D NMR spectroscopy. All three samples produced comparable gel filtration profiles consisting of two peaks, the first one right within the void volume of the column and the second one with a retention volume of 52 ml. The major difference between the three samples was the ratio between the 2 peaks. The sample produced by purification using the Q-Sepharose column and by the first peak of the HiTrap Heparin HP column showed ratios in favor of the aggregation peak, while only within the sample corresponding to the second peak

of the HiTrap Heparin HP column the ratio changed, and the portion of monomeric β-arrestin 1-382 was superior to the aggregated one (Figure 34).

All the experiments described above were performed with samples derived from GST-β-arrestin 1-382 produced in *Pichia pastoris*, and His-β-arrestin 1-382 produced in *Escherichia coli*. Neither the purification protocol with its functionality test of Heparin binding nor the NMR analysis showed differences in quality of the samples produced either in *E. coli* or *P. pastoris*. One liter of shaking flask culture from *P. pastoris* yielded typically 1.25 mg of purified β-arrestin 1-382, while *E. coli* produced only 0.35 mg per liter culture.

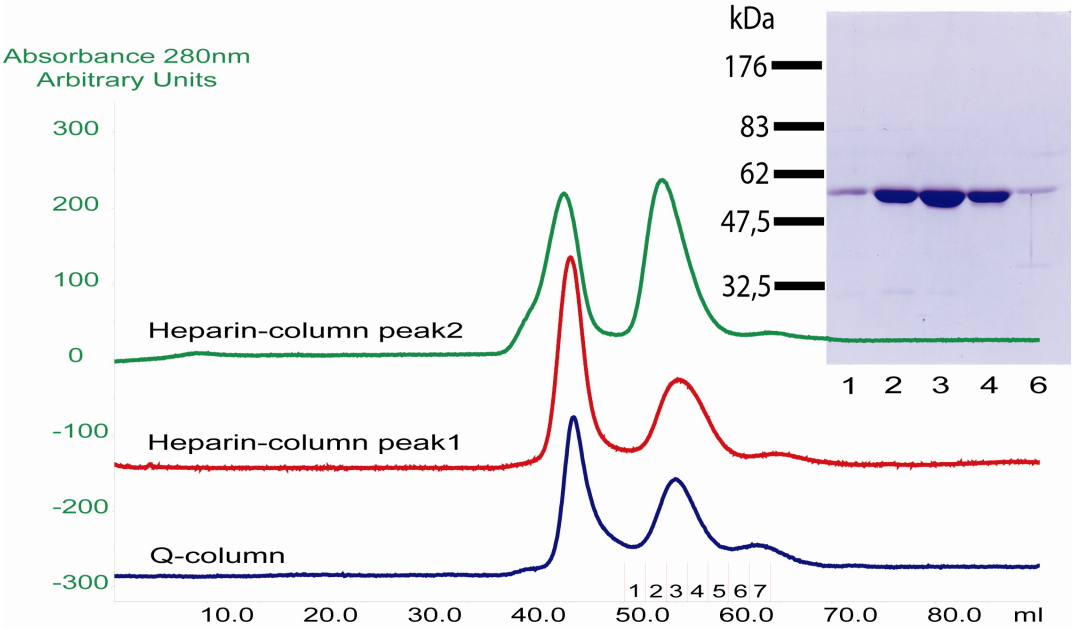

Figure 34: Upper Pannel: Superdex 75 Gel Filtration of β-arrestin 1-382, and 12% SDS-PAGE, Coomassie stained of fractions indicated above.

3.4 Interaction of NAR1 with β-Arrestin 1 *in vitro*

Samples of NAR1 purified in DM/CHS, LM/CHS or Cymal-6/CHS in the presence of nicotinic acid and asolectin were mixed with GST-β-arrestin 1-382 and Glutathione 4B Sepharose beads. SDS-PAGE and Western Blot analysis showed that NAR1 was specifically bound to the beads if the pull down experiment was done with DM/CHS (Figure 35) or LM/CHS as detergents. If Cymal-6/CHS was used as detergent, NAR1 was not retained on the beads. Still, it is obvious from SDS-PAGE analysis that only a small fraction of NAR1 was bound by β-arrestin 1, since it could only be visualized by Western-blotting.

Furthermore, the β_2-adrenergic receptor could be bound in the same manner to GST-β-arrestin 1-382 (data not shown). The β_2-adrenergic receptor was bound more efficiently, and could be visualized on silver stained SDS-PAGE yet, as for NAR1, the majority of the receptor was not retained.

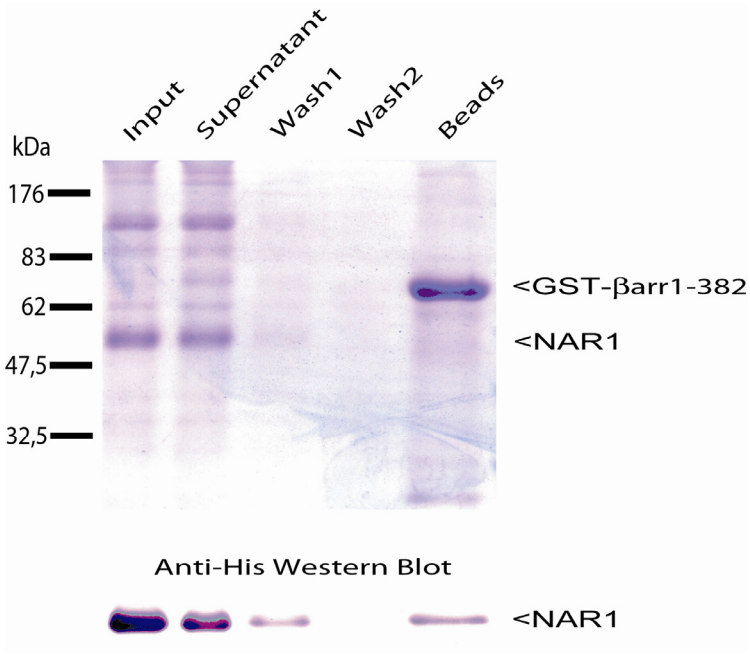

Figure 35: Pull Down experiment using GST-β-arrestin 1-382 as bait for activated NAR1 receptor. 12 % SDS-PAGE analysis and Anti-His Western-Blot.

3.5 Activity Measurements of Solubilized & Purified NAR1

Only substoichiometric amounts of NAR1 were bound by β-arrestin1. Therefore it was to be assessed which fraction of the receptor was in an active state, capable of being bound by β-arrestin1-382. Given that the addition of detergent impairs the standard radioligand filtration assay, as demonstrated above, other methods had to be tested.

- Since NAR1 already proved to be bound by immobilized metal affinity resins, NAR1 was immobilized onto these beads, allowed to capture radioligand nicotinic acid, and excess, free, radioactive material was removed by washing. This method was again evaluated for the detergents that were found to be promising in above mentioned experiments. DM/CHS, α-LM/CHS, Cymal-6/CHS, C12E9/CHS and Fos-14/CHS were compared, but none produced an observable binding signal, despite the fact that the receptor was highly enriched compared to membrane binding assays.

- The use of streptavidin coated plates that had been proven successful in demonstrating binding activity for A_{2A}-adenosine receptor [67], failed to produce a result with NAR1. [^{3}H]-nicotinic acid was not retained, and no signal was observed.

- In gel filtration assays that had been used to demonstrate ligand binding activity of the β_2-adrenergic receptor [68], the separation of bound from free radioactive material is achieved by differential retention times of the receptor ligand complex and the free ligand. The equilibrated reaction mix containing the radio ligand and the receptor are loaded onto the column. The radio ligand which is bound to the receptor molecule will travel faster through the column, while free radio ligand will take longer to pass through, thus separating bound from free material. NAR1 functionality was assessed by this method, again with the five above mentioned detergents. Best results were obtained with α-LM/CHS, which produced only a miniscule signal, two-fold above background, while NAR1 handled in other detergents failed to produce any signal at all.

- **Equilibrium Dialysis**

  Equilibrium dialysis is a method for determining the binding activity in a given sample of soluble proteins [91]. Its advantage over the above described methods relies on the fact that the fraction of bound ligand is measured as an increase in radioactivity compared to the reference compartment. The removal of free ligand is not required, and concentration dependent disassembly of the complex does not occur during separation. This experimental method was adapted for NAR1 binding analysis, and a preparation of purified NAR1 was assayed on its binding ability. As with the previous attempts, no productive binding of radioligand was detected.

- **Scintillation Proximity Assay**

  Similar scintillation proximity assays are a technique that does not require the separation of free and bound radioactivity. The scintillant is embedded in a small bead, which is covered with an affinity matrix. Binding of a receptor to the affinity ligands on the beads and, in turn, the binding of a radiolabeled ligand to the receptor, will concentrate radioactivity around the bead, and increase the stimulation of the scintillant within the bead, resulting in a signal. This method had been shown to identify a synthetic agonist for the CRHT2 receptor [92]. A preparation of NAR1 was

subjected to these experiments, which were performed in collaboration with Dr. Irvin Winkler at Sanofi-Aventis Deutschland GmbH, but demonstrated no detectable activity of the receptor.

- **Saturation Transfer Difference Spectroscopy**

  The only method that was finally capable of demonstrating activity of NAR1 was Saturation Transfer Difference Spectroscopy. This is a method that targets the small molecule ligand, in this case nicotinic acid. Within an NMR Spectrometer, the compound nicotinic acid has a unique signal, its peak shifts and their magnitude is related to the concentration of the compound. In the presence of a binding protein, magnetism is transferred from the compound to the protein molecule. The detected signal for the small molecule compound is diminished, and the difference between the compound by itself and the compound in the presence of the binding protein indicates whether binding events between both partners occur. Saturation Transfer Difference

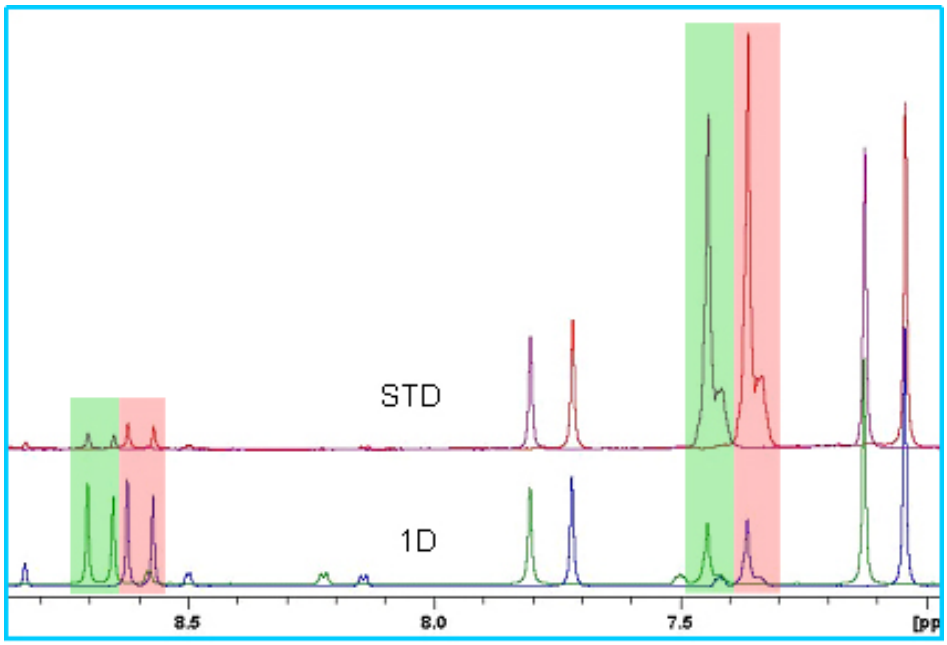

Figure 36: STD Spectra of NAR1 with Acipimox. Blue: 1D Spectra at day 1; Green: 1D Spectra at day 2 (offset by 0.1 ppm); Red: STD Spectra at day 1; Purple: STD Spectra at day 2 (offset by 0.1 ppm). The red shaded area shows specific signals of Acipimox at day 1 which reappear in the STD spectra and indicate binding. The green shaded area displays the same specific peaks for Acipimox that are diminished at day 2, indicating reduced binding due to protein instability over time.

Spectroscopy was done in collaboration with Alexis Rozenknop and Dr. Stefan Bartoschek at Sanofi-Aventis Deutschland GmbH, and remains the only method that has been able to show a binding signal for solubilized and purified NAR1. STD

measurements demonstrated binding of Acipimox and Acifran, the clinical used drugs, to NAR1 (Figure 36). STD measurements with each compound in a reference buffer did not show any signal, indicating that binding observed in samples is specific.

3.6 Reconstitution of NAR1 into Liposomes

Since activity measurements of NAR1 in solution appeared to be far from straightforward, and the functionality of membrane proteins is intimately linked with its correct placement into the lipid bilayer, the reconstitution of NAR1 into lipid vesicles was attempted.

There are a number of ways to reconstitute membrane proteins into lipid vesicles. The simplest method is to mix preformed liposomes with solubilized membrane protein in excess detergent. The detergent will render the liposomes accessible for incorporating proteins, and subsequent detergent removal results in proteoliposomes. DM/CHS solubilized and purified preparations of NAR1 were used for this kind of reconstitution experiment. Vesicles obtained were analyzed in two ways. First, binding activity was measured by the standard radioligand binding assay. Second, freeze fracture imaging of prepared vesicles was performed to visualize and estimate the content of protein incorporated into the lipid bilayer. Activity measurements remained without result, which is in good agreement with the results obtained by freeze fracture images taken by Dr. Winfried Haase. The liposomes that are seen in these images are devoid of protein, while in between the liposomes irregular structures are observed which most likely represent larger aggregates of the protein.

At low concentrations detergent molecules exist in solution as monomers, but above a certain concentration, the cmc, in equilibrium between monomers and micelles. On the other hand, detergent molecules will dissolve in the lipid bilayer of added vesicles resulting in a different equilibrium between detergent molecules dissolved in lipid membranes, in free monomers and micelles, if the concentration of free monomers is still above the cmc. To prevent detergent molecules from being removed from the solution, lipid vesicles were presaturated with detergent, just below the point of bilayer disruption, as monitored by light scattering at 550 nm. These presolubilized lipids were mixed with purified NAR1 and the detergent was subsequently removed by BioBead addition. Recovered activity by this method did not exceed 2 % of that measured in membranes.

The second approach began from a different point. Solubilized lipids were included in the purification buffers of NAR1. Due to the fact that lipids can already associate with the membrane protein in solution, mixed micelles are formed containing NAR1 and lipids. The removal of detergent molecules should lead to the association of mixed micelles to form larger mixed micelles eventually leading to membrane fragments and finally vesicles containing membrane protein.

Removal of detergent was accomplished by various methods, the first and simplest being the incubation with BioBeads. A second one was the removal of detergent with cyclodextrins. Two further attempts were based on dilution, one being a very controlled dilution using gel filtration and the other one by dilution into buffer without detergent, resulting in a quick drop of the detergent concentration below cmc values and thus initiating the aggregation of lipid molecules along with membrane protein to form vesicles.

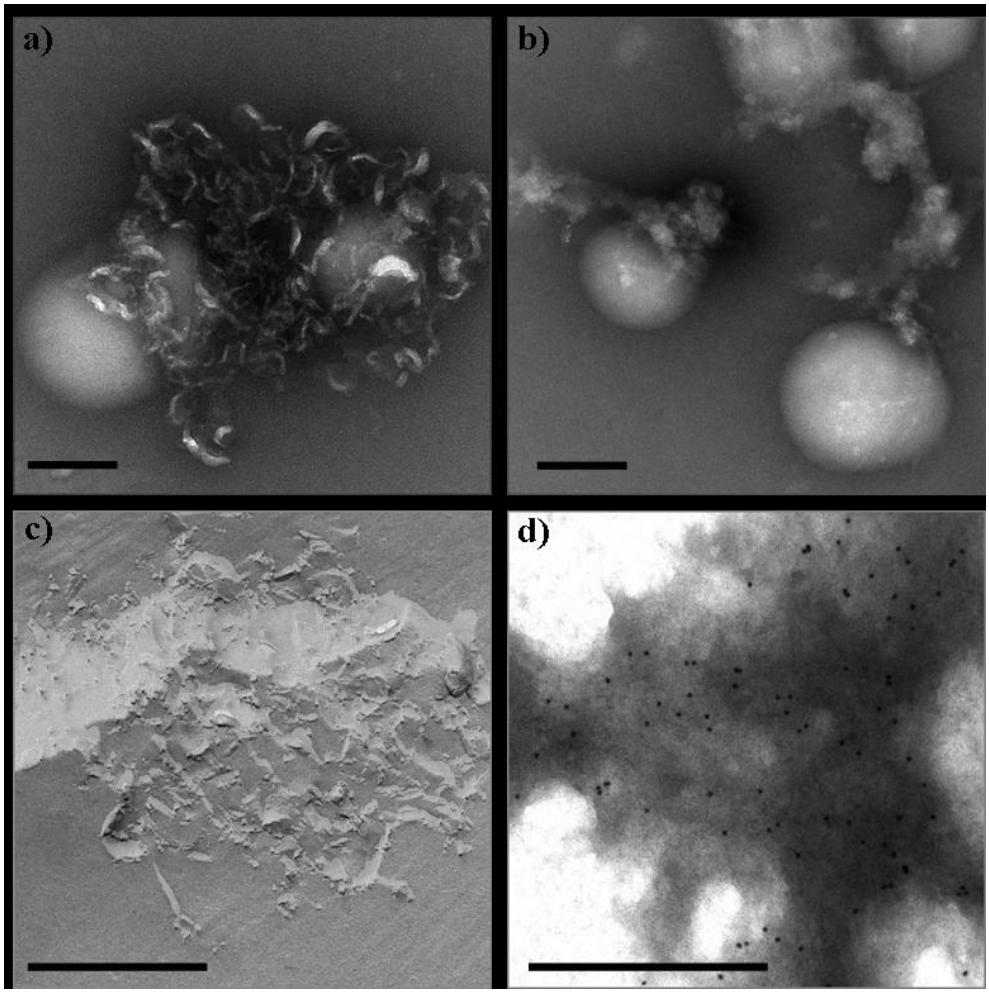

Figure 37: a + b) Electron Microscopic Negative Stain Imaging of NAR1 Reconstituted into Liposomes; c) Electron microscopic freeze fracture imaging of NAR1 reconstituted into liposomes; d) Electron microscopic image of Immuno-Gold labelling of NAR1. The black bar indicates 1 µm.

The reconstitution experiments were analyzed again by the functional radioligand binding assay and electron microscopic studies (Figure 37). Functional analysis yielded activities of a maximum of 12 % of values measured in membranes despite purification and enrichment of NAR1. This value was achieved by the gel filtration method. The rapid dilution method yielded 5 % of the ligand binding observed in crude membranes. All other methods yielded no notable activity recovery.

Electron microscopic freeze fracture imaging, performed by Dr. Götz Hofhaus, showed the same results as described above: no vesicles that contained protein were found. Only a very small number of vesicles were seen, while mostly irregular shaped structures were observed, that resembled lipid protein aggregates but not functionally reconstituted protein (Figure 37c). Since in freeze fracture images only few vesicles were observed, negatively stained images of the sample were produced. The analysis of these indicated a similar conclusion. Mostly irregular aggregated multi-lamellar lipid protein sheets were observed (Figure 37 a, b). To confirm that these structures are the ones that contain NAR1 protein, an antibody labeling of the vesicle preparation was performed by Dr. Götz Hofhaus. NAR1 protein was prevalently found within these dense structures, and not in the few regular vesicles (Figure 37d).

3.7 NMR Measurements of β-Arrestin 1-382

As with the only high resolution structure available for GPCRs, that of rhodopsin, all structures of arrestin are in its unliganded form. Nevertheless, rearrangements of arrestin upon receptor engagement have been demonstrated [3]. To address the question of how liganded β-arrestin 1-382 looks like, it was grown and purified metabolically labeled [^{15}N] variant to obtain [^{1}H]-[^{15}N] 2D NMR TROSY spectra and a receptor derived peptide was added. TROSY spectra obtained by Dr. Marco Betz (Johann Wolfgang Goethe-Universität, Frankfurt am Main) led to the observation that the spectral properties of β-arrestin 1 are improved by higher temperature. The peak dispersion was best at 37 °C, while measurements at 25 °C and at 10 °C reduced the quality of the 2D spectra (Figure 38). But even at 37 °C the TROSY spectra did not yield a single peak for each amino acid, which is a prerequisite for NMR structure determination. Still, a number of the side-chain amide [^{15}N]-[^{1}H] correlation peaks were degenerate, which resembles the general pattern of peaks characteristically obtained from intrinsically unfolded proteins. Yet the information obtained from a TROSY experiment is not always sufficient to discriminate between a folded protein with degenerate proton

chemical shifts, i. e. a molten globule that can be driven to complete folding under certain circumstances or a protein that exists in equilibrium of folded and unfolded states, and a largely disordered and unstructured protein. Therefore, [^{1}H]-[^{15}N] NOESY (HetNOE) spectra were recorded. In some cases such experiments can distinguish between intrinsically unfolded proteins and those that exist in a dynamic equilibrium of

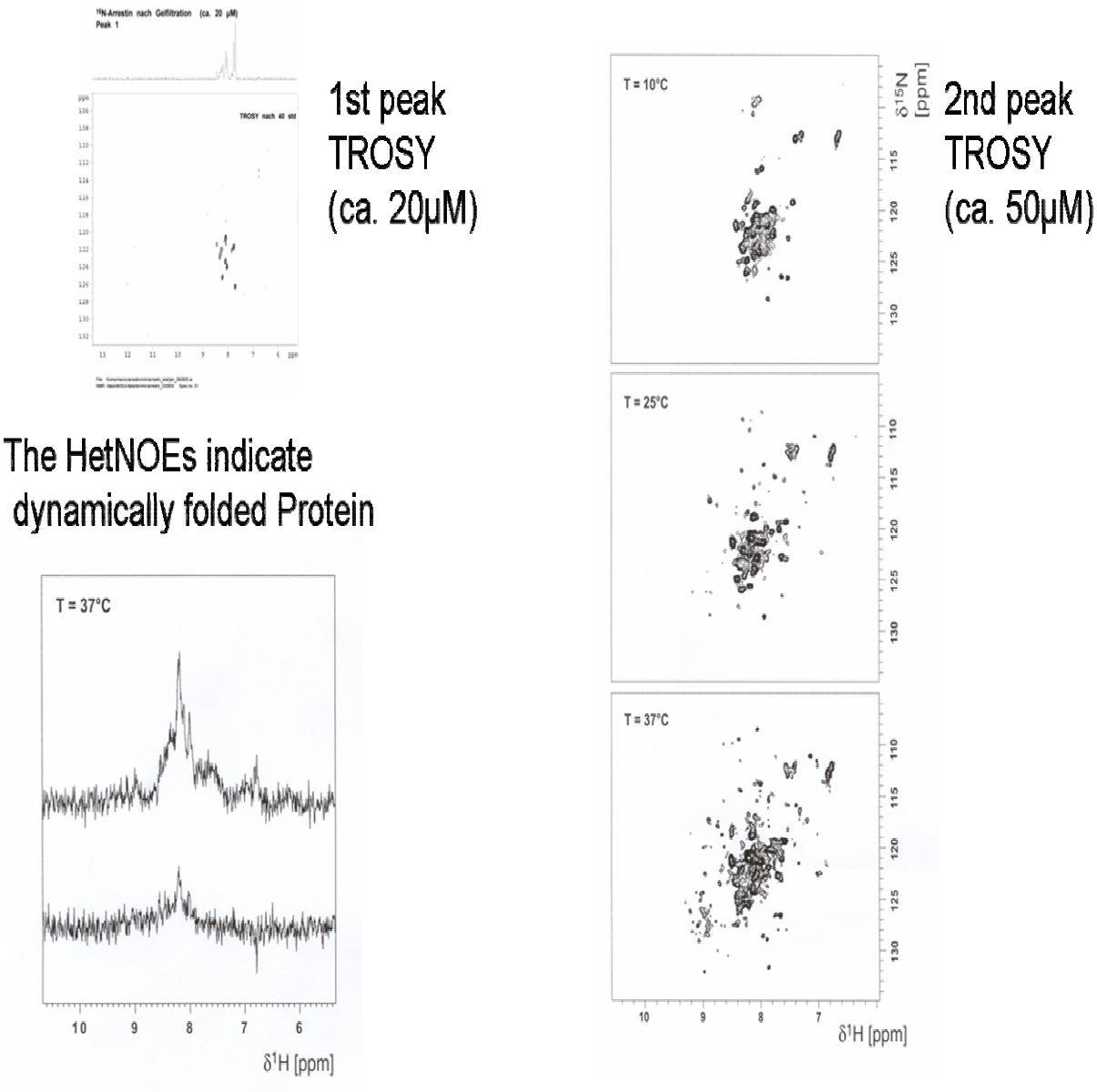

Figure 38: 2D [^{1}H]-[^{15}N] TROSY spectra of β-arrestin 1-382. Upper left: Void volume peak of gel filtration. Right Pannel: Second peak of gel filtration, spectra recorded at 10°C, 25°C and 37°C. Lower left: HetNOE spectra, upper trace: at [^{15}N] saturation, lower trace: below [^{15}N] saturation.

unfolded and folded states [10, 93]. HetNOE measurements for [^{15}N]-β-arrestin 1-382 indicated the latter (Figure 38).

Addition of a peptide with the sequence N-CIDRYLAVVHAVFAL-C derived from the CCR5 chemokine receptor that had been shown to bind β-arrestin1 with an affinity of 12 µM

[94] did not lead to observable changes in the [^{1}H]-[^{15}N] 2D NMR TROSY spectra that would indicate interaction between β-arrestin 1-382 and the peptide (data not shown).

4 Discussion

4.1 Production of the human GPCR HM74A in *P. pastoris*

The human GPCR HM74A, along with most other human GPCRs, is an important drug target for the pharmaceutical industry. The successful clinical use of nicotinic acid within the last 50 years underlines this fact. To facilitate a rational approach for the discovery of new drugs that enhance blood lipid profiles, having HM74A as target, high resolution structural data is needed. Despite the fact that the crystallization of membrane proteins, and especially GPCRs, remains a difficult and challenging task, with the crystallization of bovine rhodopsin in 2000 [37] showed that it is a feasible goal. Nevertheless, rhodopsin remains unique among GPCRs, since it is very abundant in native tissue, covalently bound to its ligand and its quality, folding state and conformation can be monitored by spectroscopic methods. For most other GPCRs, the first step in the long way to obtaining a high resolution crystal structure is the heterologous large scale production of the target.

The present work's focus lies on the heterologous production of the human gene HM74A, whose protein product is termed NAR1, a GPCR, in the methylotrophic yeast *Pichia pastoris*. Until recently, most structures of integral membrane proteins deposited in the Protein Data Bank (PDB) represented either heterologously expressed bacterial or archaebacterial proteins, or membrane proteins that could be isolated from native tissues, either from prokaryotes or eukaryotes. Only recently were the structures of the voltage-gated potassium channel from rat and that of the spinach aquaporin determined after heterologous production in *Pichia pastoris*. Other successes were the rabbit calcium ATPase (*Saccharomyces cerevisiae*) and rat aquaporin (baculovirus infected insect cells). Furthermore, it has been shown previously that *P. pastoris* facilitates the high level production of GPCRs [79, 82, 83]. Despite the fact, that other heterologous host systems for the overexpression of recombinant proteins are commercially available, *P. pastoris* has certain advantages. Although mammalian GPCRs have been produced at higher levels in mammalian cell culture systems [95], production scale up is hampered by limitations of costly large scale and high density cell cultivation. Similar limitations exist for baculovirus transfected insect cells, where the virus production is a long and tedious process, and cultivation of large cell masses is expensive. Compared to other yeast systems, *P. pastoris* offers the advantage of being easily fermentable to high cell densities at relatively low costs. Furthermore, the robust and inducible target protein expression is accomplished by the simple addition of methanol. In contrast to expression in *E.*

coli, the eukaryotic *P. pastoris* offers analogous pathways for the integration of membrane proteins into the lipid bilayer as mammalian cells, which are different in bacteria. This promotes the production of functional GPCRs, and measurable activity within membranes. Nevertheless, the expression level is influenced by vast number of other factors such as the integration machinery, the folding and quality control apparatus and the transport machinery. If any one is overwhelmed by the produced protein amount, yeasts can activate an Unfolded Protein Response (UPR) that leads to the degradation of target proteins and the shut down of further protein production [96, 97]. *E. coli* based systems follow two strategies i) the first favors the high yield production of unfolded GPCRs in inclusion bodies and subsequent refolding to obtain functional material [53], while ii) the second relies on functional production of receptors integrated into the membrane [98, 99] (for review see [97]). Although both of these *E. coli* based methods yielded amounts suitable for structural studies, the refolding protocol up to 3 mg pure receptor [100], and the functional expression up to 0.4 mg/ml (~0.4 pmol/mg) [99], no crystal structures have yet been obtained, either for a GPCR or for any other eukaryotic membrane protein expressed heterologously in *E. coli* [99].

4.1.1 Multi-Copy Clone Selection

The stable integration of multiple copies of the vector into the *P. pastoris* genome determines the gene dosage effect. In combination with a strong promoter, multiple copies of a single gene give rise to a higher number of messenger RNA molecules, and should increase the target protein expression level. The G418 high throughput screen that allows for the selection of multi-copy clones is based on this gene dosage effect. Nevertheless, in the case of NAR1 clone selection it displayed inconsistencies. Some colonies grew on intermediate antibiotic concentrations, but not on lower ones, and since it had been shown that the highest expression of a given GPCR does not always correlate with the highest copy number a second high throughput screen was employed. The direct expression colony blot enabled the selection of clones with high levels of target protein expression [65]. This is important, since the copy number does not always correlate with the level of target protein overexpression. Still, the direct expression colony blot alone was not capable of unambiguously identifying or verifying clones selected based on G-418 screening. Selection of the intersection of positive clones that were obtained by these two methods resulted in the identification of high level expression clones for the pPIC9K fhT-NAR1-Tbio construct. The nano9-tag, although praised as robust affinity handle and detection tag [101] failed to produce signals in the direct expression

colony blot and Western blots, and rendered those constructs useless for further purification experiments. Activity was subsequently demonstrated for the chosen constructs in the functional radioligand binding assay, enabling the assessment of the effect of the three different C-terminal tags, the biotinylation/stab tag, β-arrestin 1-382 and β-arrestin 1-fl. Although an enhanced pharmacological profile has been reported for the fusion of β-arrestin 1 to the C-terminus of the neurokinin NK1 receptor, resulting in an increased agonist binding affinity, no such effect was observed for the fusion of β-arrestin 1 to NAR1. The fusion of NK1 and β-arrestin 1 was studied in COS-7 cells, which have a different lipid composition in membranes than does *P. pastoris* [102]. Lipids, in particular acidic lipids, have been shown to be crucial for the interaction of β-arrestin 1 *in vitro* [23]. Furthermore, mammalian cells contain a large number of proteins that interact with GPCRs and β-arrestins that modulate the binding of ligand and receptor, and homologs might not be present in *P. pastoris*. Either of these differences could explain the altered functionality of the *P. pastoris* produced β-arrestin 1 fusion.

4.1.2 Pharmacological Characterization

The binding affinity, K_d, provides a good assessment for the quality of the produced protein. In native tissues the affinity of NAR1 for nicotinic acid has been reported to be between 60 nM and 90 nM [13, 16, 103-105]. The affinities that were measured for the *P. pastoris* produced constructs lay between 140 nM and 252 nM and are well in the range of what could be expected for a heterologously overexpressed protein. Furthermore, the K_i values for agonists Acifran and Acipimox are similarly lowered. It has been observed previously that agonist binding is diminished in a heterologous expression system. This effect can be explained in part by different membrane lipid composition and the absence of allosteric modulators that are present in native tissue. GPCRs have been found to be sensitive to the presence or the absence of their signaling partners, especially their cognate heterotrimeric G proteins, resulting in a low affinity state regarding agonist binding [106-108]. These findings might as well be one explanation for the long incubation time of 2 hours during the binding assay that is in contrast to the rapid response *in vivo*, where reduced free fatty acid levels in plasma occur in mouse already 15min after nicotinic acid injection [15]. Nevertheless, the saturation binding experiments on membranes were performed at room temperature, ~15 °C below body temperature in mice, explaining the delayed occurrence of the maximum response. Furthermore, a physiological response might not require the saturation of all

available binding sites, for the calculation of the total amount of receptor present in a given membrane preparation it is crucial. The notion that measured binding events are due to a degradation product of the radioligand can be ruled out by the fact, that membrane preparations of *P. pastoris* cells that were transformed with either the empty pPIC9K vector or the β_2-adrenergic receptor did not show any specific binding.

4.1.3 Expression Optimization of NAR1

Optimization of the NAR1 production level was achieved by two measures i) decreasing the growth temperature from 30 °C to 22 °C and ii) the addition of DMSO to the culture medium.

- That beneficial effect on heterologous protein production of lowering the temperature has been observed many times previously [98, 109, 110], and likely has several causes. At lower temperature the cell's metabolism is slowed, decreasing the speed of translation and allowing more time for the machinery to insert the nascent membrane proteins into the lipid bilayer. Additionally, the population of produced proteins is allowed more time to acquire the correct folding and ensure extended time for the cell's chaperones to aid in adopting the correct fold. Furthermore protease activity is decreased, reducing protein degradation.
- The way DMSO exerts its beneficial effect on protein production levels is not clear. DMSO has not only been shown to modify membrane properties [111], it furthermore changes gene expression profiles in yeasts and upregulates genes involved in lipid metabolism [112, 113]. For the production of NAR1, the addition of 2 % DMSO was found best and increased the production level 1.5 fold.

The fact that ligands might serve as a folding template and stabilize proteins has been exploited for protein overexpression efforts, and in particular for GPCRs [80, 83, 114]. In some cases, the addition of ligand to the growth media increased the expression level up to seven-fold [79]. Nevertheless, this effect was not observed for the production of NAR1, as addition of nicotinic acid to the expression media had no effect on the level of functional NAR1 production.

Another parameter assessed by André et al. [79] was the addition of histidine to the growth media. Whereas histidine addition resulted in one to two fold increase in production of all receptors tested, it had no effect on the production level of NAR1.

Under optimized conditions NAR1 expression levels reached 42 pmol/mg, which corresponds to ~0.4 mg/l culture. Compared to the 20 receptors tested for *P. pastoris* expression by André

et al. [79], the production level can be considered as reasonably good. Of the three categories defined by André et al., - those that displayed low level expression (binding < 2 pmol/mg), mid range expression (binding 2-20 pmol/mg) and high level expression (binding > 20 pmol/mg) - NAR1 would belong accordingly to the high level expression receptors.

It has been observed that the use of an antagonist in radioligand binding assays revealed significantly more binding activity on the same membrane samples than was seen with the use of an agonist. Therefore it can be speculated that the actually produced amount of receptor is larger than what could be measured.

In their native environment, membrane proteins face two different compartments, the cytosol son one side and the extracellular matrix on the other. These two compartments not only differ in their oxidizing properties, but also with respect to the concentrations of various ions and metabolites. With the preparation and solubilization of membranes, this sidedness is abolished.

The fact that sodium ions act on GPCRs as allosteric modulators of agonist affinity was shown for the opioid receptors as early as 1974 [115]. Since then, this effect has been observed for other receptors [116-118], and shown to involve a conserved aspartic acid residue in transmembrane helix 2. This aspartic acid is present as Asp73 in the second transmembrane segment of NAR1. Therefore, it is not surprising that this effect could also be shown for NAR1, and was reported in 2001 [13]. On the other hand it was shown that the binding of antagonists, as in the case of A_{2A}-adenosine receptor [86, 87] is enhanced by sodium ions. Given the fact that antagonists for NAR1 are not known to date, this study could only confirm that sodium ions inhibit the binding of nicotinic acid to NAR1. Concentrations of 100 mM reduced the specific agonist binding to 20 %, while other cations like potassium, lithium or ammonium had a less detrimental effect, and at similar concentrations reduced binding to only 60 % of the reference value without salt.

As already mentioned, a disulfide bridge between extracellular loops 2 and 3 is common among family A GPCRs. This disulfide bridge can only form in the oxidizing environment of the extracellular space. Its importance to receptor function has been shown previously, and reduction by DTT abolishes ligand binding capability [119]. It has been argued that the disulfide bond stabilizes the receptor, yet other receptors, such as the cannabinoid receptor CB1, do not have this conserved disulfide bond [120], and are not sensitive to reducing agents (Chandramouli Reddy, personal communication). NAR1 does have this conserved disulfide bond and it is required for its function, since as little as 500 µM DTT reduces the binding activity of NAR1 by 50 %. This observation demonstrates that the disulfide bridge is crucial

to the structural integrity and function of NAR1. This fact has to be kept in mind for further experiments that involve the reconstitution of NAR1 with β-arrestins, as these are purified in the presence of high concentrations of DTT.

Imidazole is commonly used to elute His-tagged proteins from IMAC columns, and therefore hardly avoidable in preparations of HisTrap purified NAR1. Histidine resembles the nicotinic acid scaffold as does imidazole. It shares a similar scaffold with its ligand, nicotinic acid, thus the effect of imidazole effect on the binding of NAR1 was tested, and found to impair nicotinic acid binding already in membranes. Concentrations of 250 mM reduced the observable binding to less than 30 % of the original value. Whether this is due to imidazole competing with nicotinic acid or for a different reason is unknown.

The organic solvent DMSO is required for the preparation of stock solutions of Acifran and Acipimox, because both have a low solubility in water. Along with the addition of Acifran or Acipimox to the activity test DMSO is inevitably added. Therefore its effect was tested, and found that small amounts of up to 1 % will be tolerated, although diminishing the observable binding to 60 %.

4.1.4 Solubilization

One of the crucial steps of membrane protein purification is the extraction from the membrane. This is routinely achieved by the solubilization of the membrane with detergents. At concentrations below the cmc detergents partition into the lipid bilayer and change the membrane properties. In some cases they even compete with ligand for receptor binding sites [121], or block the access to the ligand binding site of the receptor. These effects might already influence the NAR1 radioligand binding assay and were tested by adding detergent at concentrations below cmc. Most tested detergents did not interfere with the assay format at concentrations below the cmc. But as soon as the cmc was approached, no more binding could be observed. The explanation for this effect could be the denaturation of the receptor by detergents during the removal of the surrounding membrane. However, the measured decrease in ligand binding does not necessarily mean the loss of function of NAR1. For a number of receptors, a reduced affinity has been reported upon solubilization [122]. Lowered affinity would be harder to measure with standard techniques like radioligand binding assays. The fact, that titration of detergents to the binding assay abolished observable binding as soon as the cmc is approached suggests an interference of the detergents with the receptor ligand interaction. Furthermore, the treatment of the glass fiber filters with PEI creates a surface for

electrostatic interactions between PEI laced glass fibers and charged filtrates [122]. Phospholipids carry charges and membrane fragments with embedded membrane proteins exhibit different electrostatic properties than solubilized receptors in detergent micelles. Thus, the interaction between solubilized NAR1 and the filters might not occur anymore and be the cause for not observed ligand binding. In addition, partial binding was regained by the removal of detergents DM, LM and Cymal-6 from solubilizate with BioBeads. BioBead treatment leads to the reduction of the detergent concentration, leading to reconstitution of the solubilized lipids into vesicles accommodating membrane proteins. Thus, the solubilization event does not denature NAR1 completely.

4.1.5 Purification

The initial purification step of NAR1 using a HisTrap HP column allowed robust enrichment of NAR1, but the preparations were not of the desired purity. The first strategy to eliminate impurities that bound to the HisTrap HP column was a second pass over the same column after enzymatic removal of the decahistidine tag on NAR1. The impurities would bind the resin again, while NAR1 devoid of the decahistidine-tag should pass through the column. Unfortunately, enzymatic removal of the engineered tags with TEV protease decreased the protein's stability and the cleaved NAR1 precipitated. In addition to the detergent, the hydrophilic tags might have shielded further hydrophobic patches and stabilized the receptor conformation, while without them NAR1 integrity was lost and it aggregated. Since the removal of the hydrophilic engineered tags resulted in precipitation of NAR1, purification strategies that required enzymatic cleavage failed. A systematic screen, varying pH, detergents, detergent concentration and salt concentration was performed to identify buffer conditions that would promote protein stability, but none was identified that tolerated removal of the tags. Therefore further purification was attempted with the tagged version of NAR1. Various chromatographic media were tested: HiTrap Blue material, ion exchange resins and the affinity matrix immobilized monomeric avidin. Immobilized monomeric avidin makes use of the C-terminal Bio-tag as an affinity ligand for purification and had been used successfully for the purification of the adenosine A_{2A} receptor [67]. In conjunction with the initial HisTrap HP purification step, immobilized monomeric avidin allowed pure and stable protein to be obtained at pH 9. Adjusting the pH from the physiological pH of 7.5 to pH 9 yielded a NAR1 preparation that was sufficiently stable to give a single peak on a Superose 6 gel filtration column, using DM as detergent. Nevertheless, substantial amounts of NAR1 protein were lost

on the immobilized monomeric avidin column. It is conceivable that only properly folded biotinylation domains are biotinylated in *P. pastoris*, and that due to overexpression only partial biotinylation takes place. Non biotinylated receptor molecules are inevitably lost by this method. Additionally, non-specific binding to the column was observed, so that only little of the receptor could be eluted specifically. These are potential explanations for the low yield of this strategy.

4.1.6 Activity Measurements & Reconstitution

To assess functionality of NAR1, two different approaches were initiated. First, ligand binding assays of the solubilized, purified protein, and second the reconstitution of purified NAR1 into liposomes, to mimic its native environment.

4.1.6.1 Activity Measurements of Solubilized & Purified NAR1

GPCRs are very flexible proteins that can adopt a multitude of pharmacologically different conformations [123], and detergent solubilization likely increases this flexibility. It has been observed that the ligand binding affinity of solubilized receptors can decrease [122] or disappear completely [124] and kinetics may be altered.

During a radioligand binding filtration experiment an equilibrium between free and receptor-bound radioligand is established, which is changed during the washing steps, since washing buffers do not contain any radioligand. Although the time for washing was always kept as short as possible, substantial amounts of weakly bound ligand can be released from the receptor, and therefore not be detected anymore.

Another method for the separation of receptor-bound from free radioligand was gel filtration that had been used previously for the characterization of β_2-adrenergic receptor binding sites upon solubilization [68]. But no activity was observed for NAR1.

A completely different method is a scintillation proximity assay, and has successfully been used to demonstrate radio ligand binding to GPCRs [125, 126]. If the receptor is bound to the affinity ligand coated bead, a very high density of receptor molecules surrounding the scintillant is achieved, and the decay of bound radioligand will stimulate light emission. This method did not show activity for solubilized NAR1 and was also not successful in demonstrating activity on crude membranes containing NAR1 used as reference. Interestingly, it was found for the α2-adrenergic receptor that, although radioligand binding could be observed by SPA in membranes, the assay could not be adopted for the solubilized

receptor. For this solubilized receptor, filtration assays were also unsuccessful, but receptor functionality could be demonstrated by surface plasmon resonance experiments [127].

A standard procedure for the observation of binding events to soluble proteins is equilibrium dialysis. It is routinely used in clinics for the determination of the binding of a certain radio ligand to blood plasma samples [91]. The binding reaction was dialyzed against a buffer that did not contain radio ligands. By diffusion, an equilibrium of free radio ligand is achieved between both compartments. Bound radio ligand increases the amount of radioactivity in the sample compartment, and binding is measured as a difference between both compartments. This method has a number of drawbacks. It is slow, has a low reproducibility and a low signal to noise ratio [121]. These drawbacks might already explain the failure of this procedure, since it could not demonstrate the activity of NAR1.

As a last method NMR based Saturation Transfer Difference was tested. This method relies on the transfer of magnetism from the receptor to the ligand. Each chemical compound has a unique set of peaks in an NMR spectrum and the peak height corresponds to the concentration of the ligand. If the ligand is bound by the receptor, magnetism is transferred from the receptor to the ligand, diminishing its observable signal. Thus, the comparison of a reference spectrum containing only ligand in an appropriate buffer with a spectrum obtained from a sample containing ligand with receptor indicates binding if peaks for the ligand are observed. By this means ligand binding activity of NAR1 could be demonstrated. Furthermore, the diminishing of the signal from one day to the next further demonstrated the limited stability of purified NAR1 in solution. Although promising, this experiment was only able to provide a qualitative answer to the question of receptor activity, and quantification of the data was not possible. Although the method of saturation transfer difference spectroscopy is becoming more and more a standard method for the detection of binding events between small molecules and proteins, this appears to be the first application of the method to a solubilized GPCR.

4.1.6.2 Reconstitution of NAR1 into Liposomes

It has been mentioned previously, that the measurement ligand binding on solubilized receptors is difficult. Since measuring ligand binding was far from straightforward for solubilized NAR1, its reconstitution into membranes was attempted. It was hoped that restoring the constraining influence of a lipid bilayer might also restore ligand affinity and binding activity. To achieve this reconstitution of NAR1 into liposomes, purified NAR1 was

combined with lipid vesicles or detergent saturated vesicles and detergent was removed by treatment with BioBeads. This method has been used for the functional reconstitution of the CCR5 receptor [128], but similar experiments with NAR1were unsuccessful.

In another set of experiments NAR1 was mixed with detergent solubilized lipids rather than with preformed liposomes. At this stage mixed micelles exist that are composed of i) detergent and membrane protein, ii) detergent and lipids and iii) detergent, lipid and membrane protein. During subsequent detergent removal, these mixed micelles should associate with each other and eventually form proteoliposomes. The reconstitution of NAR1 was attempted by different methods, i) removal of detergent by BioBeads as was shown for the reconstitution of the metabotropic glutamate receptor [129], ii) removal of detergent by cyclodextrins [70] which was used for the reconstitution of the histamine H1 receptor [130], iii) a controlled slow dilution by gel filtration, used for the reconstitution of the β_2-adrenergic receptor [69] and iv) by a fast dilution into large volume of buffer without detergent [69, 71, 131]. None of these methods yielded functionally reconstituted NAR1. Although a variety of methods under different conditions were tested, the right conditions were either not found or NAR1 was not in a state allowing successful reconstitution.

4.2 Multi-Host Expression of β-Arrestins

For the production of a complex with NAR1, β-arrestin 1 was cloned in three different versions i) the full length coding sequence, ii) a truncation version comprising residues 1-393, corresponding to one of the crystallized fragments of bovine β-arrestin 1 with the constitutively activating mutation R169E, that renders β-arrestin active in the absence of receptor phosphorylation and iii) the shortest version containing residues 1-382, corresponding to the second crystallized fragment of bovine β-arrestin 1, which is by itself constitutively active, capable of binding the unphosphorylated receptor. Similar versions of β-arrestin 2 were cloned also.

Although the structure of β-arrestin 1 is derived from the bovine homologue, the similarity between human and bovine β-arrestin 1 isoforms is 99 %, and for reasons of scientific significance human β-arrestins were chosen for expression and recomplexation with human NAR1. Thus proteins from the same source organism were used.

The comparative heterologous expression in two different host organisms, namely the bacterial expression in *E. coli* and in parallel the eukaryotic expression in the methylotrophic yeast *P. pastoris* was set up to compare protein yields. That the expression of bovine β-

arrestin 1 in *E. coli* was feasible had been shown before, not at least by its crystallization [64] but its expression was labor intensive. Hoping to boost the production similar expression was tested in the eukaryotic yeast system *P. pastoris*. In *P. pastoris* only four times more protein was expressed than in *E. coli*. This four fold increase does not justify the increase in labor and time that is needed for the cultivation and breakage of yeast cells, and alterations of the construct always will need rescreening for multi-copy clones that is not required with *E. coli*. Furthermore, metabolic labeling for NMR experiments or selenomethionine labeling for phase determination in X-ray diffraction experiments is by far easier accomplished with *E. coli* than in *P. pastoris*.

It was found that the shortest version of β-arrestin 1 (β-arrestin1-382) was expressed better than the full length version and the construct version β-arrestin 1-393 R169E. Furthermore β-arrestin 1 constructs were expressed significantly better than constructs of β-arrestin 2 regardless of the tag and host organism. The reason for this difference remains elusive, but this might explain as well the existence of x-ray crystal structures for all arrestins [64, 132-134] except β-arrestin 2.

Purification of β-arrestin 1-382 was accomplished essentially as described by Han et al. 2001 [64]. The major difference being the replacement of the initial HiTrap Heparin purification by an affinity purification step, either on a HisTrap HP column or Glutathione 4B Sepharose for His-tagged and GST-tagged versions respectively. The purification with a GST-tag allowed for simple pull down interaction experiments with NAR1 and detection via the decahistidine-tag. The second purification step utilized a HiTrap Heparin HP column and elution by a linear salt gradient. Heparin and phosphorylated light activated rhodopsin had been shown to bind visual Arrestin in a competitive manner [135]. Therefore the HiTrap Heparin HP column can be considered as a ligand column and furthermore binding of β-arrestin demonstrates its functionality.

Further evaluation of the quality of β-arrestin 1-382 was done by NMR spectroscopic studies, with [^{15}N] labeled samples from *P. pastoris* and *E. coli*. The spectral properties of β-arrestin 1-382 are not sufficient for NMR assignment of residues and structure determination. However, TROSY spectra in combination with HetNOE measurements indicate that β-arrestin 1-382 exists in a dynamic equilibrium or molten globule like state. Nevertheless, proteins with these spectral qualities might sill be good targets for crystallization experiments as had been shown by Yee et al. [93]. Potential explanations for the low quality of spectral properties are the fact that arrestins do dimerize and tetramerize [136-138]. This is not only clear from the crystal structure, where the asymmetric unit consists of two β-arrestin 1-382

molecules [64], it had furthermore been shown that β-arrestin forms dimers in the cytoplasm [138], which are believed to be an inactive storage form of β-arrestins. In addition, it had been shown that β-arrestins dimerize at high concentrations [136], hence the high concentration of β-arrestin 1-382 (0.1 μM) in NMR experiments might have promoted this dimerization. The monomer of β-arrestin 1-382 has a molecular weight of ~44 kDa, which is already challenging for standard NMR spectroscopic methods of structure determination. The dimer with a molecular mass of ~88 kDa is certainly even more challenging.

This might also be one explanation why interaction mapping of β-arrestin 1-382 with a peptide derived from the second intracellular loop of the human CCR5 receptor failed to produce observable peak shifts, although the peptide had been shown in surface plasmon resonance experiments to interact with β-arrestin 1 before [94]. In the case of dimer formation, peak shifts might not be resolved, or more likely in its inactive storage form as a dimer, β-arrestin 1-382 might not be capable of interacting with the peptide.

4.3 Interaction of NAR1 with β-Arrestin 1

4.3.1 Interaction of NAR1 with β-Arrestin 1 *In Vivo*

The crystallization of membrane proteins is a difficult task, since they have to be removed from their native membranous environment and their hydrophilic surface areas are often small and do not allow the formation of stable crystal contacts. A strategy to overcome this problem is complexation with antibody fragments. Since the raising of an antibody that binds NAR1 in a conformation dependent manner, is also a difficult task, using alternative proteins that might fulfill a similar function was attempted. β-arrestins appeared to be that promising alternative. It is sufficiently big, its binding was determined to be in the low nanomolar range [139], and it is sensitive to the active conformation of the receptor. Furthermore it might help overcome stability problems, lock the receptor in its agonist bound conformation and increase its solubility.

Recent experiments reported consensus sequences for the interaction of GPCRs with β-arrestin within the second intracellular loop [140]. The reported sequence starts with the conserved DRY motive, and further important is a proline residue in position 9 (numbering starts with D of the DRY motif). The amino acid sequence in the second intracellular loop of NAR1 contains these residues (Figure 39), and therefore the interaction with β-arrestins was likely. Nevertheless as the interaction between both proteins has not yet been demonstrated, therefore their interaction *in vivo* had to be confirmed. This was achieved by laser scanning

microscopy of cells cotransfected with a NAR1-GFP construct and two versions of CFP-β-arrestin 1. Two versions of β-arrestin were chosen because, for the interaction of full length β-arrestin with NAR1 not only is the conformation of the receptor important, but also phosphorylation of serine and threonine residues within its cytoplasmic domains. This phosphorylation is achieved by a cognate GRK. Since it is not known which GRK phosphorylates NAR1 *in vivo* and whether it is present in BHK and HEK host cells, a second version of β-arrestin was employed that does not require phosphorylation. Truncation of β-arrestin 1 at residue 382 results in a phosphorylation insensitive version that only depends on the activated receptor conformation. Both versions of β-arrestin 1 could be shown to migrate from the cytoplasm to the membrane upon addition of nicotinic acid and activation of NAR1.

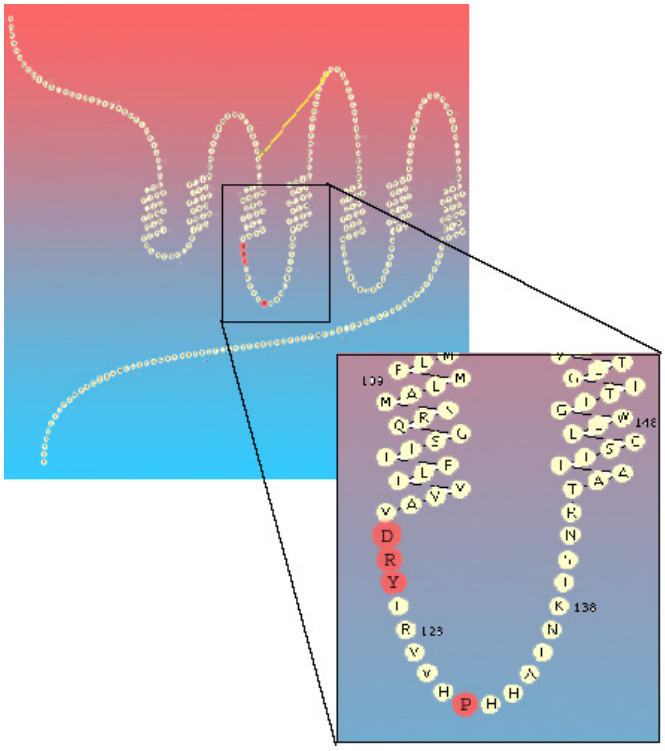

Figure 39: Snake-like plot of NAR1. The 2nd intracellular loop is magnified and contains the DRY motif and the downstream proline residue that are important for β-arrestin binding.

4.3.2 Interaction of NAR1 with β-Arrestin 1 *In Vitro*

After proof of the interaction of β-arrestin1-fl and β-arrestin 1-382 with NAR1 *in vivo*, the reconstitution of purified β-arrestin 1-382 and NAR1 was attempted. Since it had been shown previously that the interaction of visual arrestin and rhodopsin could only be established *in vitro* in the presence of lipids, but not in purified delipidated state of rhodopsin [23], NAR1

was mixed with GST-β-arrestin 1-382 in the presence of asolectin and the agonist nicotinic acid. The interaction was analyzed by a pull down assay using Glutathione 4B Sepharose matrix, capturing GST-β-arrestin 1-382, and bound NAR1. This interaction could be demonstrated for NAR1 samples purified in DM+CHS and LM+CHS, but not for NAR1 purified with Cymal-6+CHS. Although roughly stoichiometric amounts of NAR1 and GST-β-arrestin 1-382 were used as input at quantities producing a clearly visible band in Coomassie stained SDS-PAGE, the amount of bound NAR1 had to be visualized by much more sensitive Western blotting, while the band for GST-β-arrestin 1-382 that was captured on the beads was still visible in Coomassie stain. Thus, clearly sub-stoichiometric amounts of NAR1 were bound by β-arrestin 1-382. Therefore the question that arises immediately is why NAR1 could not be captured quantitatively. Since GST-β-arrestin 1-382 bound to heparin during its purification, and heparin was shown to competitively inhibit the interaction between visual arrestin and rhodopsin, it has to be considered functional and should not be the cause for the partial interaction. NAR1's activity regarding nicotinic acid binding was established by STD studies. Potential reasons for the low stoichiometric binding might be the interference of detergents with the interaction of NAR1 and β-arrestin 1, or the removal of the membrane, since β-arrestin is expected to partially insert its amphipathic N-terminal helix 1 into the membrane bilayer for strong binding of GPCRs. Yet, the low amount of NAR1 captured corresponds well to similar experiments performed by C. Krettler using the β_2-adrenergic receptor. These experiments demonstrated the same low ratio of receptor bound to GST-β-arrestin 1-382, although the ability of the β_2-adrenergic receptor to bind ligand in solubilized form had been shown.

Another intriguing explanation for this inefficient capturing might be the interaction of arrestins with receptor dimers (Figure 40). Very little is known to date about the stoichiometry of the interactions of a GPCR with arrestins, whether they bind a monomeric receptor, a dimer or a higher order oligomeric state. Although this is highly speculative, more and more evidence accumulates in favor of this interpretation. Recent AFM studies showed that rhodopsin is present in native membranes as a densely packed array of dimers [6, 49]. High concentrations of detergent and the purification of rhodopsin abolish this dimeric state [141]. The loss of lipids during purification abolishes the interaction of visual arrestin with rhodopsin *in vitro*, but can be rescued by the addition of lipids [23]. The existence of dimers and higher order oligomers has also been shown for the β_2-adrenergic receptor *in vivo* [18, 19]. Recent modeling experiments compared the interactions of the cytoplasmic face of the rhodopsin monomer with i) the N-domain cavity of visual arrestin, ii) the C-domain, iii) the

N- and C-domain of visual arrestin forming a pincer, and iv) the cytoplasmic domains of a rhodopsin dimer with one being engaged to the N-domain and the other to the C-domain simultaneously, and found that the interaction of visual arrestin with the dimer should be twice as favorable as that with a monomer [22].

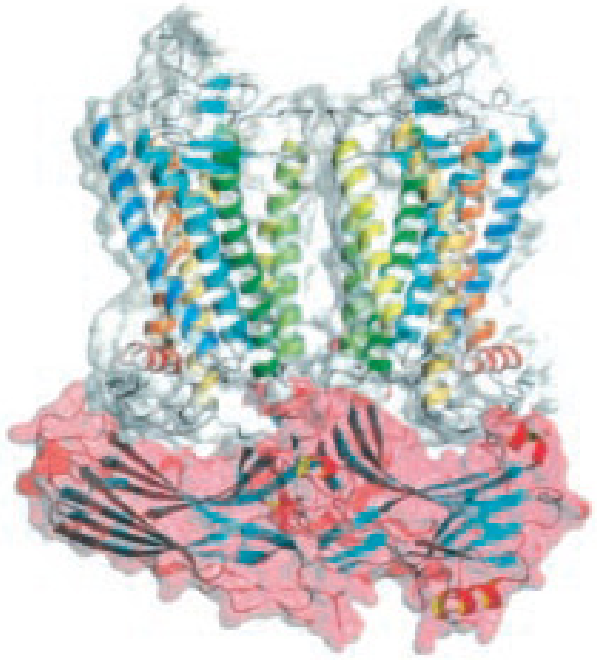

Figure 40: Hypothetical model of visual arrestin (red) binding a dimer of rhodopsin [6]

Since most production and purification strategies so far aimed at producing a uniform sample that in most cases corresponded to a monomeric form of the receptor according to gel filtration analysis, and dimerization is abolished by detergent addition [141], it might be that these strategies were prone to abolish the reconstitution between receptors and β-arrestins. All other experiments that demonstrated the interaction of wild type arrestins or constitutively active variants as in this study were performed with either reconstituted receptors, receptors in native membranes or in living cells, disregarding the oligomeric states of the receptor [90, 139, 142-146]. The only report that measured quantitatively the affinity for the β_2-adrenergic receptor and β-arrestin 1, and determined it to be 1.8 nM [140], used reconstituted receptors and found a stoichiometry of one β-arrestin 1 molecule for three molecules of β_2-adrenergic receptors. It was argued in this case that phosphorylation occurred only at one third of the molecules of the receptor population giving rise to a 1:1 stoichiometry. But given that these experiments were performed before the dimerization of receptors became widely accepted, and furthermore one activated receptor molecule within the dimer might be enough for the interaction with arrestins, these conclusions might have to be reconsidered. One photon can

only activate only one molecule of rhodopsin, but already might lead to the recruitment of visual arrestin to a rhodopsin dimer.

Nevertheless it has to be kept in mind that this present study was exclusively performed with a constitutively active β-arrestin 1 variant and unphosphorylated receptors that have a somewhat lower binding affinity than that of wild type arrestins to phosphorylated receptors, and this could be the explanation for the low yields of reconstitution. Discovering conditions that favor the dimeric form of receptors might overcome this issue and lead to a higher yield of complex reconstitution and support crystallization of the complex.

4.4 Conclusion

This present PhD work is the first report about heterologous large scale expression of the human GPCR NAR1, and the only one to date that is capable of supplying quantities suitable for future structural studies. Additionally, it could be shown that the heterologously produced receptor resembles the pharmacological profile of the native receptor. Therefore the produced material can be used for biochemical and biophysical *in vitro* studies of NAR1 in membranes to elucidate the binding and signaling mechanism of this receptor. Furthermore, its solubilization and purification was successfully achieved, although it will require additional work to find conditions that preserve the receptor in a fully active state throughout solubilization and purification, and a simpler assay to prove this than NMR STD measurements. Similarly more effort has to be put into the reconstitution of the receptor into liposomes, since all attempts failed so far.

This is the first report about the interaction of NAR1 with β-arrestin 1 *in vivo* and *in vitro*. Although the reconstitution of the complex of NAR1 with β-arrestin 1-382 *in vitro* was very inefficient, the results are promising and indicate that crystallization of the complex will be feasible in the future. Nevertheless will it take substantial amounts of work to develop a solid protocol for the formation of this complex, since the potential explanations for the low yield at present are manifold.

5 References

1. Hunte, C., von Jagow, G. & Schägger, H. (2003) *Membrane Protein Purification and Crystallization*
A practical guide, 2 edn, Academic Press.
2. Offermanns, S. (2006) The nicotinic acid receptor GPR109A (HM74A or PUMA-G) as a new therapeutic target, *Trends in Pharmacological Sciences. 27*, 384-390.
3. Xiao, K., Shenoy, S. K., Nobles, K. & Lefkowitz, R. J. (2004) Activation-dependent Conformational Changes in {beta}-Arrestin 2, *J. Biol. Chem. 279*, 55744-55753.
4. Jacoby, E. B., Rochdi; Gerspacher, Marc; Seuwen, Klaus. (2006) The 7TM G-Protein-Coupled Receptor Target Family, *ChemMedChem. 1*, 760-782.
5. Fredriksson, R. & Schioth, H. B. (2005) The Repertoire of G-Protein-Coupled Receptors in Fully Sequenced Genomes, *Mol Pharmacol. 67*, 1414-1425.
6. Liang, Y., Fotiadis, D., Filipek, S., Saperstein, D. A., Palczewski, K. & Engel, A. (2003) Organization of the G Protein-coupled Receptors Rhodopsin and Opsin in Native Membranes, *J. Biol. Chem. 278*, 21655-21662.
7. Lefkowitz, R. J., Rajagopal, K. & Whalen, E. J. (2006) New Roles for ß-Arrestins in Cell Signaling: Not Just for Seven-Transmembrane Receptors, *Molecular Cell. 24*, 643-652.
8. Perez, D. M. (2005) From Plants to man: The GPCR "Tree of Life", *Molecular Pharmacology. 67*, 1383-1384.
9. Pike, N. B. (2005) Flushing out the role of GPR109A (HM74A) in the clinical efficacy of nicotinic acid, *J. Clin. Invest. 115*, 3400-3403.
10. Snyder, D. A., Chen, Y., Denissova, N. G., Acton, T., Aramini, J. M., Ciano, M., Karlin, R., Liu, J. F., Manor, P., Rajan, P. A., Rossi, P., Swapna, G. V. T., Xiao, R., Rost, B., Hunt, J. & Montelione, G. T. (2005) Comparisons of NMR spectral quality and success in crystallization demonstrate that NMR and X-ray crystallography are complementary methods for small protein structure determination, *Journal of the American Chemical Society. 127*, 16505-16511.
11. Altschul, R. H., A; Stephen, JD. (1955) Influence of nictinic acid on serum cholesterol in man, *Archives of Biochemistry. 54*, 558-559.
12. Carlson, L. (1963) Studies on the effect of nicotinic acid on catecholamine lipolysis in adipose tissue in vitro, *Acta Medica Scandinavica. 173*, 719-722.

13. Lorenzen, A., Stannek, C., Lang, H., Andrianov, V., Kalvinsh, I. & Schwabe, U. (2001) Characterization of a G Protein-Coupled Receptor for Nicotinic Acid, *Mol Pharmacol. 59*, 349-357.

14. Soga, T., Kamohara, M., Takasaki, J., Matsumoto, S.-I., Saito, T., Ohishi, T., Hiyama, H., Matsuo, A., Matsushime, H. & Furuichi, K. (2003) Molecular identification of nicotinic acid receptor, *Biochemical and Biophysical Research Communications. 303*, 364-369.

15. Tunaru, S., Kero, J., Schaub, A., Wufka, C., Blaukat, A., Pfeffer, K. & Offermanns, S. (2003) PUMA-G and HM74 are receptors for nicotinic acid and mediate its anti-lipolytic effect. *9*, 352-355.

16. Wise, A., Foord, S. M., Fraser, N. J., Barnes, A. A., Elshourbagy, N., Eilert, M., Ignar, D. M., Murdock, P. R., Steplewski, K., Green, A., Brown, A. J., Dowell, S. J., Szekeres, P. G., Hassall, D. G., Marshall, F. H., Wilson, S. & Pike, N. B. (2003) Molecular Identification of High and Low Affinity Receptors for Nicotinic Acid, *J. Biol. Chem. 278*, 9869-9874.

17. Springael, J.-Y. U., Eneko; Parmentier, Marc. (2005) Dimerization of chemokine receptors and its functional consequences, *Cytokine & Growth Factor Reviews. 16*, 611-623.

18. Salahpour, A., Angers, S., Mercier, J.-F., Lagacé, S. M. & Bouvier, M. (2004) Homodimerization of the beta2-Adrenergic receptor as a Prerequisite for Cell Surface Targeting, *Journal of Biological Chemistry. 279*, 33390-33397.

19. Angers, S., Salahpour, A. & Bouvier, M. (2001) Biochemical and biophysical demonstration of GPCR oligomerization in mammalian cells, *Life Sciences. 68*, 2243-2250.

20. Overton, M. C., Chinault, S. L. & Blumer, K. J. (2003) Oligomerization, Biogenesis, and Signaling Is Promoted by a Glycophorin A-like Dimerization Motif in Transmembrane Domain 1 of a Yeast G Protein-coupled Receptor, *Journal of Biological Chemistry. 278*, 49396-49377.

21. Filipek, S., Krzysko, K. A., Fotiadis, D., Liang, Y., Saperstein, D. A., Engel, A. & Palczewski, K. (2004) A concept for G protein activation by G-protein-coupled receptor dimers: the transducin/rhodopsin interface, *Photochemical &Photobiological Sciences. 3*, 628-638.

22. Modzelewska, A., Filipek, S., Palczewski, K. & Park, P. S.-H. (2006) Arrestin Interaction With Rhodopsin, *Cell Biochemistry and Biophysics. 46*, 1-15.

23. Sommer, M. E., Smith, W. C. & Farrens, D. L. (2006) Dynamics of Arrestin-Rhodopsin Interactions - Acidic Phospholipids enable binding of Arrestin to purified rhodopsin in detergent, *Journal of Biological Chemistry. 281*, 9407-9417.

24. Bryson, B. (2003) *A Short History Of Nearly Everything*.

25. Rodbell, M. (1980) The role of hormone receptors and GTP-regulatory in membrane transduction, *Nature. 284*, 17-22.

26. Gomperts, B. D. K., Ijsbrand M; Tatham, Peter ER. (2003) *Signal Transduction*, Academic Press.

27. Pawson, T. (2002) Regulation and targets of receptor tyrosine kinases, *European Journal of Cancer. 38*, 3-10.

28. McLysaght, A., Hokamp, K. & Wolfe, K. H. (2002) Extensive genomic duplication during early chordate evolution. *31*, 200-204.

29. Gu, X., Wang, Y. & Gu, J. (2002) Age distribution of human gene families shows significant roles of both large- and small-scale duplications in vertebrate evolution. *31*, 205-209.

30. Josefsson, L.-G. (1999) Evidence for kinship between diverse G-protein coupled receptors, *Gene. 239*, 333-340.

31. Borkovich, K. A., Alex, L. A., Yarden, O., Freitag, M., Turner, G. E., Read, N. D., Seiler, S., Bell-Pedersen, D., Paietta, J., Plesofsky, N., Plamann, M., Goodrich-Tanrikulu, M., Schulte, U., Mannhaupt, G., Nargang, F. E., Radford, A., Selitrennikoff, C., Galagan, J. E., Dunlap, J. C., Loros, J. J., Catcheside, D., Inoue, H., Aramayo, R., Polymenis, M., Selker, E. U., Sachs, M. S., Marzluf, G. A., Paulsen, I., Davis, R., Ebbole, D. J., Zelter, A., Kalkman, E. R., O'Rourke, R., Bowring, F., Yeadon, J., Ishii, C., Suzuki, K., Sakai, W. & Pratt, R. (2004) Lessons from the Genome Sequence of Neurospora crassa: Tracing the Path from Genomic Blueprint to Multicellular Organism, *Microbiol. Mol. Biol. Rev. 68*, 1-108.

32. Pandey, S. & Assmann, S. M. (2004) The Arabidopsis Putative G Protein-Coupled Receptor GCR1 Interacts with the G Protein {alpha} Subunit GPA1 and Regulates Abscisic Acid Signaling, *Plant Cell. 16*, 1616-1632.

33. Chen, J.-G., Pandey, S., Huang, J., Alonso, J. M., Ecker, J. R., Assmann, S. M. & Jones, A. M. (2004) GCR1 Can Act Independently of Heterotrimeric G-Protein in Response to Brassinosteroids and Gibberellins in Arabidopsis Seed Germination, *Plant Physiol. 135*, 907-915.

34. Probst, W. S., LA; Schuster, DI; Brosius, J; Sealfon, SC. (1992) Sequence alignment of the G-protein coupled receptor superfamily, *DNA and Cell Biology. 11*, 1-20.

35. Kolakowski, L. J. (1994) GCRDb: a G-protein-coupled receptor database, *Receptors and Channels. 2*, 1-7.

36. Pierce, K., Permont, RT, Lefkowitz, RJ. (2002) Seven-transmembrane receptors, *Nature Reviews Molecular Cell Biology. 3*, 639-650.

37. Palczewski, K., Kumasaka, T., Hori, T., Behnke, C. A., Motoshima, H., Fox, B. A., Trong, I. L., Teller, D. C., Okada, T., Stenkamp, R. E., Yamamoto, M. & Miyano, M. (2000) Crystal Structure of Rhodopsin: A G Protein-Coupled Receptor, *Science. 289*, 739-745.

38. Pebay-Peyroula, E., Rummel, G., Rosenbusch, J. P. & Landau, E. M. (1997) X-ray Structure of Bacteriorhodopsin at 2.5 Angstroms from Microcrystals Grown in Lipidic Cubic Phases, *Science. 277*, 1676-1681.

39. Okada, T. & Palczewski, K. (2001) Crystal structure of rhodopsin: implications for vision and beyond, *Current Opinion in Structural Biology. 11*, 420-426.

40. Gether, U. (2000) Uncovering Molecular Mechanisms Involved in Activation of G Protein-Coupled Receptors, *Endocr Rev. 21*, 90-113.

41. Kristiansen, K. (2004) Molecular mechanisms ligand binding, signaling, and regulation within the superfamily of G-protein-coupled receptors: molecular modeling and mutagenisis approaches to receptor structure and function, *Pharmacology & Therapeutics. 103*, 21-80.

42. Vassilatis, D. K., Hohmann, J. G., Zeng, H., Li, F., Ranchalis, J. E., Mortrud, M. T., Brown, A., Rodriguez, S. S., Weller, J. R., Wright, A. C., Bergmann, J. E. & Gaitanaris, G. A. (2003) The G protein-coupled receptor repertoires of human and mouse, *PNAS. 100*, 4903-4908.

43. Fredriksson, R., Lagerstrom, M. C., Lundin, L.-G. & Schioth, H. B. (2003) The G-Protein-Coupled Receptors in the Human Genome Form Five Main Families. Phylogenetic Analysis, Paralogon Groups, and Fingerprints, *Mol Pharmacol. 63*, 1256-1272.

44. Caron, M. S., Y; Pitha, J; Kociolek, K; Lefkowitz RJ. (1979) Affinity chromatography of the beta-adrenergic receptor, *Journal of Biological Chemistry. 254*, 2923-2927.

45. Dixon, R. A. F., Kobilka, B. K., Strader, D. J., Benovic, J. L., Dohlman, H. G., Frielle, T., Bolanowski, M. A., Bennett, C. D., Rands, E., Diehl, R. E., Mumford, R. A., Slater, E. E., Sigal, I. S., Caron, M. G., Lefkowitz, R. J. & Strader, C. D. (1986) Cloning of the gene and cDNA for mammalian [beta]-adrenergic receptor and homology with rhodopsin, *Nature. 321*, 75-79.

46. Krauss, G. (2003) *Biochemistry of Signal Transduction and Regulation*, 3rd edn, Wiley-VCH.

47. Lefkowitz, R. J. & Shenoy, S. K. (2005) Transduction of Receptor Signals by {beta}-Arrestins, *Science. 308*, 512-517.

48. Franco, R., Casado, V., Mallol, J., Ferrada, C., Ferre, S., Fuxe, K., Cortes, A., Ciruela, F., Lluis, C. & Canela, E. I. (2006) The Two-State Dimer Receptor Model: A General Model for Receptor Dimers, *Mol Pharmacol. 69*, 1905-1912.

49. Fotiadis, D., Liang, Y., Filipek, S., Saperstein, D. A., Engel, A. & Palczewski, K. (2003) Atomic-force microscopyRhodopsin dimers in native disc membranes, *Nature. 421*, 127-128.
50. Karnik, S. G., Camelia; Patil, Supriya; Saad, Yasser; Takezako, Takanobu. (2003) Activation of G-protein-coupled receptors: a common molecular mechanism, *Trends in Endocrinology and Metabolism. 14*, 431-437.
51. Bissantz, C., Bernard, P., hibert, M. & Rognan, D. (2003) Protein-based virtual screening of chemical databases. II. Are homology models of G-Protein Coupled Receptors suitable targets?, *Proteins. 50*, 5-25.
52. Evers, A. & Klebe, G. (2004) Successful Virtual Screening for a Submicromolar antagonist of the Neurokinin-1 receptor Based on a Ligand-Supported Homology Model, *Journal of Medicinal Chemistry. 47*, 5381-5392.
53. Baneres, J.-L. & Parello, J. (2003) Structure-based Analysis of GPCR Function: Evidence for a Novel Pentameric Assembly between the Dimeric Leukotriene B4 Receptor BLT1 and the G-protein, *Journal of Molecular Biology. 329*, 815-829.
54. Harrison, C. (2006) Targeting the hotspot of G-protein interactions, *Nature Reviews Drug Discovery. 5*.
55. Bonacci, T. M. M., Jennifer L; Yuan, Chujun; Lehmann, David M, Malik, Sundeep; Wu, Dianqing; Font, Jose L; Bidlack, Jean M; Smrcka, Alan M. (2006) Differential Targeting of Gβγ-Subunit Signaling with Small Molecules, *Science. 312*, 443-446.
56. Iwata, S., Ostermeier, C., Ludwig, B. & Michel, H. (1995) Structure at 2.8 A resolution of cytochrome c oxidase from Paracoccus denitrificans, *Nature. 376*, 660-669.
57. Hunte, C., Koepke, J., Lange, C., Rossmanith, T. & Michel, H. (2000) Structure at 2.3 A resolution of the cytochrome bc(1) complex from the yeast Saccharomyces cerevisiae co-crystallized with an antibody fragment, *Structure. 8*, 669-684.
58. Zhou, Y., Morais-Cabral, J., Kaufman, A. & Mackinnon, R. (2001) Chemistry of ion coordination and hydration revealed by a K+ channel-Fab complex at 2.0 A resolution, *Nature. 414*, 43-48.
59. Ostermeier, C., Iwata, S., Ludwig, B. & Michel, H. (1995) Fv fragment-mediated crystallization of the membrane protein bacterial cytochrome c oxidase, *Nature Structural Biology. 2*, 842-846.
60. (1975) Coronary Drug Project Research Group: Clofibrate and niacin in coronary heart disease, *The Journal of the American Medical Association. 231*, 360-381.

61. Canner, P., Berge, K., wenger, N., Stamler, J., Friedman, L., Prineas, R. & friedewald, W. (1986) Fifteen year mortality in Coronary DrugProject patients: long-term benefit with niacin, *Journal of the American College of Cardiology. 8*, 1245-1255.

62. Taggart, A. K. P., Kero, J., Gan, X., Cai, T.-Q., Cheng, K., Ippolito, M., Ren, N., Kaplan, R., Wu, K., Wu, T.-J., Jin, L., Liaw, C., Chen, R., Richman, J., Connolly, D., Offermanns, S., Wright, S. D. & Waters, M. G. (2005) (D)-{beta}-Hydroxybutyrate Inhibits Adipocyte Lipolysis via the Nicotinic Acid Receptor PUMA-G, *J. Biol. Chem. 280*, 26649-26652.

63. Hanahan, D., Jessee, J. & Bloom, F. R. (1991) Techniques for transformation of E. coli in *Methods in Enzymology* pp. 63-113.

64. Han, M., Gurevich, V. V., Vishnivetskiy, S. A., Sigler, P. B. & Schubert, C. (2001) Crystal Structure of [beta]-Arrestin at 1.9 A: Possible Mechanism of Receptor Binding and Membrane Translocation, *Structure. 9*, 869-880.

65. Boettner, M., Prinz, B., Holz, C., Stahl, U. & Lang, C. (2002) High-Throughput screening for expression of heterologous proteins in the yeast *Pichia pastoris*, *Journal of Biotechnology. 99*, 51-62.

66. Cheng, Y. & Prussof, W. H. (1973) Relation between the inhibition constant (K1) and the concentration of inhibitor which causes 50 per cent inhibition (50) of an enzymatic reaction, *Biochemical Pharmacology. 22*, 3099-3108.

67. Prual, C. (2006) *Production of the human adenosine A_{2A} receptor in Pichia pastoris, its isolation and purification and the selection of a specific single-chain Fv fragment by phage display*, Johann Wolfgang Goethe - Universität, Frankfurt am Main.

68. Caron, M. G. & Lefkowitz, R. J. (1976) Solubilization and Characterization of the β-adrenergic Receptor Binding Sites of Frog Erythrocytes, *Journal of Biological Chemistry. 251*, 2374-2384.

69. Cerione, R. A. & Ross, E. M. (1991) Reconstitution of Receptors and G Proteins in Phospholipid Vesicles in *Methods in Enzymology 292* pp. 329-342, Academic Press.

70. DeGrip, W. J., VanOOstrum, J. & Bovee-Geurts, P. H. M. (1998) Selective detergent-extraction from mixed detergent/lipid/protein micelles using cyclodextrin inclusion compounds: a novel generic approach for the preparation of proteoliposomes, *Biochemical Journal. 330*, 667-674.

71. Ambudkhar, S. V., Lelong, I. H., Zhang, J. & Cardarelli, C. (2002) Purification and Reconstitution of Human P-Glycoprotein in *Methods in Enzymology* pp. 492-504, Academic Press.

72. Wigler, M., Pellicer, A., Silverstein, S. & Axel, R. (1978) Biochemical transfer of single-copy eucaryotic genes using total cellular DNA as donor, *Cell. 14*, 725-731.
73. Graham & Eb, V. d. (1973) A New Technique for the Assay of Infectivity of Human Adenovirus 5 DNA, *Virology. 52*, 456-467.
74. Smith, P., Krohn, R., Hermanson, G., Mallia, A., Gartner, F., Provenzano, M., Fujimoto, E., Goeke, N., Olson, B. & Klenk, D. (1985) Measurement of protein using bicinchoninic acid, *Analytical Biochemistry. 150*, 76-85.
75. Tornqvist, H. & Belfrage, P. (1976) Determination of protein in adipose tissue extracts, *Journal of Lipid Research. 17*, 542-545.
76. Laemmli, U. (1970) Cleavage of structural proteins during the assembly of the head of bacteriophage T4, *Nature. 227*, 680-685.
77. Fling, S. P. & Gregerson, D. S. (1986) Peptide and Protein Molecular Weight Determination by Electrophoresis Using a High-Molarity tris Buffer System without Urea, *Analytical Biochemistry. 155*, 83-88.
78. Mikkelsen, S. R. & Cortón, E. (2004) *Bioanalytical Chemistry*, Wiley.
79. Andre, N., Cherouati, N., Prual, C., Steffan, T., Zeder-Lutz, G., Magnin, T., Pattus, F., Michel, H., Wagner, R. & Reinhart, C. (2006) Enhancing functional production of G protein-coupled receptors in Pichia pastoris to levels required for structural studies via a single expression screen, *Protein Science. 15*, 1115-1126.
80. Grünewald, S., Haase, W., Molsberger, E., Michel, H. & Reiländer, H. (2004) Production of the human D2S receptor in the methylotrophic yeast *P. pastoris*, *Receptors and Channels. 10*, 37-50.
81. Reiländer, H. & Weiß, H. M. (1998) Production of G-protein-coupled receptors in yeast, *Current Opinion in Biotechnology. 9*, 510-517.
82. Weiß, H. M., Haase, W., Michel, H. & Reiländer, H. (1995) Expression of functional mouse 5-HT5a serotonin receptor in the methylotrophic yeast Pichia pastoris: pharmacological characterization and localization, *FEBS Letters. 377*, 451-456.
83. Weiß, H. M., Haase, W., Michel, H. & Reiländer, H. (1998) Comparative biochemical and pharmacological characterization of the mouse $5HT_{5a}$ 5-hydroxytryptamine receptor and the human b2 Adrenergic receptor produced in the methylotrophic yeast Pichia pastoris, *Biochemical Journals. 330*, 1137-1147.
84. Maritini, L., Hastrup, H., Holst, B., Fraile-Ramos, A., Marsh, M. & Schwartz, T. W. (2002) NK1 Receptor fused to β-Arrestin Displays a Single-Component, High-Affinity Molecular Phenotype, *Mol Pharmacol. 62*, 31-37.

85. Ivanovic, A. (2001) *Klonierung rekombinanter Histamin H1 - rezeptoren und deren Charakterisierung, Solubilisierung und Reinigung nach heterologer Produktion*, Johann Wolfgang Goethe - Universität, Frankfurt am Main

86. Gao, Z.-G. & Ijzerman, A. P. (2000) Allosteric Modulation of A2A Adenosine Receptors by Amiloride Analogues and Sodium Ions, *Biochemical Pharmacology. 60*, 669-679.

87. Gao, Z.-G., Jiang, Q., Jacobson, K. A. & Ijzerman, A. P. (2000) Site-Directed Mutagenesis Studies of Human A2A Adenosine Receptors: Involvement of Glu13 and His278 in Ligand Binding and Sodium Modulation, *Biochemical Pharmacology. 60*, 661-668.

88. Julenius, K., Molgaard, A., Gupta, R. & Brunak, S. (2005) Prediction, conservation analysis and structural characterization of mammalian mucin-type O-glycosylation sites, *Glycobiology. 15*, 153-164.

89. Gupta, R., Jung, E. & Brunak, S. (2004) Prediction of N-glycosylation sites in human proteins., *in preparation*.

90. Kovoor, A., Celver, J., Abdryashitov, R. I., Chavkin, C. & Gurevich, V. V. (1999) Targeted construction of phosphorylation-independent beta-arrestin mutants with constitutive activity in cells, *Journal of Biological Chemistry. 274*, 6831-6834.

91. Jusko, W. & Gretch, M. (1976) Plasma and tissue protein binding of drugs in pharmakokinetics, *Drug Metabolism Reviews. 5*, 43-140.

92. Gervais, F. G., Moerello, J.-P., Beaulieu, C., Sawyer, N., Denis, D., Greig, G., Malebranche, A. D. & O'Neill, G. P. (2005) Identification of a Potent and Selective Synthetic Agonist at the CRTH2 Receptor, *Molecular Pharmacology. 67*, 1834-1839.

93. Yee, A. A., Savchenko, A., Ignachenko, A., Lukin, J., Xu, X. H., Skarina, T., Evdokimova, E., Liu, C. S., Semesi, A., Guido, V., Edwards, A. M. & Arrowsmith, C. H. (2005) NMR and x-ray crystallography, complementary tools in structural proteomics of small proteins, *Journal of the American Chemical Society. 127*, 16512-16517.

94. Hüttenrauch, F., Nitzki, A., Lin, F.-T., Höning, S. & Oppermann, M. (2002) beta-Arrestin Binding to CC Chemokine Receptor 5 Requires Multiple C-terminal Receptor Phosphorylation Sites and Involves a Conserved Asp-Arg-Tyr Sequence Motif, *Journal of Biological Chemistry. 277*, 30769-30777.

95. Hassaine, G., Wagner, R., Kempf, J., Cherouati, N., Hassaine, N., Prual, C., André, N., Reinhart, C., Pattus, F. & Lundstrom, K. (2006) Semliki Forest virus vectors for overexpression of 101 G protein-coupled receptors in mammalian host cells, *Protein Expression & Purification. 45*, 343-351.

96. Griffith, D. A., Delipala, C., Leadsham, J., Jarvis, S. M. & Oesterheldt, D. (2003) a novel expression system for the overproduction of quality-controlled membrane proteins, *FEBS Letters. 553*, 45-50.

97. Grisshammer, R. (2006) Understanding recombinant expression of membrane proteins, *Current Opinion in Biotechnology. 17*, 337-340.

98. Tian, C., Breyer, R. M., Kim, H. J., Karra, M. D., Friedman, D. B., Karpay, A. & Sanders, C. R. (2005) Solution NMR Spectroscopy of the Human Vasopression V2 Receptor, A G Proteiin-Coupled Receptor, *The Journal of the American Chemical Society. 127*, 8010-8011.

99. Grisshammer, R., White, J. F., Trinth, L. B. & Shiloach, J. (2005) Large-scale expression and purification of a human G-protein-coupled receptor for structure determination - an overview, *Journal of Structural and Functional Genomics. 6*, 159-163.

100. Baneres, J.-L., Martin, A., Hullot, P., Girard, J.-P., Rossi, J.-C. & Parello, J. (2003) Structure-based Analysis of GPCR Function: Conformational Adaptation of both Agonist and Receptor upon Leukpotriene B_4 Binding to Recombinant BLT1, *Journal of Molecular Biology. 329*, 801-814.

101. Lamla, T. & Erdmann, V. A. (2004) The Nano-tag, a streptavidin-binding peptide for the purification and detection of recombinant proteins, *Protein Expression & Purification. 33*, 39-47.

102. Opekarova, M. & Tanner, W. (2003) Specific lipid requirements of membrane proteins - a putative bottleneck in heterologous expression, *Biochim Biophys Acta. 1610*, 11-22.

103. Lorenzen, A., Stannek, C., Burmeister, A., Kalvinsh, I. & Schwabe, U. (2002) G protein-coupled receptor for nicotinic acid in mouse macrophages, *Biochemical Pharmacology. 64*, 645-648.

104. Tang, Y., Zhou, L., Gunnet, J. W., Wines, P. G., Cryan, E. V. & Demarest, K. T. (2006) Enhancement of arachidonic acid signaling pathway by nicotinic acid receptor HM74A, *Biochemical and Biophysical Research Communications. 345*, 29-37.

105. Tunaru, S., Lattig, J., Kero, J., Krause, G. & Offermanns, S. (2005) Characterization of Determinants of Ligand Binding to the Nicotinic Acid Receptor GPR109A (HM74A/PUMA-G), *Mol Pharmacol. 68*, 1271-1280.

106. Figler, R. A., Graber, S. G., Lindorfer, M. A., Yasuda, H., Linden, J. & Garrison, J. (1996) Reconstitution of recombinant bovine A1 adenosine receptors in Sf9 cell membranes with recombinant G proteins of defined composition, *Molecular Pharmacology. 50*, 1587-1595.

107. Figler, R. A., Lindorfer, M. A., Graber, S. G., Garrison, J. C. & Linden, J. (1997) Reconstitution of Bovine A_1 Adenosine Receptors and G Proteins in Phospholipid Vesicles: βγ-Subunit Composition Influences Guanine Nucleotide Exchange and Agonsit Binding, *Biochemistry. 36*, 16288-16299

108. McIntire, W. E., Myung, C.-S., MacCleery, G., Wang, Q. & Garrison, J. C. (2002) Reconstitution of G Protein-Coupled Receptors with Recombinant G Protein α and βγ Subunits in *Methods in Enzymology* pp. 372-393.

109. Li, Z., Xiong, F., Lin, Q., d'Anjou, M., Dauqulis, A., Yang, D. & HEW, C. (2001) Low-temperature increases the yield of biologically active herring antifreeze protein in Pichia pastoris, *Protein Expression & Purification. 21*, 438-445.

110. Mattanovich, D., Gasser, B., Hohenblum, H. & Sauer, M. (2004) Stress in recombinant protein producing yeasts, *Journal of Biotechnology. 113*, 121-135.

111. Yu, Z. & Quinn, P. (1998) The modulation of membrane structure and stability by dimethyl sulphoxide, *Molecular Membrane Biology. 15*, 59-68.

112. Murata, Y., Watanabe, T., Masanori, S., Momose, Y., Nakahara, T., Oka, S.-i. & Iwahashi, H. (2003) Dimethyl Sulfoxide Exposure Facilitates Phospholipid Biosynthesis and Cellular Membrane Proliferation in Yeast Cells, *Journal of Biological Chemistry. 278*, 33185-33193.

113. Zhang, W., Needham, D., Coffin, M., Rooker, A., Hurban, P., Tanzer, M. & Shuster, J. (2003) Microarray analyses of the metabolic responses of Saccharomyces cerevisiae to organic solvent dimethyl sulfoxide, *Journal of Industrial Microbiology and Biotechnology. 30*, 57-69.

114. King, K., Dohlman, H. G., Thorner, J., Caron, M. G. & Lefkowitz, R. J. (1990) Control of yeast mating signal transduction by mammalian β2-adrenergic receptor and Gs α subunit, *Science. 250*, 121-123.

115. Pert, C. B. & Snyder, S. H. (1974) Opiate Receptor Binding of Agonist and Antagonist Affected Differentially by Sodium, *Molecular Pharmacology. 10*, 868-879.

116. Horstman, D. A., Brandon, S., Wilson, A. L., Guyer, C. A., Cragoe, E. J. J. & Limbird, L., E. (1990) An Aspartate Conserved among G-protein Receptors Confers Allosteric Regulation of α_2-Adrenergic Receptors by Sodium, *Journal of Biological Chemistry. 265*, 21590-21595.

117. Kong, H., Raynor, K., Yasuda, K., Moe, S. T., Portoghese, P. S., Bell, G. I. & Terry, R. (1993) A Single Residue, Aspartic Acid 95, in the δ Opioid Receptor Specifies Selective High Affinity Agonist Binding, *Journal of Biological Chemistry. 268*, 23055-23058.

118. Neve, K. A., Cumbay, M. G., Thompson, K. R., Yang, R., Buck, D. C., Watts, V. J., Durand, C. J. & Teeter, M. M. (2001) Modeling and Mutational Analysis of a Putative Sodium-Binding Pocket on the Dopamine D2 Receptor, *Molecular Pharmacology. 60*, 379-381.

119. Lin, S., Gether, U. & K., K. B. (1996) Ligand Stabilization of the β_2 Adrenergic Receptor: Effect of DTT on Receptor Conformation Monitored by Circular Dichroism and Fluorescence Spectroscopy, *Biochmistry. 35*, 14445-14451.

120. Shire, D., Calandra, B., Delpech, M., Dumont, X., Kaghad, M., Le Fur, G., Caput, D. & Ferrara, P. (1996) Structural Features of the Central Cannabinoid CB1 Receptor Involved in the Binding of the Specific CB1 Antagonist SR141716A*, *Journal of Biological Chemistry. 271*, 6941-6946.

121. Grünewald, S. (1997) *Produktion des humanen Dopamin D2S Rezeptors in Insektenzellen: Biochemische und pharmakologische Charakterisierung soie Entwicklung eines in vivo Rekonstitutionssystems zur Untersuchung der G Protein Kopplung*, Johann Wolfgang Goethe Universität, Frankfurt am Main.

122. Haga, T., Haga, K. & Hulme, E. C. (1990) Solubilization, purification, and molecular characterization of receptors: principles and strategy in *Receptor Biochemistry*
A Practical Approach (Hulme, E. C., ed), Oxford.

123. Schwartz, T. W. & Holst, B. (2006) Ago-Allosteric Modulation and Other Types of Allostery in Dimeric 7TM Receptors, *Journal of Receptors and Signal Transduction. 26*, 107-128.

124. Demoliou-Mason, C. D. & Barnard, E. A. (1990) Opioid Receptors in *Receptor Biochemistry*
A Practical Approach (Hulme, E. C., ed), Oxford.

125. Berry, J. A., Burgess, A. J. & Towers, P. J. (1991) Scintillation Proximity Assay: competitive binding studies with [^{125}I]endothelin-1 in human placenta and porcine lung, *J. Cardiovasc. Pharmacol. 17*, 143-145.

126. Murray, W. V., Lalan, P. & Gill, A. (1993) Substituted pyrrolidin-2-one biphenyltetrazoles as angiotensin II antagonists, *Bioorganic & Medicinal Chemistry letters. 3*, 369-374.

127. Sen, S. (2005) *Functional Studies on alpha2-Adrenergic Receptor Subtypes*, University of Helsinki, Helsinki.

128. Devesa, F., Chams, V., Dinadayala, P., Stella, A., Ragas, A., Auboiroux, H., Stegmann, T. & Poquet, Y. (2002) Functional reconstitution of the HIV receptors CCR5 and CD4 in liposomes, *European Journal of Biochemistry. 269*, 5163-5174.

129. Eroglu, C., Cronet, P., Panneels, V., Beaufils, P. & Sinning, I. (2002) Functional reconstitution of purified metabotropic glutamate receptor expressed in the fly eye, *EMBO reports. 3*, 491-496.

130. Ratnala, V. R. P., Swarts, H. G. P., VanOOstrum, J., Leurs, R., DeGroot, H. J. M., Bakker, R. A. & DeGrip, W. J. (2004) Large-scale overproduction, functional purification and ligand affinities of the His-tagged human histamine H1 receptor, *European Journal of Biochemistry. 271*, 2636-2646.

131. Chazot, J. A. & Strange, P. G. (1992) Coupling of D_2 dopamine receptors to G-proteins in solubilized preparations of bovine caudate nucleus, *Biochemical Journal. 281*, 369-375.

132. Granzin, J., Wilden, U., Choe, H., Labahn, J., Krafft, B. & Buldt, G. (1998) X-ray crystal structure of arrestin from bovine rod outer segments, *Nature. 391*, 918-921.

133. Hirsch, J., Schubert, C., Gurevich, V. V. & Sigler, P. B. (1999) The 2.8 A crystal structure of visual arrestin: a model for arestin's regulation, *Cell. 97*, 257-69.

134. Sutton, R., Vishnivetskiy, S. A., Robert, J., Hanson, S. M., Raman, D., Knox, B., Kono, M., Navarro, J. & Gurevich, V. V. (2005) Crystal structure of cone arrestin at 2.3A: evolution of receptor specificity, *Journal of Molecular Biology. 354*, 1069-1080.

135. Buczylko, J., Gutmann, C. & Palczewski, K. (1991) Regulation of rhodopsin kinase by autophosphorylation, *Proceedings of the National Academy of Sciences of the United States of America. 88*, 2568-2572.

136. Imamoto, Y., Tamura, C., Kamikubo, H. & Kataoka, M. (2003) Concentration-dependent Tetramerization of Bovine Visual Arrestin, *Biophysical Journal. 85*, 1186-1195.

137. Storez, H., Scott, M. G. H., Issafras, H., Burtey, A., Benmerah, A., Muntaner, O., Piolot, T., Tramier, M., Coppey-Moisan, M., Bouvier, M., Labbé-Jullié, C. & Marullo, S. (2005) Homo- and Hetero-oligomerization of β-Arrestins in Living Cells, *Journal of Biological Chemistry. 280*, 40210-40215.

138. Milano, S. K., Kim, Y.-M., Stefano, F. P., Benovic, J. L. & Brenner, C. (2006) Nonvisual Arrestin Oligomerization and Cellular Localization Are Regulated By Inositol Hexakisphosphate Binding, *J Biol Chem. 281*, 9812-9823.

139. Söhlemann, P., Hekman, M., Puzicha, M., Buchen, C. & Lohse, M. J. (1995) Binding of purified recombinant β-arrestin to guanine-nucleotide-binding-protein-coupled receptors, *European Journal of Biochemistry. 232*, 464-472.

140. Marion, S., Oakley, R. H., Kim, K.-M., Caron, M. G. & Barak, L. S. (2006) A beta-Arrestin Binding Determinant Common to the Second Intracellular Loops of Rhodopsin Family G Protein-coupled Receptors, *J. Biol. Chem. 281*, 2932-2938.

141. Jastrzebska, B., Maeda, T., Zhu, L., Fotiadis, D., Filipek, S., Engel, A., Stenkamp, R. E. & Palczewski, K. (2004) Functional Characterization of Rhodopsin Monomers and Dimers in Detergent, *Journal of Biological Chemistry. 279*, 54663-54675.

142. Gurevich, V. V., Palsrylaarsdam, R., Benovic, J. L., Hosey, M. M. & Onorato, J. J. (1997) Agonist-Receptor-Arrestin, an Alternative Ternary Complex with High Agonist Affinity, *Journal of Biological Chemistry. 272*, 28849-28852.

143. Oakley, R. H., Laporte, S. A., Holt, J. A., Barak, L. S. & Caron, M. G. (1999) Association of β-Arrestin with G Protein-coupled Receptors during Clathrin-mediated Endocytosis Dictates the Profile of Receptor Resensitization, *Journal of Biological Chemistry. 274*, 32248-32257.

144. Oakley, R. H., Laporte, S. A., Holt, J. A., Barak, L. S. & Caron, M. G. (2001) Molecular Determinats Underlying the formation of Stable Intracellular G Protein-coupled Receptor-β-Arrestin Complexes after Receptor Endocytosis, *Journal of Biological Chemistry. 276*, 19452-19460.

145. Krasel, C., Bünemann, M., Lorenz, K. & Lohse, M. J. (2005) β-Arrestin Binding to the β_2-Adrenergic Receptor Requires Both Receptor Phosphorylation and Receptor Activation, *Journal of Biological Chemistry. 280*, 9528-9535.

146. Hanson, S. M. & Gurevich, V. V. (2006) The Differential Engagement of Arrestin Surface Charges by the Various Functional Forms of the Receptor, *J. Biol. Chem. 281*, 3458-3462.

6 Abbreviations

7TM	7 Trans Membrane
ACTH	Adrenocorticotropic Hormone
ADP	Adenosine Di-Phosphate
Amp	Ampicillin
AP-2	Adaptor Protein 2
BCIP	5-Bromo-4-chloro-3-indolylphosphate
BGH	Bovine Growth Hormone
BHK	Baby Hamster Kidney
BSA	Bovine Serum Albumin
cAMP	Cyclic Adenosine Mono-Phosphate
cAR	cAMP Receptor
CFP	Cyan Fluorescent Protein
cGMP	cyclic Guanosine Mono-Phosphate
CGRF	Calcitonin Gene-Related Peptide
CHS	Cholesteryl Hemisuccinate
CIAP	Calf Intestinal Alkaline Phosphatase
CMV	Cauliflower Mosaic Virus
CRD	Cysteine Rich Domain
CRF	Corticotropin-releasing Factor
DAG	Diacylglycerol
Dermal DC	Dermal Dendritic Cell
DM	n-decyl-ß-D-maltopyranoside
DMEM	Dulbecco's Modified Eagles Medium
DMF	Dimethylformamide
DMSO	Dimethyl sulfoxide
DNA	Deoxyribonucleic Acid
dNTP	Deoxyribonucleotides
DP	Prostaglandin D2
DTT	Dithiothreitol
EDTA	Ethylenediaminetetracetic Acid
EL	Extracellular Loop

EGFR	Epidermal Growth Factor Receptor
EP2	Prostaglandin E2
EP4	Prostaglandin E4
ERK	Extracellular Signal Regulated Kinase
F_{ab}	Fragment Antigen Binding
FCS	Fetal Calf Serum
Fv	Variable Fragment
FYVE	Fab1, YOTB/ZK632.12, Vac1, and EEA1
GABA	γ-Aminobutyricacid
GAP	GTPase Activating Protein
GDP	Guanosine Di-Phosphate
GEF	Guanosine Nucleotide Exchange Factor
GFP	Green Fluorescent Protein
GHRH	Growth Hormone Releasing Hormone
GIP	Gastric Inhibitory Polypeptide
GPCR	G-Protein Coupled Receptor
Grb2	Growth Factor Receptor-Bound Protein 2
GRK	G-Protein Coupled Receptor Kinase
GST	Glutathione-S-Transferase
GTP	Guanosine Tri-Phosphate
HDL	High Density Lipoprotein
HEK	Human Embryonic Kidney
HEPES	4-(2-hydroxyethyl)-1-piperazineethanesulfonic acid
HetNOE	Heteronuclear Overhauser Effect
HIS4	Histidinol Dehydrogenase
IL	Intracellular Loop
IP3	Inositol Trisphosphate
IPTG	Isopropyl β-D Thiogalactoside
IR	Insulin Receptor
IRS1	Insulin Receptor Substrate 1
JNK	c-Jun N-terminal Kinase
Kan	Kanamycin
LDL	Low Density Lipoprotein
LM	n-dodecyl-β-D-maltopyranoside

MAP	Mitogen Activated Protein
MAPK	Mitogen Activate Protein Kinase
MCS	Multiple Cloning Site
MSH	Melanin Stimulating Hormone
NAD+	Nicotinamide Adenine Dinucleotide
NADP+	Nicotinamide Adenine Dinucleotide Phosphate
NAR1	Nicotinic Acid Receptor 1
NBT	Nitrobluetetrazolium
NMR	Nuclear Magnetic Resonance
NO	Nitric Oxide
NSF	N-maleimide Sensitive Factor
NK1	Neurokinin 1
OD	Optical Density
PACAP	Pituary Adenylate Cyclase Activated Polypeptide
PAGE	PolyAcrylamide Gel Electrophoresis
PBS	Phosphate Buffered Saline
PCR	Polymerase Chain Reaction
PDZ	PSD95/SAP90, Discs large, Zonula occludens-1
PE	Phosphatidylethanolamine
PEI	Polyethyleneimine
PGD2	Prostaglandin D2
PGE2	Prostaglandin E2
PH	Pleckstrin Homology
PI3-Kinase	Phosphatidyl-Inositol 3 Kinase
PIP2	Phosphatidylinositol-(4,5)-Bisphosphate
PKA	Protein Kinase A
PKC	Protein Kinase C
PMSF	Phenylmethylsulfonylfluoride
PtdIns(4,5)-P	Phosphatidylinositol-(4,5)-Bisphosphate
PtdIns(3,4,5)-P	Phosphatidylinositol-(3,4,5)-Trisphosphate
PTH	Parathyroid Hormone
PTHrP	Parathyroid Hormone-Related Protein
PTK	Protein Tyrosine Kinase
PTB	Phospho-Tyrosine Binding

PUMA-G	Protein Upregulated in Macrophages by Interferon γ
PVDF	Polyvinylidenfluorid
RGS	Regulator of G-Protein Signaling
RTK	Receptor Tyrosine Kinase
SDS	Sodium Dodecyl Sulfate
SH2	Src-Homology 2
SH3	Src-Homology 3
Shc	Src Homology 2 domain Containing
SPA	Scintillation Proximity Assay
Src	v-src sarcoma (Schmidt-Ruppin A-2) viral oncogene homolog (avian)
STAT	Signal Transducer and Activator of Transcription
STD	Saturation Transfer Difference
TBS	Tris Buffered Saline
TBST	Tris Buffered Saline + Tween20
TEMED	N,N,N'N'-tetramethylethylenediamine
TEV	Tobacco Etch Virus
TM	Transmembrane Helix
VIP	Vasoactive Intestinal Peptide
VLDL	Very Low Density Lipoprotein
YNB	Yeast Nitrogen Base

7 Appendix

7.1 Amino Acid Sequneces

7.1.1 Proteins

7.1.1.1 NAR1 (human)

N-terminus:

MNRHHLQDHFLEIDKKNCCVFRDDFIVKVLPPVLGLEFIFGLLGNGLALWIFCFHLKS
WKSSRIFLFNLAVADFLLIICLPFLMDNYVRRWDWKFGDIPCRLMLFMLAMNRQGSII
FLTVVAVDRYFRVVHPHHALNKISNRTAAIISCLLWGITIGLTVHLLKKKMPIQNGGA
NLCSSFSICHTFQWHEAMFLLEFFLPLGIILFCSARIIWSLRQRQMDRHAKIKRAITFIM
VVAIVFVICFLPSVVVRIRIFWLLHTSGTQNCEVYRSVDLAFFITLSFTYMNSMLDPVV
YYFSSPSFPNFFSTLINRCLQRKMTGEPDNNRSTSVELTGDPNKTRGAPEALMANSGE
PWSPSYLGPTSP –C-terminus

7.1.1.2 β-Arrestin 1 (human)

N-terminus:

MGDKGTRVFKKASPNGKLTVYLGKRDFVDHIDLVDPVDGVVLVDPEYLKERRVYV
TLTCAFRYGREDLDVLGLTFRKDLFVANVQSFPPAPEDKKPLTRLQERLIKKLGEHAY
PFTFEIPPNLPCSVTLQPGPEDTGKACGVDYEVKAFCAENLEEKIHKRNSVRLVIRKV
QYAPERPGPQPTAETTRQFLMSDKPLHLEASLDKEIYYHGEPISVNVHVTNNTNKTV
KKIKISVRQYADICLFNTAQYKCPVAMEEADDTVAPSSTFCKVYTLTPFLANNREKR
GLALDGKLKHEDTNLASSTLLREGANREILGIIVSYKVKVKLVVSRGGLLGDLASSDV
AVELPFTLMHPKPKEEPPHREVPENETPVDTNLIELDTNDDDIVFEDFARQRLKGMKD
DKEEEEDGTGSPQLNNR –C-terminus

7.1.1.3 β-Arrestin 2 (human)

N-terminus:

MGEKPGTRVFKKSSPNCKLTVYLGKRDFVDHLDKVDPVDGVVLVDPDYLKDRKVF
VTLTCAFRYGREDLDVLGLSFRKDLFIATYQAFPPVPNPPRPPTRLQDRLLRKLGQHA
HPFFFTIPQNLPCSVTLQPGPEDTGKACGVDFEIRAFCAKSLEEKSHKRNSVRLVIRKV
QFAPEKPGPQPSAETTRHFLMSDRSLHLEASLDKELYYHGEPLNVNVHVTNNSTKTV
KKIKVSVRQYADICLFSTAQYKCPVAQLEQDDQVSPSSTFCKVYTITPLLSDNREKRG

LALDGKLKHEDTNLASSTIVKEGANKEVLGILVSYRVKVKLVVSRGGDVSVELPFVL
MHPKPHDHIPLPRPQSAAPETDVPVDTNLIEFDTNYATDDDIVFEDFARLRLKGMKD
DDYDDQLC -C-terminus

7.1.2 Recombinant Tags

7.1.2.1 Flag-Tag

N-terminus: DYKDDDDK –C-terminus

7.1.2.2 His-Tag (Decahistidine Tag)

N-terminus: HHHHHHHHHH –C-terminus

7.1.2.3 Nano9-Tag

N-terminus: DVEAWLGAR –C-terminus

7.1.2.4 GST-Tag

N-terminus:
MSPILGYWKIKGLVQPTRLLLEYLEEKYEEHLYERDEGDKWRNKKFELGLEFPNLPY
YIDGDVKLTQSMAIIRYIADKHNMLGGCPKERAEISMLEGAVLDIRYGVSRIAYSKDF
ETLKVDFLSKLPEMLKMFEDRLCHKTYLNGDHVTHPDFMLYDALDVVLYMDPMCL
DAFPKLVCFKKRIEAIPQIDKYLKSSKYIAWPLQGWQATFGGGDHPPKSDLEVLFQGP
LGSDLNSDDSTDDEAHPRKPIPTWARGTPLSQAIIHQYYQPPNLLELFGTILPLDLEDIF
KKSKPRYHKRTSSAVWNSPPLQGARVPSSLAYSLKKH–C-terminus

7.1.2.5 TEV cleavage site

N-terminus: ENLYFQG –C-terminus

7.1.2.6 Bio-Tag

N-terminus:
GGGTGGAPAPAAGGAGAGKAGEGEIPAPLAGTVSKILVKEGDTVKAGQTVLVLEAM
KMETEINAPTDGKVEKVLVKERDAVQGGQGLIKIG –C-terminus

7.1.2.7 Stab-Tag

N-terminus:

GGGTGGAPAPAAGGAGAGKAGEGEIPAPLAGTVSKILVKEGDTVKAGQTVLVLEAM
RMETEINAPTDGKVEKVLVKERDAVQGGQGLIKIG –C-terminus

7.1.2.8 GFP

N-terminus:

MVSKGEELFTGVVPILVELDGDVNGHKFSVSGEGEGDATYGKLTLKFICTTGKLPVP
WPTLVTTLTYGVQCFSRYPDHMKQHDFFKSAMPEGYVQERTIFFKDDGNYKTRAEV
KFEGDTLVNRIELKGIDFKEDGNILGHKLEYNYNSHNVYIMADKQKNGIKVNFKIRH
NIEDGSVQLADHYQQNTPIGDGPVLLPDNHYLSTQSALSKDPNEKRDHMVLLEFVTA
AGITLGMDELYK –C-terminus

7.1.2.9 CFP

N-terminus:

MVSKGEELFTGVVPILVELDGDVNGHKFSVSGEGEGDATYGKLTLKFICTTGKLPVP
WPTLVTTLTWGVQCFSRYPDHMKQHDFFKSAMPEGYVQERTIFFKDDGNYKTRAEV
KFEGDTLVNRIELKGIDFKEDGNILGHKLEYNYISHNVYITADKQKNGIKANFKIRHNI
EDGSVQLADHYQQNTPIGDGPVLLPDNHYLSTQSALSKDPNEKRDHMVLLEFVTAA
GITLGMDELYK –C-terminus

7.2 Acknowledgements

I would like to thank:

- Prof. Hartmut Michel for accepting me as a PhD student, his kind supervision of the project and enduring faith in it.
- Prof. Clemens Glaubitz for supervising the thesis as a representative of Johann Wolfgang Goethe-University and his support.
- Dr. Christoph Reinhart for excellent supervision of my thesis project, his kind support throughout the whole time, discussions and enduring support, and help in the preparation of the manuscript of this thesis.
- Dr. Krishna Saxena at Johann Wolfgang Goethe-University for his commitment, help in all aspects of the project, especially in genetic engineering, protein expression and purification, support and fruitful discussions and help in compiling my results.
- Dr. Stephen Marino for help and discussions on general GPCR work, his support with mammalian cell culture, the use of Semliki-Forest Virus mediated protein expression, binding assays, discussions of binding data and the correction of the manuscript.
- Dr. Nicolas André and Dr. Cécile Prual for help with *P. pastoris* and binding assays.
- Gabi Maul for help with *P. pastoris*, binding assays and day to day support in the lab.
- Sabine Gemeinhart for help and discussions on protein purification and crystallization and P. pastoris transformation as well as direct-expression colony blotting
- Marc Böhm for help and support with Äkta and SMART systems and discussions
- Sebastian Richers for help with mass spectrometry
- Christoph Krettler for experiments with β-arrestin and the β_2-adrenergic receptor
- Dr. Danka Elez and Dr. Darui Huo for help with Semliki-Forest Virus mediated protein expression
- Christian Peter for introduction to mammalian cell culture
- Hanne Müller and Conny Münke for help in the lab
- All other members of the Molecular Membrane Biology Department for help and discussion or the fun we had
- Dr. Götz Hofhaus for help with reconstitution experiments and all aspects of electron microscopy

- Dr. Winfried Haase for electron microscopy
- Dr. Carville Bevans for help with reconstitution experiments and lipid handling
- Taryn Kirsch for help with Reconstitution experiments
- Solveigh McCormack and Rosemarie Schmidtell for all the papers and additional things
- All other members of the Max-Planck-Institute of Biophysics for support and discussions
- Dr. Marco Betz, Dr. Martin Vogtherr, Dr. Ulrich Schieborr and Dr. Bettina Elshorst for help with NMR experiments on β-arrestin and discussions
- Heinz Schewe for help with confocal microscopy
- Steffen Gurke for help support and discussion on *in vivo* experiments with NAR1 and β-arrestin and confocal microscopy

- Sanofi-Aventis Deutschland GmbH for funding of the project
- Dr. Thomas Klabunde and Dr. K. Ulrich Wendt for coordination of the project
- Dr. Stefan Bartoschek, Dr. Elke Duchardt and Alexis Rozenknop for performing NMR-STD experiments
- Dr. Oliver Boschheinen, Ingo Focken, Thomas Jürgens and Thorsten Gleich at Protein Production
- Dr. Irvin Winkler and Heike Kohler for SPA experiments
- Dr. Jochen Kruipp and Dr. Thomas Wendrich for SPR experiments

I would like to thank:

- My parents Brunhild and Klaus Griesbach for their love and their enduring support throughout my life. You are the ones who made all this possible!
- Taryn Kirsch for her everlasting love, for being there and being the sunshine in my life when the sun refused to shine.
- All my family Hella Griesbach, Erna Kruse and Bernd Kruse for support and being their.
- Dr. Krishna Saxena for all his scientific support and all the cocktails we drank.

- All my friends Uwe Hering, Rainer Döhring, Martin Hager, Marvin Schäfer, Steffen Gurke for enduring support, discussions and cheering me up when required.
- My friends at the FTGII Volleyball Squad Jonas Hutzenlaub, Axel and Susi Morgner, Robert Schäl and all the rest of the team for all the great times and beers we had.
- Michael J. Eck, MD-PhD, Derek Ceccarelli, PhD, Jamie Friedman, PhD, Hyun-Kyu Song, PhD and Prof. Irmgard Sinning for helping me with my first steps into scientific life.
- Everybody else I forgot unintended.

7.3 Resume

Personal Data	• Date of Birth:	19.09.1977
	• Place of Birth:	Augsburg
	• Marital Status:	Single
	• Nationality:	German

Education	• June 2003	Started PhD at the Max-Planck-Institute for Biophysics, Frankfurt in the Department of Prof. H. Michel, expected graduation May 2007
	• April 2003	Graduation in Biology at Ruprecht-Karls University, Heidelberg (Average Grade: 1.2)
	• Mar. 2002 - Oct. 2002	Diploma thesis: „Structure Function Analysis of the XLP protein SAP", Dana-Farber Cancer Institute, Boston, MA, USA, Supervisor Michael J. Eck, MD-PhD
	• Sept. 2001 - Jan. 2002	Exchange Student at University of Massachusetts, Boston, USA
	• July 2000	Received First Diploma (Average Grade: 1.8)
	• Oct. 1998	Started Biology at the Ruprecht-Karls-University, Heidelberg
	• 1987-1997	Attended Carl-Benz-Gymnasium in Ladenburg Leaving Degree: Abitur (Average Grade: 1.3)

Publications	Chan B, Lanyi A, Song HK, Griesbach J, Simarro-Grande M, Poy F, Howie D, Sumegi J, Terhorst C, Eck MJ. SAP couples Fyn to SLAM immune receptors. Nat Cell Biol. 2003 Feb;5(2):155-60.

Working Experience	• Sept. 2001- March 2002	Internship at the Dana-Farber Cancer Institute, Boston, MA, USA, in the Laboratory of Michael J. Eck, MD-PhD
	• Aug. 2000	Internship at SunGene GmbH&Co. KGaA
	• 1999-2003	Employee of the Studentenwerk Heidelberg
	• Sept. 1997- Sept. 1998	Civil Service at the Johann-Peter-Hebel-Heim in Mannheim-Gartenstadt: Attending and homework supervision of the children in the group as well as housekeeping duties